**Omaha Public Power District**

1623 HARNEY ■ OMAHA, NEBRASKA 68102 ■ TELEPHONE 536-4000 AREA CODE 402

December 29, 1982
LIC-82-410

Mr. Robert A. Clark, Chief
U. S. Nuclear Regulatory Commission
Office of Nuclear Reactor Regulation
Division of Licensing
Operating Reactors Branch No. 3
Washington, D.C. 20555

Reference: Docket No. 50-285

Dear Mr. Clark:

Fort Calhoun Station Cycle 8
Reload Amendment Application

Omaha Public Power District transmitted the subject amendment application, dated November 22, 1982, to the Commission to request approval of several changes to the Fort Calhoun Station Technical Specifications to accommodate Cycle 8 operation. The District's justification and analysis for these proposed changes were provided as revised sections to the Fort Calhoun Station Updated Safety Analysis Report (USAR), which were included in Attachment B to the subject application. Page 2 of Attachment B also identified two accident analyses, "Loss of Coolant Flow Incident" and "Loss of Coolant Accident", which were incomplete and, as such, were not submitted with the amendment application. Revised USAR Sections 14.6, "Loss of Coolant Flow Incident", and 14.15, "Loss of Coolant Accident", were recently completed and are attached in support of our reload application.

Sincerely,

W C Jones

W. C. Jones
Division Manager
Production Operations

WCJ/TLP:jmm

Attachment

cc: LeBoeuf, Lamb, Leiby & MacRae
1333 New Hampshire Avenue, N.W.
Washington, D.C. 20036

A001

## 14.6 LOSS OF COOLANT FLOW INCIDENT

### 14.6.1 General

A loss of normal coolant flow may result from either a loss of electrical power to one or more of the four reactor coolant pumps or from a mechanical failure, such as shaft seizure, of a single pump. Simultaneous mechanical failure of two or more pumps, however, is not considered credible.

The following failure modes for the loss of coolant flow incident were investigated assuming an initial thermal power of 102% (of 1500 MWt) and four reactor coolant pumps in operation:

a. Loss of power to one pump;

b. Loss of one auxiliary transformer (two pumps in opposite loops);

c. Simultaneous loss of power to all four pumps;

d. Seized rotor on one pump.

Case (a) has not been analyzed because it is covered by the more limiting case (b). Case (b) can result from a single failure (electrical or mechanical) in an auxiliary transformer, provided 4160 V buses 1A1 and 1A3 or 1A2 and 1A4 are fed from a common source. Feeding of buses 1A1 and 1A3 or 1A2 and 1A4 through a common auxiliary transformer is not a normal plant operation (See Technical Specification 2.7). This is also the worst loss of flow incident that can occur from a single electrical failure (See Section 8.3). Case (c), the loss of a-c power to the reactor coolant pumps, may result from either the complete loss of a-c power to the plant or the failure of the fast transfer breakers to close after a loss of off-site power. In the event that this incident does occur, the high rotational energy in the pumps (N = 1185 rpm, I = 71,000 lb-ft$^2$ per pump) will cause the core flow rate to drop at such a rate that the minimum DNBR is always in excess of 1.30 using the W-3 correlation, i.e. at which point there is a 95% probability at a 95% confidence level that DNB does not occur (Reference 1). Case (d), the worst loss of flow incident resulting from mechanical failure, is considered to be of extremely low probability. It is assumed that the rotor shears instantaneously leaving a low inertia (~1000 lb-ft$^2$) impeller attached to a bent shaft. This latter combination comes to a halt immediately, causing a sharp drop in the flow rate and rapid reduction in DNBR.

Reactor trip for the loss of coolant flow incident is initiated by a low coolant flow rate as determined by a reduction in the sum of the steam generator hot to cold leg pressure drops. This signal is compared with a setpoint which is a function of the number of reactor coolant pumps in operation (which current Technical Specifications require to be four). For a complete loss of flow at full power, a trip would be initiated when the flow rate drops to 93 percent of full flow (95 percent minus 2 percent uncertainty). The corresponding trip initiation time for the two pump loss of flow incident occurs when the core flow rate drops to 92.4 percent of its initial value.

### 14.6.2 Method of Analysis

#### 14.6.2.1 Electrical Failure

The electrical failure mode is responsible for the loss of power to the reactor coolant pumps in cases (a) through (c). There were three steps which were performed in the analysis of these cases in Cycle 1; current transient analysis code versions may combine some of the steps. The three analysis steps are:

a. The time dependent core and individual loop flow rates and steam generator pressure drops are determined by solving the conservation equations for mass flow rate and momentum. The general forcing functions for the fluid momentum equations consist of the pump torque values as given by the manufacturer's four quadrant curves wherein the torque is related to the pump angular velocity and discharge rate.

b. The core flow rate was furnished as input into the transient-thermal hydraulics code which includes reactor kinetics and CEA scram worth. The CEA scram worth used assumes that the most reactive CEA is stuck in the fully withdrawn position. CEA motion is initiated after a 0.4 second delay time, following a low flow trip signal. The scram worth vs. time function is chosen for a top peaked neutron flux. Even though a top peaked axial shape results in a faster termination of the event than for a bottom shaped flux, DNBR is minimized due to a lower initial steady state available overpower margin. The moderator temperature coefficient of reactivity chosen is the most positive allowed by Technical Specifications to augment the positive reactivity feedback. In Cycle 1 the value was $+0.1 \times 10^{-4} \Delta\rho/°F$ and currently is $+0.5 \times 10^{-4} \Delta\rho/°F$. The least negative fuel temperature coefficient of reactivity (Doppler) is used with a 0.8 multiplier. Output from the code includes the transient surface heat flux in both the core average and hot channels.

c. The transient heat fluxes and average channel mass velocity are used as input to another computer program which performs open channel pressure balancing calculations and determines the DNB ratio using the W-3 correlation for the hot channel as a function of time and axial position. This value is then compared to the limiting value of 1.30.

#### 14.6.2.2 Mechanical Failure

The Seized Rotor event, which is the result of a mechanical failure, is conservatively assumed to result in a 0.1 second rampdown of the core flow from its initial value to the asymptotic three-pump value. This is much more rapid than realistically can be expected.

For the Seized Rotor case a DNBR analysis was performed to determine the maximum number of fuel rod failures which could occur. A DNBR value was calculated for the maximum total integrated radial peaking factor ($F_R^T$) assuming the three-pump core flow rate and distribution, the initial maximum inlet temperature, the initial minimum RCS pressure, and the maximum DNB LCO heat flux. The value of $F_R$ was allowed to vary so that a curve of DNBR versus $F_R$ could be constructed. Using a pin census based on $F_R$ in 0.01 increments the number of

pins which fail in a given interval was calculated by multiplying the number of pins in the interval by the probability of failure for the $F_R$ interval's minimum DNBR. This failure probability is specific to a 14x14 fuel rod array using the CE-1 DNBR correlation. The total number of fuel rod failures was determined by summing the failures of all the $F_R$ intervals.

Based on the analyses for both the limiting cycle (Cycle 1) and Cycle 8, less than 1% of the fuel rods in the core would fail. This assures that the radiological releases are within a small fraction of the 10CFR100 guidelines.

### 14.6.3 Results

Figure 14.6-1 shows the transient relative flow rate through the core (normalized to full core flow) for the two-pump coastdown case. The transient value of the minimum hot channel DNBR for the reference (or current) cycle's analysis of this incident starting at full power (102% of 1500 MWt) four-pump operation, is 1.76. This value is less limiting than that of the Cycle 1 analysis which resulted in a DNBR of 1.50. Figure 14.6-2 shows a plot of the reference cycle and limiting cycle (Cycle 1) results of DNBR vs. time.

Figure 14.6-3 shows the transient relative core flow rate for the simultaneous loss of power to all four reactor coolant pumps, with flow rate governed by the rotating energy in the pumps plus a small fluid inertia. The transient value minimum hot channel DNBR for the reference (or current) cycle is 1.77. The Cycle 1 analysis is the most limiting of the fuel cycles of operation having a minimum DNBR of 1.51. Figure 14.6-4 shows that the time of minimum DNBR (for the limiting cycle) occurs approximately 3 seconds after the initiation of the flow coastdown.

The seized rotor event was reanalyzed for Cycle 8 using methods outlined in Section 14.6.2.2. The percentage of fuel rods calculated to fail for the Cycle 8 Seized Rotor event is 0.13% which is bounded by the limiting cycle (Cycle 1) value of 0.25%. The Cycle 1 failure criteria was overly conservative because it assumed that if a rod experienced a DNBR less than 1.30 (using the W-3 correlation) it would fail. Thus, the consequences of a seized rotor event during Cycle 8 are bounded by Cycle 1 and are acceptable. By maintaining the fuel failures at less than 1.0% of the total number of fuel rods, it is ensured that the radiological releases will be small with respect to the 10CFR100 guidelines.

### 14.6.4 Conclusions

For full power loss of flow incidents, where the affected pumps are able to coast down, there is a considerable margin between the minimum transient value of the DNBR and the limiting value of 1.30 (using the W-3 correlation). For the case of Seized Rotor, with the assumption of complete loss of flow in the affected loops within 0.1 second, the minimum transient DNB ratio drops below 1.30 (using the W-3 correlation) for Cycle 1 and 1.19 (using the CE-1 correlation) for Cycle 8 for some rods. However, given the small number of rods that have been conservatively calculated to fail for this incident, the potential radiological releases would be a small fraction of the 10CFR100 limits.

## 14.6.5 SECTION 14.6 REFERENCES

1. Prediction of Departure from Nucleate Boiling for an Axially Non-Uniform Heat Flux Distribution, Tong, L. S., Journal of Nuclear Energy, 1967, Vol. 21, pp 241-248.

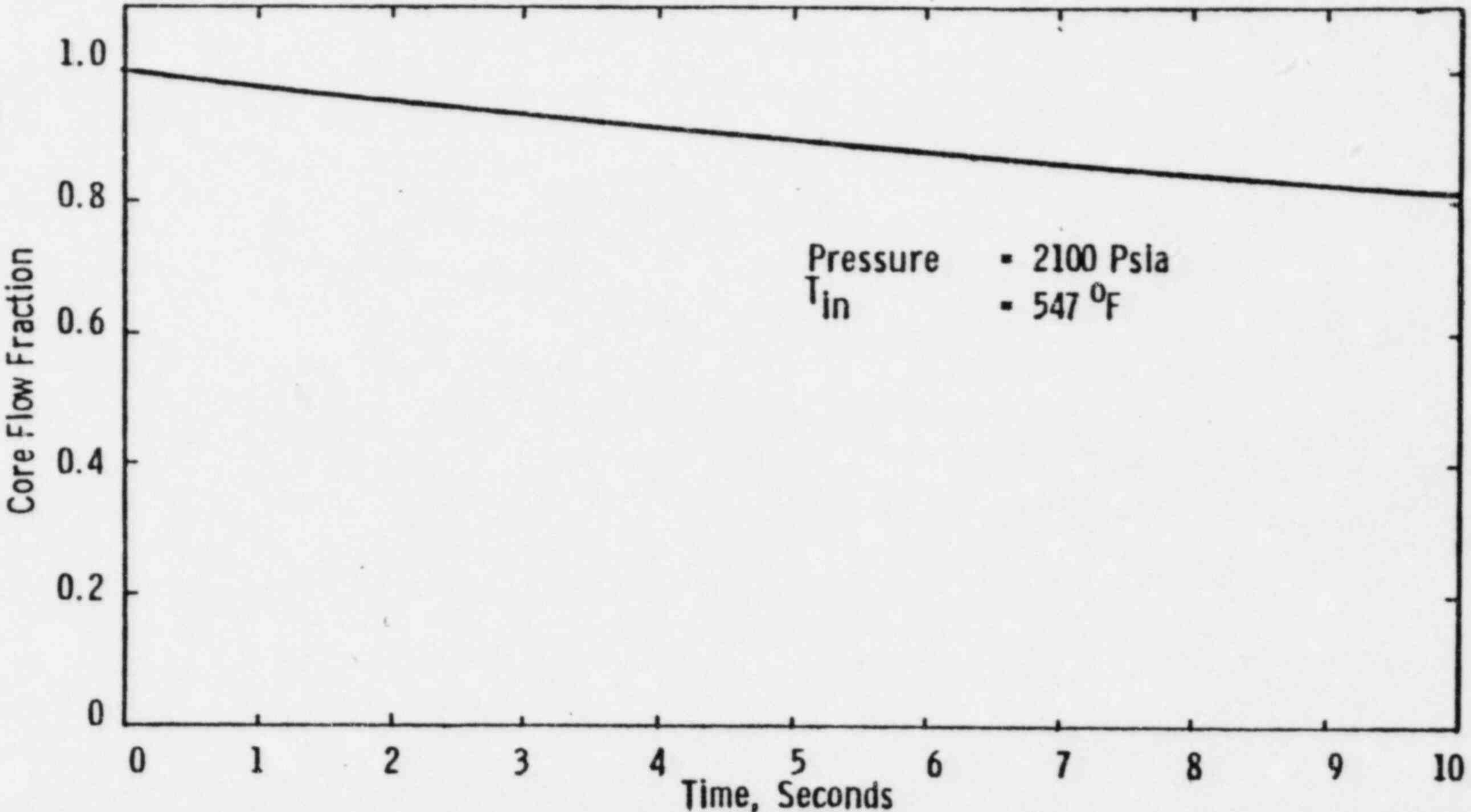


NOTE:
Loss Of Two Pumps In Opposite Loops From A Full Power Initial Condition

Loss Of Coolant Flow Incident
Core Flow vs Time

Omaha Public Power District
Fort Calhoun Station-Unit No.1

Figure
14.6-1

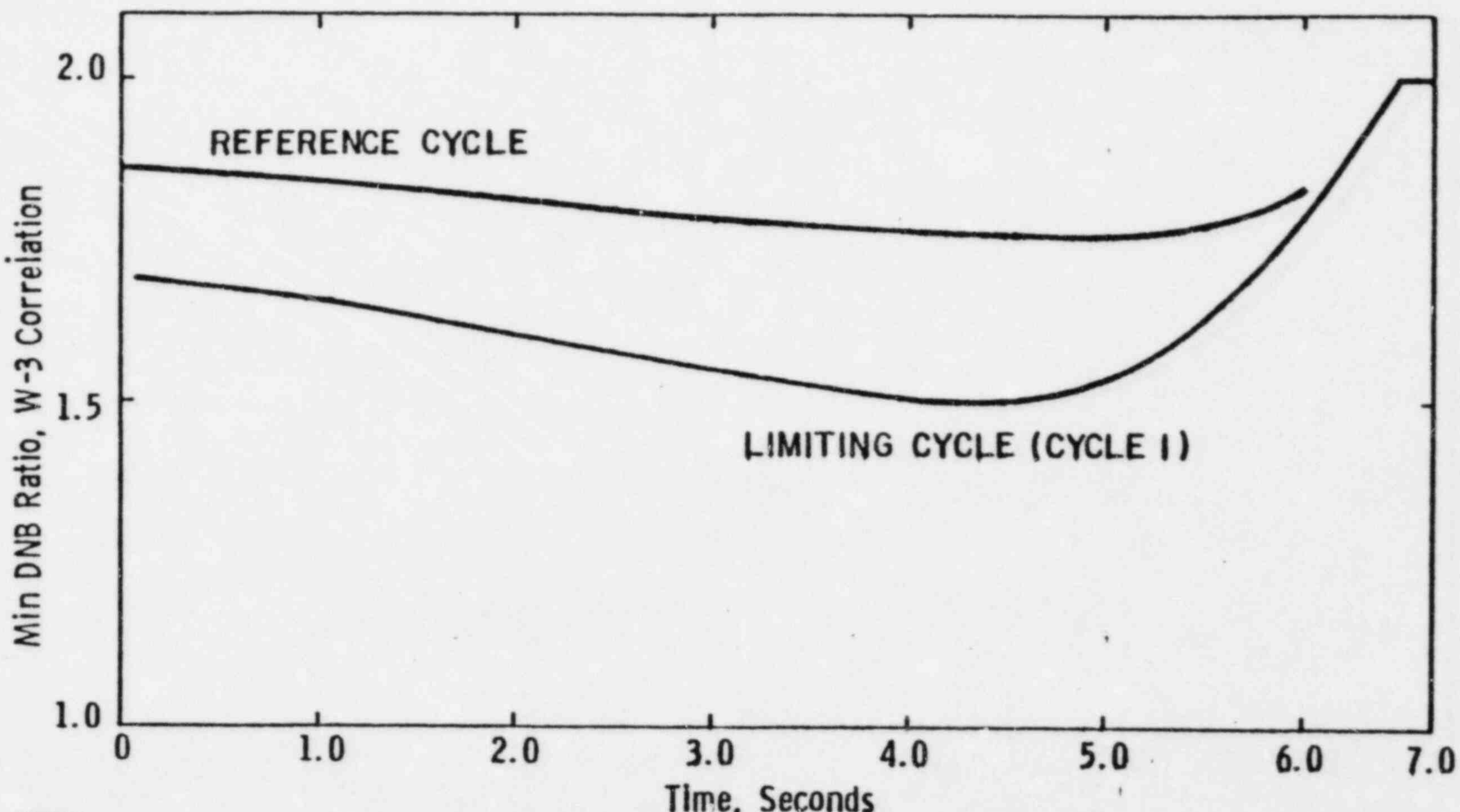


NOTE:
Loss Of Two Pumps In Opposite Loops
From A Full Power Initial Condition

Omaha Public Power District
Fort Calhoun Station-Unit No.1

Loss Of Coolant Flow Incident
Minimum DNBR vs Time

Figure
14.6-2

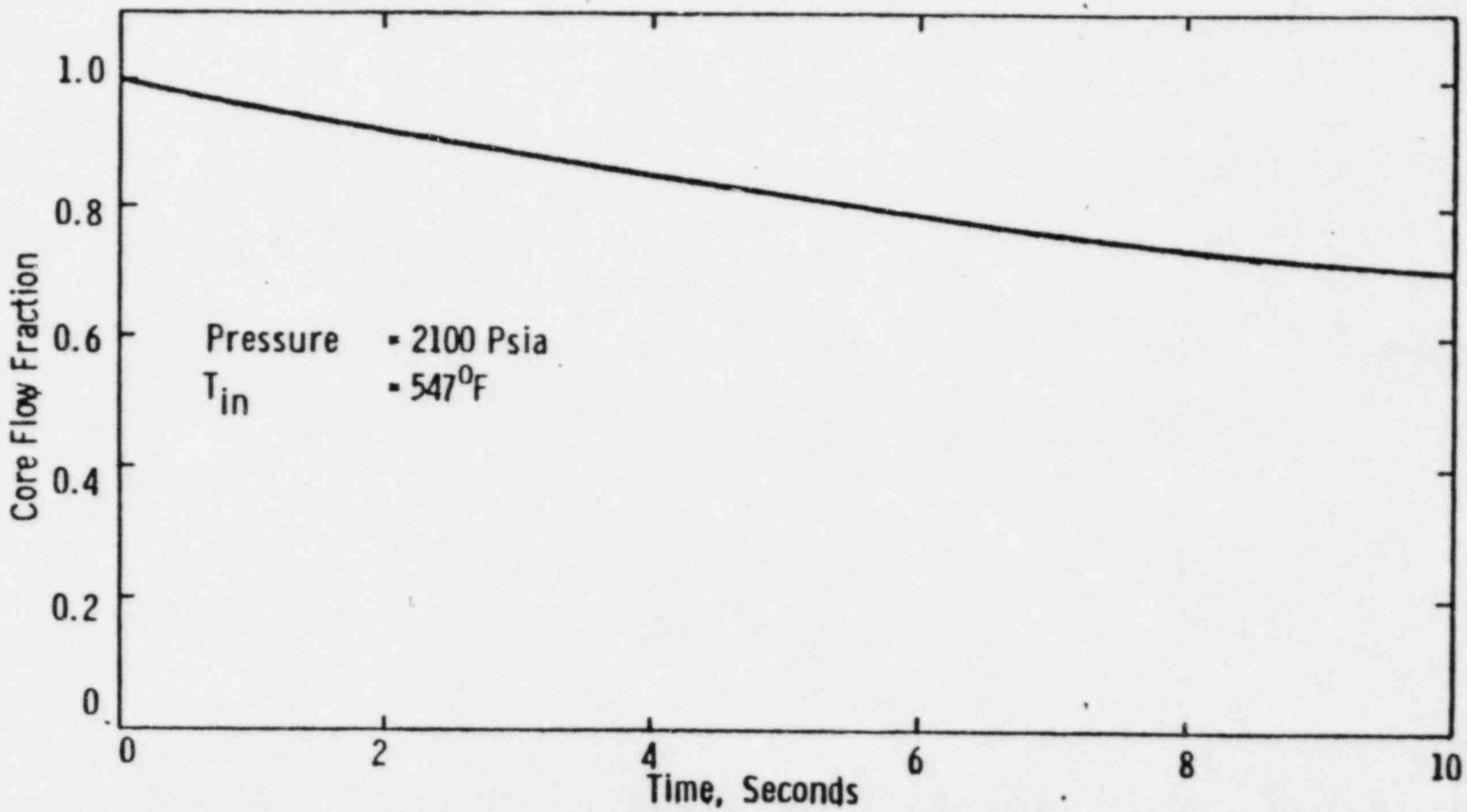


NOTE:
A Complete Loss Of All Four Pumps From A Full Power Initial Condition.

Loss Of Coolant Flow Incident
Core Flow vs Time

Omaha Public Power District
Fort Calhoun Station-Unit No.1

Figure 14.6-3

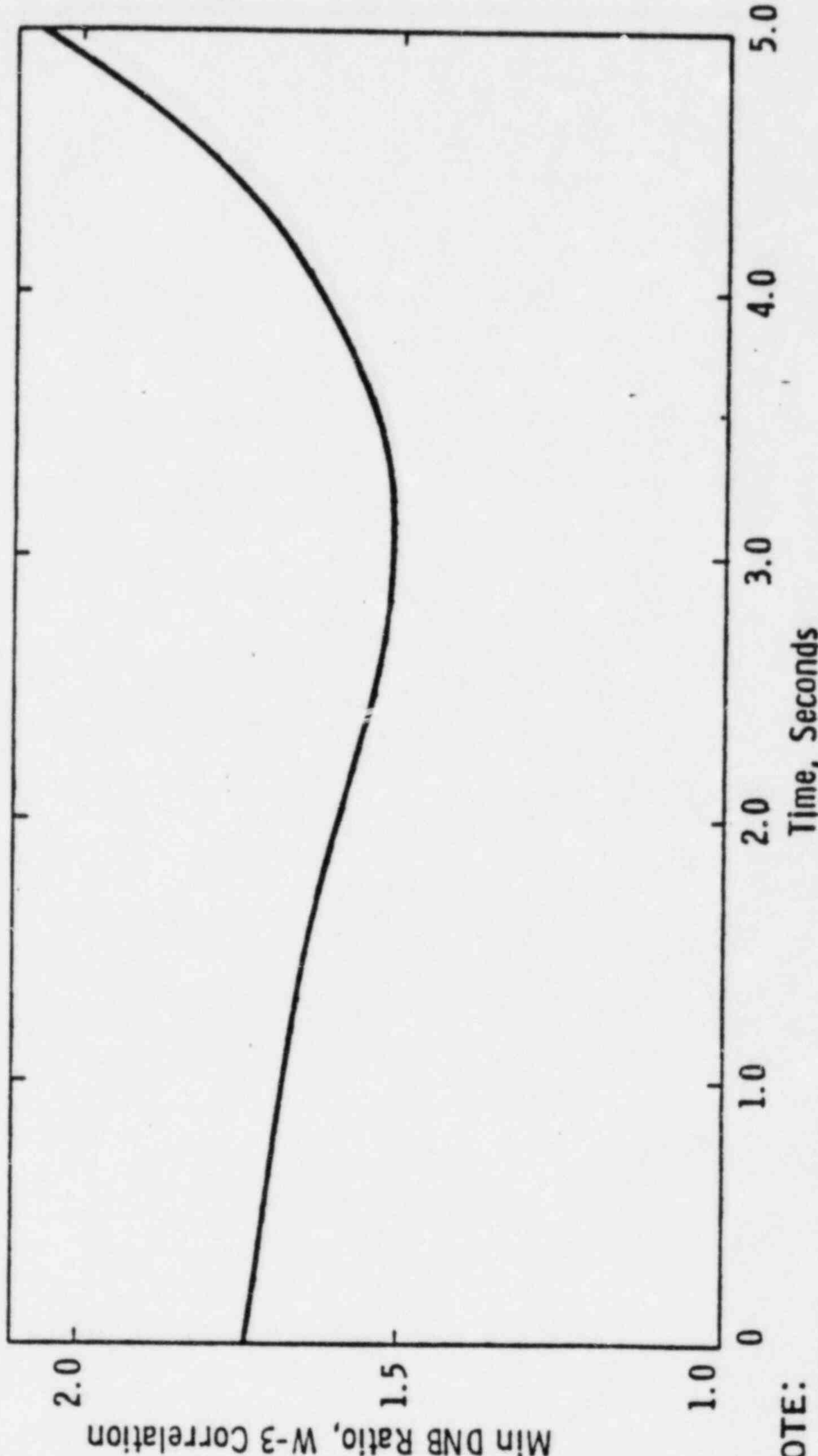


NOTE:
LIMITING CYCLE (CYCLE I)
COMPLETE LOSS OF POWER FOR ALL FOUR MAIN COOLANT PUMPS

| Loss Of Coolant Flow Incident<br>Minimum DNBR vs Time | Omaha Public Power District<br>Fort Calhoun Station-Unit No. 1 | Figure<br>14.6-4 |
|---|---|---|

## 14.15 LOSS-OF-COOLANT ACCIDENT

### 14.15.1 General

A loss-of-coolant accident (LOCA) is defined as a breach of the reactor coolant system boundary which results in interruption of the normal mechanism for removing heat from the reactor core. Emergency core cooling is provided to prevent clad and fuel melting which could occur as a result of decay heat and possible chemical reactions. The Emergency Core Cooling System (ECCS) provides adequate protection for the core in the unlikely event of a LOCA.

The safety injection system, which provides the emergency core cooling, consists of three high-pressure pumps, two low-pressure pumps, and four safety injection tanks. Emergency operation of the pumps is initiated either by a low-low pressurizer pressure signal or by a high containment building pressure signal. Water is delivered to the reactor coolant system from the safety injection tanks when the cold leg pressure drops below the driving head which consists of nitrogen gas (minimum gas pressure = 240 psig) within the safety injection tanks plus an elevation head. Thus, the tanks operate as a passive system requiring no manual or automatic action for their operation.

The injection water for the high- and low-pressure pumps is supplied from the borated (1700 ppm) safety injection and refueling water (SIRW) tank. The minimum usable inventory of this tank is 283,000 gallons. When the SIRW tank is nearly emtpy, water is recirculated from the containment sump, as described in Section 6.2.

The ECCS is designed such that its calculated cooling performance following a postulated LOCA conforms to the criteria specified in 10CFR Part 50.46. The models used for the evaluation of ECCS performance during the various postulated LOCA's include the required and acceptable features specified in Appendix K to 10CFR Part 50.46, and ECCS performance has been calculated for a number of postulated LOCA's of different sizes, locations, and other properties sufficient to provide assurance that the entire spectrum of postulated LOCA's is covered.

The LOCA analysis confirms adequate core cooling for the break spectrum up to and including the 32 inch double-ended break, assuming minimum availability of the safety injection system corresponding to the following assumptions. The entire contents of all four safety injection tanks are assumed to be available for emergency core cooling, but the contents of one of the tanks are assumed to be lost through the break in the reactor coolant system. In addition, for the three high-pressure safety injection pumps (HPSI's) and the two low-pressure safety injection pumps (LPSI's), it is assumed that two high pressure and one low pressure pumps operate for the large break analysis while only one of each type is assumed to operate in the small break analysis[1]. For the large break LOCA, it is assumed that 25% of the combined HPSI - LPSI discharge rate and the flow from one safety injection tank is lost through the break in the reactor coolant system. For the small break LOCA, 25% of the HPSI flow, 50% of the LPSI flow, and the flow from one safety injection tank is assumed to be lost through the break.

14.15.2 Method of Analysis

The method of analysis used for the larger size breaks (double-ended hot leg down to 0.5 $ft^2$) is somewhat different from the method used for the intermediate and small breaks. In addition, the large break analysis was performed by Exxon Nuclear Company, but the small break analysis was performed by Combustion Engineering. The large break model and analysis are described in Section 14.15.2.1, and the small break model and analysis are described in Section 14.15.3.1.

A complete large break LOCA analysis for operation of the Fort Calhoun Station at 1500 Mwt was performed for Cycle 6 in two stages. This analysis represents the base case and perterbations for any of the assumptions will be addressed by a reanalysis of the limiting break. First a complete spectrum analysis for the larger break sizes, which demonstrated compliance with the criteria of 10 CFR Part 50.46, was performed and reported.[17] Following the completion of this complete spectrum analysis, some errors and changes were identified in the input data used for that analysis, and the NRC requested a reassessment of the effects of flow blockage on the analysis using a new NRC flow blockage model[18]. Therefore, a reanalysis was performed of the large break determined to be the most limiting by the complete spectrum analysis, and the results were reported.[19] Since the effects of the input and model changes on the results for the most limiting break are small and since similar effects would occur for other large break sizes, reanalysis of the most limiting break is sufficient to demonstrate compliance with the criteria of 10CFR Part 50.46. In the following sections, the analysis and results are described for both stages of the large break LOCA analysis.

The limiting range break was reanalyzed for Cycle 8 to accommodate an increase in the intergrated radial peaking factor, $F_R^T$, from 1.65 to 1.85 and an increased peak pellet burnup from 48,000 MWD/MTU to 52,000 MWD/MTU.

14.15.2.1 LOCA Analysis for Large Breaks

Background

The Exxon Nuclear Company (ENC) WREM-IIA model was used for the Cycle 6 large break analysis. This model includes the following computer codes: RELAP4-EM/ENC28F for blowdown and hot channel analyses; REFLEX for core reflood analysis; CONTEMPT-LT/22, as modified in CSB 6-1 for containment back pressure analysis; TOODEE2/MAY79 for heatup analysis. System models and nodalization used for the ENC WREM-IIA computer codes have been presented in the Fort Calhoun Example Problem Document XN-NF-79-45[2] and the generic PWR ECCS Evaluation Model Update ENC WREM-IIA Document XN-NF-78-30.[3] The analytical techniques used are further described in XN-75-41, Volumes I and II, and supplements[4], XN-76-44[5], XN-76-36[6], XN-NF-78-25[7], and XN-76-27 plus supplements[8].

The Cycle 8 large break analysis[20] utilized the ENC EXEM/PWR evaluation model[21], which gives greater benefits to exposed fuel cases than the ENC WREM-IIA model. These benefits primarily result from the incorporation of radiation heat transfer and steam cooling models into the reflood and heatup models used in EXEM/PWR.

For the purpose of LOCA analyses, a LOCA is defined as a hypothetical rupture of the Reactor Coolant System piping, up to and including the double-ended rupture of the largest pipe in the Reactor Coolant System or of any line connected to that system up to the first closed valve.

Should a major break occur, depressurization of the Reactor Coolant System results in a pressure decrease in the pressurizer. A reactor trip signal occurs when the pressurizer low-pressure trip setpoint is reached. (No credit for the reactor trip was conservatively assumed in the large break analysis). A Safety Injection Actuation Signal (SIAS) occurs when either the pressurizer pressure low-low or containment high pressure setpoints are reached. (The safety analysis conservatively assumes that no SIAS condition exists until after the latter of these two setpoints is reached). These countermeasures will limit the consequences of the accident in two ways:

1. Reactor trip and borated water injection complement void formation in causing rapid reduction of power to a residual level corresponding to fission product decay heat.

2. Injection of borated water provides heat transfer from the reactor core and prevents excessive clad temperatures.

At the beginning of the blowdown phase, the entire Reactor Coolant System contains subcooled liquid which transfers heat from the core by forced convection cooling. After the break develops, the time to departure from nucleate boiling (DNB) and post DNB core heat transfer (both transition and film boiling occurring) are calculated in accordance with Appendix K of 10CFR Part 50.46. As the core becomes uncovered, both turbulent and laminar forced convection to steam are considered as core heat transfer mechanisms.

When the Reactor Coolant System pressure falls below 255 psia, the Safety Injection Tanks begin to inject borated water. The conservative assumption is made that water from one Safety Injection Tank bypasses the core and goes out through the break until the termination of bypass.

Large Break Modeling Considerations

The Fort Calhoun Station is a two steam generator - four reactor coolant pump Combustion Engineering pressurized water reactor with a dry containment. The reactor coolant system is nodalized into control volumes representing reasonably homogenous regions, interconnected by flow-paths or "junctions" as described in XN-NF-77-45.[2] The nodalized system blowdown model schematic used by RELAP4-EM in both WREM-IIA and EXEM/PWR is given in Figure 14.15-1.

One percent of the steam generator tubes were assumed to be uniformly plugged. The unbroken loop was assumed symmetrical and modeled the same as the broken loop except for the break nodalization and the pressurizer. Pump performance curves characteristic of the Fort Calhoun pumps were used in the analysis. System imput parameters are given in Table 14.15.1.

TABLE 14.15-1

FORT CALHOUN DATA

| | |
|---|---|
| Primary Heat Output, MWt | 1500* |
| Primary Coolant Flow, lbm/hr | $7.233 \times 10^7$ |
| Primary Coolant Volume, $ft^3$ | 12,031** |
| Operating Pressure, psia | 2100 |
| Inlet Coolant Temperature, °F | 545 |
| Reactor Vessel Volume, $ft^3$ | 2986 |
| Pressurizer Volume, Total, $ft^3$ | 900 |
| Pressurizer Volume, Liquid, $ft^3$ | 500 |
| Accumulator Volume, Total, $ft^3$ (one of four) | 1300 |
| Accumulator Volume, Liquid, $ft^3$ | 825 |
| Accumulator Pressure, psia | 255 |
| Steam Generator Heat Transfer Area, $ft^2$ (one of two) | 47,184 |
| Steam Generator Secondary Flow, lbm/hr | $3.38 \times 10^6$ |
| Steam Generator Secondary Pressure, psia | 853 |
| Reactor Coolant Pump Head, ft | 201 |
| Reactor Coolant Pump Speed, rpm | 1192 |
| Moment of Inertia, lbm-$ft^2$/rad | 71,000 |
| Cold Leg Pipe, I.D., in | 24.0 |
| Hot Leg Pipe, I.D., in | 32.0 |
| Pump Suction Pipe, I.D., in | 24.0 |
| Fuel Assembly Rod Diameter, in*** | 0.442 |
| Fuel Assembly Rod Pitch, in*** | 0.580 |
| Fuel Assembly Pitch, in*** | 8.180 |
| Fueled (Core) Height, in*** | 128.0 |
| Fuel Heat Transfer Area, $ft^2$ | 28,892 |

TABLE 14.15-1 (Continued)

| | |
|---|---|
| Fuel Total Flow Area, $ft^2$ | 32.579 |
| Steam Generator Tube Plugging (Assumed uniform) | 1% |

* Primary Heat Output used in analysis is: 1.02 x 1500 = 1530 MWt.
** Includes total accumulator and pressurizer volumes.
*** ENC fuel parameters

The reactor core is modeled with heat generation rates determined from kinetics equations with reactivity feedback and with decay heating as required by Appendix K of 10CFR Part 50.46. The axial power profile used for the break spectrum analysis is a top skewed curve with an axial peaking factor of 1.52 for Cycle 6 and 1.33 for Cycle 8.

The values for the primary coolant system core inlet temperatures and the steam generator secondary side pressure were set at 545°F and 853 psia, respectively.

The containment backpressure for the analysis of the postulated LOCA was evaluated in accordance with the discussion presented in XN-75-41, Supplement 5, Section 4.6 (4). The condensing heat transfer coefficient is modeled in accordance with Branch Technical Position CSB 6-1, "Minimum Containment Pressure Model for PWR ECCS Performance Evaluation" (9). The containment parameters used in the containment analysis to determine the ECCS backpressure are presented in Table 14.15-2

TABLE 14.15-2

DRY CONTAINMENT DATA

Containment Physical and Thermal Parameters

| | |
|---|---|
| Net Free Volume | $1.05 \times 10^6 ft^3$ |
| Outside Air Temperature | -17°F |
| Initiation Time for: | |
| Spray Flow | 55.0 sec |
| Fan Coolers | 25.0 sec |
| Containment Initial Conditions: | |
| Temperature | 85°F |
| Pressure | 14.7 psia |
| Relative Humidity | 80% |
| Containment Spray Water: | |
| Temperature | 40°F |
| Flow Rate (Total, 3 pumps) | 5100 gpm |
| Fan Air Cooler Capacity (total 4 coolers) | |

TABLE 14.15-2 (Continued)

| Vapor Temperature (°F) | Capacity (Btu/hr) |
|---|---|
| 150 | $0.50 \times 10^8$ |
| 185 | $1.38 \times 10^8$ |
| 244 | $3.00 \times 10^8$ |
| 288 | $4.37 \times 10^8$ |
| 320 | $5.20 \times 10^8$ |

Thermal Conductivity and Volumetric Heat Capacity

| Materials | Thermal Conductivity (Btu/hr-ft$^2$-°F) | Volumetric Heat Capacity (Btu/ft$^3$-°F) |
|---|---|---|
| Steel | 26.0 | 59.0 |
| Structural Concrete | 0.85 | 32.0 |
| Paint for Steel Surfaces | 1.5 | 57.6 |
| Paint for Concrete Surfaces | 0.3 | 43.2 |

Cycle 6 Break Spectrum Results

The Cycle 6 break spectrum calculations included configurations for double-ended cold-leg guillotine pipe breaks (DECLG) with discharge coefficients ($C_D$) of 1.0, 0.6 and 0.4. Split break configurations of the cold-leg (DECLS) pipe were calculated both with a break area equal to twice the cross sectional pipe area (6.28 ft$^2$) and with break areas reduced to 0.6, 0.4 and 0.08 times this value. The break spectrum analysis was performed for a core composed of Exxon Nuclear Company fuel at nominal Beginning-of-Cycle (BOC) conditions.

Using the large break analytic model, transient system behavior is determined by solving the governing conservation equations for mass, energy, and momentum. Energy transport, flow rates and heat transfer are determined from appropriate correlations. Table 14.15-3 presents the timing and sequence of events as determined for the large guillotine break configuration with discharge coefficients of 1.0, 0.6 and 0.4 and the split break configuration with break areas of 6.28, 3.77, 2.51 and 0.5 square feet. In general, the transient events occur slower for smaller discharge coefficients or break sizes.

Table 14.15-4 presents the peak clad temperatures and maximum metal-water reaction results for the above spectrum of break sizes. This range of break sizes was determined to include the limiting case for peak clad temperature. The maximum peak cladding temperature of 2092°F was calculated for the double-ended cold-leg guillotine break configuration ($C_D$ = 1.0) with a total linear heat generation of 15.53 kw/ft ($F_Q$ = 2.53) for ENC fuel (102% of 15.22 kw/ft). The maximum local metal-water reaction is less than 9%, all well below the limits set by the criteria of 10CFR Part 50.46.

Since there is usually margin between the value of the peak linear power density used in this analysis and the value expected in operation, a lower peak clad temperature would be obtained by using the peak linear power density expected during operation.

For the results discussed below, the hot spot is defined to be the location of maximum peak clad temperature. This location is given in Table 14.15-4 for each break size analyzed.

TABLE 14.15-3
CYCLE 6
FORT CALHOUN LARGE BREAK EVENTS
Time (Seconds)

| Event | Guillotine Breaks | | | Split Breaks | | | |
|---|---|---|---|---|---|---|---|
| | DECLG ($C_D$=1.0) | DECLG ($C_D$=0.6) | DECLG ($C_D$=0.4) | 1.0 DECLS (6.28 $ft^2$) | 0.6 DECLS (3.77 $ft^2$) | 0.4 DECLS (2.51 $ft^2$) | 0.08 DECLS (0.5 $ft^2$) |
| Start | 0.0 | 0.0 | 0.0 | 0.0 | 0.0 | 0.0 | 0.0 |
| Initiate Break | 0.05 | 0.05 | 0.05 | 0.05 | 0.05 | 0.05 | 0.05 |
| Safety Injection Signal | 0.55 | 0.66 | 0.81 | 0.56 | 0.61 | 0.72 | 2.77 |
| Accumulator Injection, Intact Loop(s) | 16.50 | 18.20 | 22.40 | 16.50 | 17.20 | 20.20 | 89.36 |
| Pressurizer Empties | 8.40 | 8.45 | 8.50 | 8.40 | 8.40 | 8.45 | 9.50 |
| End-of-Bypass | 19.63 | 21.54 | 25.89 | 19.53 | 20.39 | 23.38 | 93.57 |
| Safety Injection Flow, SIS | 20.45 | 20.56 | 20.71 | 20.48 | 20.51 | 20.61 | 22.67 |
| Start of Reflood | 32.76 | 34.91 | 39.36 | 32.64 | 33.64 | 36.70 | 107.40 |
| Peak Clad Temperature Reached (sec) | 159.5 | 165.5 | 181.1 | 171.0 | 161.6 | 164.1 | 337.6 |

TABLE 14.15-4
CYCLE 6
FORT CALHOUN LARGE BREAK RESULTS

| Event | Guillotine Breaks | | | Split Breaks | | | |
|---|---|---|---|---|---|---|---|
| | DECLG ($C_D$=1.0) | DECLG ($C_D$=0.6) | DECLG ($C_D$=0.4) | 1.0 DECLS (6.28 $ft^2$) | 0.6 DECLS (3.77 $ft^2$) | 0.4 DECLS (2.51 $ft^2$) | 0.08 DECLS (0.5 $ft^2$) |
| Peak Cladding Temperature, °F | 2092 | 2041 | 1995 | 2051 | 2045 | 1972 | 1756 |
| Peak Temperature Location, ft From Bottom | 7.97 | 7.97 | 7.97 | 7.97 | 7.97 | 7.97 | 7.47 |
| Local Zr/$H_2O$ Reaction (Max.), % | 8.0 | 6.5 | 5.1 | 6.5 | 6.8 | 5.3 | 3.3 |
| Local Zr/$H_2O$ Location, ft From Bottom | 7.47 | 7.47 | 7.47 | 7.47 | 8.22 | 8.22 | 7.47 |
| Total $H_2$ Generation, % of total Zr Reacted | <1% | <1% | <1% | <1% | <1% | <1% | <1% |
| Hot Rod Burst Time, sec | 33.03 | 35.84 | 41.49 | 32.83 | 33.89 | 51.3 | 228.6 |
| Hot Rod Burst Location. ft. From Bottom | 7.47 | 7.47 | 6.99 | 7.47 | 7.47 | 7.47 | 7.47 |
| Linear Heat Generation Rate, kw/ft at BOCREC | 0.8055 | 0.7947 | 0.7708 | 0.8071 | 0.8009 | 0.7847 | 0.6242 |

Numerous analyses and sensitivity studies have been performed on PWR systems using the ENC ECCS evaluation model. These studies have demonstrated the adequacy of the system nodalization used. In addition, these studies have shown that for transient conditions similar to those calculated for the Fort Calhoun reactor during the LOCA, the reactor coolant inlet pipe or cold leg is the worst break location. The small break analysis, described in Section 14.15.2.2, demonstrates that the large breaks represent the most limiting LOCA conditions for Fort Calhoun.

LOCA Axial Power Profile Analysis

The break spectrum LOCA analysis presented in Section 14.15.2.1 identified the limiting break for the Fort Calhoun Reactor to be a double-ended guillotine break in the pump discharge line with a discharge coefficient of 1.0 (1.0 DECLG break). The break spectrum analysis was performed with a power profile having the axial peak located at 0.7 of core height and a total peaking factor of 2.53. That analysis was expanded to define the ECCS limits for additional axial power distributions and to show the sensitivity of peak cladding temperature (PCT) to axial power peaking.

The three axial power shapes which were evaluated are shown in Figures 14.15-2 to 14.15-4. The shape shown in Figure 14.15-2 has the peak power located at 0.7 of core height, and the two additional shapes have the power peak located at 0.8 and 0.9 of core height.

The results of the analyses are summarized in Table 14.15-5 and in Figure 14.15-4A, which shows the limits on total peaking as a function of core height.

TABLE 14.15-5
CYCLE 6
RELATIVE TOTAL PEAKING VERSUS AXIAL
PEAK LOCATION WITH A CONSTANT PCT

| Peak Location (inches) (X/L) | Relative Core Height, L | Relative Peaking |
|---|---|---|
| 79.08 | 0.7 | 1.0 |
| 92.26 | 0.8 | 0.945 |
| 105.44 | 0.9 | 0.874 |

As the location of the axial peak rises in the core, it is necessary to reduce the peak linear heat generation rate (LHGR), since it takes longer for the ECCS fluid to cool the higher core elevations in the reflood portion of the transient.

The total peaking obtained at the 0.7 of core height elevation is also applied to lower core elevations as shown in Figure 14.15-4A. This is conservative, because the dominant influence on PCT in the axial studies is the time to terminate the temperature rise for the high-powered regions of the core. With power peaking lower in the core, reflood temperature transients will be terminated

earlier with a consequent reduction in PCT at the assumed peak power limit. Reactor operation with total peaking less than or equal to the value defined by the $F_Q$ versus core height curve in Figure 14.15-4A assures that 10CFR Part 50.46 criteria are not exceeded.

Cycle 6 Reanalysis of the Most Limiting Break

As described in Section 14.15.1, some errors were discovered and changes were required in the input data used in the large break spectrum analysis. The following is a list of the modifications made to the input to correct the errors and take into account the changes:

1. The ENC fuel cladding outside diameter was increased from 0.440 in. to 0.442 in.,

2. The two hot leg volumes in the reactor primary coolant system were reduced by approximately 15 cubic feet each,

3. The fluid volumes contained in the lower downcomer, lower head, and lower plenum regions of the reactor vessel were reduced by about 160 $ft^3$, and

4. The flow rate data used in the single channel heatup calculations was corrected.

In addition, in response to an NRC request, the model used to account for the effects of flow blockage was changed.

After incorporating these changes, a reanalysis was performed of the large break determined to be the most limiting by the complete spectrum analysis (1.0 DECLG). Since the effects of these revisions are small and since similar effects would occur for other large break sizes, the 1.0 DECLG break remains the most limiting large break.

In the reanalysis of the 1.0 DECLG break with the identified changes, the system representation, all other input data, and the code versions used were identical to those used in the previous large break spectrum analysis. Limiting break event times from the reanalysis results for both ENC and CE fuels are given in Table 14.15-6. Blowdown results from the revised calculation are shown in Figure 14.15-5 through 14.15-11. Blowdown Hot Channel results are given in Figures 14.15-12 through 14.15-17. The blowdown results are somewhat different than those from the previous analysis as a direct result of the reduced system volume.

Containment pressure and normalized power are given in Figures 14.15-18 and 14.15-19. The calculation for the containment pressure was performed to include the revised mass and energy released during both blowdown and reflood.

TABLE 14.15-6
CYCLE 6
FORT CALHOUN LIMITING
LARGE BREAK EVENT TIMES
(1.0 DECLG BREAKS)

| | ENC FUEL BOL TIME (seconds) | CE FUEL BOL TIME (seconds) |
|---|---|---|
| Initiate Break | 0.05 | 0.05 |
| Safety Injection Signal | 0.55 | 0.55 |
| Accumulator Injection, Intact Loop(s) | 15.9 | 15.9 |
| Pressurizer Empties | 8.35 | 8.35 |
| End-of-bypass | 19.02 | 19.07 |
| Safety Injection Flow, SIS | 20.45 | 20.45 |
| Start of Reflood | 30.23 | 30.27 |
| Peak Clad Temperature Reached | 208. | 229. |

The reflood results which are obtained using the revised containment pressure are given in Figures 14.15-20 through 14.15-23 and the cladding heatup results are given in Figure 14.15-24 for ENC fuel at beginning-of-life. Final heatup results for both ENC and CE fuels are provided in Table 14.15-7.

Comparison of reanalysis results with the results of the previous analysis shows only small differences in the thermal-hydraulic behavior of the two cases. The principal differences are a faster blowdown and a reduced refill time as a direct result of the smaller system volume input to the analysis. The correction of single-channel flow data and use of the NRC blockage model affect only the final heatup portion of the transient.

A recalculation of axial profile sensitivity with a power peak at the 90% core elevation and a peaking magnitude determined by Figure 14.15-5 (0.874 times the 70% core height value) resulted in a PCT 18°F below the PCT for the 70% core height reference case. Thus, the axial peaking limit relationship given in Figure 14.15-4A remains applicable for the revised analysis.

Cycle 6 Limiting Break Heatup Analysis Results Including Rod Internal Pressure Uncertainties and Exposure Sensitivity

This section describes the results of the fuel rod internal pressure uncertainty and exposure sensitivity analyses, which support an ECCS allowable total peaking $F_Q^T$, of 2.53 for both ENC and CE fuel types.

A complete LOCA calculation for the limiting 1.0 DECLG break was performed for CE fuel as part of the large break spectrum analysis. The calculational models and assumptions were identical to those for the ENC fuel calculation. The only difference in the calculations was that the core was modeled with CE fuel rather than ENC fuel. Since there are only relatively small differences between these fuel types, the blowdown and heatup transients for both ENC and CE fuel types are very similar. Beginning-of-life peak cladding temperatures differed by only 21°F for the two fuel designs.

ECCS heatup calculations require consideration of rod internal pressure uncertainties in order to conservatively maximize the calculated flow blockage in the hot rod heatup calculations. The heatup analysis models are identical to those detailed and referenced for Prairie Island.[10]

Table 14.15-1 summarizes the key system parameters for the exposure heatup analysis. These parameters apply to the analyses for both ENC and CE fuel. The core upper and lower plenum boundary conditions used for the BOL and exposed fuel hot channel calculations are from the respective limiting break blowdown calculations, and the reflood rates versus time for the heatup calculations are for the limiting break reflood calculations.

Table 14.15-7 provides the heatup analysis results for ENC and CE fuel types at beginning-of-life. The respective heatup transients for ENC and CE fuel are given in Figures 14.15-24 and 14.15-25. These heatup results include allowances for the upper bound uncertainties on rod internal pressure. The calculated PCT's are 1980°F for ENC fuel and 2012°F for CE fuel. Maximum local metal water reaction is less than 7.0% in both cases. These results support an ECCS allowable total peaking factor of 2.53 for BOL.

TABLE 14.15-7
CYCLE 6
EXPOSURE HEATUP ANALYSES RESULTS FOR ENC AND CE FUEL

| Exposure Peak Pellet Burnup (PPBU) (MWD/MTU) | ENC FUEL BOL | ENC FUEL 48,000 (EOL) | CE FUEL BOL | CE FUEL 32,600 | CE FUEL 42,400 (EOL) |
|---|---|---|---|---|---|
| Total Peaking, $F_Q^T$ | 2.53 | 2.53 | 2.53 | 2.53 | 2.46 |
| Peak Clad Temperature (PCT), °F | 1980 | 2195 | 2012 | 2188 | 2190 |
| Max. Local $Zr/H_2O$ - Reaction, % | 4.6 | 9.1 | 6.2 | 9.5 | 10.1 |
| Hot Rod Burst Time, sec | 31.6 | 29.3 | 28.5 | 26.6 | 26.1 |
| Hot Rod Burst Location, ft From Bottom | 7.47 | 7.47 | 7.47 | 7.47 | 7.47 |
| Time of PCT, sec | 208 | 252 | 229 | 235 | 254 |
| PCT Location, ft From Bottom | 8.22 | 8.22 | 8.22 | 8.22 | 8.22 |

TABLE 14.15-7 (Continued)

| Exposure Peak Pellet Burnup (PPBU) (MWD/MTU) | ENC FUEL BOL | ENC FUEL 48,000 (EOL) | CE FUEL BOL | CE FUEL 32,600 | CE FUEL 42,400 (EOL) |
|---|---|---|---|---|---|
| Max, $Zr/H_2O$ Reaction Location, ft | 8.22 | 8.22 | 8.22 | 8.22 | 8.22 |
| Linear Heat Generation Rate, kw/ft at BOCREC | 0.8218 | 0.8682 | 0.8206 | 0.8596 | 0.8338 |
| Total $H_2$ Generation, % of total Zr reacted | <1% | <1% | <1% | <1% | <1% |

End-of-life (EOL) is the most limiting fuel exposure as a consequence of burnup dependent fission gas release which has the two-fold effect of increasing stored energy (due to reduced pellet-to-clad conductance) and causing high flow blockage (due to high rod internal pressure). The heatup analysis results for ENC and CE fuel types at EOL are also given in Table 14.15-7 along with those for BOL. The PCT for ENC fuel at EOL is 2195°F. For CE fuel, the PCT is 2188°F at a peak pellet burnup of 32,600 MWD/MTU with a total peaking $F_Q^T$ equal to 2.53. At EOL, the PCT for CE fuel is 2190°F and corresponds to an $F_Q^T$ value of 2.46. The cladding heatup transients for ENC fuel at EOL and for CE fuel at exposures of 32,600 MWD/MTU and at EOL are given in Figures 14.15-26, 14.15-27 and 14.15-28, respectively. The maximum local metal-water reaction results are less than 11% for both ENC and CE fuel types.

The 2.46 total peaking in the LOCA calculations for CE fuel at end-of-life is 3% below the LOCA derived limit of 2.53. This 3% reduction in allowable total peaking for CE fuel at end-of-life is considerably less than the reduction in the actual total peaking that occurs during operation because of fissile depletion for fuel assemblies that have been exposed beyond 32,600 MWD/MTU peak pellet burnup. Thus, in practice the achievable $F_Q^T$ for exposures above 32,600 MWD/MTU peak pellet burnup will be sufficiently below the achievable $F_Q^T$ for low exposure fuel, that the high exposure fuel with a 3% reduction in ECCS allowable $F_Q^T$ will not become limiting. Therefore, a single $F_Q^T$ limit of 2.53 assures conformance with 10CFR Part 50.46 criteria for both ENC and CE fuels to the maximum exposures analyzed.

Cycle 8 Limiting Break

The limiting break of Cycle 6, the double-ended cold-leg guillotine pipe break with a $C_D$ of 1.0, was reanalyzed for Cycle 8 to accomodate the increases in $F_R^T$ from 1.65 to 1.85 and in peak pellet burnup from 48,000 MWD/MTU to 52,000 MWD/MTU. The analysis can be considered as consisting of three parts: (1) a recalculation of the Cycle 6 base case with an axial power profile peaking at 0.7 of the active core height at BOL exposure (0.7 BOL); (2) an exposure calculation which repeated the base case for EOL exposure (0.7 EOL); and (3) an axial profile study which recomputed the limiting break for the worst exposure with axial power peaks at 0.8 and 0.9 of the active core height (0.8 and 0.9 BOL cases).

The final results for an axial peak of 70% of core height which are summarized in Table 14.15-8, support a linear heat generation rate of 15.22 KW/ft which corresponds to a total peaking factor, $F_Q^T$, of 2.53. Thus, these results support operation of ENC fuel at the existing limits with the increased radial peaking and higher fuel burnup. As can be seen from Table 14.15-8 the BOL case is now more limiting than EOL and the peak clad temperature results are below the Cycle 6 analyses. This is due primarily to the steam cooling and radiation heat transfer portions (incorporated into TOODEE2) of the EXEM/PWR model which gives greater benefits to exposed fuel cases than did the ENC WREM-IIA PWR ECCS model used for Cycle 6.

TABLE 14.15-8
CYCLE 8
EXPOSURE HEATUP AND AXIAL PEAKING ANALYSIS RESULTS
FOR THE 1.0 DECLG BREAK

| Parameter | Results | | | |
|---|---|---|---|---|
| | 0.7 BOL | 0.7 EOL | 0.8 BOL | 0.9 BOL |
| Total Peaking, $F_Q^T$ | 2.53 | 2.53 | 2.53 | 2.33 |
| Peak Clad Temperature, °F | 1850. | 1700. | 2022. | 2052. |
| PCT Location, ft. from Bottom | 8.22 | 8.22 | 8.97 | 9.97 |
| Local $Zr/H_2O$ Reaction (Max), % | 2.1 | 1.2 | 3.6 | 3.6 |
| Location of Maximum Local $Zr/H_2O$ reaction, ft. from Bottom | 8.22 | 8.22 | 8.97 | 8.72 |
| Total $H_2$ Generation, % of total Zr reacted | <1.0 | <1.0 | <1.0 | <1.0 |
| Hot Rod Burst time, seconds | 30.72 | 37.92 | 30.12 | 36.72 |
| Hot Rod Burst Location, ft. from Bottom | 7.47 | 7.47 | 8.47 | 9.47 |
| Linear Heat Generation Rate, KW/ft at BOCREC | .8275 | .8455 | .8274 | .7621 |

The calculation at BOL for axial power profile peaking at 80% of core height allows the full 15.22 KW/ft LHGR corresponding to a total peaking factor of 2.53, i.e. the peak cladding temperature of 2022°F meets the 2200°F acceptance criteria of 10 CFR 50.46.

The BOL calculation performed with the axial power profile peaked at 90% of core height does not meet the 10 CFR 50.46 acceptance criteria for PCT so the LHGR had to be reduced to 14.0 KW/ft yielding an $F_Q^T$ of 2.33.

Figures 14.15-34 through 14.15-36 show the 0.7, 0.8 and 0.9 axial peaking shapes used in the analysis. Figure 14.15-37 shows a plot of the allowed total peaking factor, $F_Q^T$, as a function of the axial peaks analyzed. This figure shows an improvement over that of Cycle 6 (Figure 14.15-4A) in which the $F_Q^T$ was reduced at 80% of core height.

Table 14.15-9 summarizes the sequence of events for the limiting break. System blowdown results are shown in Figures 14.15-38 through 14.15-45. Blowdown hot channel results are shown in Figures 14.15-46 through 14.15-51. Containment pressure and extended normalized power are given in Figures 14.15-52 and 14.15-53. The containment pressure calculation includes mass and energy released during both blowdown and reflood.

TABLE 14.15-9
CYCLE 8
SEQUENCE OF EVENTS FOR 1.0 DECLG BREAK

| Event | Time of Event (seconds) |
|---|---|
| Start | 0.0 |
| Initiate Break | 0.05 |
| Safety Injection Signal | 0.55 |
| Pressurizer Empties | 8.22 |
| Accumulator Injection, Broken Loop | 8.25 |
| Accumulator Injection, Intact Loops | 15.85 |
| End of Bypass | 19.12 |
| Safety Injection Flow Begins | 20.45 |
| Start of Reflood | 30.32 |
| Accumulators Empty | 31.45 |
| Peak Clad Temperature reached | |
| 0.7 X/L, BOL | 156. |
| 0.7 X/L, EOL | 173. |
| 0.8 X/L, BOL | 137. |
| 0.9 X/L, BOL | 139. |

Reflood results are shown in Figures 14.15-54 through 14.15-57, and the TOODEE2 heatup results for 0.7 BOL, 0.7 EOL, 0.8 BOL, and 0.9 BOL are shown in Figures 14.15-58 through 14.15-61.

Comparison of the results shows little difference in thermal-hydraulic behavior during blowdown between Cycles 8 and 6. The principal differences are in the thermal performance of the hot rod, and are due to the higher radial peaking factor. During reflood, there are differences in the core flooding rate, mixture level and pressure which are attributable to the EXEM/PWR ECCS model. The largest differences are seen in the TOODEE2 results which are a considerable improvement of previous results, and more than offset the effects of the increased radial peaking.

Cycle 8 Analysis Summary

The C,cle 8 EXEM/PWR analysis for Fort Calhoun with ENC fuel, shows that with the specified increased radial peaking factor and increased exposure limits, the emergency core cooling system will continue to meet the NRC acceptance criteria as presented in 10 CFR 50.46.

That is:

(1) The calculated peak fuel element clad temperature does not exceed the 2200°F limit.

(2) The amount of fuel element cladding that reacts chemically with water or steam does not exceed 1% of the total amount of zircaloy in the reactor.

(3) The cladding temperature transient is terminated at a time when the core geometry is still amenable to cooling. The hot fuel rod cladding oxidation limits of 17% are not exceeded during or after quenching.

(4) The system long-term cooling capabilities provided for previous cores remains applicable for ENC fuel.

These acceptance criteria are satisfied if the Fort Calhoun reactor is operated at 1500 MWt within the maximum linear heat generation rate (LHGR) of 15.22 kW/ft, the radial peaking, $F_R$=1.85, the $F_Q^T$ of 2.53, and the axial profile limits shown in Figure 14.15-37.

Operation within the allowed LHGR limit and the allowed axial shape limits will neutronically preclude total peaking above the 80% core height level from reaching the limits shown in Figure 14.15-37.

ECCS Performance of Extended Burnup CE Fuel

An ECCS performance evaluation for extended burnup of CE supplied fuel assemblies[24] was conducted to demonstrate that the hottest fuel rod in the supplied assemblies has a much less limiting response than the higher power ENC assemblies. This much less limiting response demonstrates the conformance of the CE fuel to the acceptance criteria for light-water cooled reactors of 10 CFR 50.46, because conformance has been demonstrated for the higher power ENC assemblies. The analysis is applicable to CE supplied fuel assemblies with peak pellet burnups exceeding 42,400 MWD/MTU and a peak rod burnup of less than 48,000 MWD/MTU.

The expected peak linear heat generation rate (LHGR) for applicable CE fuel is less than 10.0 KW/ft with the maximum allowed peak LHGR in the core limited to 15.22 Kw/ft. The method of analysis employed demonstrates that the low linear heat generation rate in the hottest CE fuel results in a much less limiting response than the higher power ENC fuel assemblies.

Burnup dependent calculations were performed using the FATES[25] and STRIKIN-II [15] computer codes to determine the limiting condition for the ECCS performance analysis. The break size and type analyzed, 1.0 DEG/PD*, is the same as was analyzed in the previous limiting break analysis[26].

*1.0 x Double-Ended Guillotine Break in the Reactor Coolant Pump Discharge Leg.

The highest burnup CE fuel utilized with the ENC fuel assemblies is a Batch D assembly located in the center of the reactor core. The radiation enclosure in the Batch D assembly analysis used a conservative adaptation of the peak clad temperature versus time profile (Figure 14.15-62) for the surrounding pins in the higher power neighboring assemblies, which represents their radiation heat transfer contribution to the hot pin in the Batch D assembly. The more limiting pins in the assemblies adjacent to the D assembly were analyzed using the CE radiation heat transfer model[15]. A variation was necessary to conservatively represent the thermal response of those high power pins in the neighboring assemblies which are adjacent to the less limiting D pin.

Table 14.15-10 presents the Batch D assembly analysis results for the limiting 1.0 DEG/PD break. A list of the significant parameters displayed graphically is presented in Table 14.15-11. A summary of the fuel and system parameters is shown in Table 14.15-12. As can be seen from the results, the worst break analysis for the Batch D assembly yields a peak clad temperature of 1303°F which is well below the criteria. Since the maximum clad temperatures achieved are low enough, pin rupture is not predicted and the maximum local zirconium oxide percentage is only 0.13%.

TABLE 14.15-10
SUMMARY OF RESULTS FOR FORT CALHOUN
BATCH D ECCS PERFORMANCE RESULTS

| | |
|---|---|
| Break: | 1.0 DEG/PD |
| Peak Clad Temperature: | 1303°F |
| Time of Peak Clad Temperature: | 10 sec |
| Maximum Local Zirconium - Oxide (%): | 0.13 |

TABLE 14.15-11
FORT CALHOUN BATCH D
VARIABLES PLOTTED AS A FUNCTION OF TIME

| Variables | Figure Designation |
|---|---|
| Peak Clad Temperature | 14.15-63 |
| Hot Spot Gap Conductance | 14.15-64 |
| Peak Local Clad Oxidation | 14.15-65 |
| Clad Temperature, Centerline Fuel Temperature, Average Fuel Temperature and Coolant Temperature for Hottest Node | 14.15-66 |
| Hot Spot Heat Transfer Coefficient | 14.15-67 |
| Hot Rod Internal Gas Pressure | 14.15-68 |

TABLE 14.15-12
FORT CALHOUN BATCH D
GENERAL SYSTEM PARAMETERS

| Parameter | Value | |
|---|---|---|
| Reactor Power Level (102% of Nominal) | 1448 | MWt |
| Linear Heat Generation Rate (LHGR) for the Batch D fuel | 10.0 | kw/ft |
| Gap Conductance at LHGR | 2000 | BTU/hr-ft$^2$-°F |
| Fuel Centerline Temperature at LHGR | 2200 | °F |
| Fuel Average Temperature at LHGR | 1451 | °F |
| Hot Rod Gas Pressure | 1581 | psia |
| Hot Rod Burnup | 49,963 | MWD/MTU |

It should be noted that this analysis was performed at a power level of 1448 MWt (102% of 1420 MWt). Since the response of the highest power Batch D pin is much less limiting than the 10 CFR 50.46 acceptance limits, it is clear that the conclusion derived from this analysis is equally valid at the 5.6% higher power.

The analyses show that the acceptance criteria are satisfied for the extended burnup CE fuel because of the much less limiting response of the CE fuel when compared to the response of the higher power ENC fuel assemblies.

14.15.2.2 LOCA Analysis for Small Breaks

Background

For the intermediate to smaller size reactor coolant system breaks (less than 0.5 ft$^2$), the events occur over relatively long periods, and the influence of secondary side transients are more important than they are for large breaks. Therefore, the analysis model for small breaks provides a more detailed representation of the transient conditions on the secondary side of the steam generators.

There is a finite rise time for void bubbles formed in the lower vessel volume to pass through the surrounding water and into the upper steam volume. For small breaks, the bubbles boil away from the water-steam interface and maintain a "quiet" level. For larger breaks, the steam cannot escape rapidly enough and a volume swell of two-phase froth occurs. Since the blowdown flow rate is sensitive to the quality of the mixture near the break, it is important to accurately locate the steam-froth interface.

Reactor Coolant System heat removal is accomplished by flow out through the break and by the steam generators. Steam generator heat transfer is particularly important for the small and intermediate sized breaks. Although the turbine stop valves close rapidly after the reactor trip signal, heat transfer from the reactor coolant system would cause the steam generator pressure to rise until the steam dump and the bypass valves or the safety valves are actuated. In the present analysis, no credit is taken for the steam dump and bypass valves.

Small Break Modeling Considerations

The LOCA analysis for small breaks was performed using Combustion Engineering's approved Small Break Evaluation Model.[11,12] The analysis of small break LOCA's involves the use of four computer codes. Blowdown hydraulics are calculated using the CEFLASH-4AS[13] code; reflood hydraulics are calculated using the COMPERC-II code [14]; and fuel rod temperatures and clad oxidation percentages are calculated using the STRIKIN-II[15] and PARCH[16] codes.

The worst single failure for analysis of the small break LOCA is the failure to start of one of the emergency diesel generators.[11] This failure results in minimum availability of safety injection water to cool the core. Consistent with this worst single failure assumption, only the following injection pumps were assumed to be operable in the small break LOCA analysis:

1. 75% of one high pressure safety injection pump

2. 50% of one low pressure safety injection pump

In addition to the pumped injection, three of the four available safety injection tanks were assumed to be operable in the analysis of small breaks.

The small break LOCA analyses conservatively assumed that offsite power is lost upon reactor trip.[11] As a result, the injection from the above described pumps was assumed to be delayed by 30 seconds (for diesel startup and load sequencing) following a safety injection actuation signal.

Core power during blowdown is computed using standard kinetics equations with significant contributions to the reactivity from the following:

1. CEA insertion;

2. Fuel temperature Doppler effect;

4. Boron concentration in the coolant.

These feedback reactivity effects are continuously calculated during the course of the accident.

The significant general system parameters used in the small break calculations are presented in Table 14.15-13.

Small Break Spectrum Results

The ECCS performance analysis considered a spectrum of cold leg breaks in the reactor coolant pump discharge leg. The break sizes analyzed were the 0.5, 0.1, 0.075 and 0.05 $ft^2$ cold leg breaks. The times at which significant events in the performance of the ECCS occurred for each break size are listed in Table 14.15-14. Table 14.15-15 shows a summary of the hot fuel rod performance including the calculated peak clad outside surface temperatures and locations as well as the amount of core wide zirconium oxidation and the peak local oxidation on the hot rod.

TABLE 14.15-13

GENERAL SYSTEM PARAMETERS
FORT CALHOUN CYCLE 6

| Quantity | Value |
|---|---|
| Reactor power level (102% of Nominal) | 1530 MWt |
| Average linear heat rate (102% of Nominal) | 6.128 kw/ft |
| Peak linear heat rate | 15.5 kw/ft |
| Gap conductance at peak linear heat rate | 1699. BTU/hr-ft$^2$-°F |
| Fuel centerline temperature at peak linear heat rate | 3689. °F |
| Fuel average temperature at peak linear heat rate | 2278. °F |
| Hot rod gas pressure | 1200. psia |
| Hot rod burnup* | 820. MWD/MTU |
| System flow rate (total) | 71.56 x $10^6$ lbm/hr |
| Core flow rate | 68.34 x $10^6$ lbm/hr |
| Reactor vessel inlet temperature | 547.0 °F |
| Reactor vessel outlet temperature | 604.2 °F |

*At time-in-life of minimum gap conductance

TABLE 14.15-14

FORT CALHOUN CYCLE 6 (1530 Mwt)

TIMES OF INTEREST FOR SMALL BREAKS
(SECONDS)

| Break Size ($ft^2$) | HPSI and Charging Pump On (sec) | LPSI Pump On (sec) | SI Tanks Aligned (sec) | Time for SI $H_2O$ to Reach Bottom of Fuel (sec) | Time That Hot Spot Peak Clad Temperature Occurs (sec) |
|---|---|---|---|---|---|
| .5 | 39. | 101. | 96. | 100. | 214. |
| 0.1 | 46. | a | 700. | b | 718. |
| .075 | 50. | a | 1010. | b | 1034. |
| .05 | 54. | a | c | b | 1648. |

a - calculation terminated before time of LPSI pump activation

b - core never totally uncovered

c - calculation terminated before SIT actuation

d - top of core never uncovers

e - clad temperature during transient never exceeds initial fuel clad temperature

## TABLE 14.15-15

## FORT CALHOUN CYCLE 6 (1530 Mwt)

## FUEL ROD PERFORMANCE SUMMARY

| Break Size ($ft^2$) | Maximum Clad Surface Temperature (°F) | Elevation of Hot Spot (from bottom of core)(ft) | Core Wide Zirconium Oxidation (%) | Peak Local Zirconium Oxidation (%) |
|---|---|---|---|---|
| .5 | 1691. | 9.6 | < .15 | < .71 |
| .1 | 1647. | 9.6 | < .08 | < .34 |
| .075 | 1874. | 9.6 | < .24 | < 2.10 |
| .05 | 1662. | 10.1 | < .22 | < 1.34 |

These results demonstrate the .075 ft$^2$ break to be the limiting small break with a peak clad temperature and peak zirconium oxidation percentage of 1874°F and 2.10%, respectively. The analysis was performed using the limiting batch H reload fuel at the time-in-life when fuel stored energy is highest.

The transient values of parameters which most directly affect fuel rod performance are shown in Figures 14.15-29 (A through H) through 14.15-32 (A through H). The following parameters are graphically presented for each break size:

1. Normalized Total Core Power
2. Inner Vessel Pressure
3. Break Flow Rate
4. Inner Vessel Inlet Flow Rate
5. Inner Vessel Two-Phase Mixture Volume
6. Hot Spot Heat Transfer Coefficient
7. Channel Coolant Temperature at Hot Spot
8. Hot Spot Clad Surface Temperature

Figure 14.15-33 compares the peak clad temperature results of the current (1980, Cycle 6) spectrum analysis, with the results of the most recent previous (1976, Cycle 3) analysis.(1) As shown in Figure 14.15-33, the 1976 analysis included ECCS performance calculations for the 0.5, 0.35, 0.1, 0.075, and 0.05 ft$^2$ cold leg breaks. This 1976 analysis indicated the worst small break to be the 0.5 ft$^2$ break. In addition, a second peak at the low end of the break size spectrum occurred for the 0.075 ft$^2$ break. To demonstrate that these limiting small breaks (i.e., the 0.5 and 0.075) remain below the acceptance criteria, the 1980 analysis included the 0.5 ft$^2$ break (the limiting Reference 1 small break) and the 0.1, 0.075 and 0.05 ft$^2$ breaks.

As shown in Figure 14.15-33, the 1980 spectrum analysis results confirm the general shape of the 1976 results but indicate the 0.075 ft$^2$ break results in a higher peak clad temperature than the 0.5 ft$^2$ break. The following discussion explains the shift in the most limiting small break size as indicated by the 1980 analysis.

Peak clad temperatures during a small break LOCA are produced by different phenomena depending on the break size. For the 0.5 ft$^2$ break, the temperature transient is terminated during the reflood period which is controlled primarily by the Safety Injection (SI) pumps after the Safety Injection Tanks (SIT) have emptied. The 1976 analysis used conservative values for the low pressure SI pump flow. The 1980 analysis used more accurate low pressure SI pump flow. This resulted in a decrease in PCT for the 0.5 ft$^2$ break at 1530 Mwt relative to the 1976 analysis performed at 1448 Mwt. However, since the PCT's for the other smaller area breaks are controlled entirely by the SIT's and the HPSI pump flows, the low pressure SI pump data does not impact the results for these smaller area breaks.

This is because the 0.1 and 0.075 $ft^2$ breaks are characterized by a relatively slow depressurization rate and recession of the two-phase level in the core. The recession of the two-phase level and subsequent recovery is controlled by the boiloff rate due to decay heat and the rate at which the coolant is replenished by the HPSI pump flow. The transient is terminated shortly after recovery of the core two phase level with injection from the SIT's.

The 0.05 $ft^2$ break experiences behavior similar to that of the 0.1 and 0.075 $ft^2$ breaks. However, for these breaks, the recovery of the core two phase level and termination of the clad temperature transient is controlled entirely by the HPSI pump flow. It is estimated that break sizes less than 0.03 $ft^2$ will not experience core uncovery since the boiloff rate will be exceeded by the HPSI flow at a time when the two-phase level in the inner vessel is well above the top elevation of the core.

There are also logical reasons for the non-limiting nature or low peak clad temperatures for breaks between 0.5 and 0.1 $ft^2$. As the break size increases above 0.1 $ft^2$, the depressurization rates increase. The higher depressurization rates result in increased steam production during the blowdown due to increased flashing of the coolant which produces greater two phase level swell. Although the fluid inventory loss increases as the break size increases, the dominant phenomena is the increased level swell as a consequence of the higher depressurization rates. Thus, these higher depressurization rates minimize core uncovery for breaks greater than 0.1 $ft^2$ and smaller than 0.5 $ft^2$. For breaks in this range, the depressurization rates are also sufficient to actuate the safety injection tanks which quickly terminate the clad temperature transient and minimize the duration of the core uncovery period. The high pressure safety injection pumps therefore, do not play a significant role in affecting core uncovery for these breaks. However, as the break size approaches 0.5 $ft^2$, the inventory loss becomes the dominating phenomenon. Therefore, as the break size increases, the core two phase level transients are characterized by increasing core uncovery. This results in an increasing peak clad temperature characteristic as the break size approaches 0.5 $ft^2$.

14.15.2.3 Loss of Coolant Accident During Shutdown

At any time after the SIT's are isolated, the reactor coolant system pressure is 400 psia or less, and the total stress in any component will be less than the total stress at the design pressure. Therefore, the possibility of a LOCA during shutdown cooling becomes even more remote than while at power.

The pressurizer pressure low signal (PPLS) has been bypassed below 1600 psia, and the safety injection tanks will be valved out when the system temperature and pressure reach 400°F and 400 psia respectively during shutdown. Using a maximum cooling rate of 75°F/hr, the above conditions are reached in less than 2½ hours. Less than 1½ hours later, when the system temperature and pressure reach 300°F and 250 psia, the system is placed in the shutdown cooling mode. In this mode, the coolant temperature is reduced from 300°F to 140°F in about 24 hours.

This shutdown procedure will usually occur only once per year or at most, a few times per year. For each shutdown, a period of about 25 hours exist during which automatic initiation of the ECCS is not available, before refueling temperature is reached.

Bypassing of the PPLS does not bypass the containment pressure high signal (CPHS). The CPHS will still initiate safety injection and the automatic sequences involved. Furthermore, after the SIT's are isolated, the operator will still be alerted to a LOCA by a combination of the following alarms and/or indications:

1. Low pressurizer level alarm
2. Low reactor coolant system pressure
3. High containment pressure alarm
4. Containment activity alarm
5. Containment temperature
6. Containment sump level alarm
7. Shutdown cooling temperature
8. Component cooling water temperature to and from the containment air cooling and ventilating system
9. Low volume control tank level alarm

For large breaks within the reactor coolant system, all of the above alarms and indications will normally be present. As break size decreases, so will the number of indications and alarms. For the break size equal to or less than the capacity of one charging pump, the least number of indications and alarms that can be postulated to occur is three; namely, increases in: (1) containment activity, (2) temperature, and (3) temperature of the component cooling water to and from the containment atmosphere.

Upon receipt of the above indications and/or alarms, the operator should perform the following immediate actions:

1. Open HCV-2914, 2934, 2954 and 2974 S.I. tank valves.
2. If the containment pressure high signal is not present, the operator should initiate CPHS by the test switch TS-A/CPHS and/or TS-B/CPHS on panel AI-30A and B.
3. Verify that the high pressure safety injection pumps started.
4. Verify that the high pressure safety injection flow control valves open.
5. Stop the low pressure safety injection pumps and close the shutdown cooling suction isolation valves.
6. Verify that containment isolation actuation signal (CIAS) is initiated.
7. Verify that the containment air cooling and ventilating system starts.

Bypassing of the PPLS does not bypass the containment pressure high signal (CPHS). The CPHS will still initiate safety injection and the automatic sequences involved. Furthermore, after the SIT's are isolated, the operator will still be alerted to a LOCA by a combination of the following alarms and/or indications:

1. Low pressurizer level alarm
2. Low reactor coolant system pressure
3. High containment pressure alarm
4. Containment activity alarm
5. Containment temperature
6. Containment sump level alarm
7. Shutdown cooling temperature
8. Component cooling water temperature to and from the containment air cooling and ventilating system
9. Low volume control tank level alarm

For large breaks within the reactor coolant system, all of the above alarms and indications will normally be present. As break size decreases, so will the number of indications and alarms. For the break size equal to or less than the capacity of one charging pump, the least number of indications and alarms that can be postulated to occur is three; namely, increases in: (1) containment activity, (2) temperature, and (3) temperature of the component cooling water to and from the containment atmosphere.

Upon receipt of the above indications and/or alarms, the operator should perform the following immediate actions:

1. Open HCV-2914, 2934, 2954 and 2974 S.I. tank valves.
2. If the containment pressure high signal is not present, the operator should initiate CPHS by the test switch TS-A/CPHS and/or TS-B/CPHS on panel AI-30A and B.
3. Verify that the high pressure safety injection pumps started.
4. Verify that the high pressure safety injection flow control valves open.
5. Stop the low pressure safety injection pumps and close the shutdown cooling suction isolation valves.
6. Verify that containment isolation actuation signal (CIAS) is initiated.
7. Verify that the containment air cooling and ventilating system starts.
8. Verify that the emergency diesels start.

9. Secure reactor coolant pumps.

All of these actions may be initiated from the control room.

Steps 1, 2 and 3, will insure core cooling regardless of break size. For a large break, rapid depressurization will result in S.I. tank discharge while for a small break, the HPSI pump will serve to immediately feed water into the system.

The containment air cooling and ventilating system can be used to reduce the high containment building pressure and to remove decay heat from the building if it becomes necessary to stop shutdown cooling. The capacity of the containment air cooling and ventilating system will be in excess of that required since the energy release will be far less than for a LOCA at full power; thus, no spray system backup should be required. Diesels will also be started to provide a standby source of power if outside power is lost during the accident.

14.15.2.4 Steam Generator Tube Failures in Conjunction with a Double-ended Cold Leg Guillotine Break

An analysis was undertaken to determine how many steam generator tubes must fail, in conjunction with rupture of a reactor coolant system cold leg pipe, to cause steam binding sufficient to prevent emergency cooling water from rising above the midplane of the core.

The analysis showed there is no limit to the number of steam generator tubes that can rupture concurrent with a 24-inch double-ended cold leg break which will prevent water from rising to the core midplane. This is because the leaking steam generator will eventually discharge its contents to the primary system which will then blow down to the containment reducing the reactor coolant pressure to an acceptable value for refill. The nature of the refill inside the core barrel will depend upon the time at which the core pressure drops below that of the containment plus the static head of water in the downcomer annulus. Should the above condition exist shortly (about 1 minute) after the reactor coolant pressure drops to about 200 psig, then the safety injection tanks will contribute to the refill. However, should the primary system blowdown take longer, then the refill of the barrel will be based on flow from the high and low pressure safety injection pumps.

14.15.2.5 Break Size Consistent With Charging Pump Capacity

Consideration has been given to the maximum reactor coolant system break size for which the charging pumps will make up the flow loss to the containment; so that a normal shutdown may occur.

As described in Section 9.2, there are three 40 gpm charging pumps. The number of charging pumps in operation and the corresponding maximum break area for which the charging pumps will make up the flow loss are given in Table 14.15-16. The discharge rate was determined from the orifice flow equation with a value of unity employed for the discharge coefficient.

TABLE 14.15-16

MAXIMUM BREAK AREA CONSISTENT WITH CHARGING PUMP CAPACITY

| No. of Pumps | Area (ft$^2$) | Equivalent Circular Diameter (in.) |
|---|---|---|
| 1 (40 gpm) | $1.37 \times 10^{-4}$ | 0.160 |
| 2 (80 gpm) | $2.75 \times 10^{-4}$ | 0.224 |
| 3 (120 gpm) | $4.12 \times 10^{-4}$ | 0.276 |

14.15.2.6 Core and Internals Integrity Analyses

The consequences of a LOCA on the reactor internal structures have been analyzed for reactor coolant system pipe breaks up to a double-ended rupture of a 32-inch pipe. Following a pipe rupture, two types of loading occur sequentially. The first is an impulse load of 15 to 30 milliseconds duration caused by rapid system depressurization from initial subcooled conditions to saturated conditions. This initial blowdown phase is followed by a two-phase fluid blowdown which persists for time periods varying up to several seconds, depending on the size of the postulated rupture.

In the early portion of the blowdown, acoustic waves propagate through the reactor coolant system. The WHAM code[22] is used to calculate the pressure variations in the system following pipe rupture. WHAM calculates the impulse pressure loadings which the system is subjected to during passage of the pressure waves through the system.

For the saturated portion of the blowdown, the loadings on the reactor internals are associated with the fluid drag forces imposed by the high velocity two-phase fluid in its flow to the break location. The short term impulse forces are generally greater than the long term drag forces, except for the loads on some of the CEA shrouds in the case of a pipe rupture near the pressure vessel outlet nozzle.

The results of the blowdown force analyses for the reactor core support system are presented in Table 14.15-17, for a 32-inch hot leg break and for a 24-inch cold leg break, both for full power and zero power initial conditions.

## TABLE 14.15-17

## MAXIMUM PRESSURE DIFFERENCE ACROSS CORE AND CORE SUPPORT STRUCTURE

| | Pressure Difference, psi | |
|---|---|---|
| | 32 in. Outlet Pipe Break | 24 in. Inlet Pipe Break |
| Zero Power | | |
| Lower Structure | 54 | 40 |
| Reactor Core | 163 | 154 |
| Upper Guide Structure | 91 | 35 |
| Full Power | | |
| Lower Structure | 29 | 30 |
| Reactor Core | 95 | 151 |
| Upper Guide Structure | 52 | 45 |

The maximum calculated stresses and deflections during blowdown for critical reactor components are tabulated in Table 14.15-18. The table also lists the corresponding allowable values of stress, pressure, or deformation based on the design criteria specified in Section 3.2 along with the estimated values of stress, pressure, or deformation at which failure would occur. It is emphasized that the shutdown mechanism for large breaks is voiding of the core. It is not necessary for the CEA's to insert (see Section 1.5.5).

During an inlet pipe break, the core support barrel is subjected to time dependent axial loads and axially varying radial pressure differentials. Axial stresses in the core support barrel and shear and bending stresses in the lower support structure were evaluated using conservative stress analysis methods. The peak of the axial pressure pulse, calculated from WHAM, was applied as a steady loading. The SEAL-SHELL computer program was used to assure that stresses and deformation are within design limits when the barrel is subjected to the peak of the time-dependent axially varying, radial pressure distribution.

During an outlet break, the core support barrel is subjected to a time dependent upward force and external radial pressure. Loads on the upper guide structure were evaluated by calculating the acceleration of the core under the time varying axial pressure (during the subcooled portion of the LOCA) and equating the kinetic energy of the core to the strain energy of the upper guide structure and core after impact. The strain energy is then related to stresses in the system. Bending stresses in the upper guide structure were evaluated during two-phase flow by using peak values for the axially varying pressure forces during this regime. The upper guide structure, modeled as a system of continuous and discrete elements, was subjected to a pressure time history, and axial stresses were evaluated.

The analyses which have been performed indicate that design limits are not exceeded even when dynamic effects are taken into account.

TABLE 14.15-18

MAXIMUM STRESSES, PRESSURES, AND DEFLECTIONS FOR CRITICAL INTERNALS COMPONENTS RESULTING FROM A COMBINED MAJOR LOSS-OF-COOLANT INCIDENT AND MAXIMUM HYPOTHETICAL EARTHQUAKE

| Structural Component | Failure Mode and Loading Condition | Limiting Component | Failure[(1)] Condition | Allowable[(2)] Condition | Calculated Condition |
|---|---|---|---|---|---|
| Core Support Barrel | Axial tensions under axial, lateral and internal pressure & axial & lateral seismic | Girth Weld between upper & middle cylinder | 54,000 psi | 29,300 psi | 12,166 psi |
| | Buckling - external pressure | Buckling of upper cylinder | $\Delta_p$ = 805 psi | $\Delta_p$ = 537 psi | $\Delta_p$ = 362 psi |
| Lower Core Support Beam | Bending - axial pressure & seismic | Beam flange | 54,000 psi | 43,950 psi | 15,158 psi |
| | Shear - axial pressure & seismic | Junction of flange & web | 32,400 psi | 17,580 psi | 5,335 psi |
| Lower Core Support Column | Bending - axial pressure & seismic | Junction of column and support beam | 54,000 psi | 41,620 psi | 26,988 psi |
| UGS Support Beams | Bending - core impact & seismic | Center of Beam | 54,000 psi | 43,620 psi | 11,637 psi |
| UGS Flange | Bending - core impact & seismic | Junction of flange & cylinder | 54,000 psi | 43,950 psi | 18,133 psi |
| CEA Shrouds Single | Bending - core impact & seismic & lateral pressure | Center of shroud | 54,000 psi<br>Defl.>0.75 in | 43,800 psi<br>Defl.=0.50 in | 19,144 psi<br>Defl.=.315 in |
| CEA Shrouds Dual | Bending - core impact & seismic & lateral pressure | Center of shroud | 54,000 psi<br>Defl.>0.75 in | 43,305 psi<br>Defl.=0.50 in | 30,665 psi<br>Defl.=.204 in |

(1) The figures in this column represent the assumed ultimate stress for tension and bending type of failures, 60 percent of the ultimate stress for shear type of failure, the theoretical buckling stress and estimated deflection limits at which the component will no longer perform its function.

(2) The figures in this column represent the allowable stress, pressure, or deflection limits in accordance with the design basis established in Section 3.

14.15.2.7 Reactor Vessel Thermal Shock

The effect of operation of the emergency core cooling system on the reactor vessel following a loss-of-coolant has been discussed in CE report A-68-9-1, "Thermal Shock Analysis on Reactor Vessel Due to Emergency Core Cooling System Operation", by W. H. Tuppeny, et al, March 15, 1968. This was submitted as Amendment 9 to the Maine Yankee License Application (AEC Docket No. 50-309). Additional information for this condition appears in CE report A-68-10-2, "Experimental Determination of Limiting Heat Transfer Coefficients During the Quenching of Thick Steel Plates in Water", by J. H. Simon, M. W. Davis and W. H. Tuppeny, December 13, 1968. This report was placed in the public record in January, 1969. This work is discussed in Section 1.5.4.

14.15.2.8 Hydrogen Accumulation in Containment

Hydrogen accumulation in the containment is discussed in Section 14.17. The hydrogen produced by radiolysis is released to the containment building where it mixes with the steam-air atmosphere. In addition to the radiolytic hydrogen, the hydrogen produced by reaction of steam with the zircaloy cladding is considered.

To control hydrogen concentration, a purge of the containment building wo[illegible]nstituted when 3 percent (volume) hydrogen is reached. This value is below the flammability limit.

14.15.2.9 Reactor Operator Action

An analysis has been performed to determine what actions the reactor operator would have to perform or may have to perform in the unlikely event of a design basis LOCA. Consideration was also given as to the allowable time periods within which the action would or might have to be performed.

In this analysis it was assumed that all engineered safeguards and support systems functioned to fulfill the design objectives of each system. Certain additional actions may have to be performed in the unlikely event of a malfunction of portion(s) of certain system(s); however, this analysis was perfomed to specifically identify reactor operator actions that will or may be required in the event of a loss-of-coolant accident.

This analysis began by assuming a double-ended rupture of a 32-inch reactor coolant system pipe. This is followed by the response of the systems in the order and manner in which the various components of the systems are expected to function.

The results of this analysis indicate that, in the event of a LOCA with the engineered safeguards and support systems functioning to fulfill design objectives, no control actions are required by the reactor operator for several hours following the accident.

The actions which the emergency operating procedures require the operator to perform include:

a. Observations of actions automatically initiated by the engineered safeguards and support systems.

b. Observations of actions initiated by the reactor protective system.

c. Observations and acknowledgement of plant annunciator systems.

d. Observation of engineered safeguards supervisory system.

e. Observation of plant parameters such as flows, temperatures, pressure, etc.

f. Trip all reactor coolant pumps.

g. Obtain a reactor coolant system sample for boric acid concentration analysis as soon as radiation levels permit, then once per hour until reactor coolant system boron concentration has stabilized. Thereafter, samples are obtained at least once per shift.

h. Verify that the desired degree of subcooling is achieved.

i. Maintain balanced flows to the reactor coolant system loops from the safety injection and recirculation systems.

j. Monitor safeguards pump rooms sump water level for excessive leakage.

k. If the containment building air cooling and filtering system charcoal filters temperature exceeds 500°F, the operator will immediately initiate flow to the filter dousing system.

l. Actuate the Radiological Emergency Response Plan.

m. After containment air temperature approaches normal, the operator resets the charcoal filter temperature alarm points to 250°F.

The actions that may be performed by the operator include:

a. After sequential starting of the raw water and component cooling water pumps by SIAS, the operator may select two component cooling water pumps and two raw water pumps and then shut down the third component cooling water pump and the other two raw water pumps.

b. The operator may close the cooling water valves on any inoperable containment building air cooling and recirculation unit.

c. The operator may divert part of the shutdown cooling heat exchanger discharge flow to the suction of the high pressure safety injection pumps.

d. The operator may regulate component cooling water flow to the shutdown cooling heat exchangers for containment building spray temperature control.

e. The operator may restart the LPSI pumps following receipt of RAS.

The above five items are actions the operator may perform; however, these actions are not critical, and the time in which they are performed would not significantly affect the performance of the associated systems.

### 14.15.2.10 Long Term Cooling Considerations

General

An evaluation of the post-LOCA Long Term Cooling ECCS performance of Fort Calhoun Station has demonstrated conformance with criterion (5) of 10 CFR Part 50.46(b). Procedures have been defined for utilizing the ECCS to remove decay heat and thereby maintain core temperatures at acceptably low values for an indefinite period of time.

Long term cooling is initiated when the core is reflooded after a LOCA and is continued until the plant is secured. The objective of long term cooling is to maintain the core temperature at an acceptably low value while removing decay heat for the extended period of time required by the long-lived radioactivity remaining in the core. In satisfying this objective, the post-LOCA long term cooling procedures make provision for maintaining core cooling and boric acid flushing by simultaneous hot and cold leg injection for the large break LOCA, or for initiating cooldown of the reactor coolant system (RCS) if the break is sufficiently small that the success of such operation is assured. Knowledge of RCS pressure gives the plant operator a proper indication of the break size.

For the small break LOCA, cooldown of the reactor coolant system (RCS) and long term decay heat removal is provided by actuation of the pressurizer power operated relief valves (PORV's) to release steam from the RCS. This action depressurizes and maintains the RCS pressure below the HPSI pump shutoff head, allowing the HPSI pumps to flush the core and accelerate refilling of the RCS.

For the large break LOCA, the HPSI flow is injected simultaneously into the hot and cold legs. This injection mode provides cooling for the RCS and prevents boric acid accumulation in the vessel following the large break LOCA.

About three hours after the LOCA, the operator determines, based on RCS pressure, whether the small break LOCA or the large break LOCA procedures are to be implemented. If the RCS pressure is above 700 psia, then the small break procedure is appropriate and the PORV's are opened. If the RCS pressure is below 700 psia, then the large break procedure applies. The HPSI pump discharge lines are realigned so that the total injection flow is split equally between the hot and cold legs. The hot side injection is achieved by injection in the RCS through the pressurizer auxiliary spray system. Both procedures provide sufficient injection flow to both cool the core and flush the reactor vessel for an indefinite period of time.

The performance analysis of long term cooling utilized the codes and methods decribed in CENPD-254.[24] However, the procedures used for long-term cooling at Fort Calhoun differ somewhat from those described in CENPD-254. In the analysis, appropriate modifications were made to these methods and models to take into account such differences.

Small Break Procedure and Results

According to the small break LOCA procedures, cooldown of the RCS is initiated by activating the PORV's if the RCS pressure is above 700 psia. Opening of the PORV's results in cooling and reducing the RCS pressure sufficiently such that the HPSI pump refills and subcools the RCS. The refilling and subcooling of the RCS results in maintaining the boric acid concentration in the vessel well below the precipitation limit by dispersing the boron through the RCS by natural circulation.

The results of the analysis demonstrate that, for break sizes of .02 $ft^2$ or smaller, the RCS will refill and subsequently achieve a subcooled condition. The boric acid concentration in the vessel is also maintained well below the precipitation limit of 75 wt% prior to refill. In fact, the boric acid concentration is also well below the precipitation limit of 32 wt% at the minimum temperature of 228°F applicable for large breaks (saturation temperature of 20 psia).

Large Break Procedure and Results

Under the large break LOCA procedures, the boric acid accumulation is reduced by the core flushing flow which is provided by the simultaneous hot side and cold side injection from an HPSI pump. The simultaneous hot side and cold side injection mode is initiated at three hours post-LOCA if the RCS pressure is below 700 psia. Initiation of simultaneous hot and cold side HPSI flow at three hours results in a substantial and time increasing core flushing flow.

The large break long term cooling procedure applies to those break sizes for which simultaneous hot and cold side injection can both flush and cool the core. A break size of .005 $ft^2$ is the smallest for which the large break procedure applies since that is the smallest break size for which the depressurization maintains the RCS pressure sufficiently low to allow the HPSI pump to flush and cool the RCS. The small break procedure is applicable for breaks as large as 0.2 $ft^2$, and since the large break procedure is applicable for breaks as small as .005 $ft^2$, a large range of overlapping break sizes may be adequately cooled by either procedure.

The above description considered only the condition wherein offsite power is unavailable. With offsite power available, it is possible to more quickly cooldown the RCS using the turbine bypass system and thereby initiate operation of the shutdown cooling system. However, opening of the PORV's and HPSI flow is sufficient to maintain decay heat removal for an indefinite period of time such that it is not necessary to initiate operation of the shutdown cooling system to assure continued heat removal.

14.15.3 Results

The results of an analysis of a LOCA indicate that both the analysis models and the calculated performance of the ECCS are in conformance with the criteria specified in 10CFR Part 50.46; namely:

1. The calculated peak fuel rod clad temperature does not exceed the 2200°F limit.

2. The amount of fuel rod zircaloy cladding that reacts chemically with water or steam does not exceed 1% of the total amount of zircaloy in the reactor.

3. The cladding temperature transient is terminated at a time when the core geometry is still amenable to cooling. The hot fuel rod cladding oxidation limits of 17% are not exceeded during or after quenching.

4. The system long term cooling capabilities maintain acceptably low core temperatures and remove decay heat for the extended period of time required.

The Acceptance Criteria are satisfied for operation of the Fort Calhoun reactor at power levels up to 1500 MW(t) and maximum LHGR's of up to 15.22 kw/ft and within the axial profile limits given in Figure 14.15-4A. Operation within the allowed maximum LHGR limit and allowed axial offset limits will preclude total peaking factors located above the 70% of core height level from reaching the limits shown in Figure 14.15-4A.

In addition, the core and internals integrity analysis indicates that the core support structure is sufficient to hold the core in place during a loss-of-coolant accident, and vessel internals would not interfere with adequate cooling of the core.

### 14.15.4 Radiological Consequences of a LOCA

The ECCS, following a design basis LOCA (double-ended break), limits the clad temperature to well below the melting point and ensures that the reactor core remains intact and in a coolable geometry, minimizing the release of fission products to the environ. However, in order to demonstrate that the Fort Calhoun Station does not represent any undue radiological hazard to the public, the off-site doses from a postulated LOCA have been calculated based on the following assumptions:

1. The reactor core equilibrium noble gas and iodine inventories are based on long-term operation at a power level of 1500 Mwt.

2. 100 percent of the core noble gas inventory and 25 percent of the core iodine inventory are immediately available for release from the containment.

3. Of the iodine fission product inventory released to the containment, 91% is in the form of elemental iodine, 5% is in the form of particulate iodine, and 4% is in the form of organic iodine.

4. No credit is taken for spray removal of halogens even though the redundant spray systems should be effective in removing the elemental and particulate halogens.

5. The containment leak rate is 0.2 percent of the free volume for the first 24 hours, and at 50% of this leakage rate for the remaining duration of the accident.

6. The Containment Air Recirculating, Cooling and Iodine Removal System filter removal constant for halogens is 5.14 per hour based on a filtration system flow rate of 100,000 scfm (only 50 percent of the installed capacity assumed available) with removal efficiency of 90% and a containment net free volume of 1.05 E+06 ft$^3$.

7. Containment purge system is started when the hydrogen concentration in the containment reaches three (3) volume percent (NOTE: THE RADIOLOGICAL CONSEQUENCES OF HYDROGEN PURGE SYSTEM ARE FULLY DISCUSSED IN SECTION 14.17 OF THE FSAR).

8. The dispersion factor for the EAB is 4.4 E-04 sec/m$^3$, and the dispersion factor for LPZ outer boundary is conservatively assumed (based on a dispersion factor for 0 - 8 hour) as 1.57 E-05 sec/m$^3$.

Based on these assumptions, the resulting off-site doses* are as follows:

| | Thyroid (Rems) | Whole Body (Rems) |
|---|---|---|
| EAB | 8.68 E+01 | 2.45 E+00 |
| LPZ | 1.61 E+01 | 6.39 E-01 |

*The off-site doses due to the post-LOCA operation of the containment hydrogen purge system are presented in Section 14.17 of the FSAR.

14.15.4.1 Post-LOCA Doses to Control Room Personnel

In the event of a LOCA, the SIAS initiates instantaneous closure of the control room isolation dampers. The emergency air makeup system is then brought into operation such that all outside air entering the control room passes through the control room filtration system. Filtered makeup air will be used along with the control room recirculation system for the duration of the accident. The doses to the control room personnel are calculated based on the following assumptions:

1. The control room filtration system operates at 820 scfm with an iodine removal efficiency of 90 percent.

2. The recirculation system flow rate is 13,150 scfm.

3. The control room net free volume is 45,100 ft$^3$.

4. The dispersion data for the control room ventilation intake is as follows:

| | |
|---|---|
| 0 - 8 hours | 5.61 E-02 sec/m$^3$ |
| 8 - 24 hours | 3.29 E-02 sec/m$^3$ |
| 1 - 4 days | 1.26 E-02 sec/m$^3$ |
| 4 - 30 days | 3.74 E-03 sec/m$^3$ |

5. Other assumptions as listed above under Section 14.15.4.

Based on these assumptions, the doses to the control room personnel for the duration of the accident are:

| | |
|---|---|
| Thyroid | 56.0 Rems |
| Whole Body | 3.2 Rems |

14.15.5 Conclusions

The LOCA analysis demonstrates that the ECCS provides adequate core cooling, by keeping the core in a coolable geometry, over the entire spectrum of breaks, including a double-ended hot leg guillotine.

The results of radiological consequences show that the thyroid and whole body doses, using the conservative assumptions, are well within the limits of 10CFR Part 100.

14.15.6 SECTION 14.15 REFERENCES


1. Omaha Public Power District submittal, Letter from T. E. Short to George E. Lear, NRC, dated December 12, 1976.

2. Exxon Nuclear Company, "Fort Calhoun LOCA Analyses at 1500 MWT Using ENC WREM-IIA PWR ECCS Evaulation Model - Large Break Example Problem", XN-NF-79-45, May 1979.

3. Exxon Nuclear Company, "Exxon Nuclear Company WREM-Based Generic PWR ECCS Evaluation Model Update ENC WREM-IIA", XN-NF-78-30.

4. Exxon Nuclear Company, "Exxon Nuclear Company WREM-Based Generic PWR ECCS Evaluation Model", XN-75-41:

   a. Volume I, July 1975
   b. Volume II, August 1975
   c. Volume III, Revision 2, August 1975
   d. Supplement 1, August 1975
   e. Supplement 2, August 1975
   f. Supplement 3, August 1975
   g. Supplement 4, August 1975
   h. Supplement 5, Revision 5, October 1975
   i. Supplement 6, October 1975
   j. Supplement 7, November 1975

5. Exxon Nuclear Company, "Revised Nucleate Boiling Lockout for ENC WREM-Based ECCS Evaluation Models", XN-76-44, September, 1976.

6. Exxon Nuclear Company, "Exxon Nuclear Company WREM-Based Generic PWR ECCS Evaluation Model (ENC-WREM-II) - 4-Loop PWR With Ice Condenser, Large Break Example Problem", XN-76-36, August, 1976.

7. Exxon Nuclear Company, "Big Rock Point Example LOCA Analysis Using the Exxon Nuclear Company Non-Jet Pump BWR Evaluation Model - Large Break Example Problem", NX-NF-78-25, Revision 1, September 1978.

8. Exxon Nuclear Company, "Exxon Nuclear Company WREM-Based Generic PWR ECCS Evaluation Model Update ENC WREM-II", XN-76-27.

9. U. S. Nuclear Regulatory Commission, "Minimum Containment Pressure Model for PWR ECCS Performance Evaluation", Branch Technical Position CSB 601

10. Exxon Nuclear Company, "Exposure Sensitivity Study for ENC XN-1 Reload Fuel at Prairie Island Unit 1 Using the ENC-WREM-IIA PWR Evaluation Model", XN-NF-79-18, March 1979.

11. CENPD-137, Calculative Methods for the C-E Small Break LOCA Evaluation Model", August 1974 (Proprietary).

12. CENPD-137, Calculative Methods for the C-E Small Break LOCA Evaluation Model", Supplement 1, January 1977 (Proprietary).

13. CENPD-133, Supplement 1, "CEFLASH-4AS, A Computer Program for Reactor Blowdown Analysis of the Small Break Loss-of-Coolant Accident", August 1974 (Proprietary).

CENPD-133, Supplement 3, "CEFLASH-4AS, A Computer Program for Reactor Blowdown Analysis of the Small Break Loss-of-Coolant Accident", January 1977 (Proprietary).

14. CENPD-135, "COMPERC-II, A Program for Emergency Refill-Reflood of the Core", April 1974 (Proprietary).

15. CENPD-135, "STRIKIN-II, A Cylindrical Geometry Fuel Rod Heat Transfer Program", April 1974 (Proprietary).

CENPD-135, Supplement 2-P, "STRIKIN-II, A Cylindrical Geometry Fuel Rod Heat Transfer Program", (Modification), February 1975 (Proprietary).

CENPD-135, Supplement 4-P, "STRIKIN-II, A Cylindrical Geometry Fuel Rod Heat Transfer Program", August 1976 (Proprietary).

CENPD-135, Supplement 5-P, "STRIKIN-II, A Cylindrical Geometry Fuel Rod Heat Transfer Program", April 1977 (Proprietary).

16. CENPD-138, "PARCH, A FORTRAN-IV Digital Program to Evaluate Pool Boiling, Axial Rod and Coolant Heatup", August 1974 (Proprietary).

CENPD-138, Supplement 1, "PARCH, A FORTRAN-IV Digital Program to Evaluate Pool Boiling, Axial Rod and Coolant", (Modification) February 1975 (Proprietary).

CENPD-138, Supplement 2, "PARCH, A FORTRAN-IV Digital Program to Evaluate Pool Boiling, Axial Rod and Coolant Heatup", (Modification) January 1977 (Proprietary).

17. Exxon Nuclear Company, "Fort Calhoun LOCA Analysis at 1500 Mwt Using ENC WREM-IIA PWR ECCS Evaluation Model", XN-NF-79-89, September 1979.

18. D. A. Powers and R. O. Meyer, "Cladding Swelling and Rupture Models for LOCA Analysis", Draft NUREG-0630, November 8, 1979.

19. Exxon Nuclear Company, "Revised Limiting Large Break LOCA Analysis for Fort Calhoun Using the ENC WREM-IIA PWR ECCS Evaluation Model", XN-NF-79-89, Supplement 1, January 1980.

20. Exxon Nuclear Company, "Fort Calhoun Cycle 8 Large Break LOCA Analysis Using the EXEM/PWR ECCS Model, XN-NF-82-102, December 1982.

21. Exxon Nuclear Company, "ENC Evaluation Model EXEM/PWR ECCS Model Updates", XN-NF-82-20(P), Revisions 1, August, 1982.

22. Fabric and Stanislav, "Early Blowdown Waterhammer Analysis for Loss of Fluid, Test Facility", 65-28-4, AEC Control No. AT-(10-1)-1165, June 1965, Revised April 1967.

23. CENPD-254, "Post-LOCA Long Term Cooling Evaluation Model", June 1977.

24. Letter from W. C. Jones, OPPD, to R. Reid, USNRC, dated December 4, 1979.

25. CENPD-139, "CE Fuel Evaluation Model Typical Report", July 1974 (Proprietary).

26. Omaha Public Power District Cycle 4 Reload Submittal, Letter from T. E. Short to H. Voigt (LeBoeuf, Lamb, Leiby & MacRae), dated August 5, 1977.

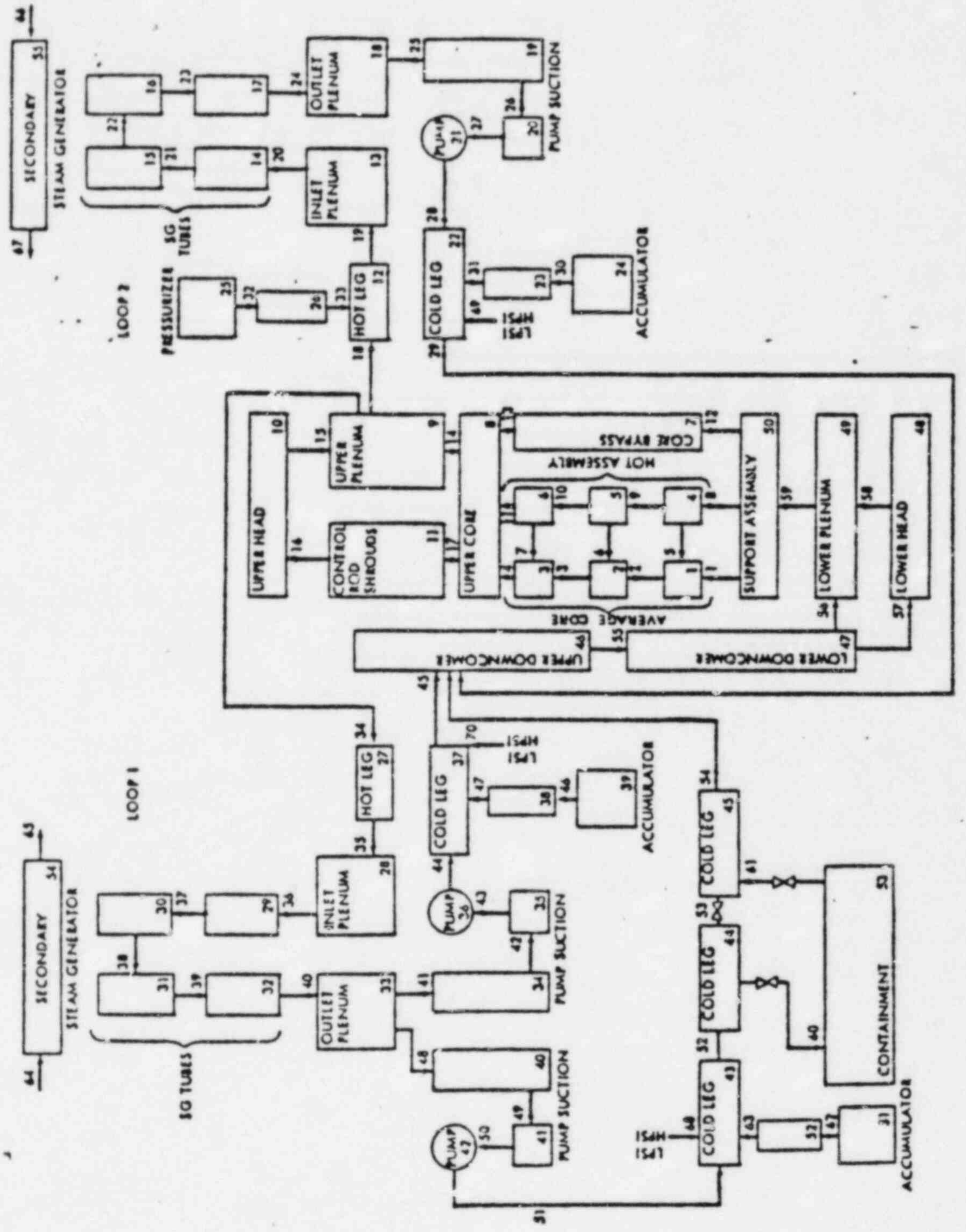


| Omaha Public Power District<br>Fort Calhoun Station<br>Unit No. 1 | System Nodalization for Large Break Blowdown LOCA Model for Fort Calhoun | FIGURE<br>14.15-1 |
|---|---|---|

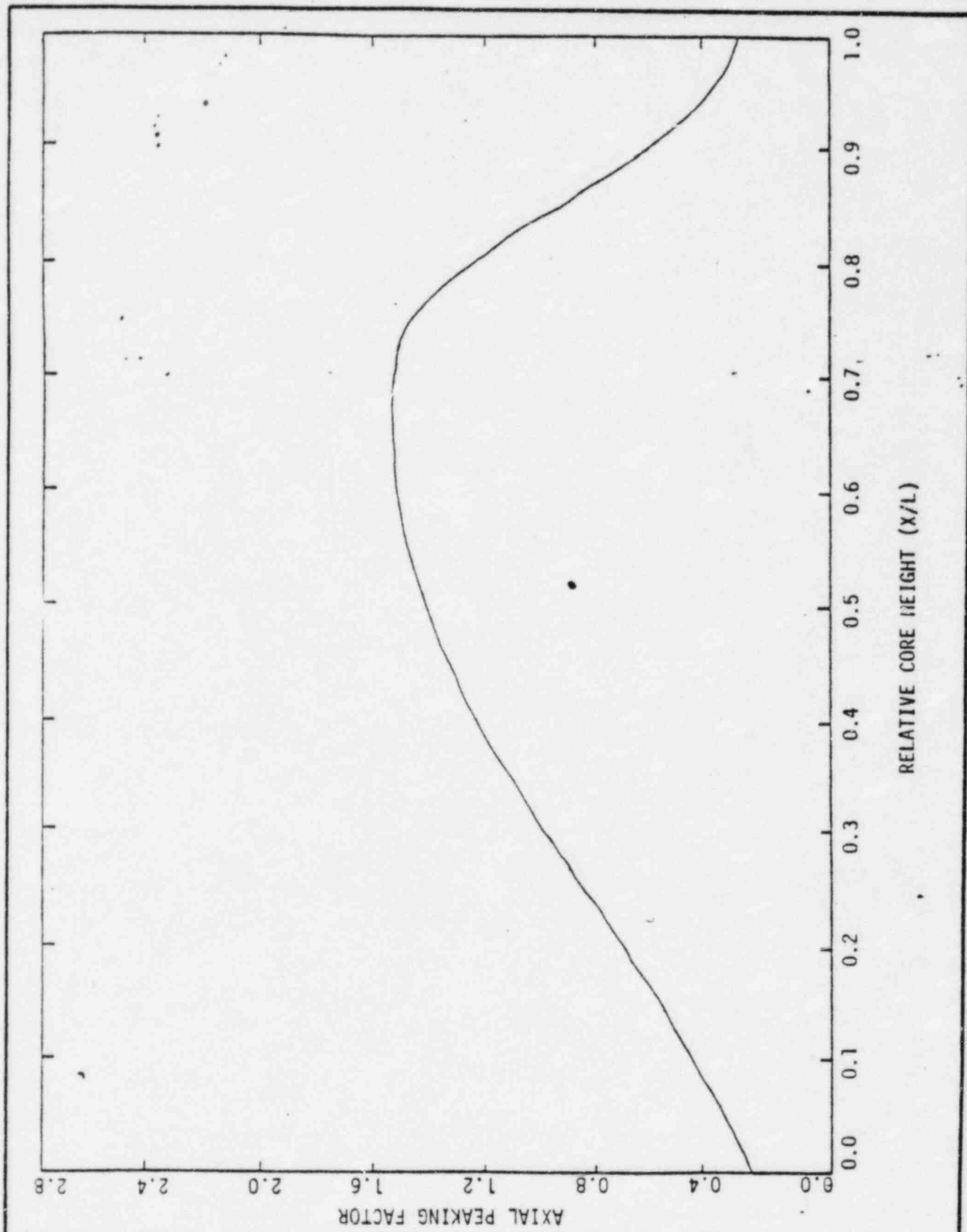


| | | |
|---|---|---|
| **Omaha Public Power District**<br>**Fort Calhoun Station**<br>**Unit No. 1** | AXIAL POWER PROFILE W/PEAK at<br>X/L = 0.7 FOR<br>ECCS ANALYSIS | Figure<br>14.15-2 |

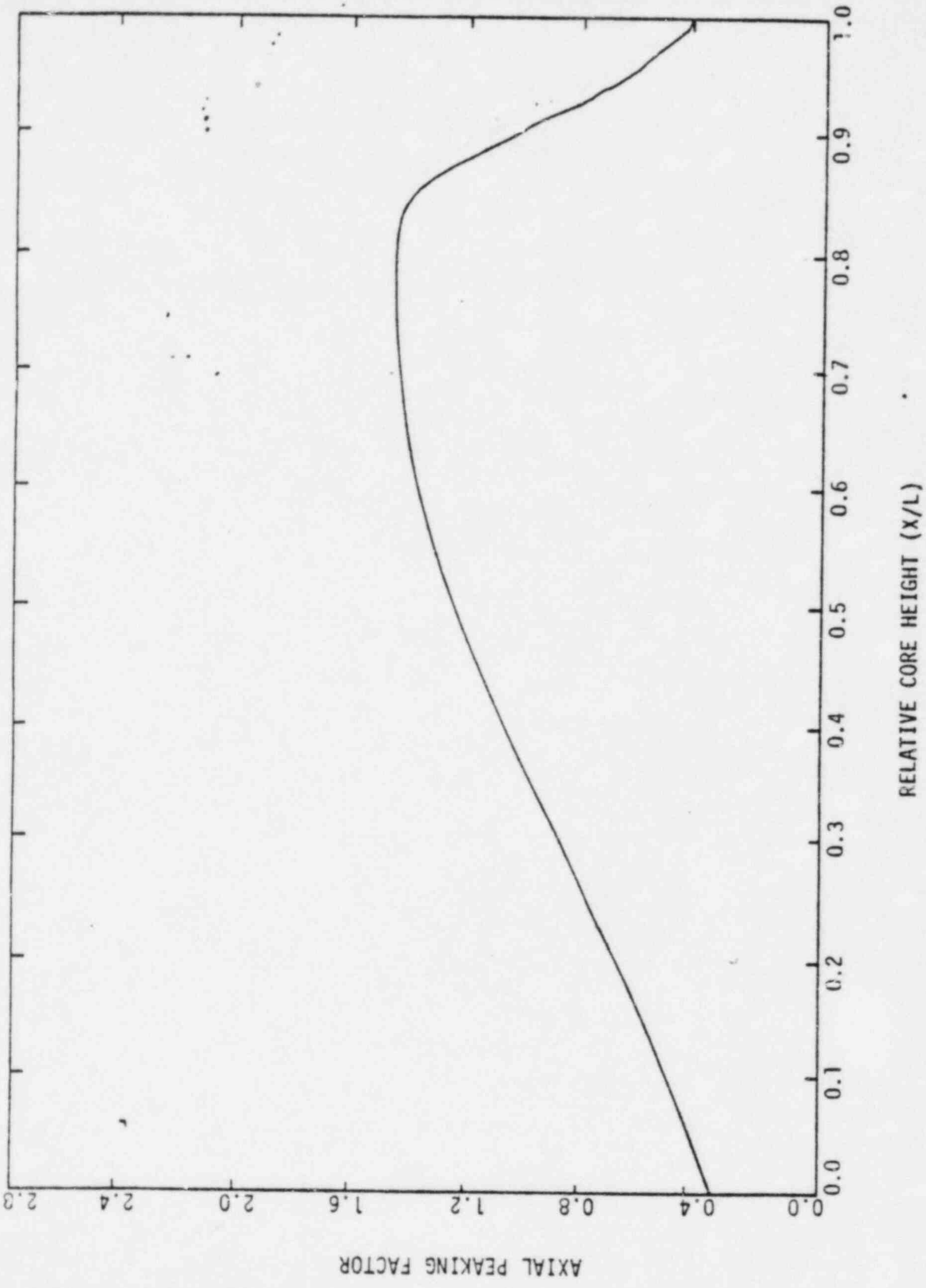


| | | |
|---|---|---|
| Omaha Public Power District<br>Fort Calhoun Station<br>Unit No. 1 | AXIAL POWER PROFILE W/PEAK<br>AT X/L = 0.8 for ECCS ANALYSIS | Figure<br>14.15-3 |

Omaha Public Power District
Fort Calhoun Station
Unit No. 1

AXIAL POWER PROFILE WITH PEAK AT X/L = 0.9 FOR FORT CALHOUN ECCS ANALYSIS

Figure 14.15-4

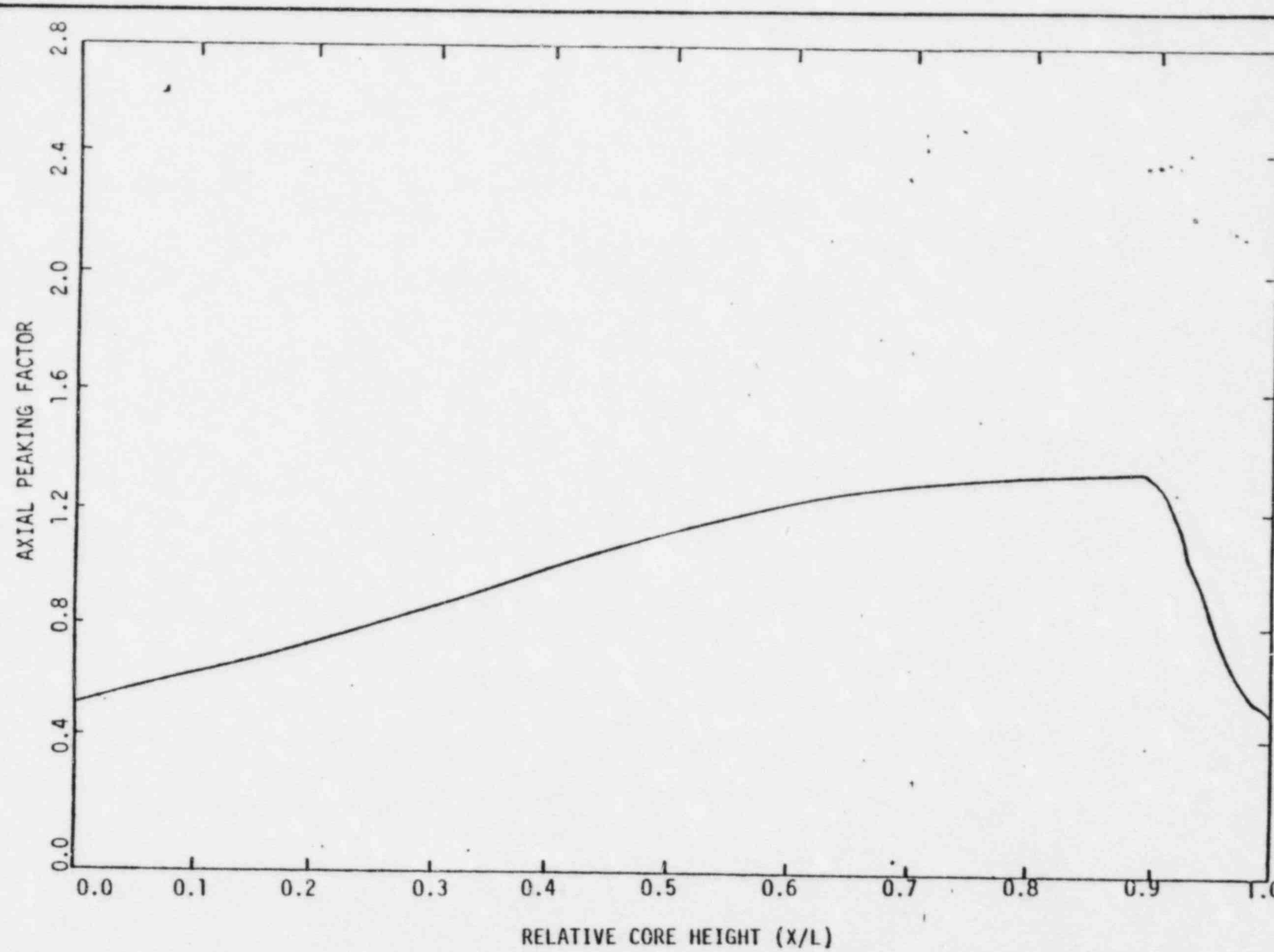

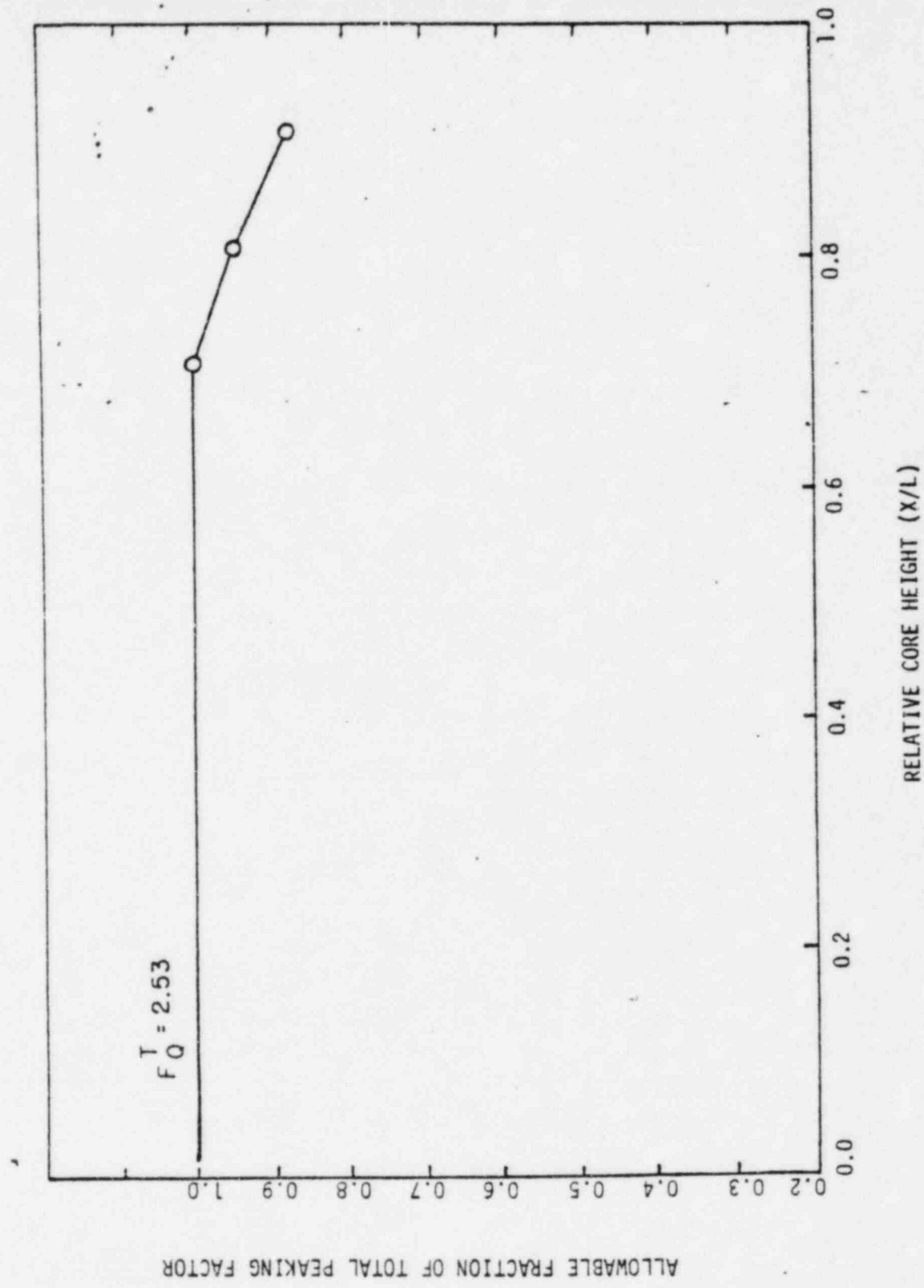


| | | |
|---|---|---|
| Omaha Public Power District<br>Fort Calhoun Station<br>Unit No. 1 | LIMITS ON TOTAL PEAKING VERSUS AXIAL POWER PEAK LOCATION | Figure 14.15-4A |

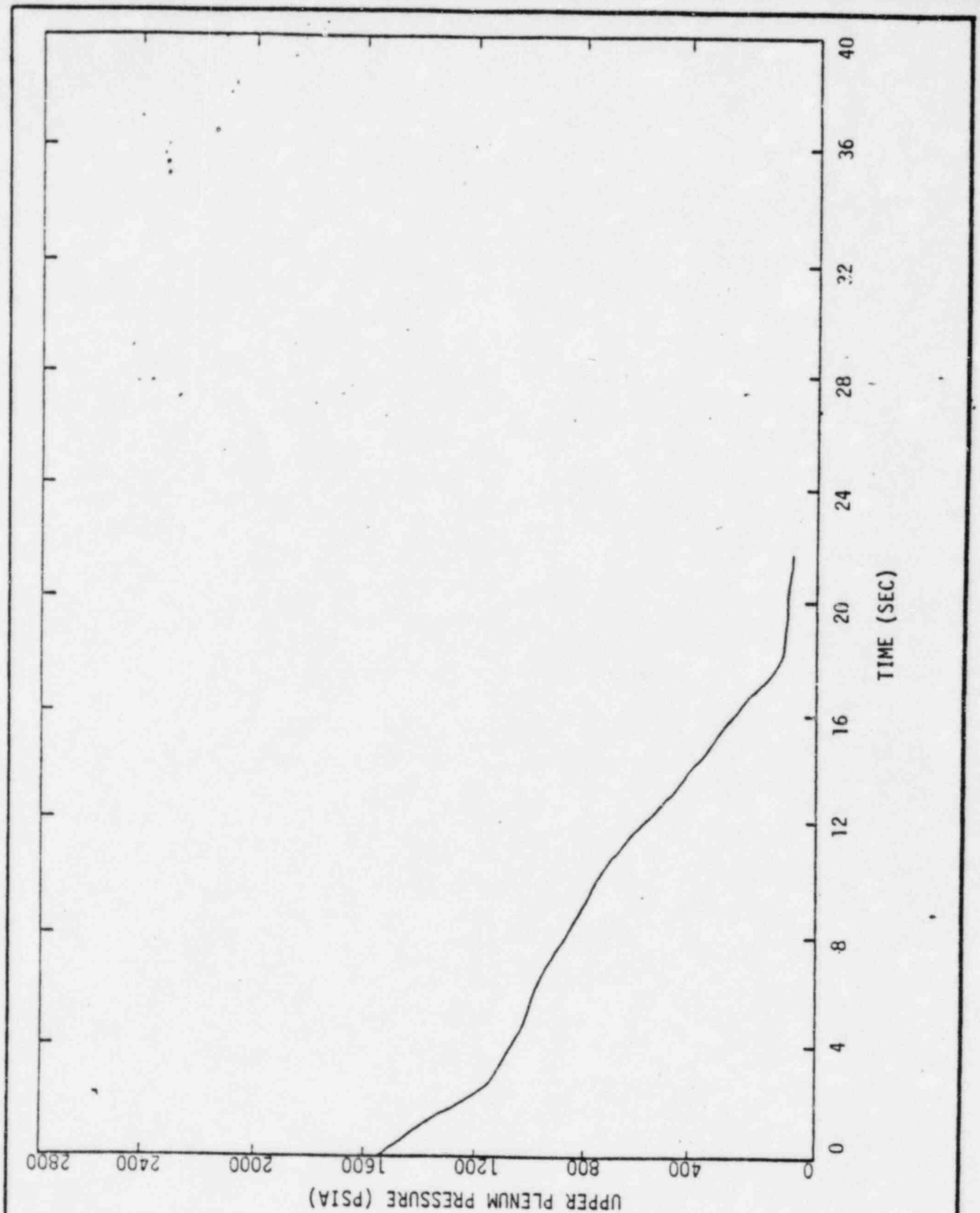


| | | |
|---|---|---|
| Omaha Public Power District<br>Fort Calhoun Station<br>Unit No. 1 | BLOWDOWN SYSTEM PRESSURE<br>1.0 DECLG BREAK | Figure<br>14.15-5 |

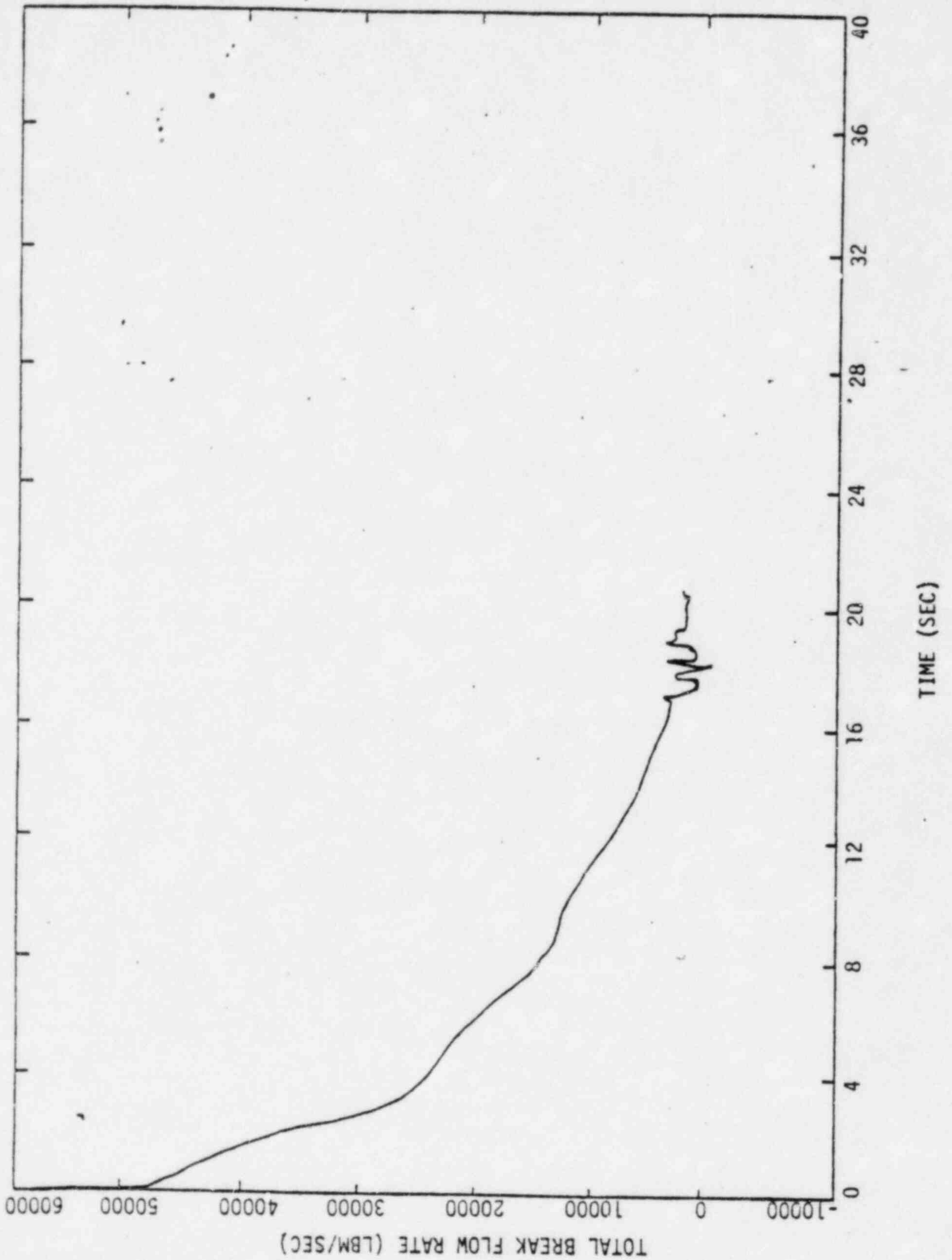


| | | |
|---|---|---|
| Omaha Public Power District<br>Fort Calhoun Station<br>Unit No. 1 | BLOWDOWN TOTAL BREAK FLOW RATE, 1.0 DECLG BREAK | Figure 14.15-6 |

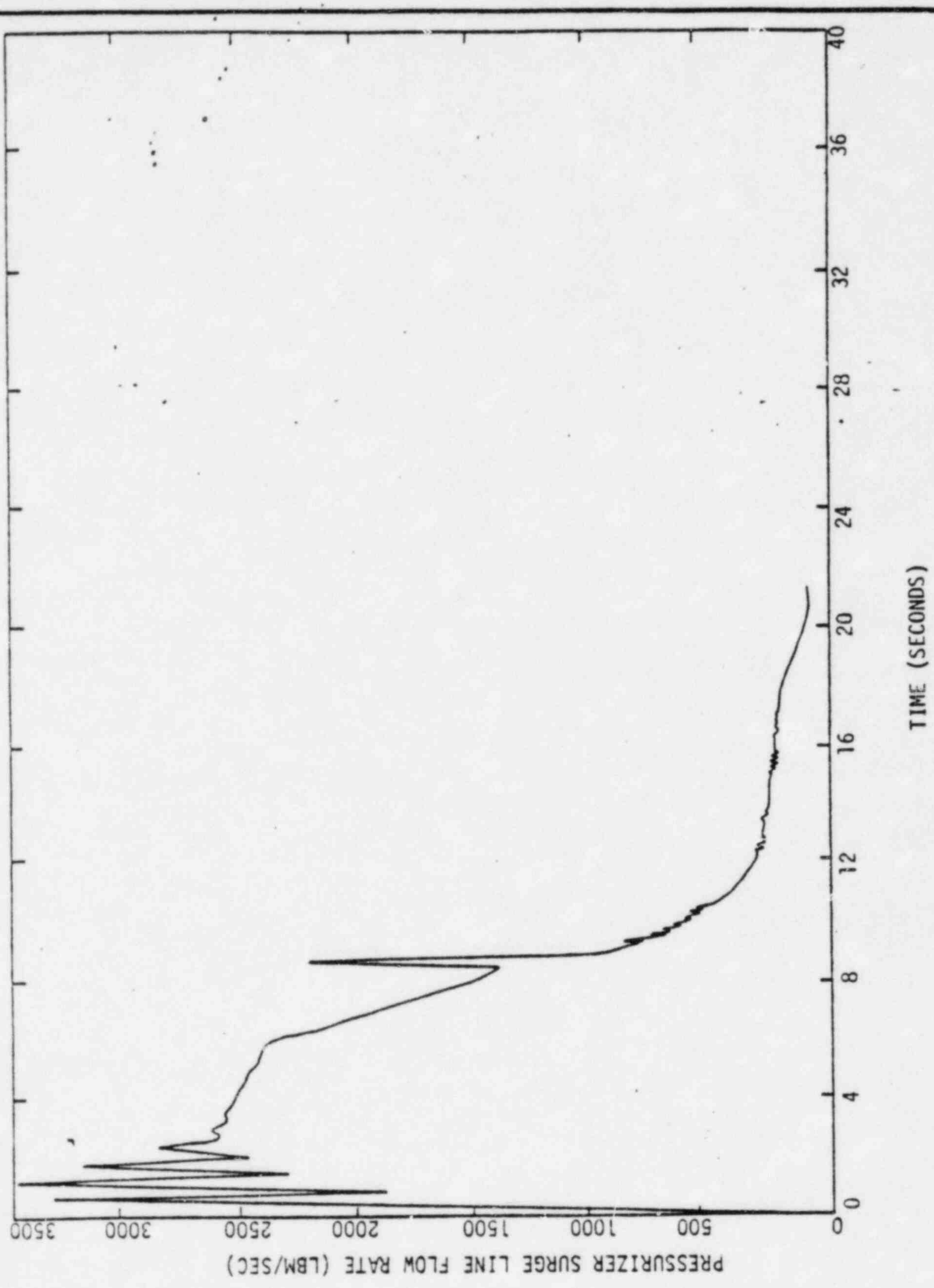


| | | |
|---|---|---|
| Omaha Public Power District<br>Fort Calhoun Station<br>Unit No. 1 | PRESSURIZER SURGE LINE<br>FLOW RATE, 1.0 DECLG BREAK | Figure<br>14.15-7 |

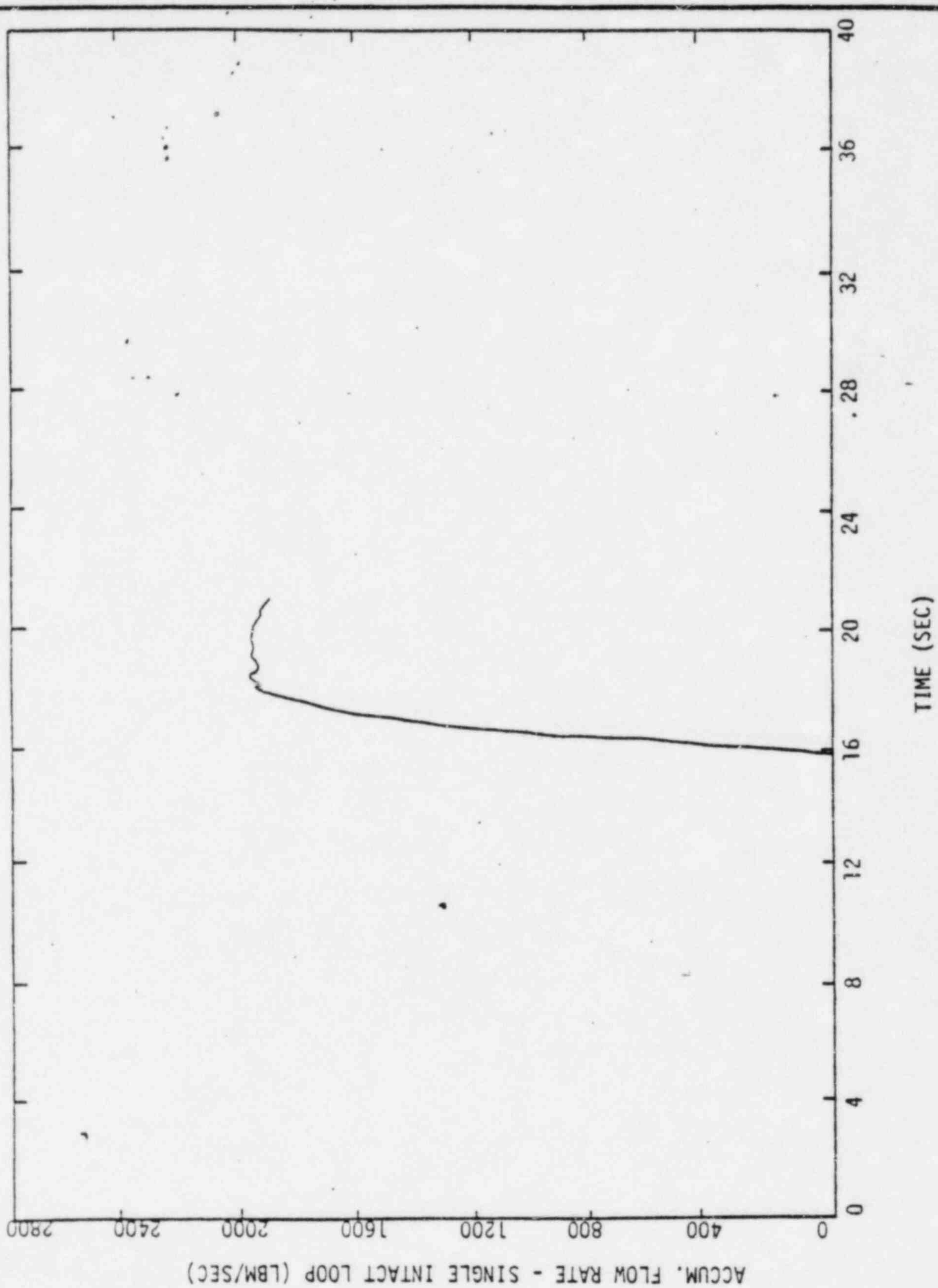


| | | |
|---|---|---|
| Omaha Public Power District<br>Fort Calhoun Station<br>Unit No. 1 | SINGLE INTACT LOOP<br>ACCUMULATOR FLOW RATE,<br>1.0 DECLG BREAK | Figure<br>14.15-8 |

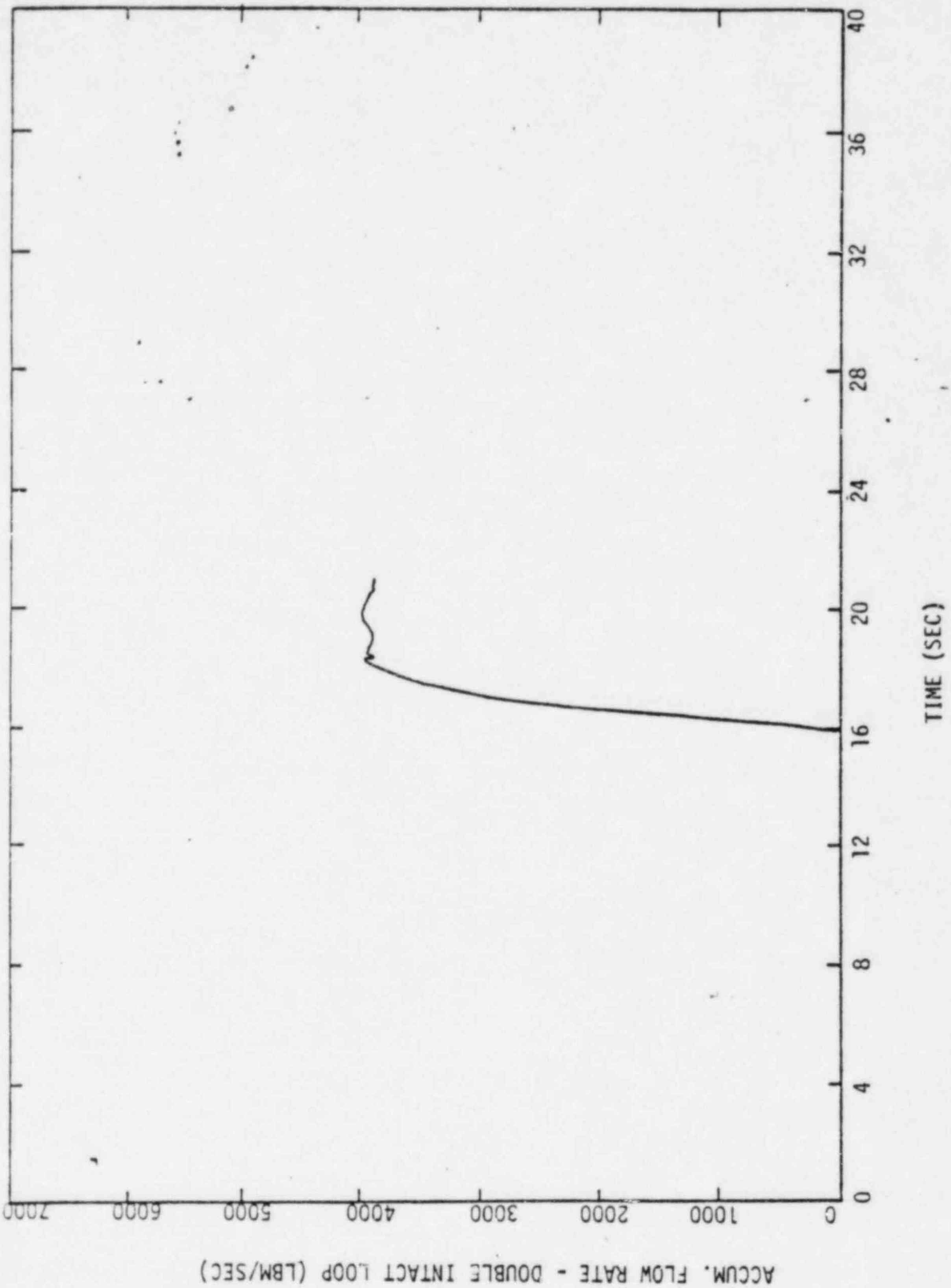


| | | |
|---|---|---|
| Omaha Public Power District<br>Fort Calhoun Station<br>Unit No. 1 | DOUBLE INTACT LOOP<br>ACCUMULATOR FLOW RATE,<br>1.0 DECLG BREAK | Figure<br>14.15-9 |

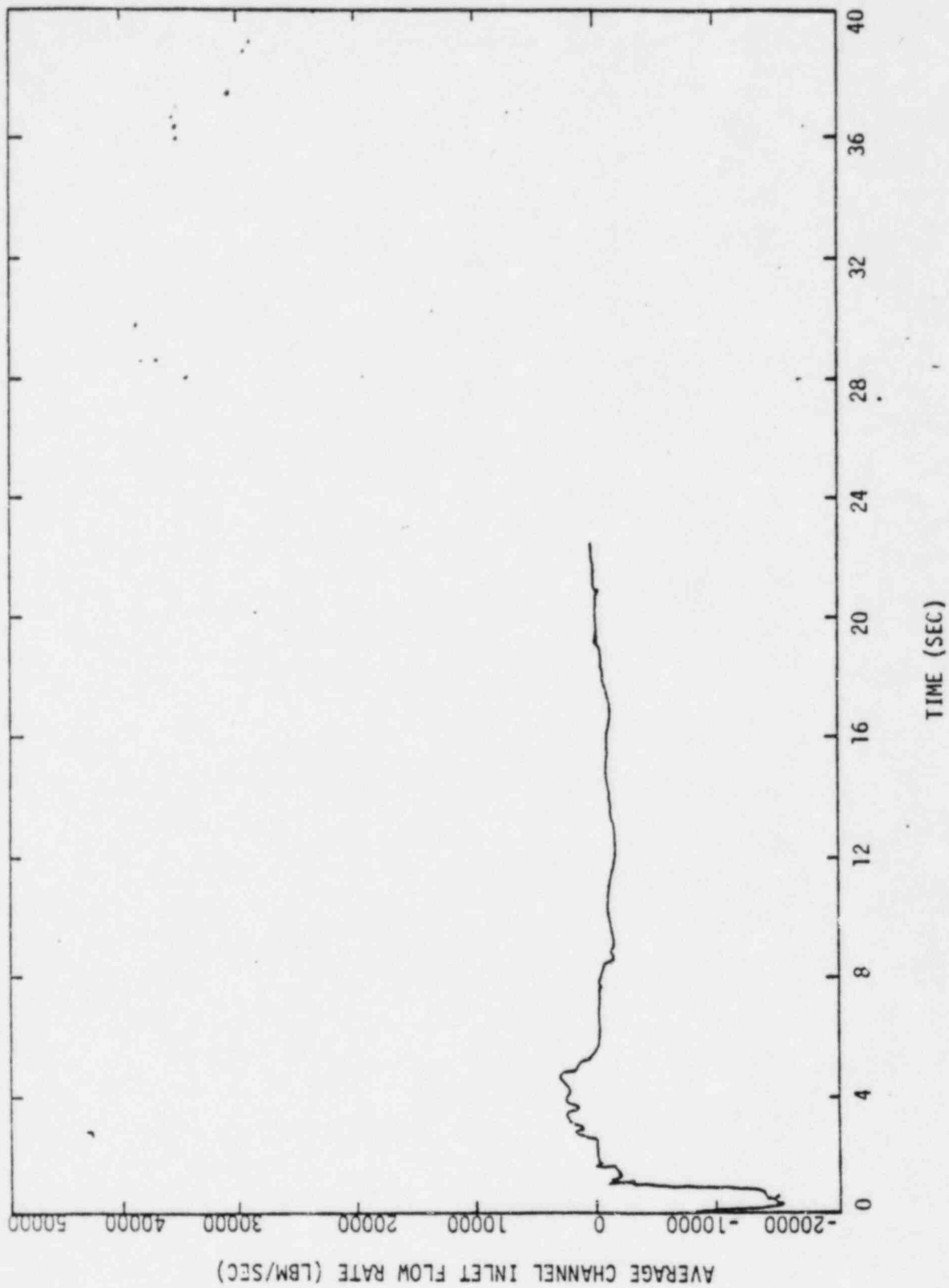


| | | |
|---|---|---|
| Omaha Public Power District<br>Fort Calhoun Station<br>Unit No. 1 | AVERAGE CHANNEL INLET<br>FLOW RATE, 1.0 DECLG BREAK | Figure<br>14.15-10 |

Omaha Public Power District
Fort Calhoun Station
Unit No. 1

AVERAGE CHANNEL OUTLET
FLOW RATE 1.0 DECLG BREAK

Figure
14.15-11

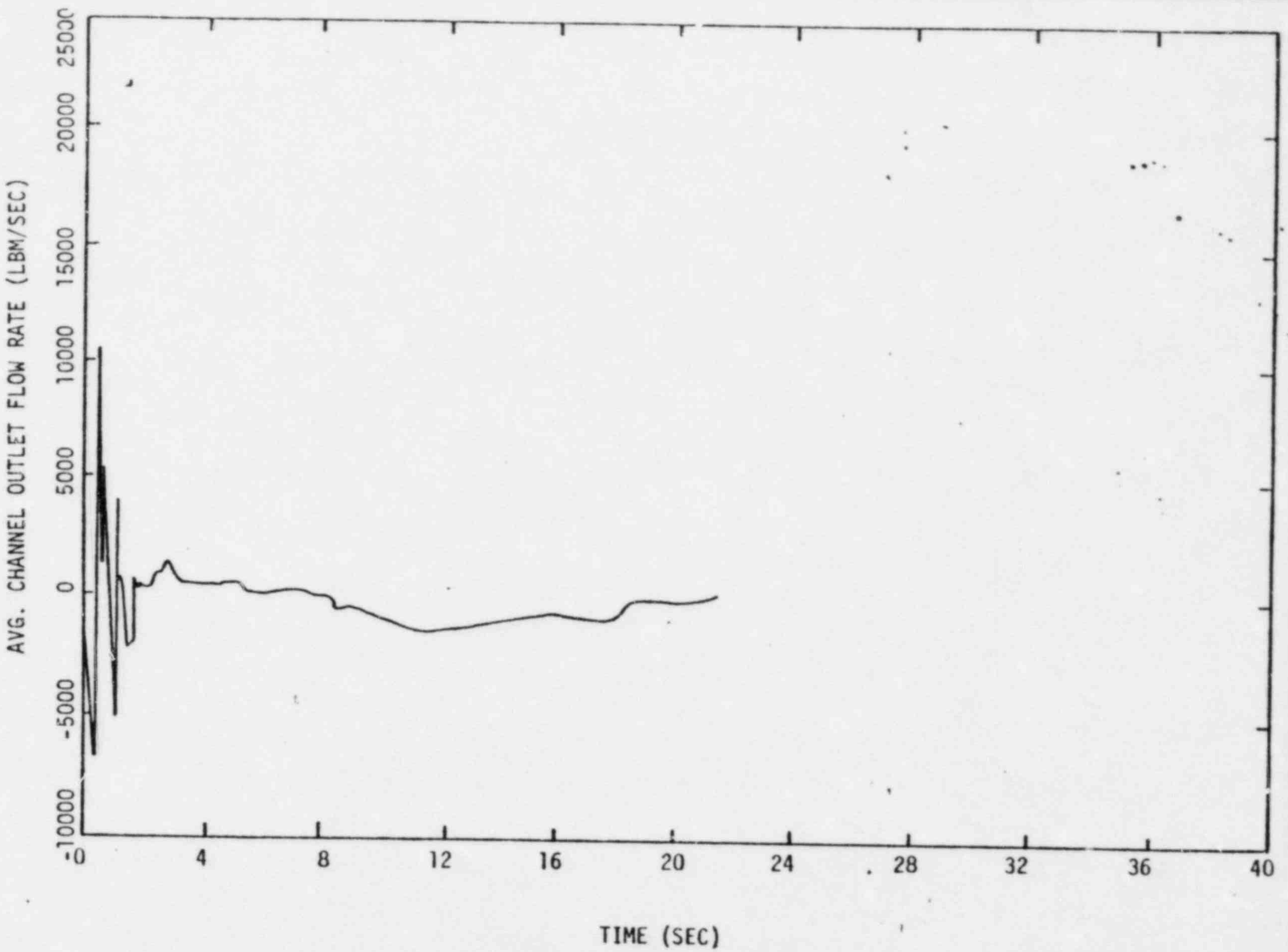

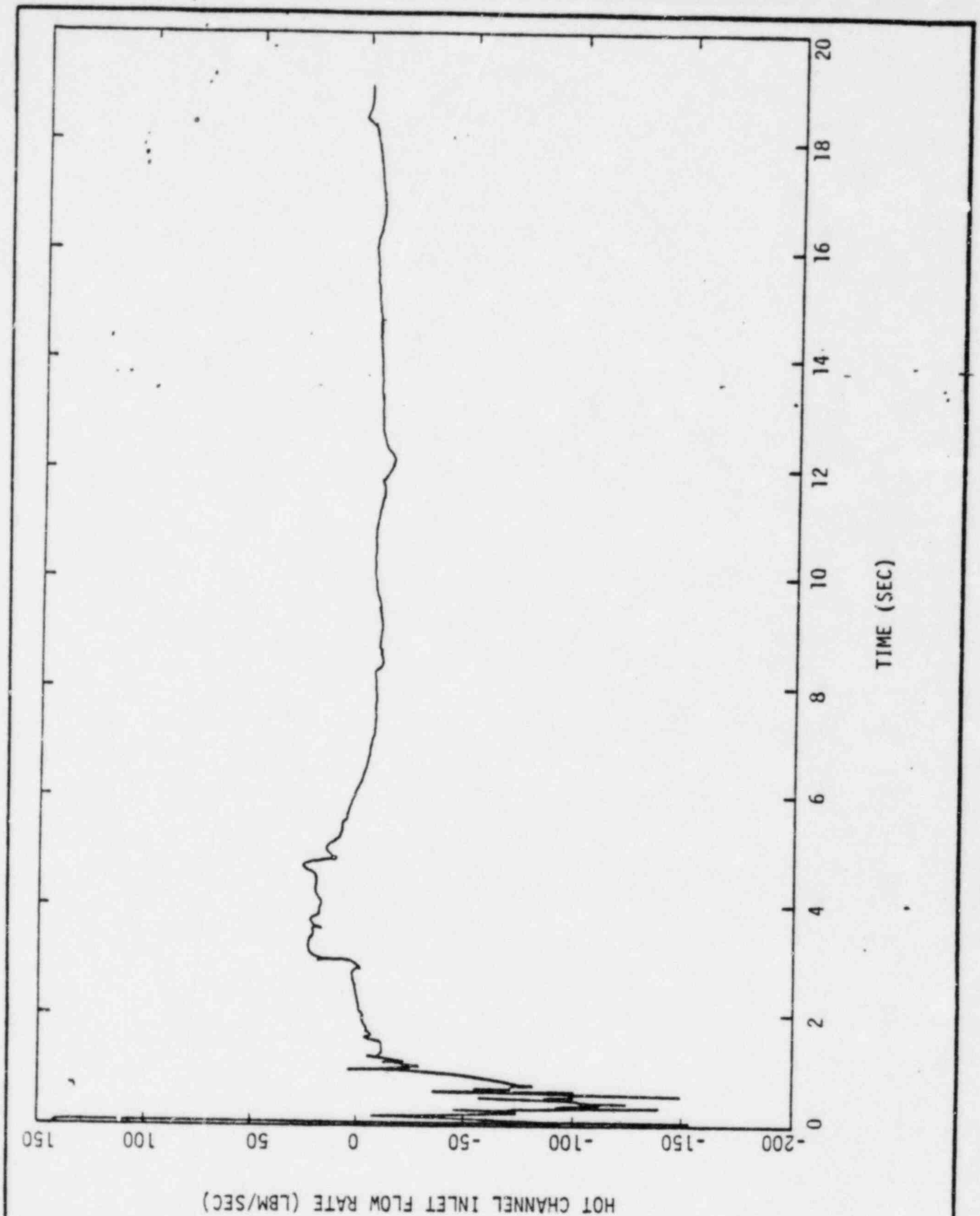


| | | |
|---|---|---|
| **Omaha Public Power District**<br>**Fort Calhoun Station**<br>**Unit No. 1** | HOT CHANNEL INLET FLOW RATE, 1.0 DECLG BREAK | Figure 14.15-12 |

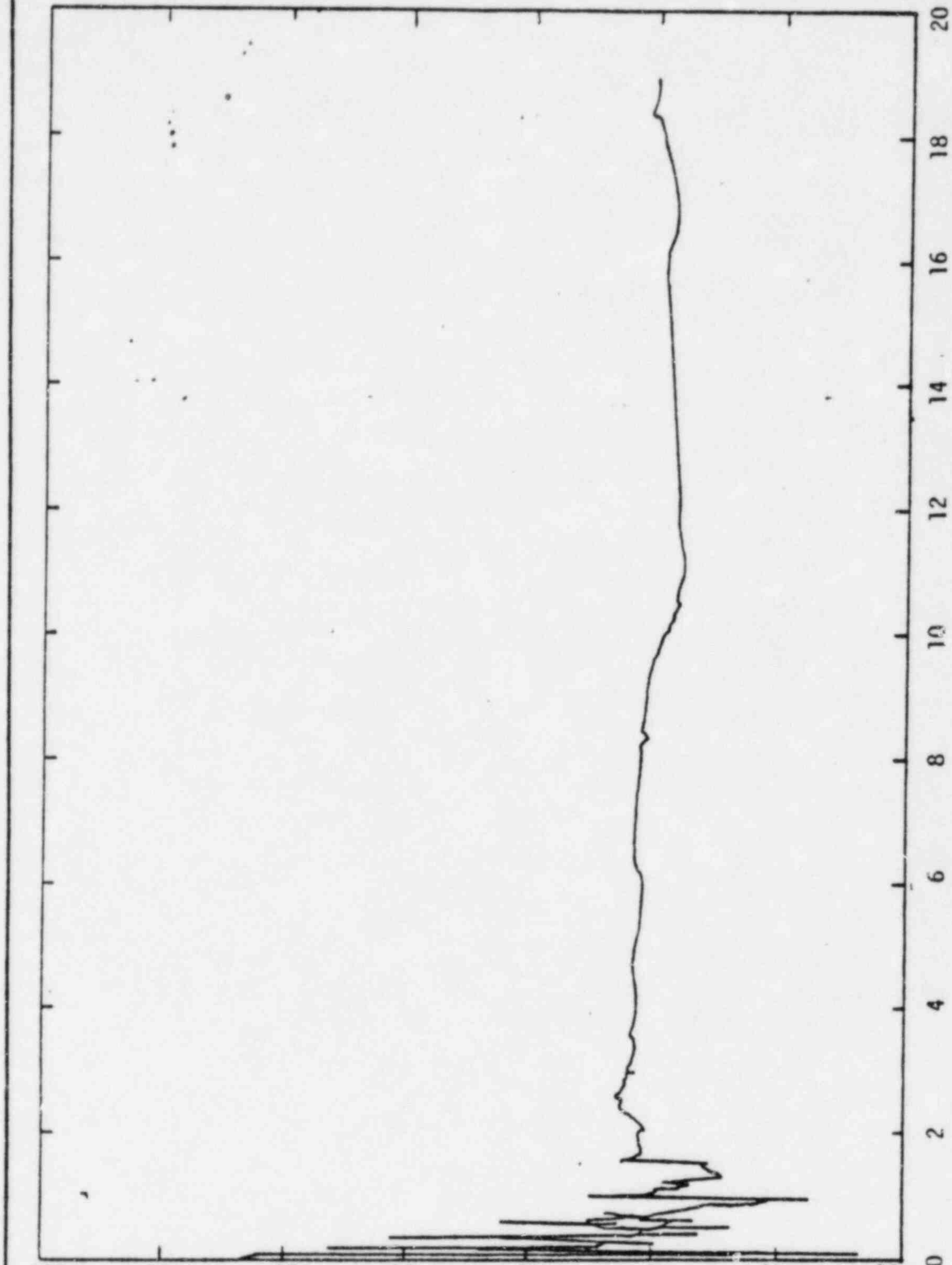


| | | |
|---|---|---|
| Omaha Public Power District<br>Fort Calhoun Station<br>Unit No. 1 | HOT CHANNEL OUTLET FLOW RATE, 1.0 DECLG BREAK | Figure 14.15-13 |

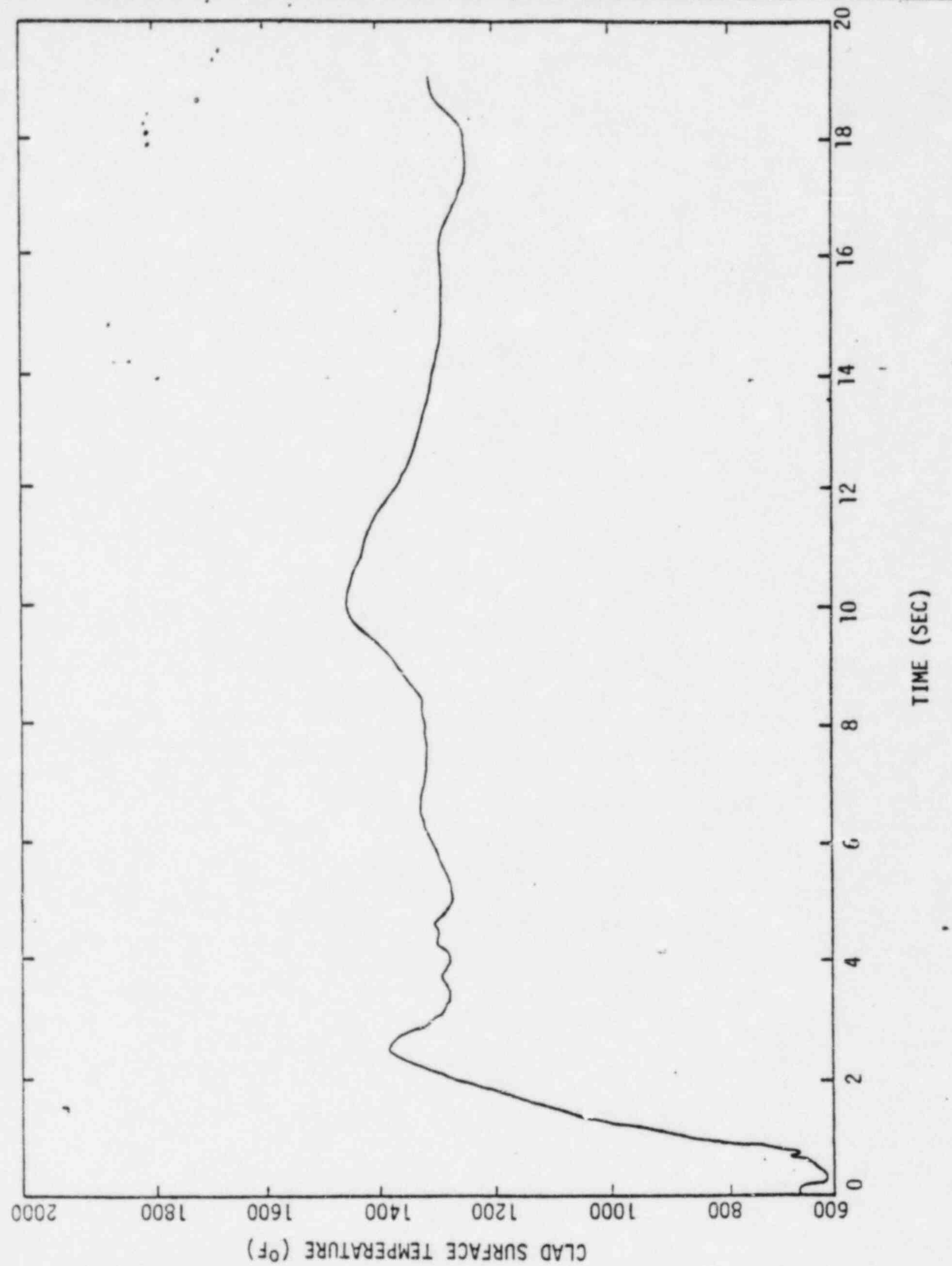


| | | |
|---|---|---|
| Omaha Public Power District<br>Fort Calhoun Station<br>Unit No. 1 | PCT NODE BLOWDOWN CLADDING SURFACE TEMPERATURE, 1.0 DECLG BREAK | Figure 14.15-14 |

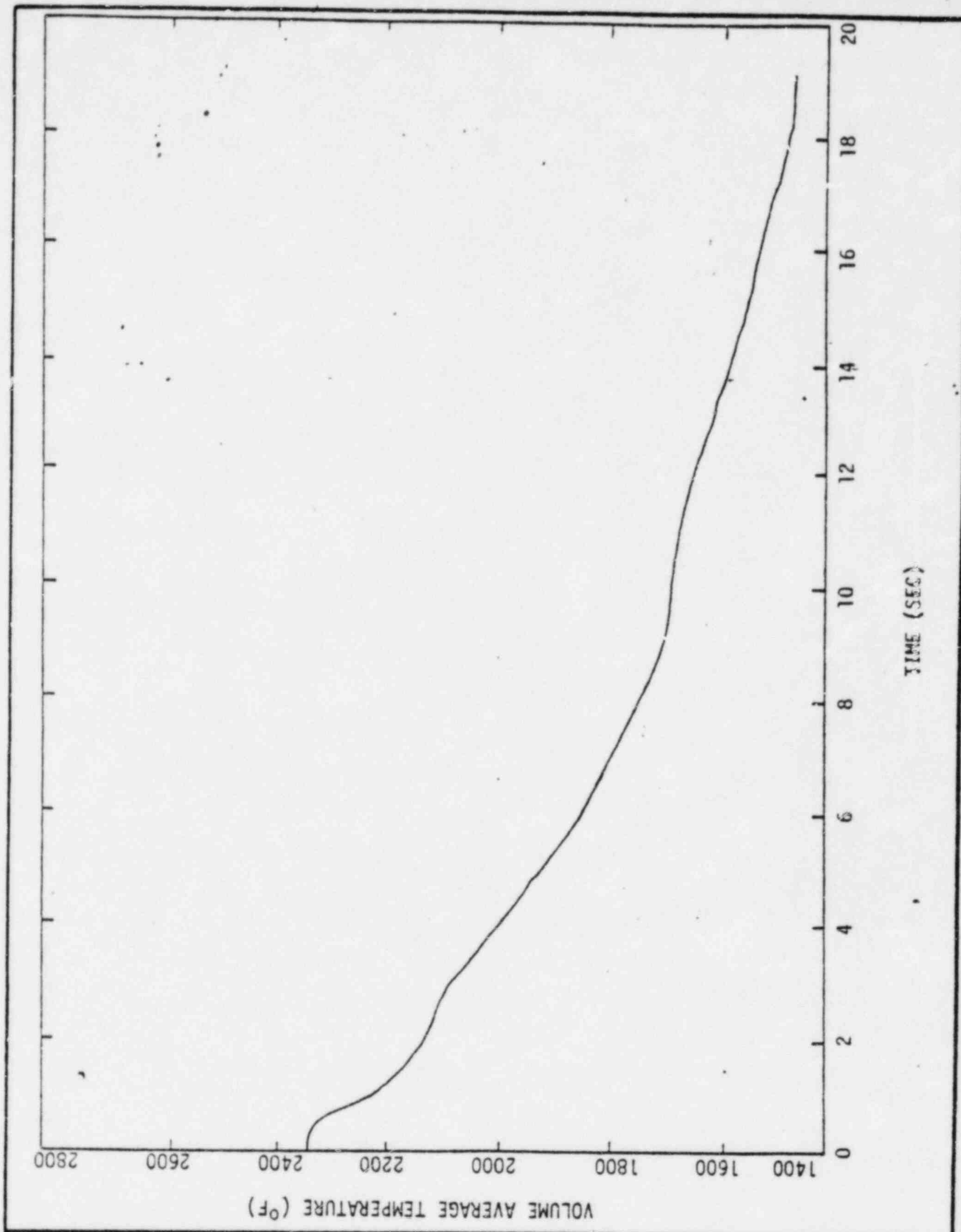


| | | |
|---|---|---|
| Omaha Public Power District<br>Fort Calhoun Station<br>Unit No. 1 | PCT NODE BLOWDOWN<br>VOLUMETRIC AVERAGE FUEL<br>TEMPERATURE, 1.0 DECLG BREAK | Figure<br>14.15-15 |

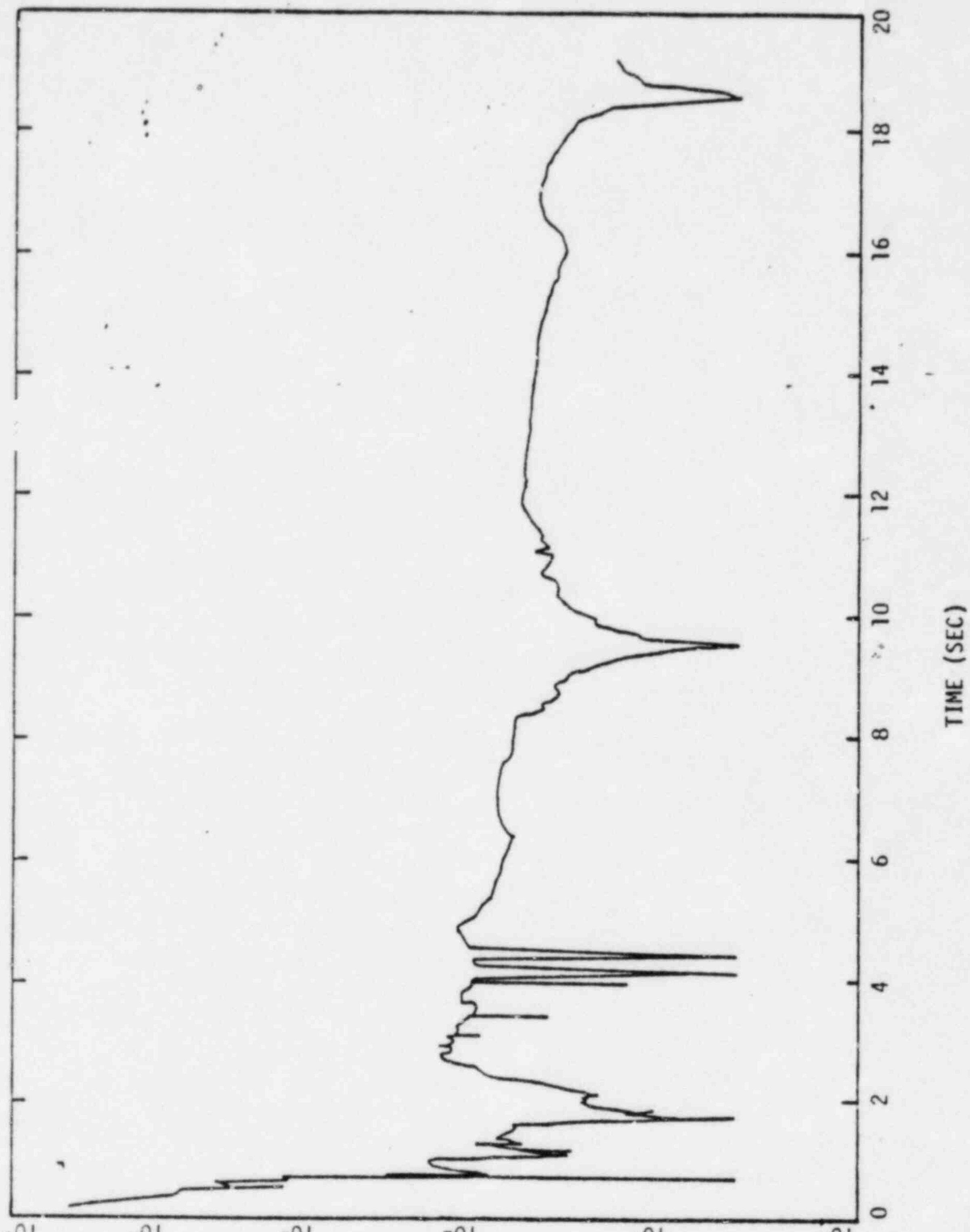


| Omaha Public Power District<br>Fort Calhoun Station<br>Unit No. 1 | PCT NODE BLOWDOWN HEAT TRANSFER COEFFICIENT, 1.0 DECLG BREAK | Figure 14.15-16 |
|---|---|---|

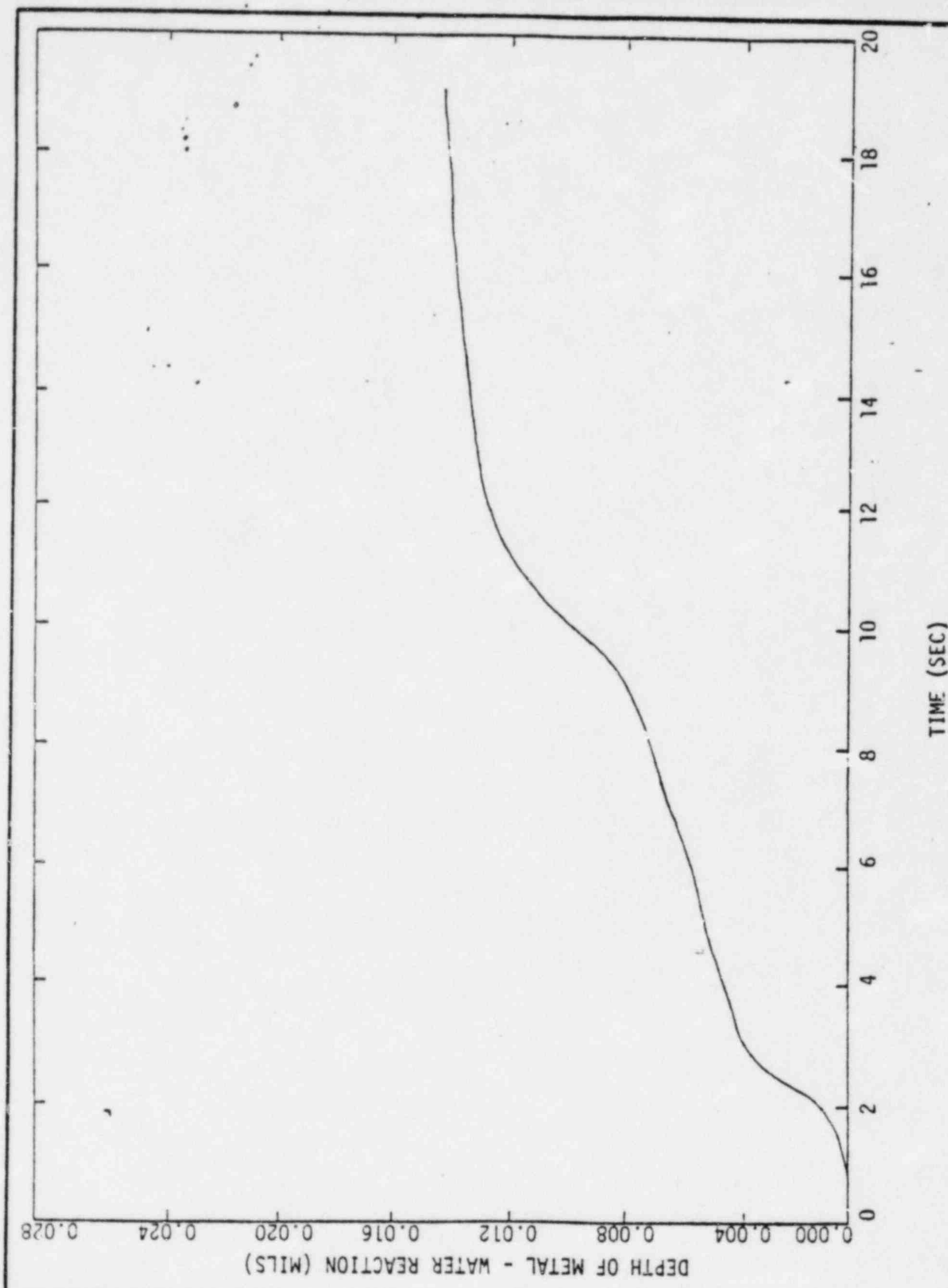


Omaha Public Power District
Fort Calhoun Station
Unit No. 1

PCT NODE BLOWDOWN DEPTH OF ZIRCONIUM - WATER REACTION, 1.0 DECLG BREAK

Figure 14.15-17

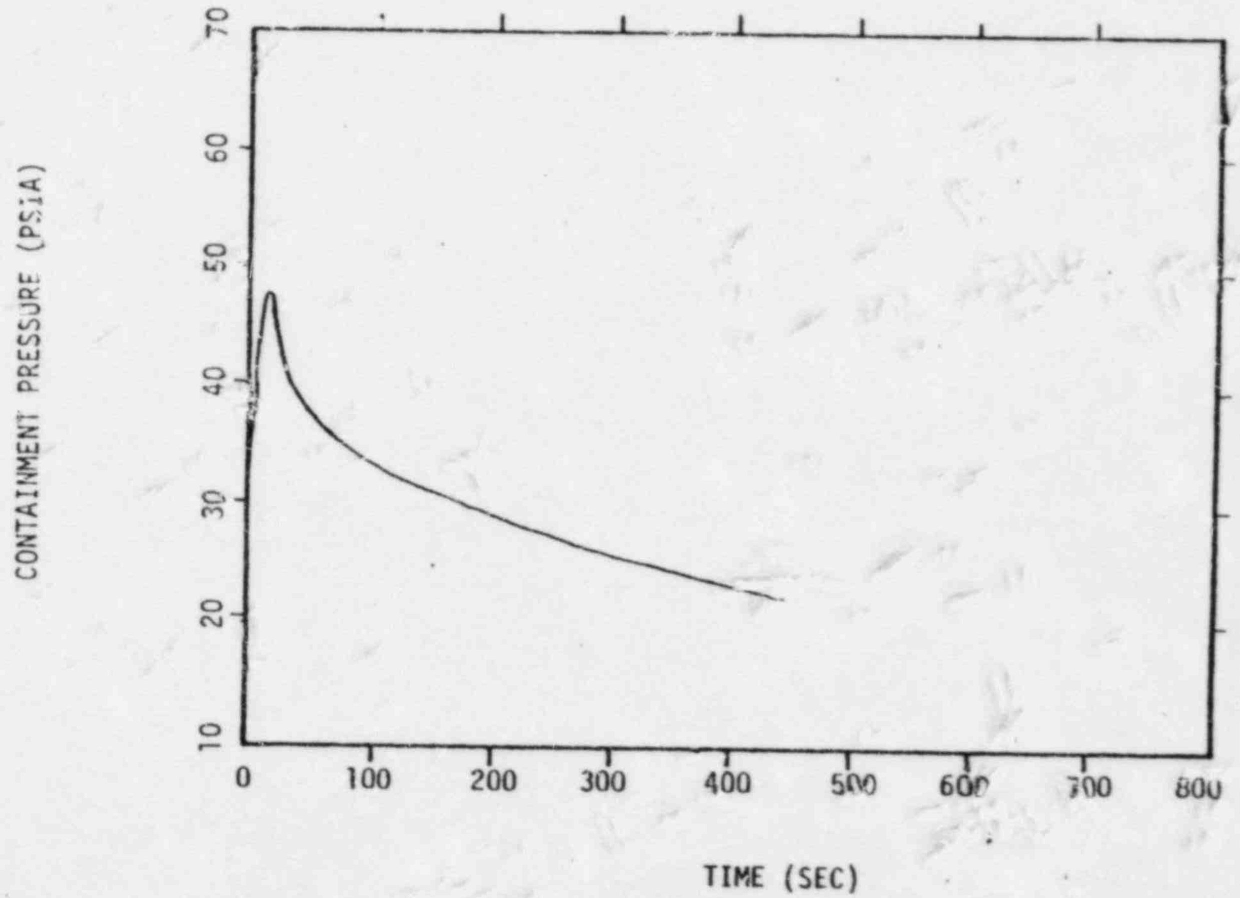


Omaha Public Power District
Fort Calhoun Station
Unit No. 1

CONTAINMENT PRESSURE
VERSUS TIME
1.0 DECLG BREAK

Figure
14.15-18

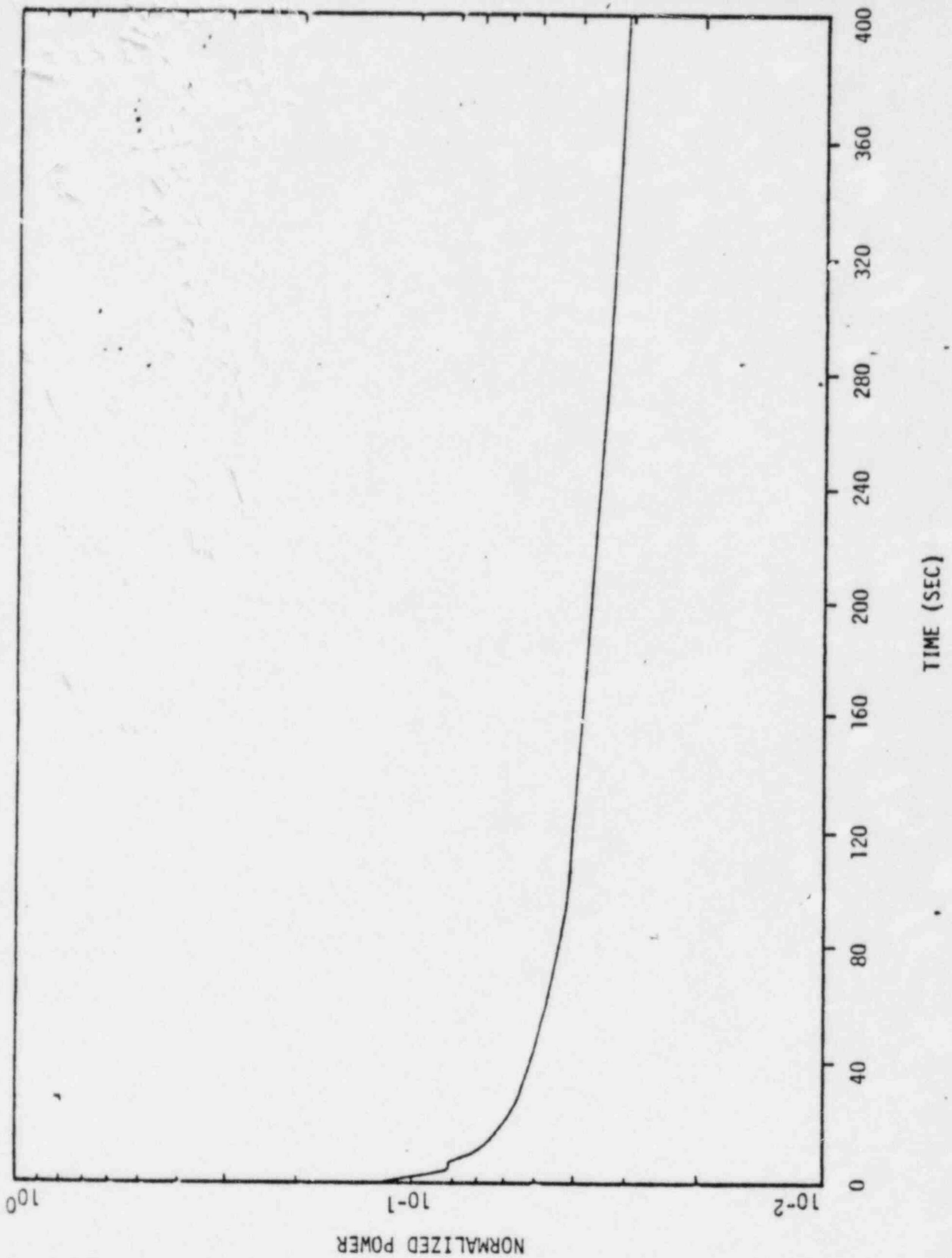


| | | |
|---|---|---|
| Omaha Public Power District<br>Fort Calhoun Station<br>Unit No. I | NORMALIZED CORE POWER,<br>1.0 DECLG BREAK | Figure<br>14.15-19 |

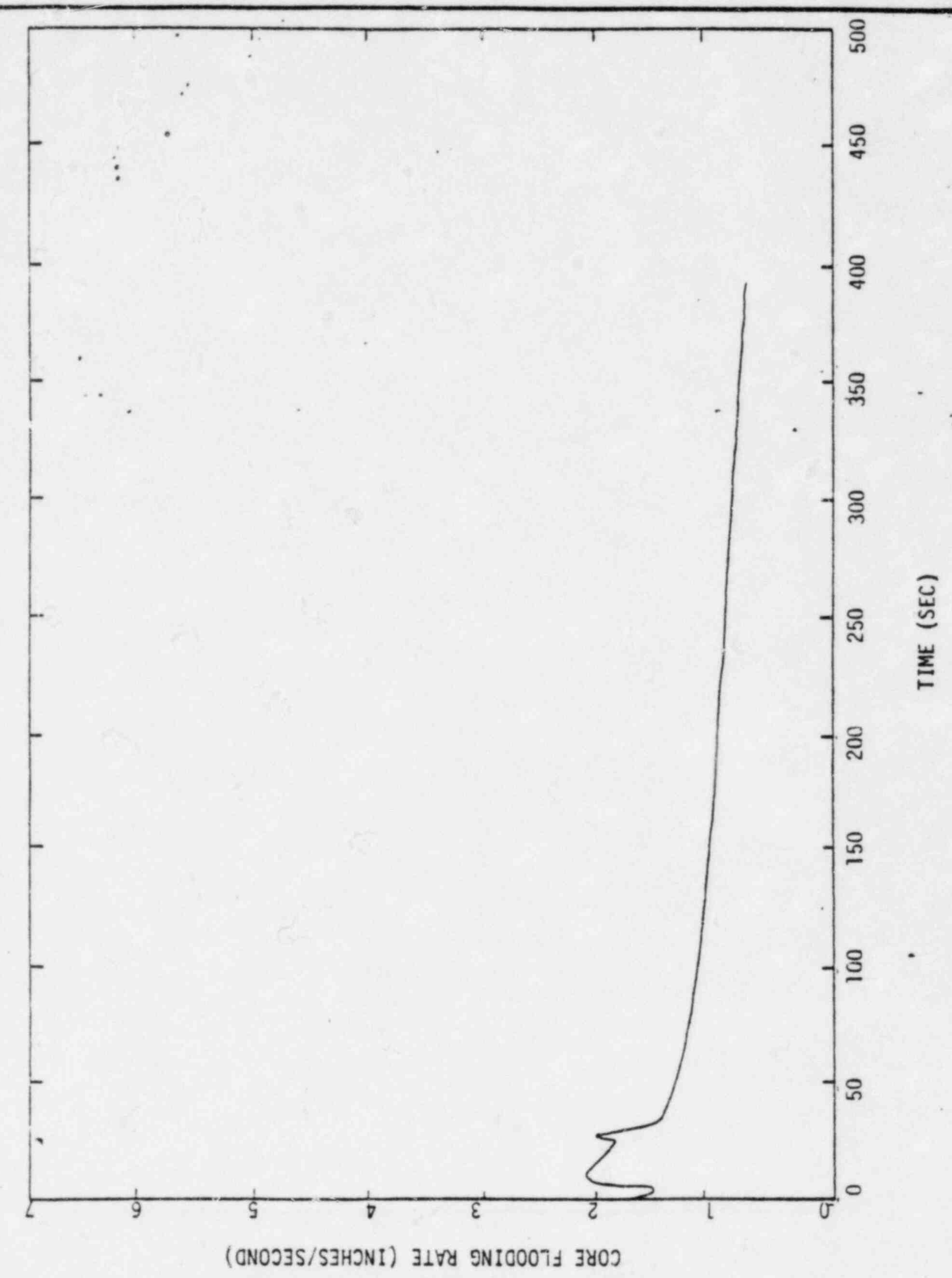


| | | |
|---|---|---|
| Omaha Public Power District<br>Fort Calhoun Station<br>Unit No. 1 | CORE REFLOODING RATE,<br>1.0 DECLG BREAK | Figure<br>14.15-20 |

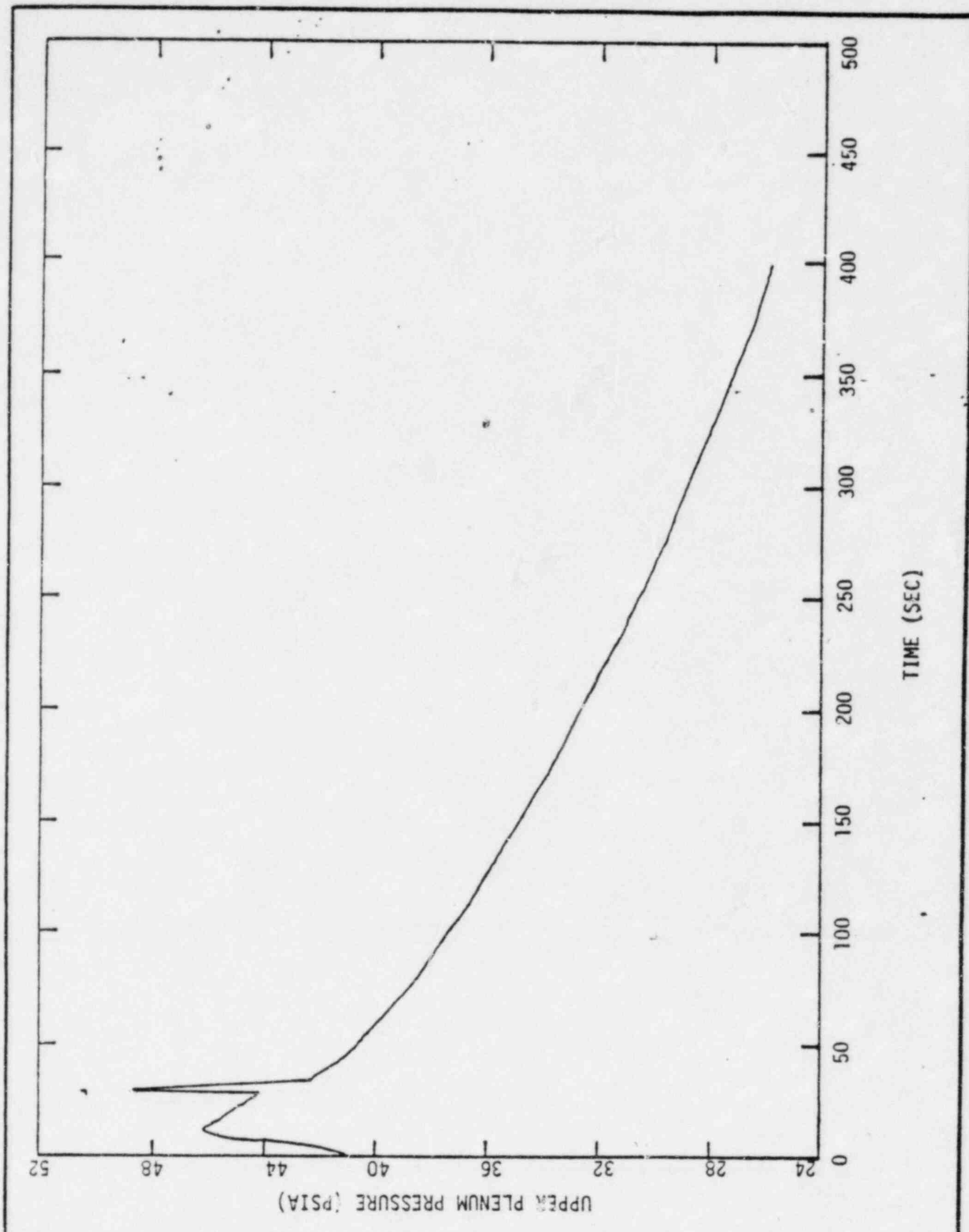


| | | |
|---|---|---|
| Omaha Public Power District<br>Fort Calhoun Station<br>Unit No. 1 | REFLOOD SYSTEM PRESSURE,<br>1.0 DECLG BREAK | Figure<br>14.15-21 |

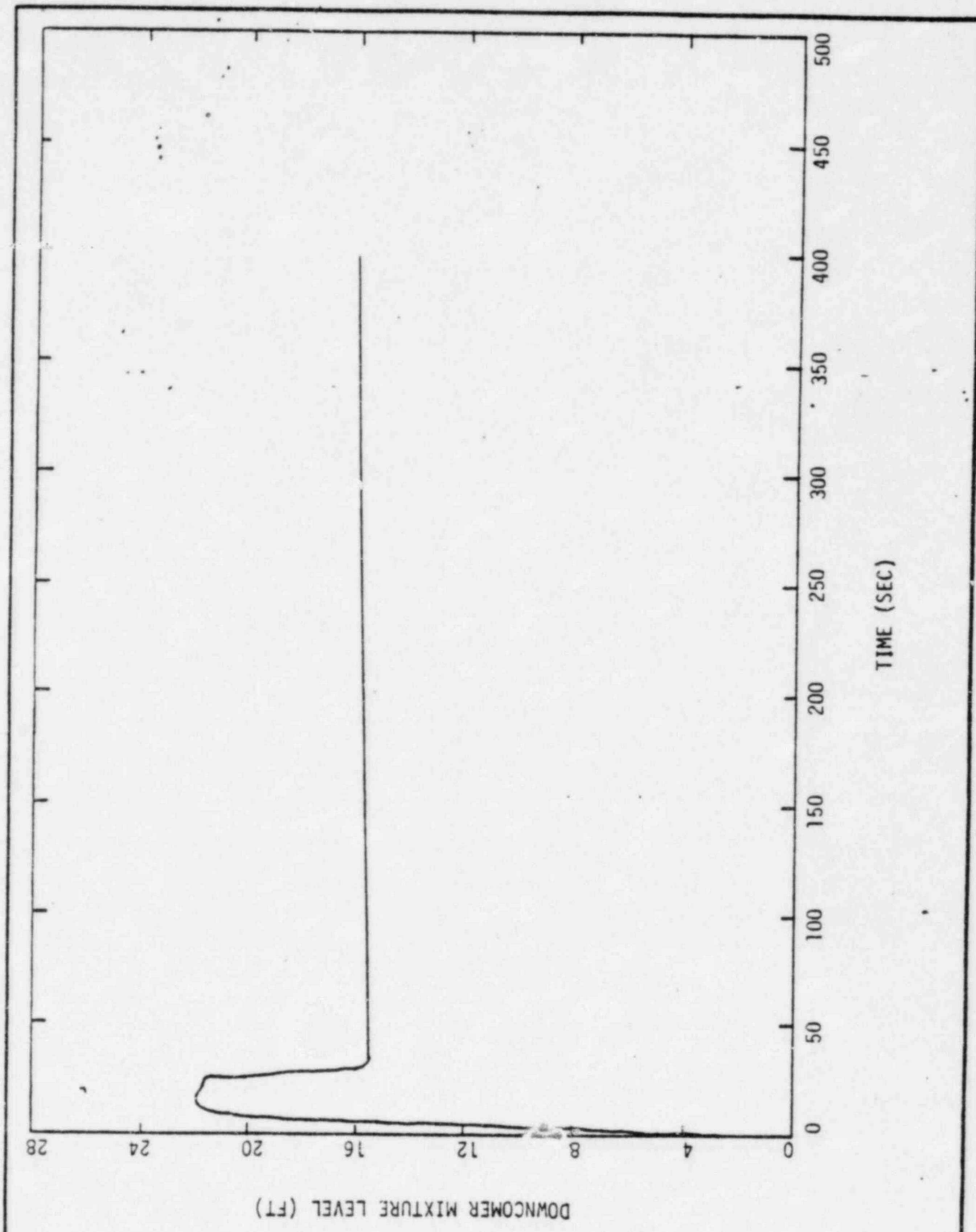


| | | |
|---|---|---|
| **Omaha Public Power District**<br>**Fort Calhoun Station**<br>**Unit No. 1** | REFLOOD DOWNCOMER MIXTURE LEVEL,<br>1.0 DECLG BREAK | Figure<br>14.15-22 |

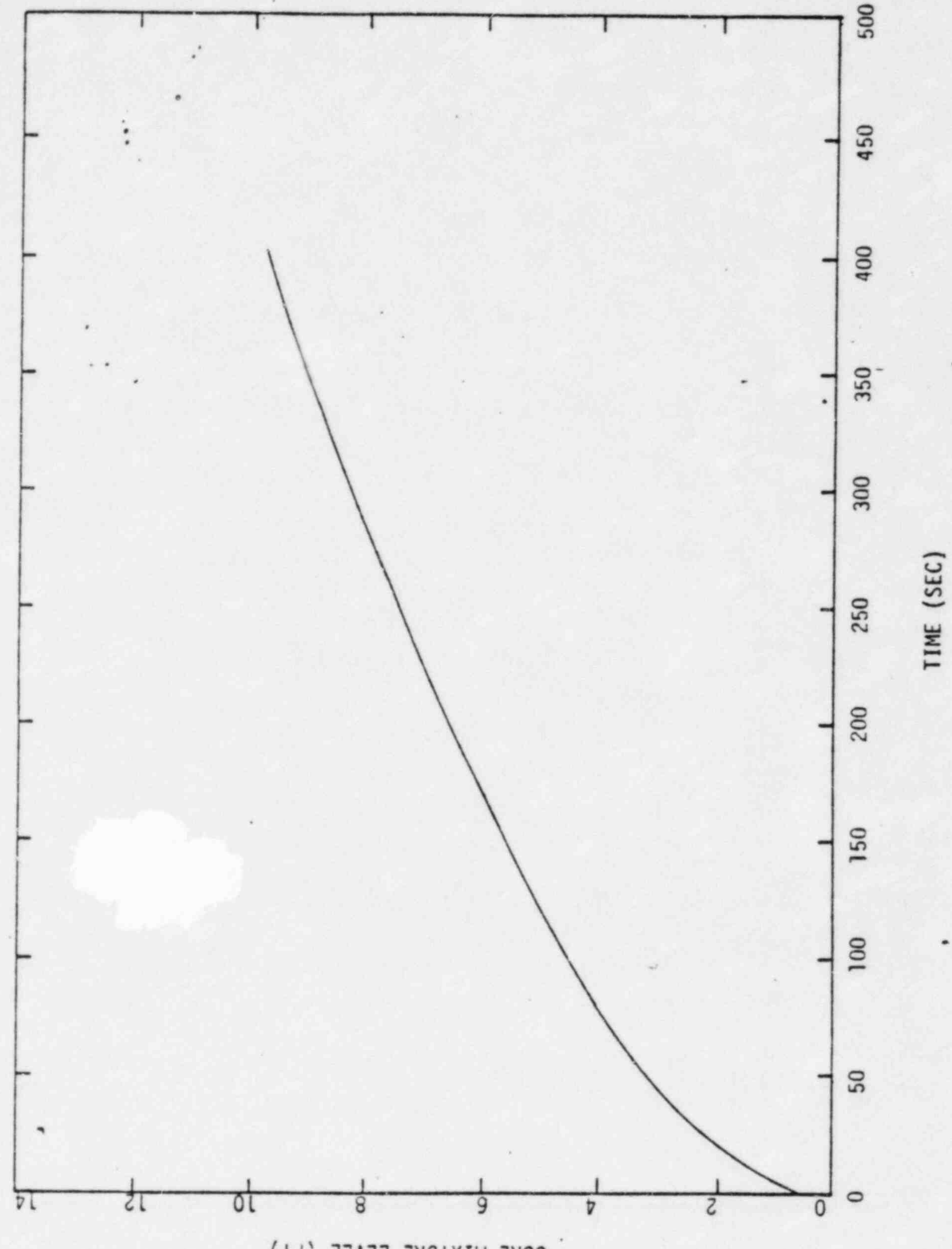


| | | |
|---|---|---|
| Omaha Public Power District<br>Fort Calhoun Station<br>Unit No. 1 | REFLOOD CORE MIXTURE LEVEL, 1.0 DECLG BREAK | Figure 14.15-23 |

Omaha Public Power District
Fort Calhoun Station
Unit No. 1

CLADDING SURFACE TEMPERATURE DURING HEATING UP OF ENC FUEL AT BOL, 1.0 DECLG BREAK

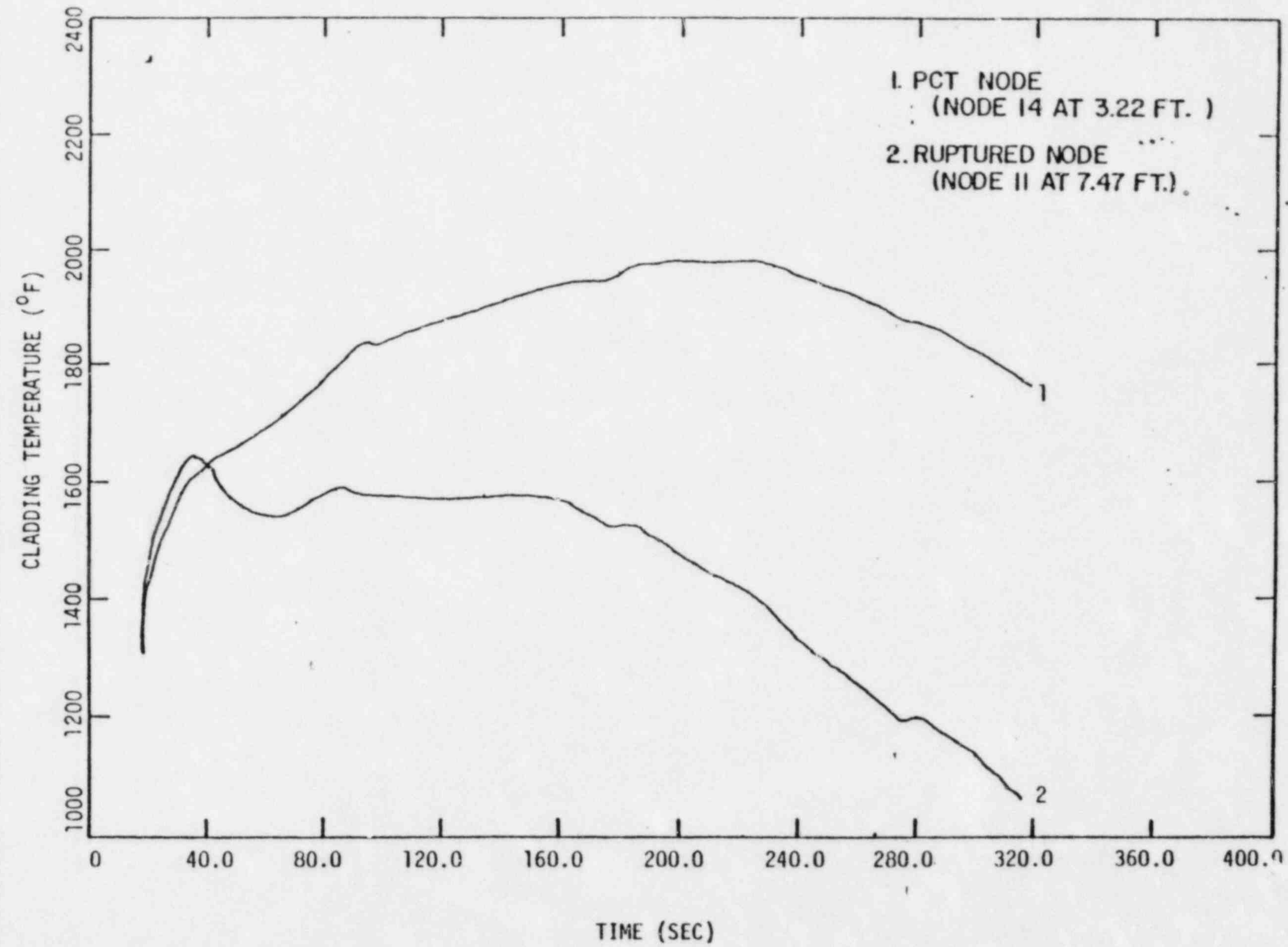


Figure 14.15-24

Omaha Public Power District
Fort Calhoun Station
Unit No. 1

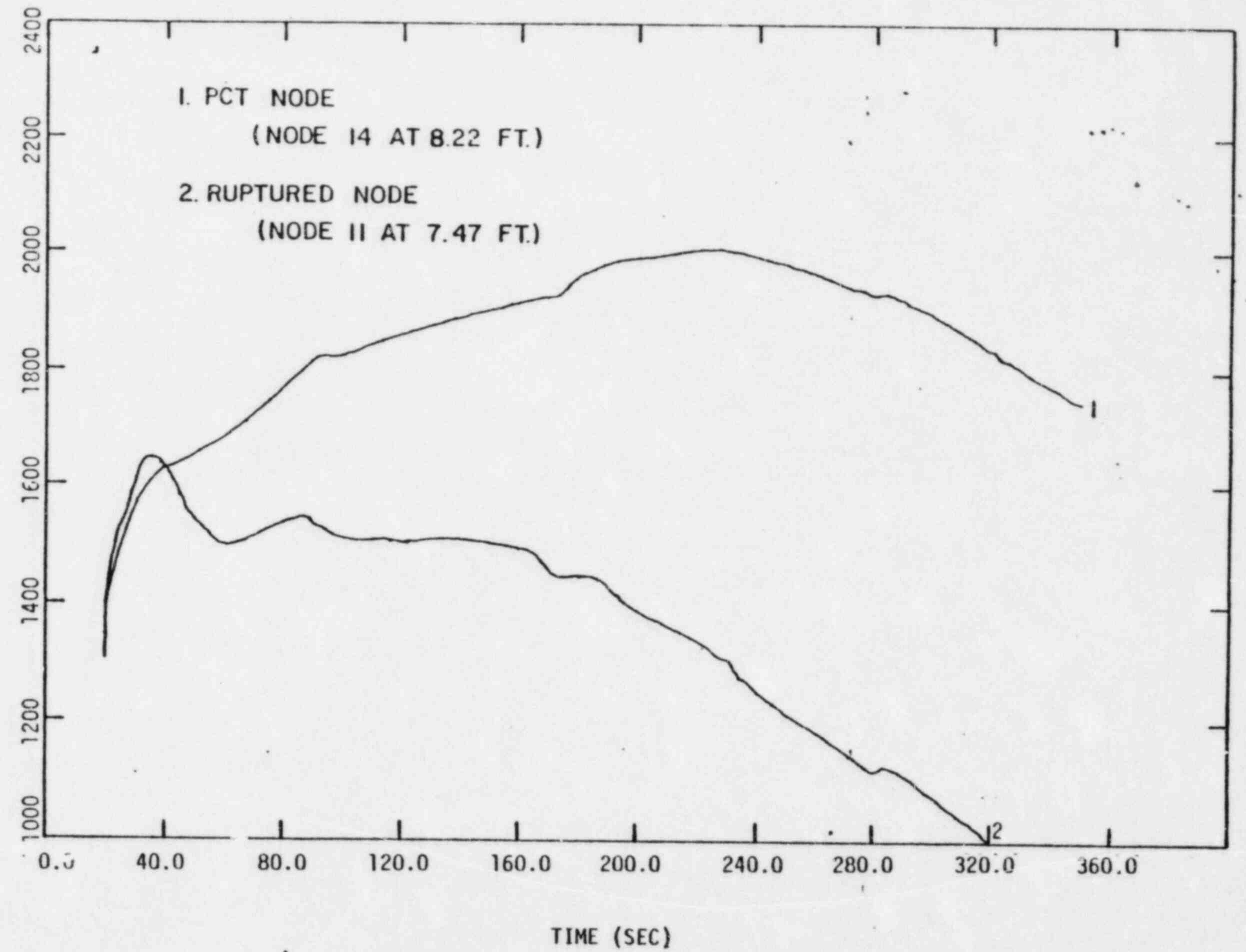


CLADDING SURFACE TEMPERATURE DURING HEATUP FOR CE FUEL AT BOL

Figure 14.15-25

Omaha Public Power District
Fort Calhoun Station
Unit No. 1

CLADDING SURFACE TEMPERATURE
DURING HEATUP FOR ENC FUEL
AT EOL

Figure
14.15-26

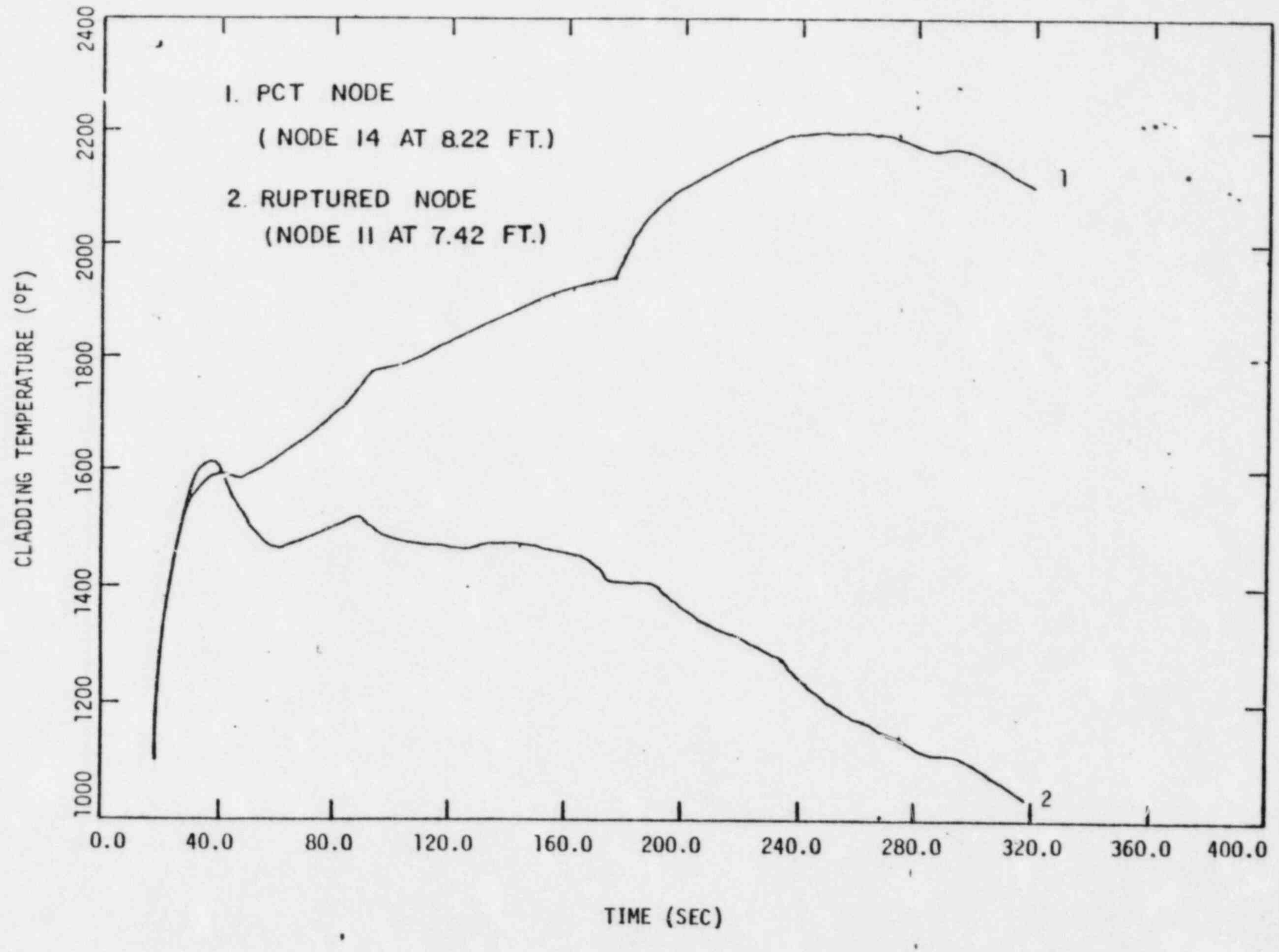

Omaha Public Power District
Fort Calhoun Station
Unit No. 1

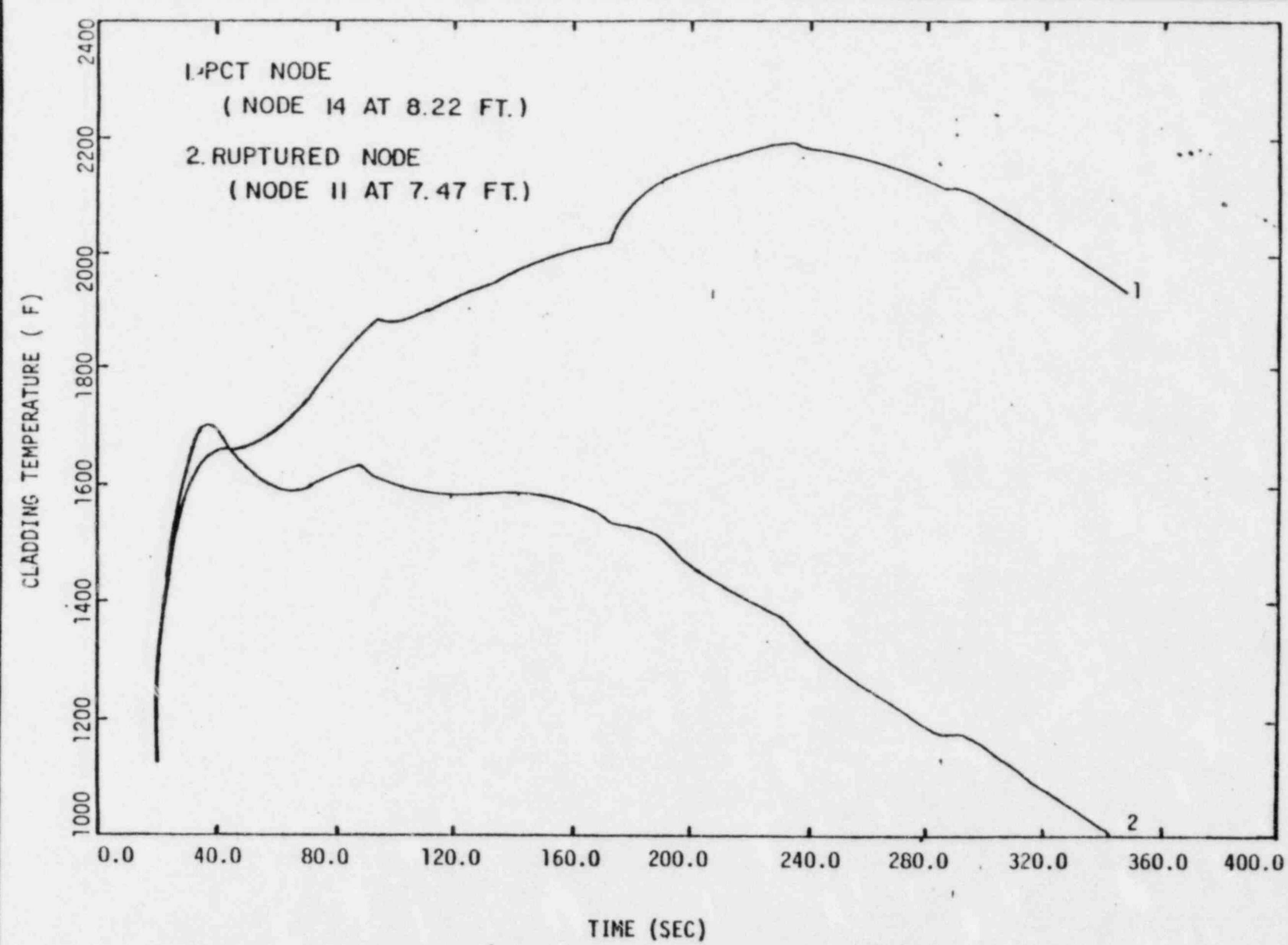


CLADDING SURFACE TEMPERATURE DURING HEATUP FOR CE FUEL AT 32,600 MWD/MTU PEAK PELLET BURNUP

Figure 14.15-27

Omaha Public Power District
Fort Calhoun Station
Unit No. 1

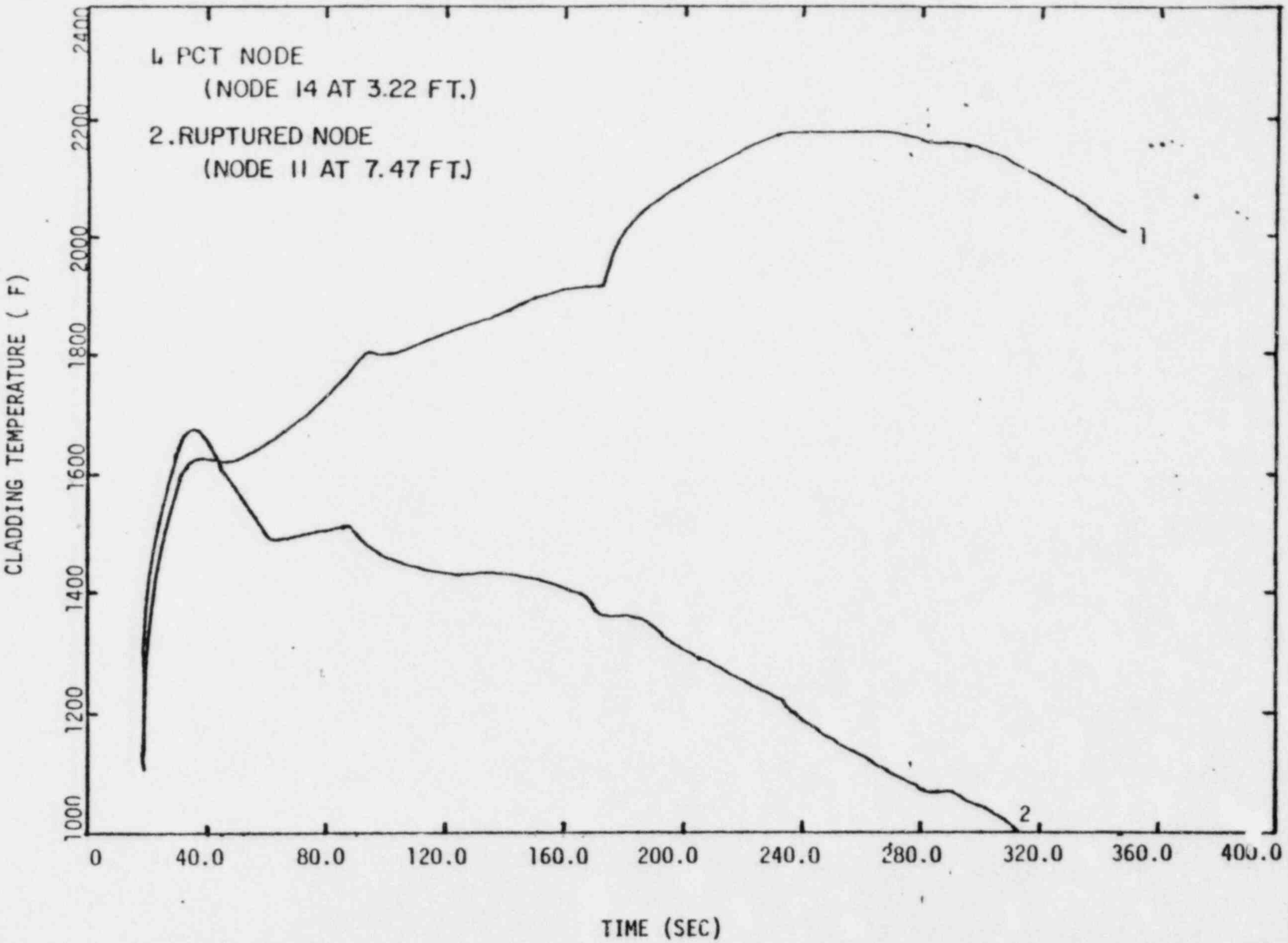


CLADDING SURFACE TEMPERATURE DURING HEATING UP FOR CE FUEL AT EOL

Figure 14.15-28

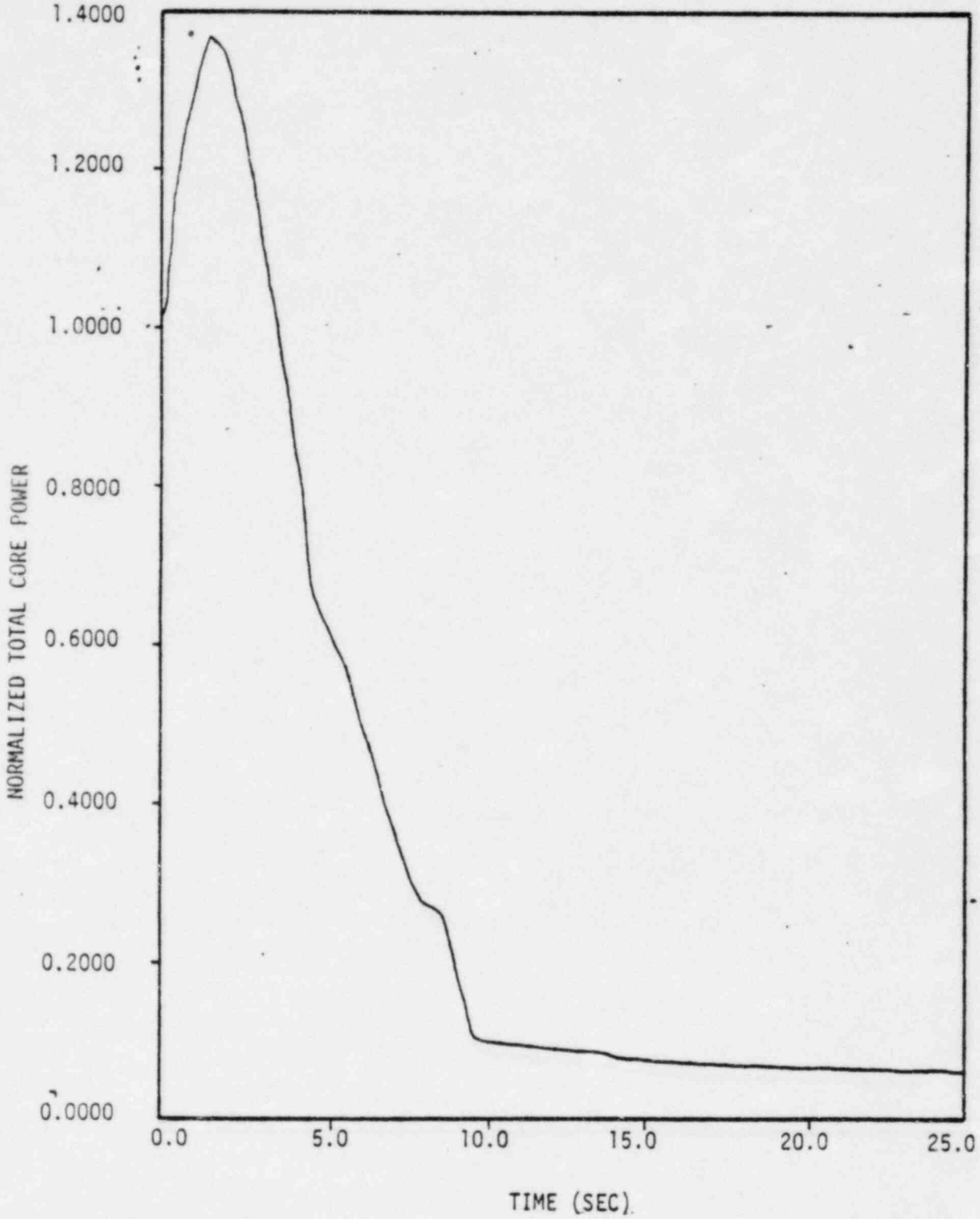


| | | |
|---|---|---|
| **Omaha Public Power District**<br>**Fort Calhoun Station**<br>**Unit No. 1** | 0.5 $FT^2$ COLD LEG BREAK AT PUMP DISCHARGE-NORMALIZED TOTAL CORE POWER (SMALL BREAK ANALYSIS) | Figure 14.15-29A |

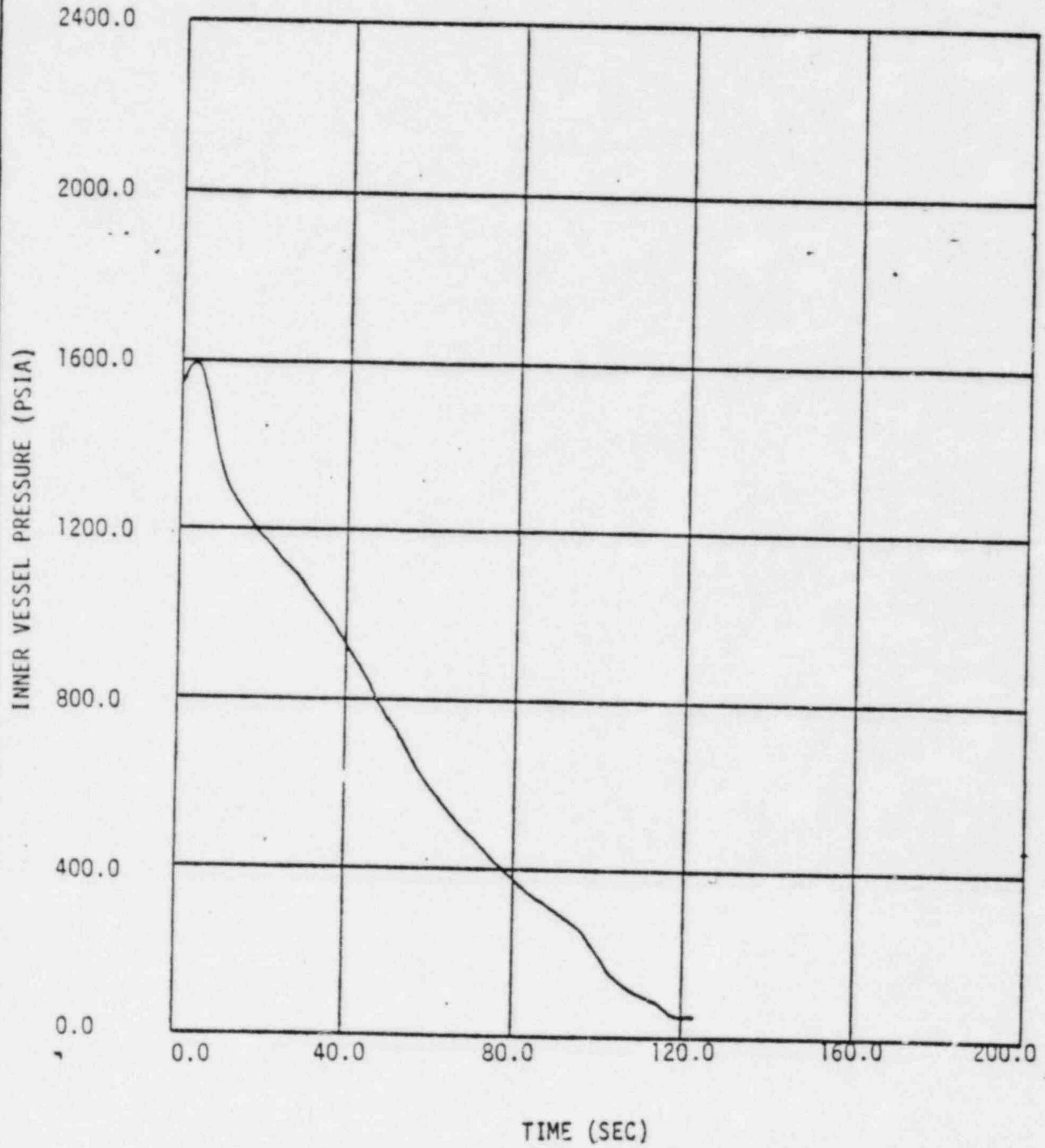


| | | |
|---|---|---|
| Omaha Public Power District<br>Fort Calhoun Station<br>Unit No. 1 | 0.5 $FT^2$ COLD LEG BREAK AT DISCHARGE-INNER VESSEL PRESSURE (SMALL BREAK ANALYSIS) | Figure 14.15-29B |

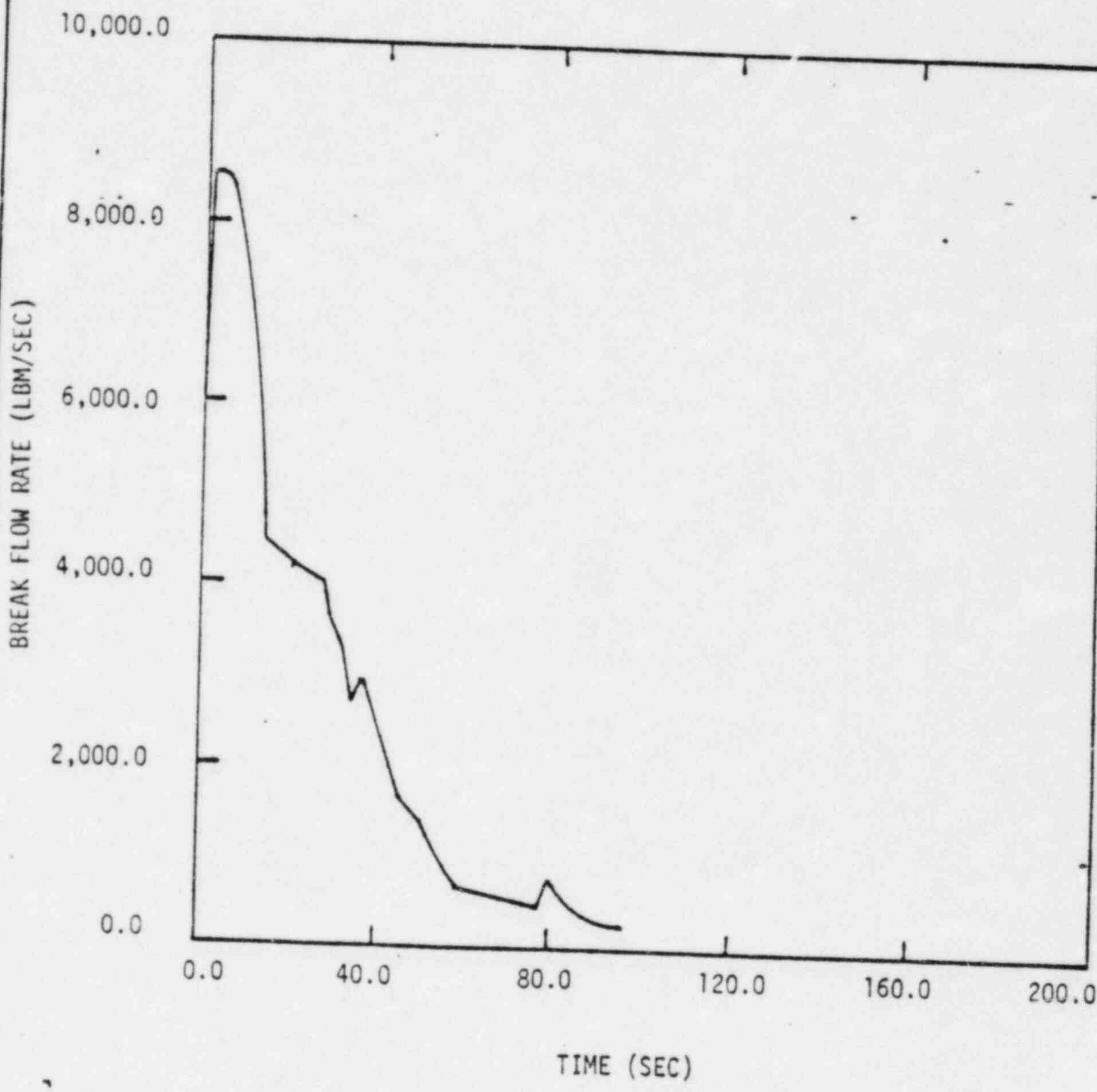


| | | |
|---|---|---|
| Omaha Public Power District<br>Fort Calhoun Station<br>Unit No. 1 | 0.5 $FT^2$ COLD LEG BREAK AT PUMP DISCHARGE-BREAK FLOW RATE (SMALL BREAK ANALYSIS) | Figure 14.15-29C |

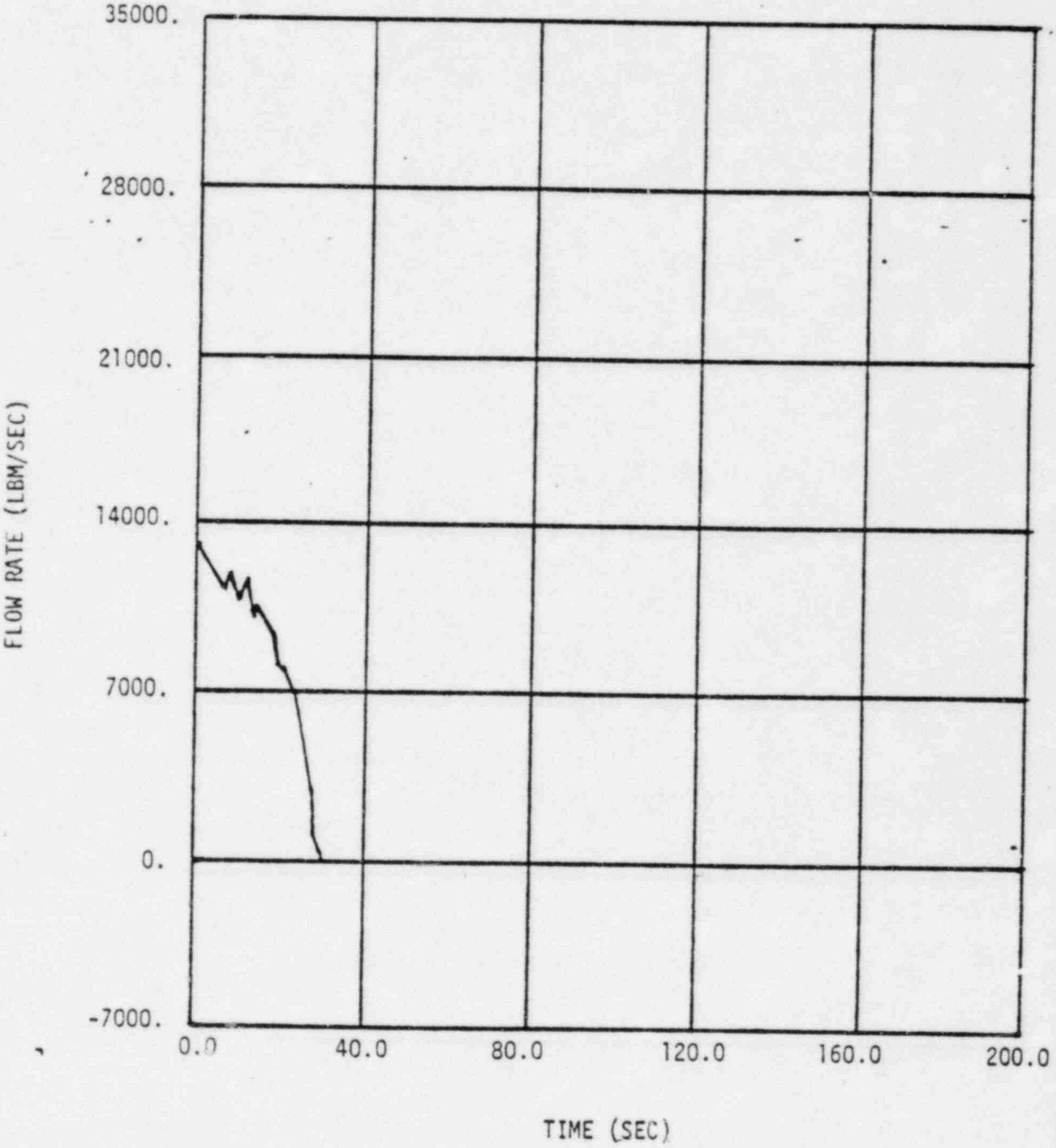


| | | |
|---|---|---|
| Omaha Public Power District<br>Fort Calhoun Station<br>Unit No. 1 | 0.5 $FT^2$ COLD LEG BREAK AT PUMP DISCHARGE-INNER VESSEL INLET FLOW RATE<br>(SMALL BREAK ANALYSIS) | Figure<br>14.15-29D |

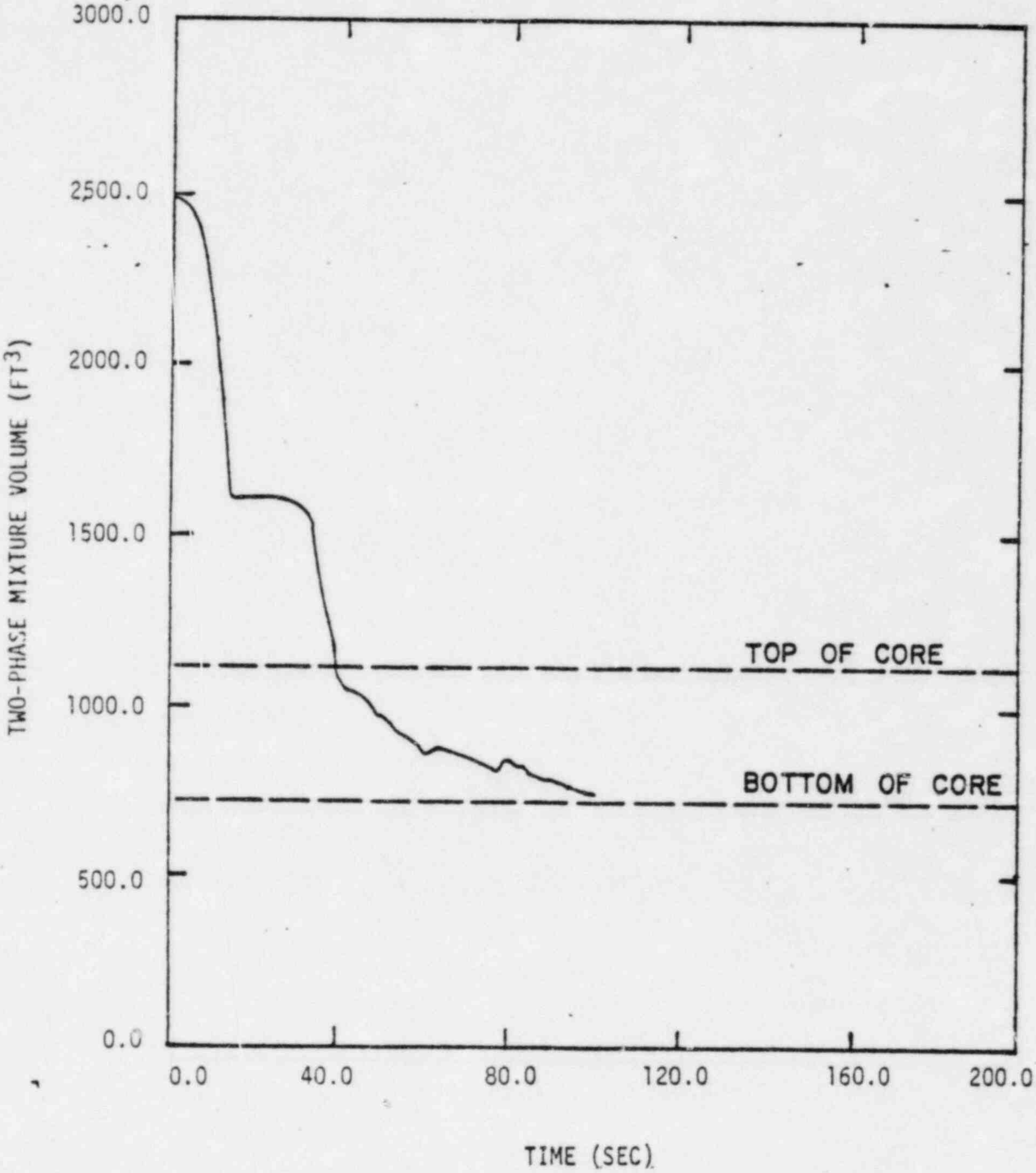


| | | |
|---|---|---|
| Omaha Public Power District<br>Fort Calhoun Station<br>Unit No. 1 | 0.5 $FT^2$ COLD LEG BREAK AT PUMP DISCHARGE-INNER VESSEL TWO PHASE MIXTURE VOLUME (SMALL BREAK ANALYSIS) | Figure 14.15-29E |

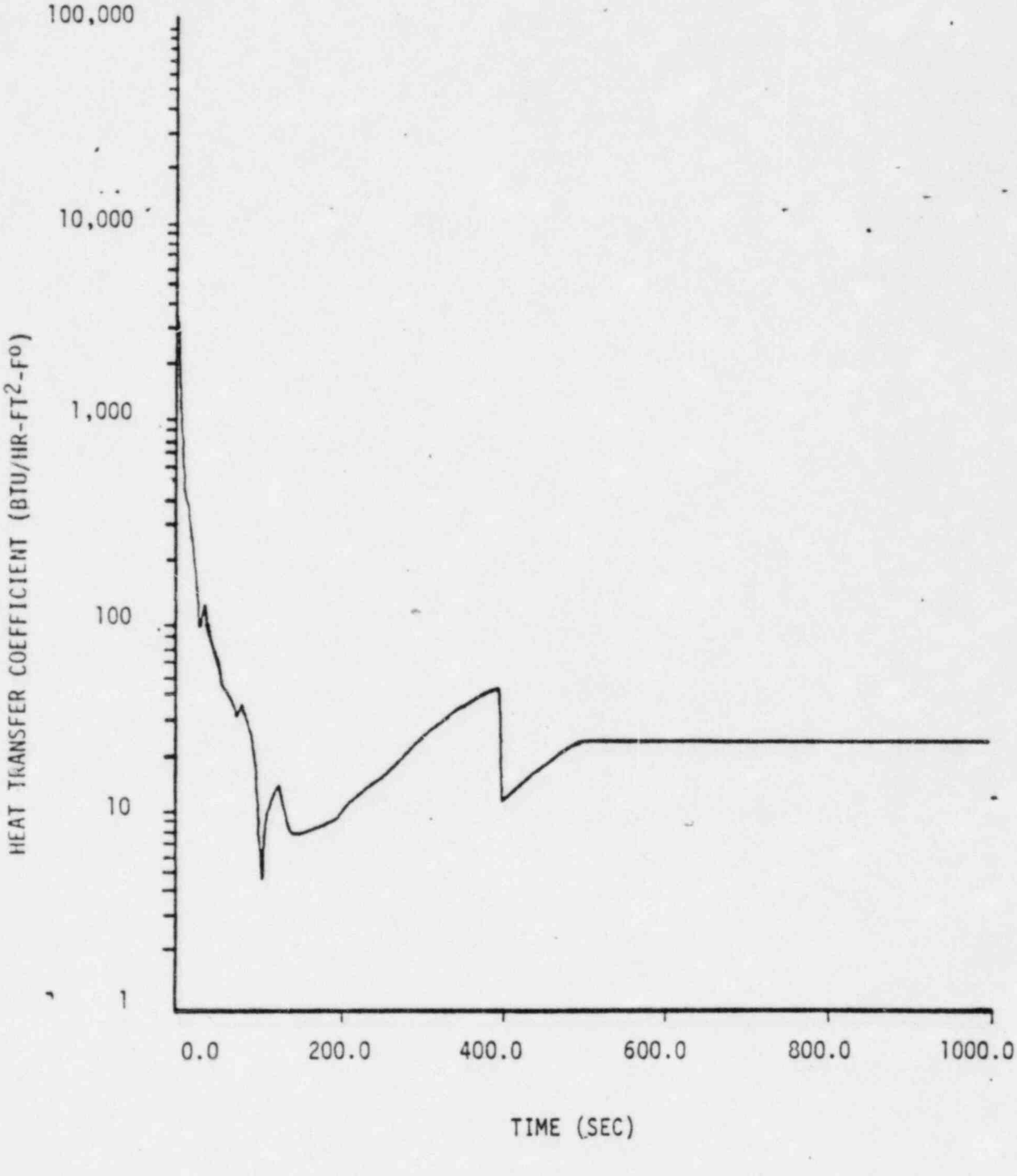


| | | |
|---|---|---|
| **Omaha Public Power District**<br>**Fort Calhoun Station**<br>**Unit No. 1** | SMALL BREAK ANALYSIS<br>0.5 $FT^2$ COLD LEG BREAK AT<br>PUMP DISCHARGE - HOT SPOT<br>HEAT TRANSFER COEFFICIENT | Figure<br>14.15-29F |

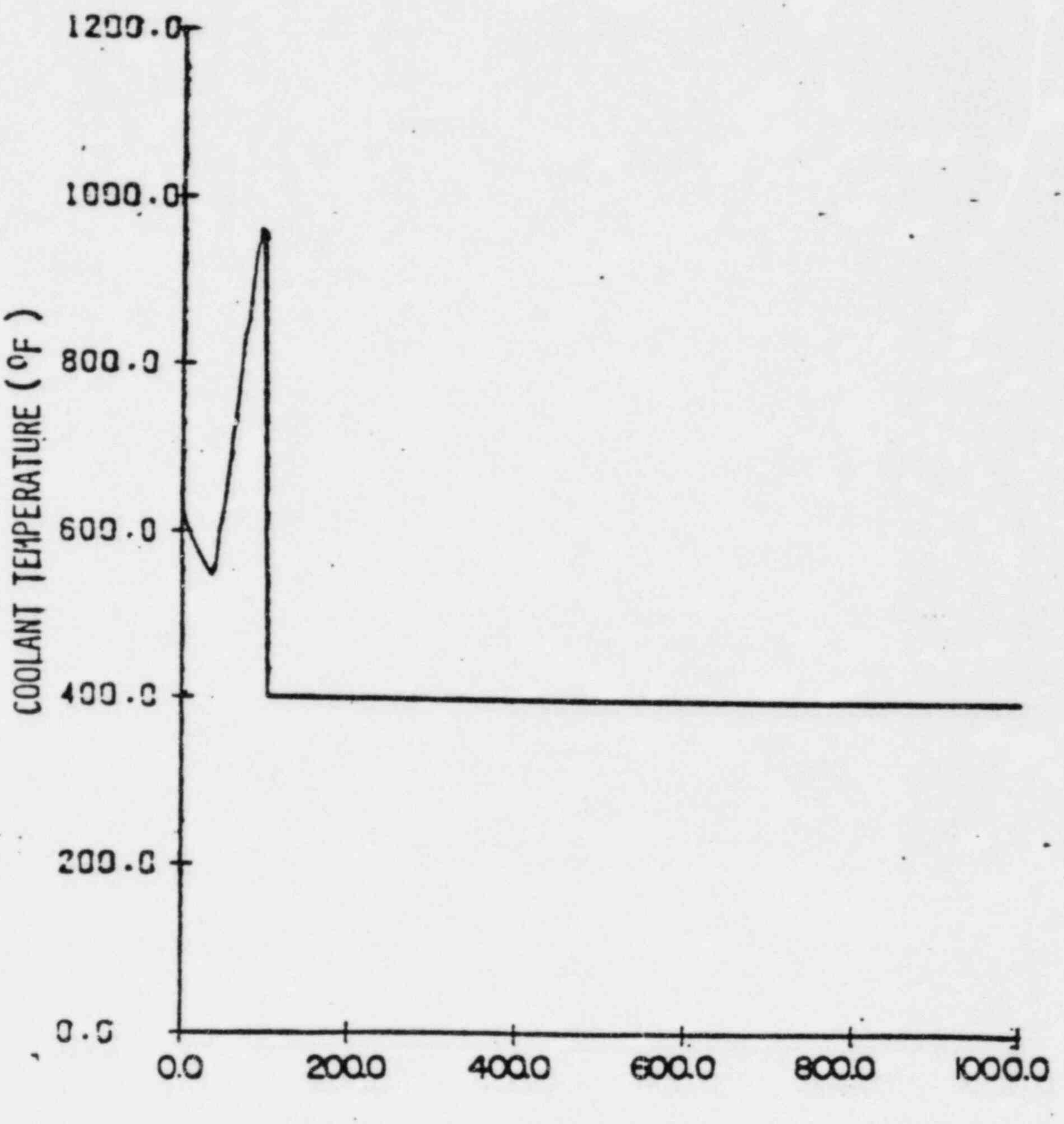


| | | |
|---|---|---|
| Omaha Public Power District<br>Fort Calhoun Station<br>Unit No. 1 | 0.5 FT² COLD LEG BREAK AT PUMP DISCHARGE, CHANNEL COOLANT TEMPERATURE AT HOT SPOT | FIGURE 14.15-29G |

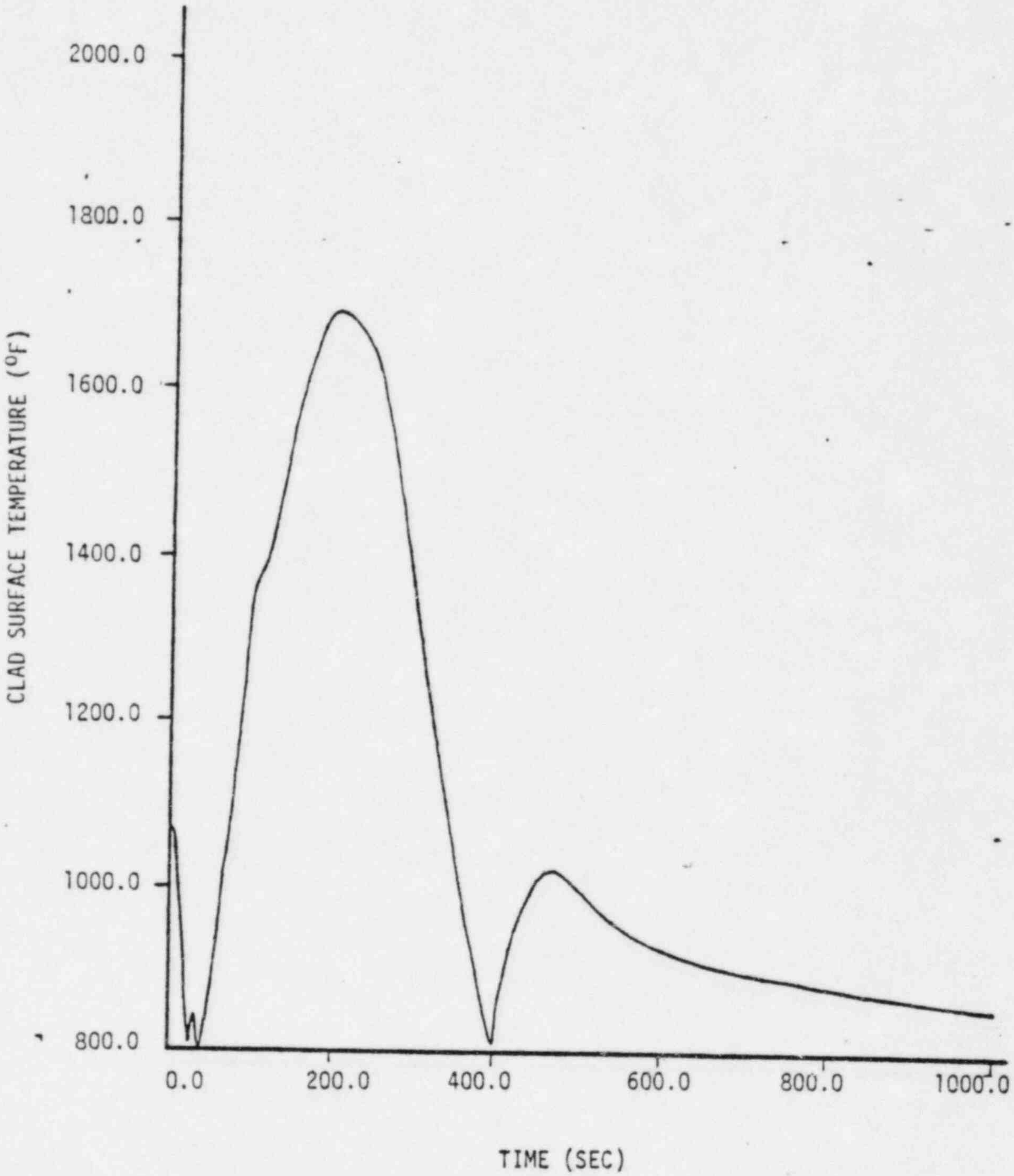


| | | |
|---|---|---|
| Omaha Public Power District<br>Fort Calhoun Station<br>Unit No. 1 | 0.5 FT COLD LEG BREAK AT PUMP DISCHARGE -<br>HOT SPOT CLAD SURFACE TEMPERATURE<br>(SMALL BREAK ANALYSIS) | Figure<br>14.15-29H |

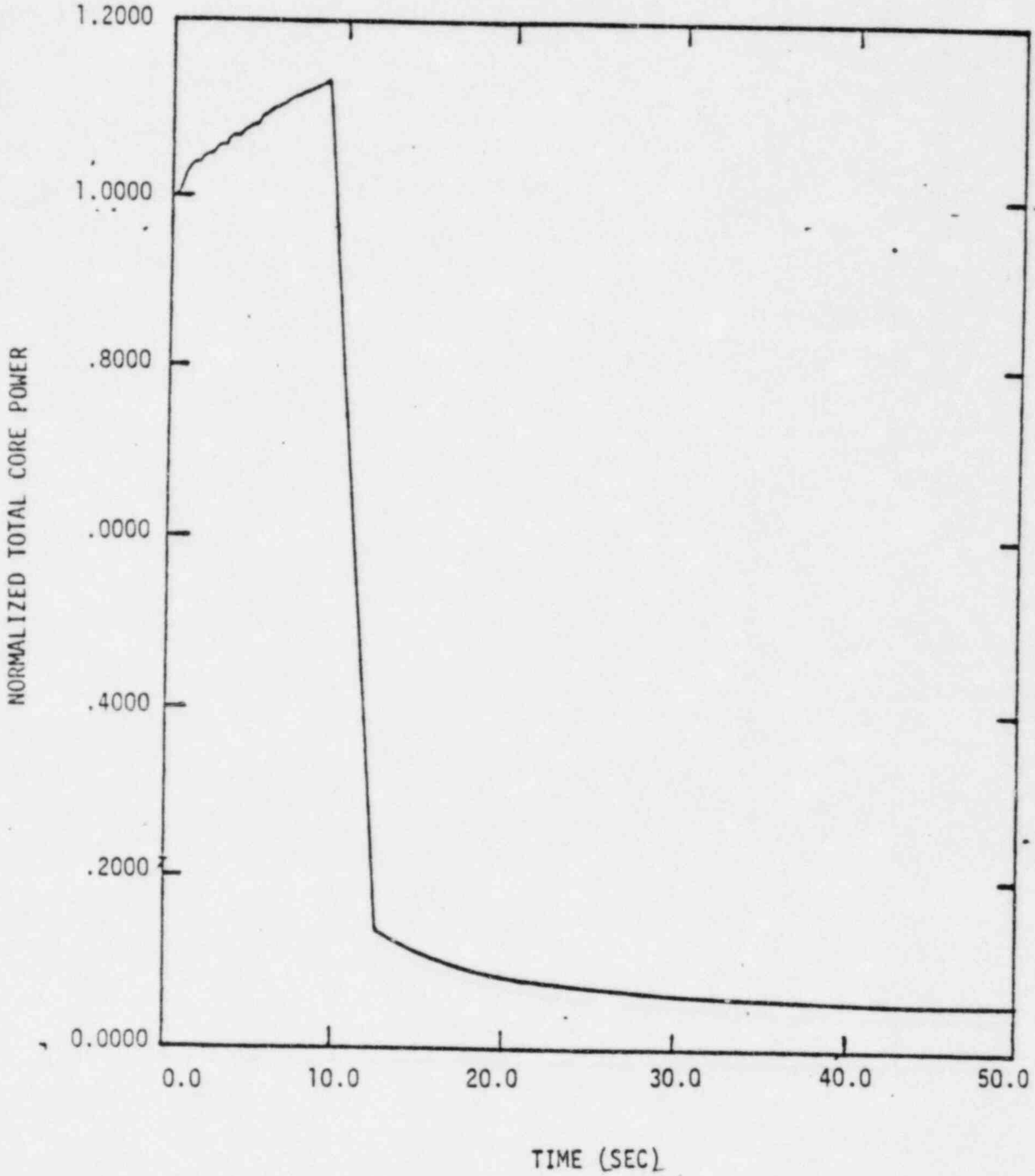


| | | |
|---|---|---|
| Omaha Public Power District<br>Fort Calhoun Station<br>Unit No. 1 | 0.1 $FT^2$ COLD LEG BREAK AT PUMP DISCHARGE-NORMALIZED TOTAL CORE POWER (SMALL BREAK ANALYSIS) | Figure 14.15-30A |

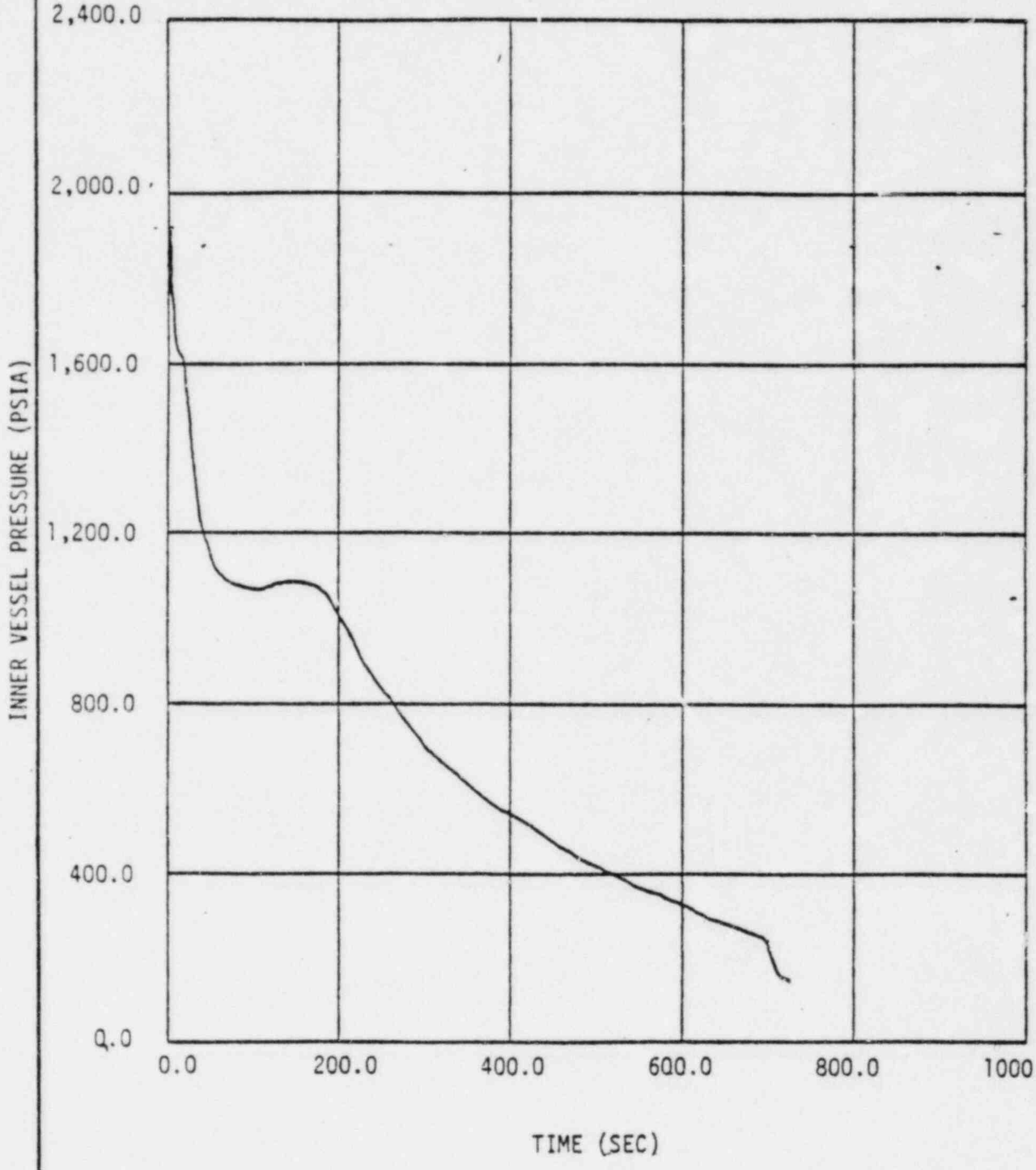


| | | |
|---|---|---|
| Omaha Public Power District<br>Fort Calhoun Station<br>Unit No. 1 | 0.1 $FT^2$ COLD LEG BREAK AT PUMP DISCHARGE-INNER VESSEL PRESSURE (SMALL BREAK ANALYSIS) | Figure 14.15-30B |

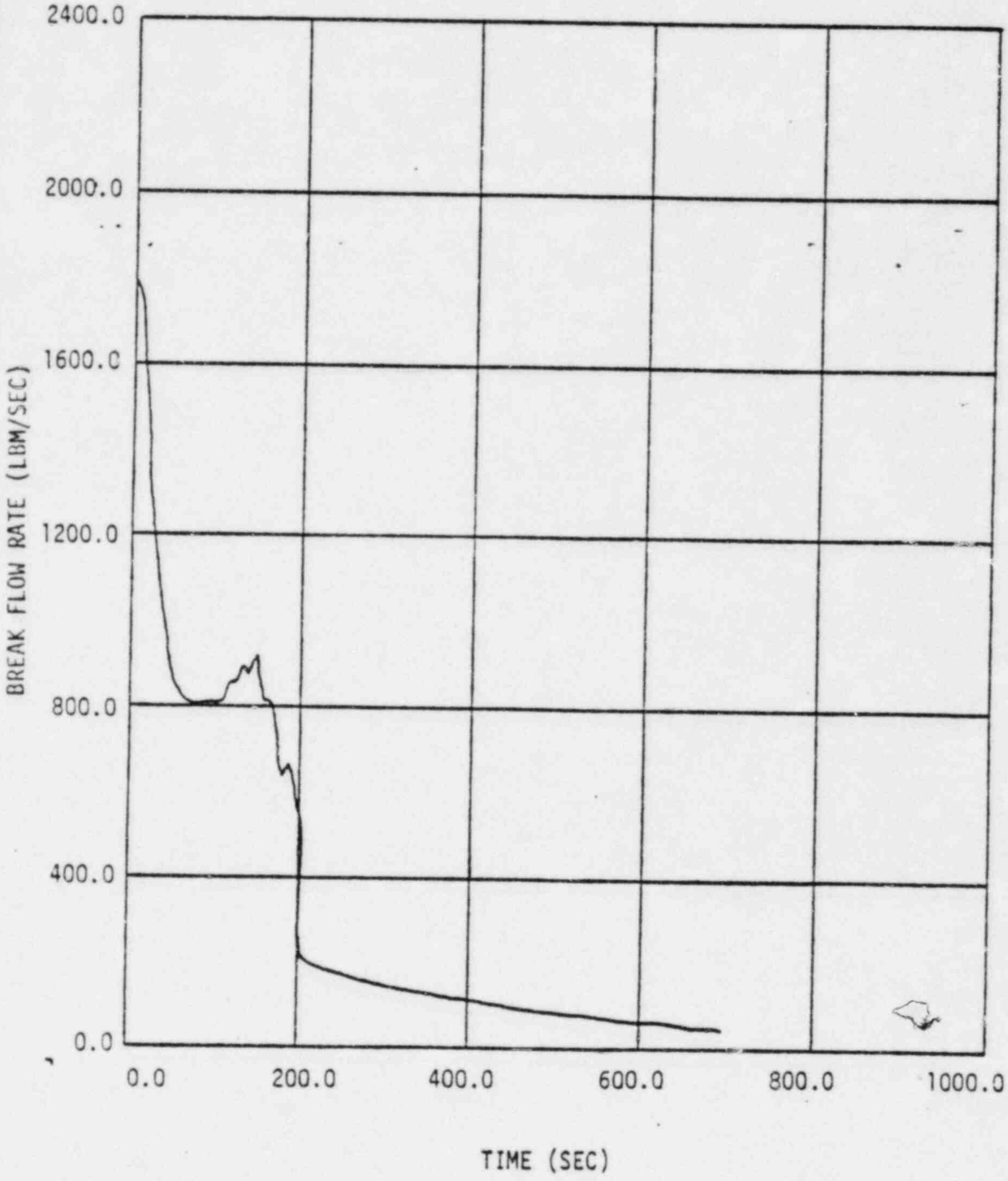


| | | |
|---|---|---|
| Omaha Public Power District<br>Fort Calhoun Station<br>Unit No. 1 | 0.1 FT$^2$ COLD LEG BREAK AT PUMP DISCHARGE-BREAK FLOW RATE (SMALL BREAK ANALYSIS) | Figure 14.15-30C |

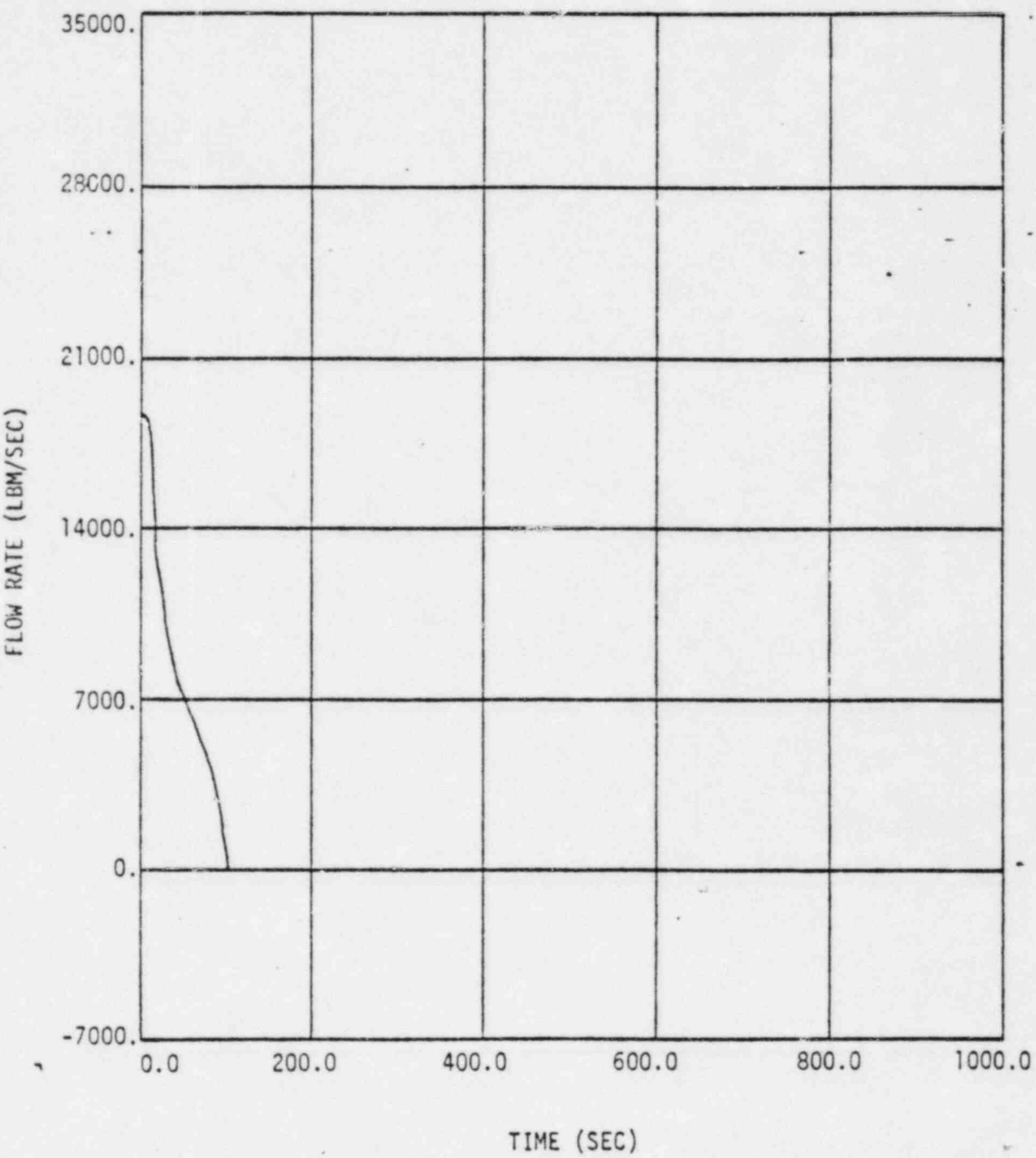


| | | |
|---|---|---|
| Omaha Public Power District<br>Fort Calhoun Station<br>Unit No. 1 | 0.1 $FT^2$ COLD LEG BREAK AT PUMP DISCHARGE - INNER VESSEL INLET FLOW RATE (SMALL BREAK ANALYSIS) | Figure 14.15-30D |

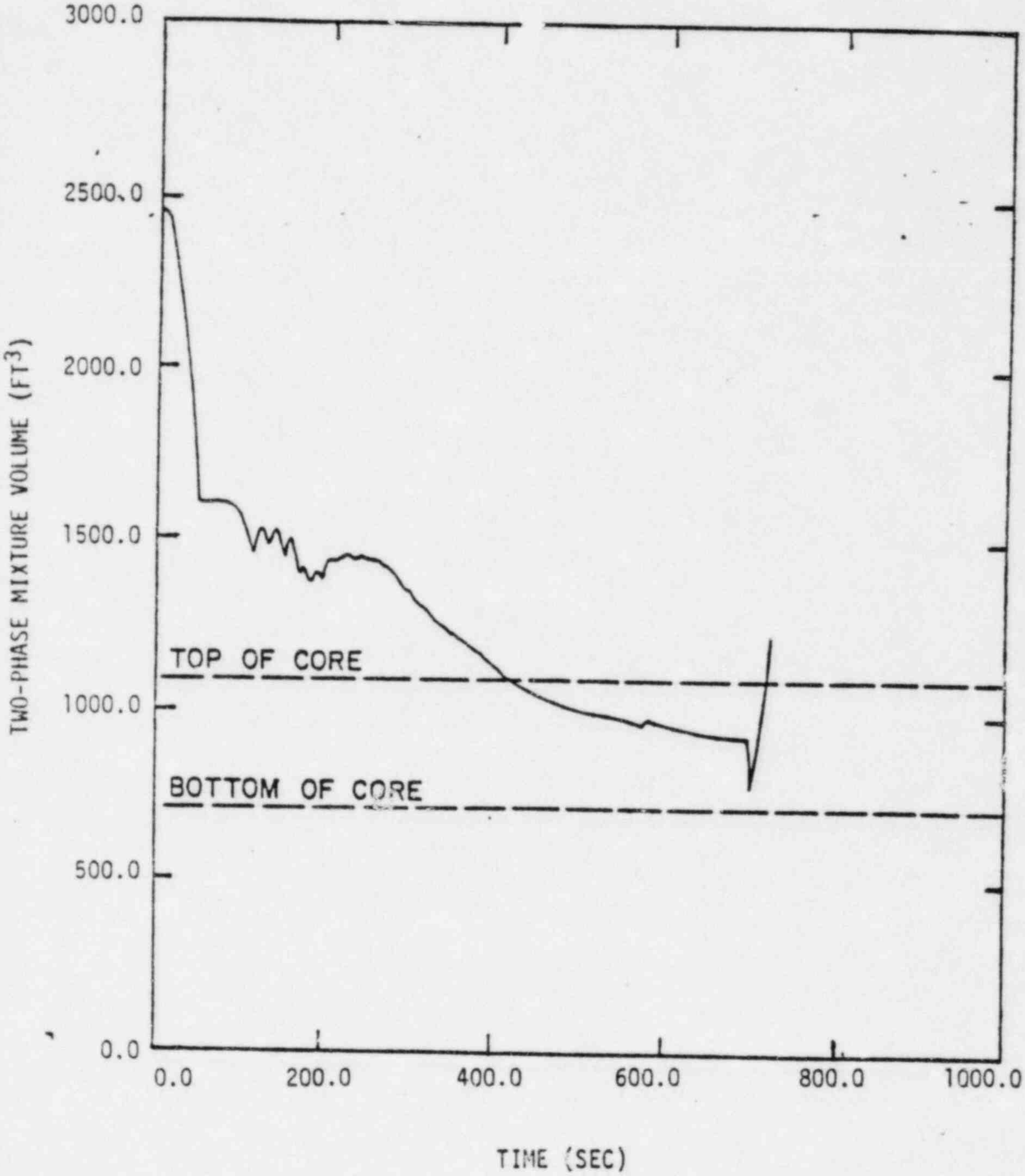


| | | |
|---|---|---|
| **Omaha Public Power District**<br>**Fort Calhoun Station**<br>**Unit No. 1** | 0.1 $FT^2$ COLD LEG BREAK AT PUMP DISCHARGE-INNER VESSEL TWO PHASE MIXTURE VOLUME (SMALL-BREAK ANALYSIS) | Figure 14.15-30E |

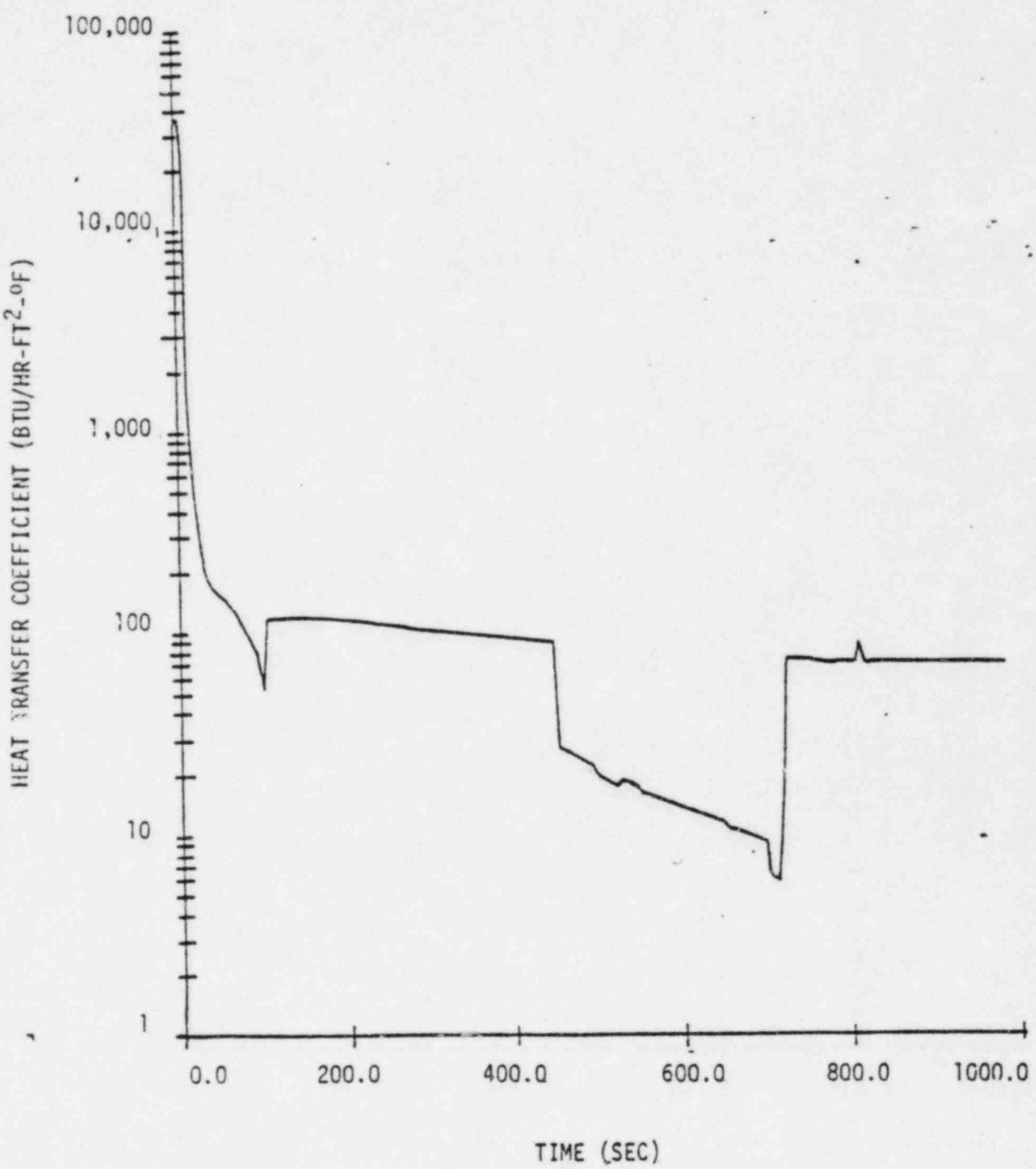


| | | |
|---|---|---|
| Omaha Public Power District<br>Fort Calhoun Station<br>Unit No. 1 | SMALL BREAK ANALYSIS<br>0.1 $FT^2$ COLD LEG BREAK AT<br>PUMP DISCHARGE - HOT SPOT<br>HEAT TRANSFER COEFFICIENT | Figure<br>14.15-30F |

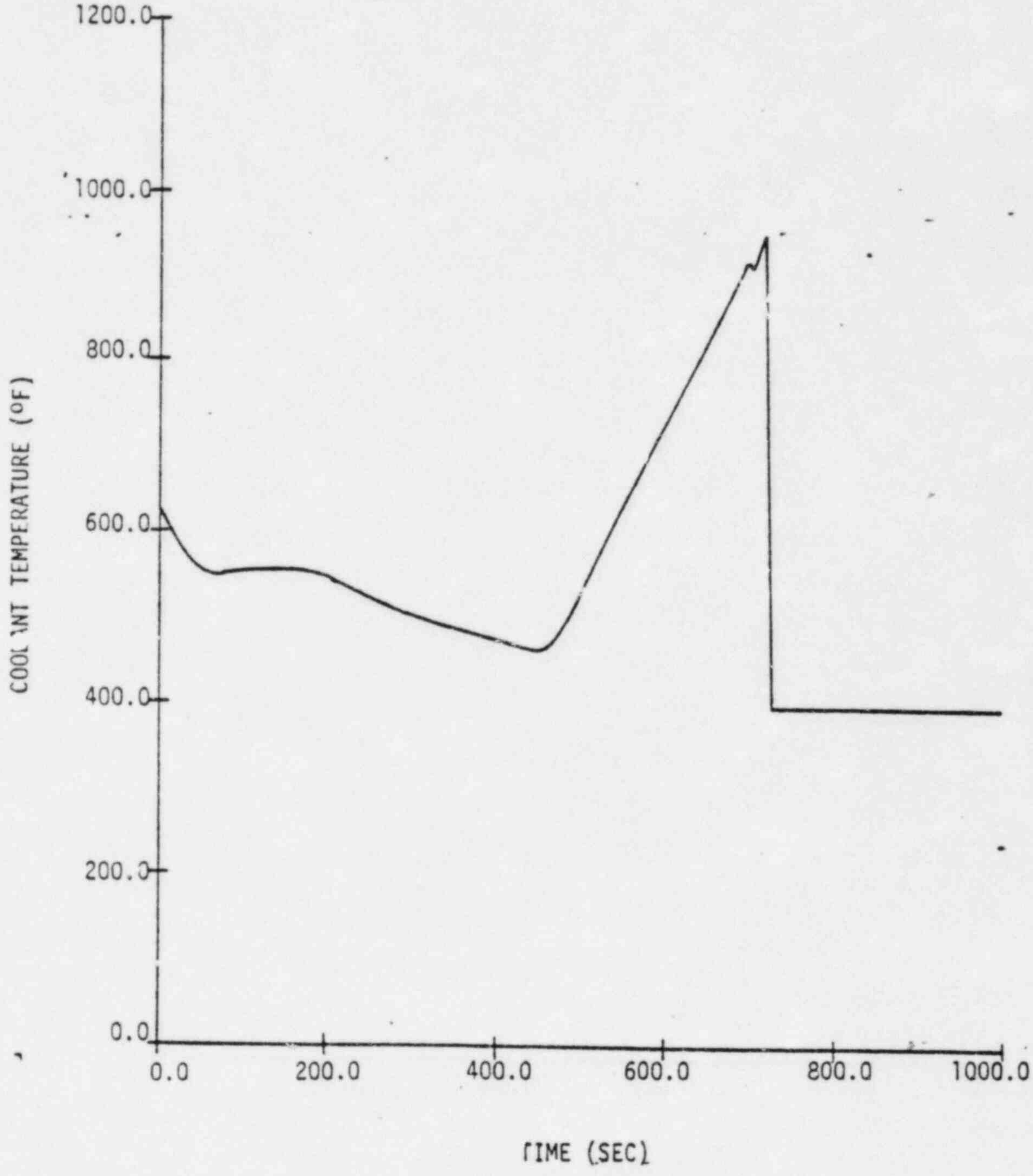


| | | |
|---|---|---|
| Omaha Public Power District<br>Fort Calhoun Station<br>Unit No. 1 | 0.1 FT$^2$ COLD LEG BREAK AT PUMP DISCHARGE-CHANNEL COOLANT TEMPERATURE AT HOT SPOT (SMALL BREAK ANALYSIS) | Figure 14.15-30G |

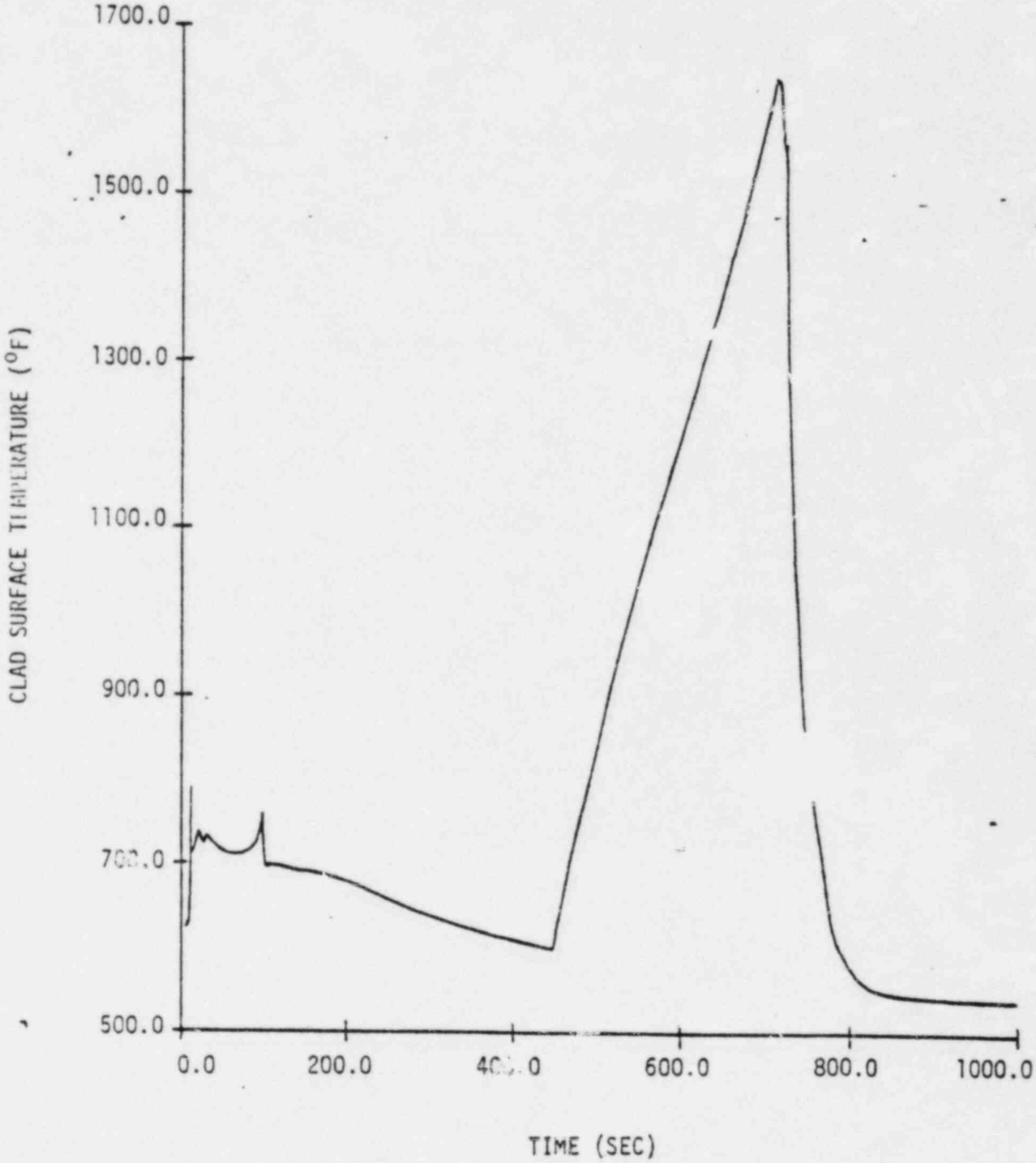


| | | |
|---|---|---|
| **Omaha Public Power District**<br>**Fort Calhoun Station**<br>**Unit No. 1** | 0.1 $FT^2$ COLD LEG BREAK AT<br>PUMP DISCHARGE-HOT SPOT<br>CLAD-SURFACE TEMPERATURE<br>(SMALL BREAK ANALYSIS) | Figure<br>14.15-30H |

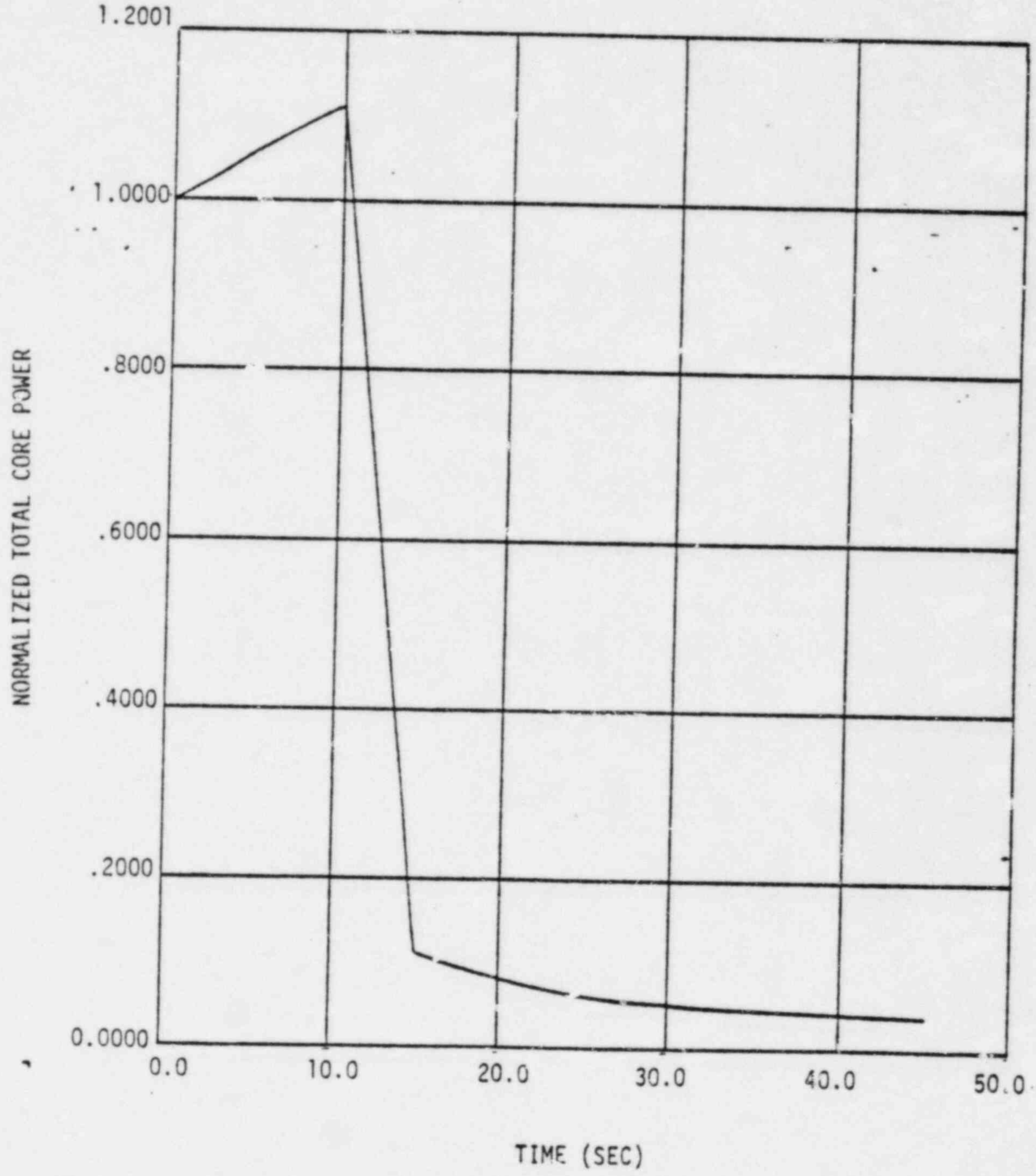


| | | |
|---|---|---|
| Omaha Public Power District<br>Fort Calhoun Station<br>Unit No. 1 | $0.075\ FT^2$ COLD LEG BREAK AT PUMP DISCHARGE-NORMALIZED TOTAL CORE POWER<br>(SMALL BREAK ANALYSIS) | Figure 14.15-31A |

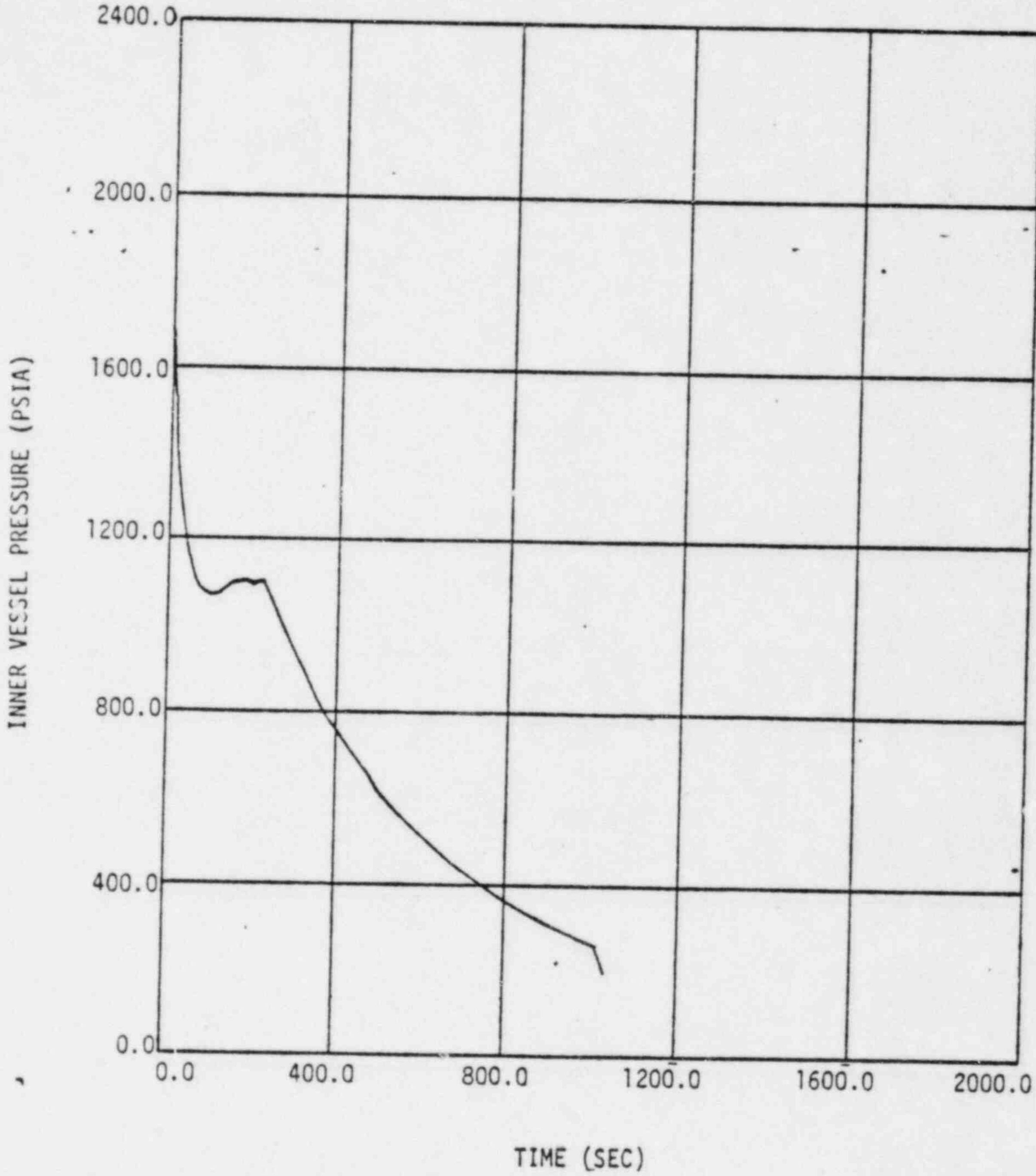


| | | |
|---|---|---|
| Omaha Public Power District<br>Fort Calhoun Station<br>Unit No. 1 | 0.075 $FT^2$ COLD LEG BREAK AT PUMP DISCHARGE-INNER VESSEL PRESSURE (SMALL BREAK ANALYSIS) | Figure 14.15-31B |

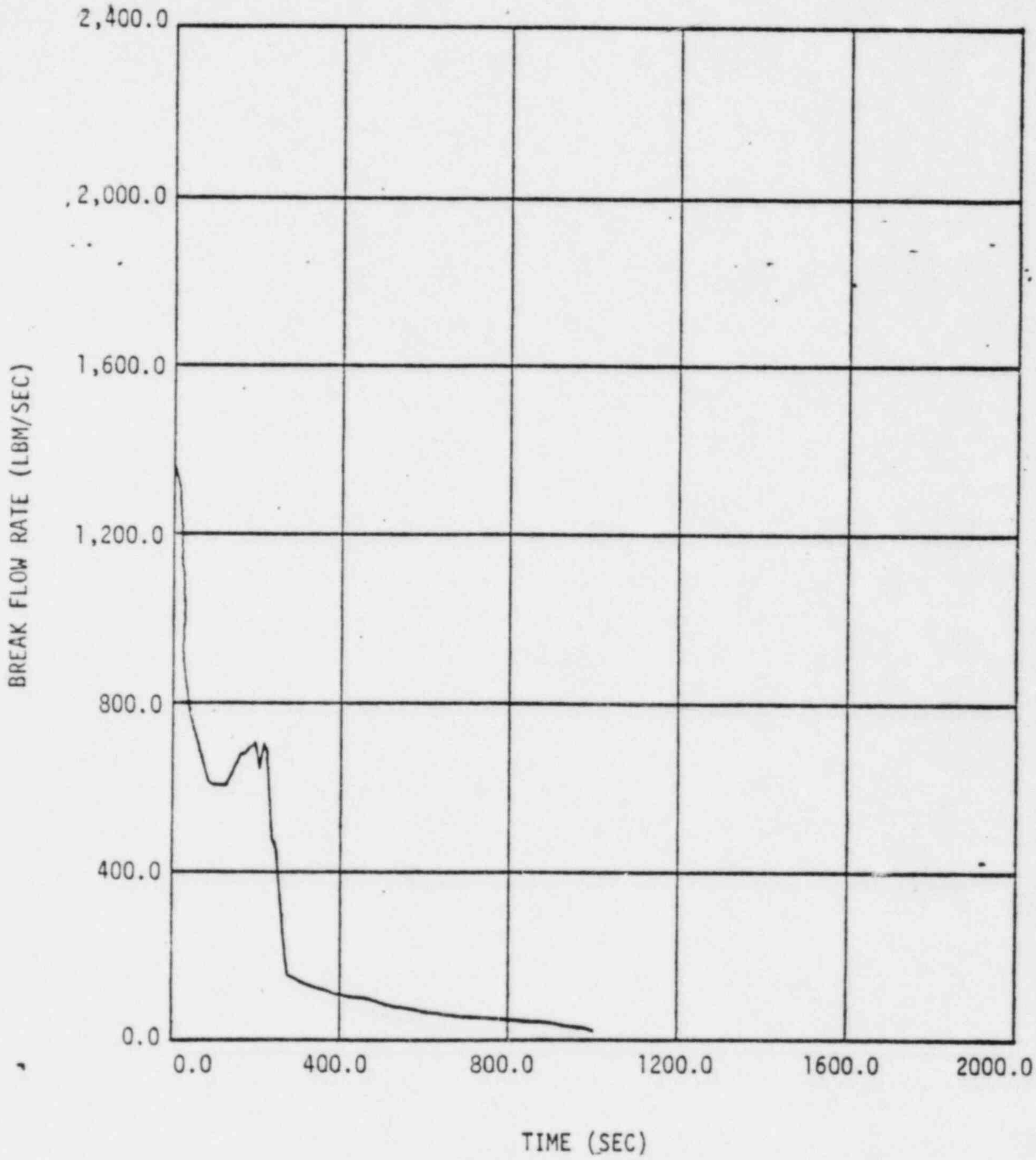


| | | |
|---|---|---|
| Omaha Public Power District<br>Fort Calhoun Station<br>Unit No. 1 | 0.075 $FT^2$ COLD LEG BREAK AT PUMP DISCHARGE - BREAK FLOW RATE (SMALL BREAK ANALYSIS) | Figure 14.15-31C |

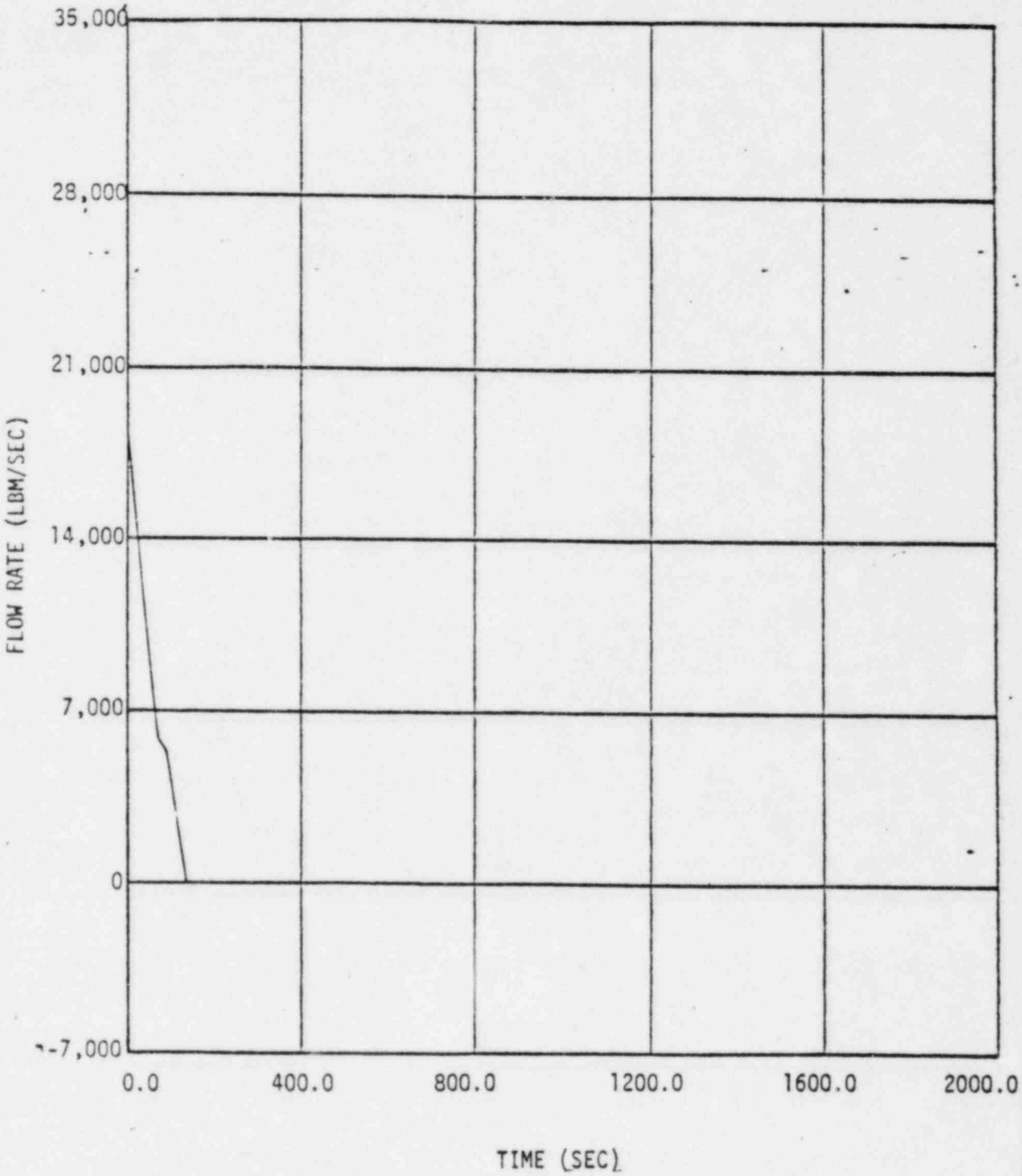


| | | |
|---|---|---|
| **Omaha Public Power District**<br>**Fort Calhoun Station**<br>**Unit No. 1** | 0.075 $FT^2$ COLD LEG BREAK AT PUMP DISCHARGE - INNER VESSEL FLOW RATE (SMALL BREAK ANALYSIS) | Figure 14.15-31D |

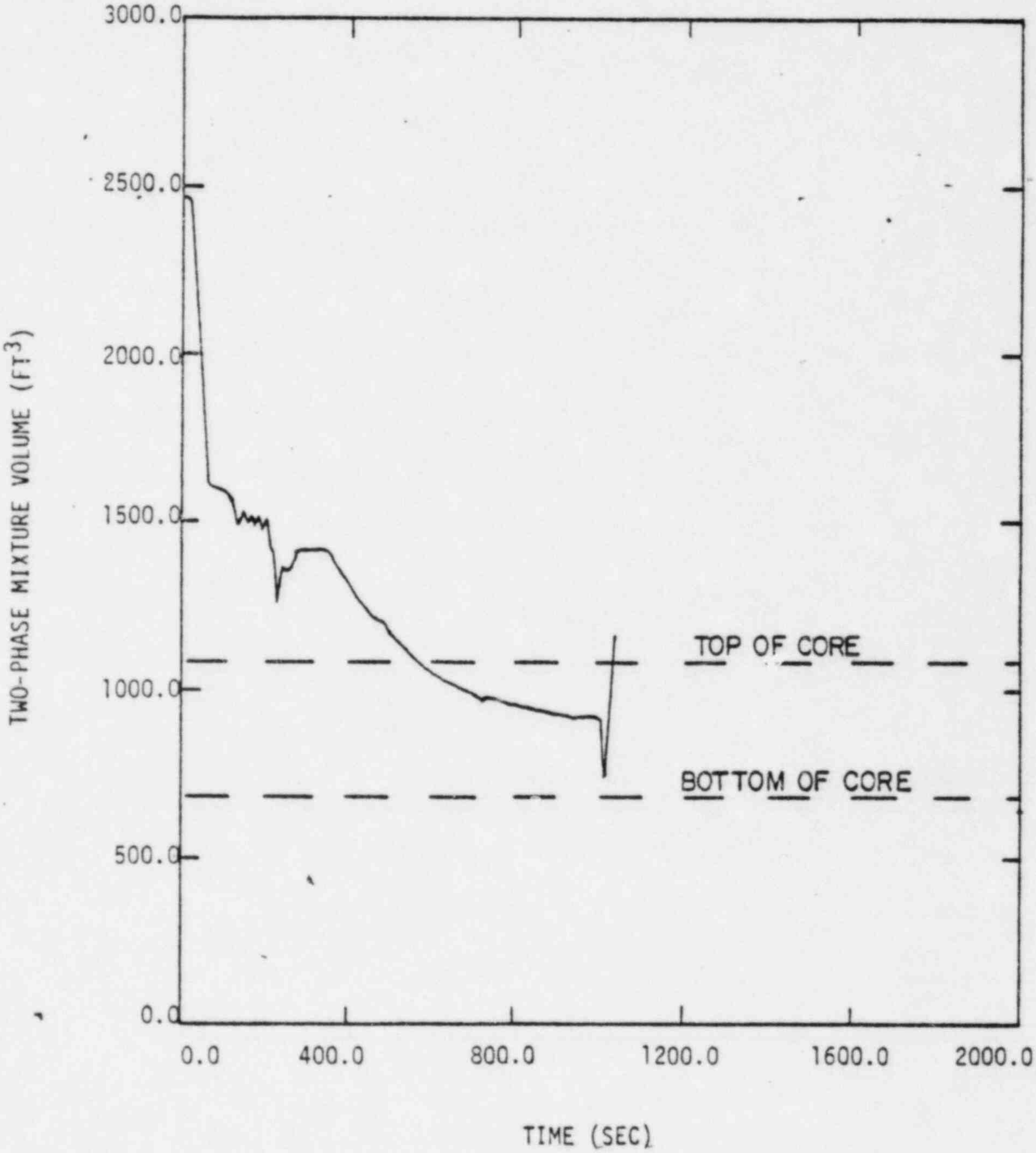


| Omaha Public Power District<br>Fort Calhoun Station<br>Unit No. 1 | 0.075 FT$^2$ COLD LEG BREAK AT PUMP DISCHARGE-INNER VESSEL TWO-PHASE MIXTURE VOLUME (SMALL BREAK ANALYSIS) | Figure 14.15-31E |
|---|---|---|

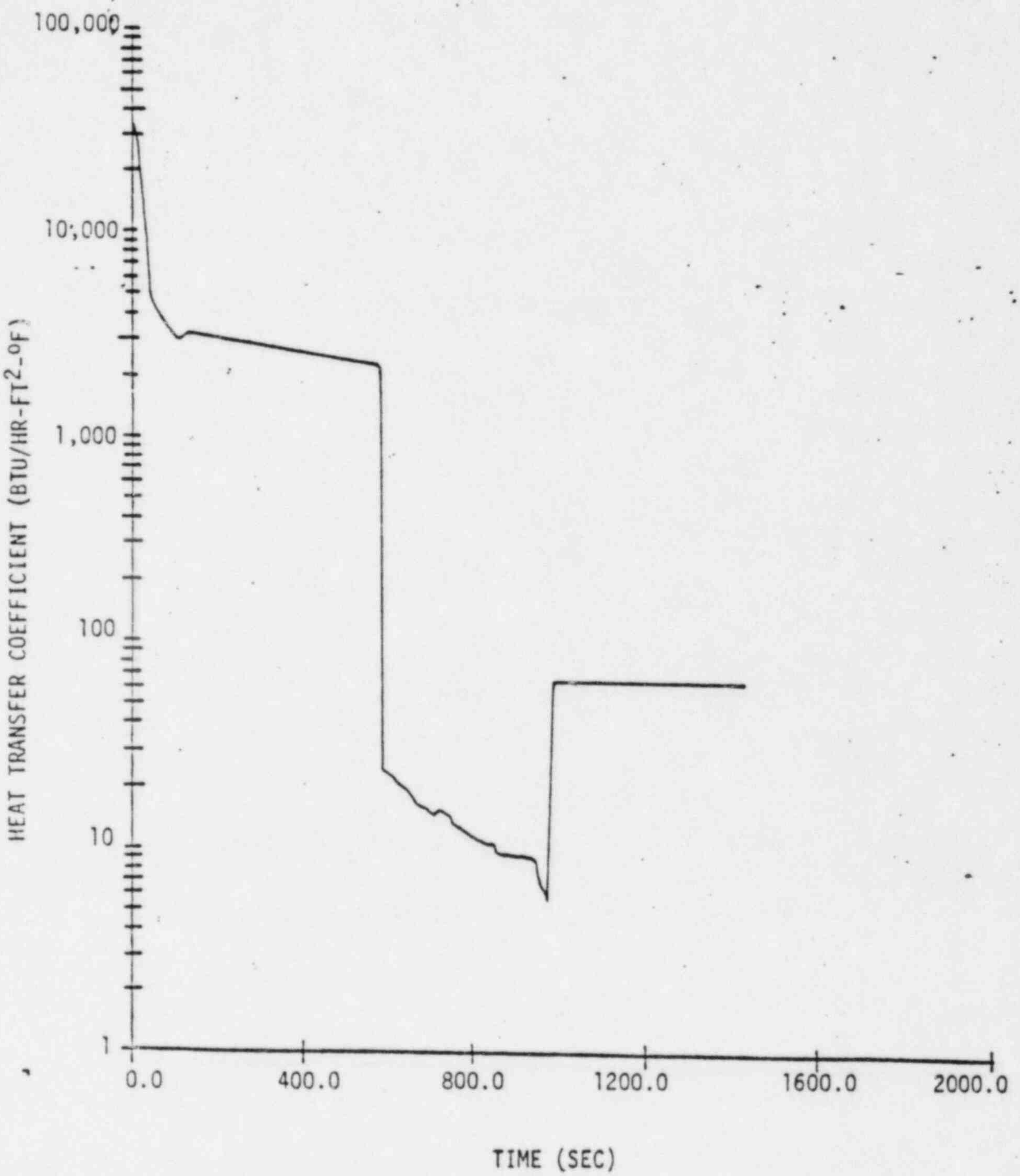


| | | |
|---|---|---|
| **Omaha Public Power District**<br>**Fort Calhoun Station**<br>**Unit No. 1** | SMALL BREAK ANALYSIS<br>.075 $FT^2$ COLD LEG BREAK AT PUMP DISCHARGE - HOT SPOT HEAT TRANSFER COEFFICIENT | Figure<br>14.15-31F |

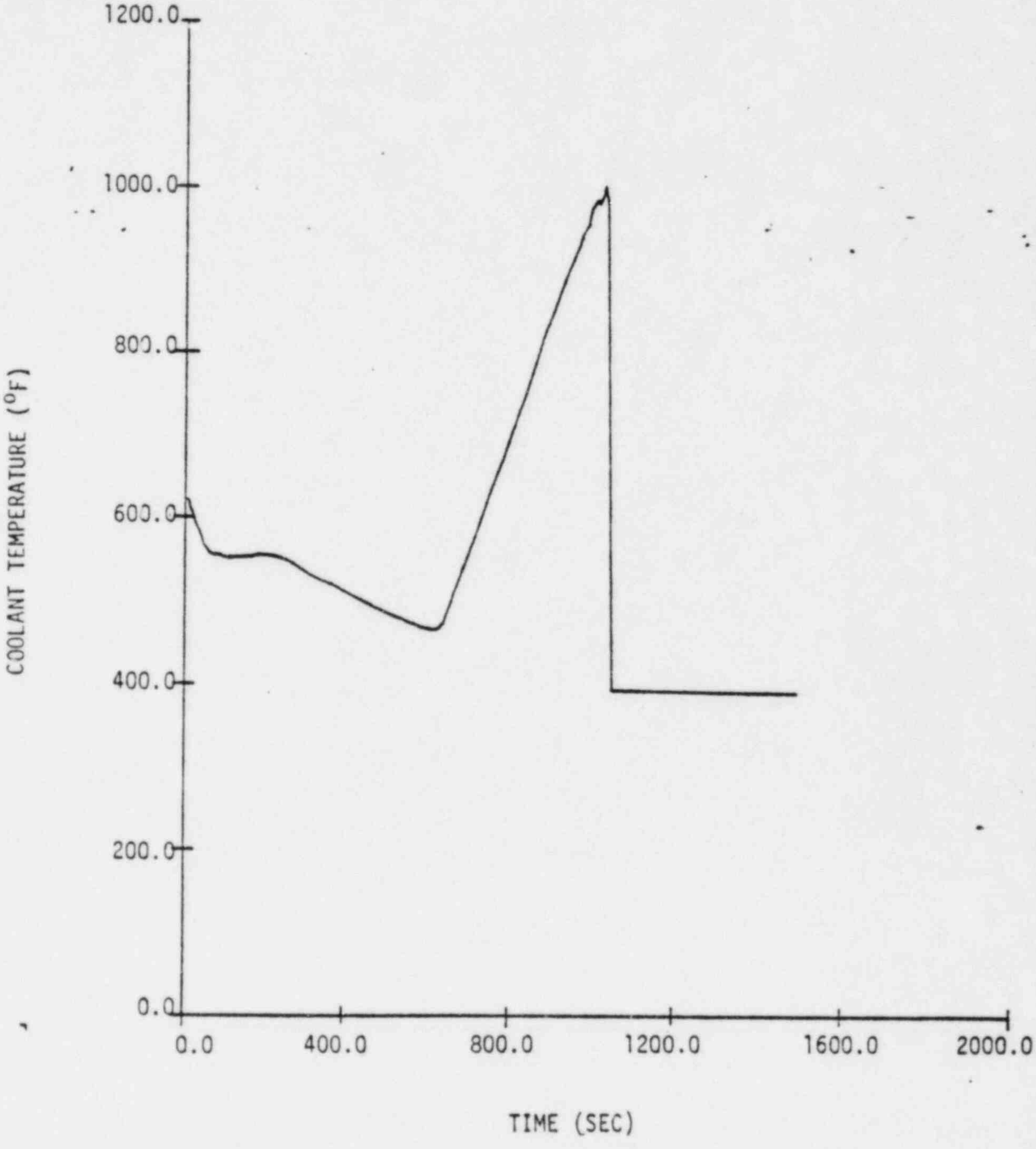


| | | |
|---|---|---|
| Omaha Public Power District<br>Fort Calhoun Station<br>Unit No. 1 | 0.075 FT$^2$ COLD LEG BREAK AT PUMP DISCHARGE-CHANNEL COOLANT TEMP. AT HOT SPOT (SMALL BREAK ANALYSIS) | Figure 14.15-31G |

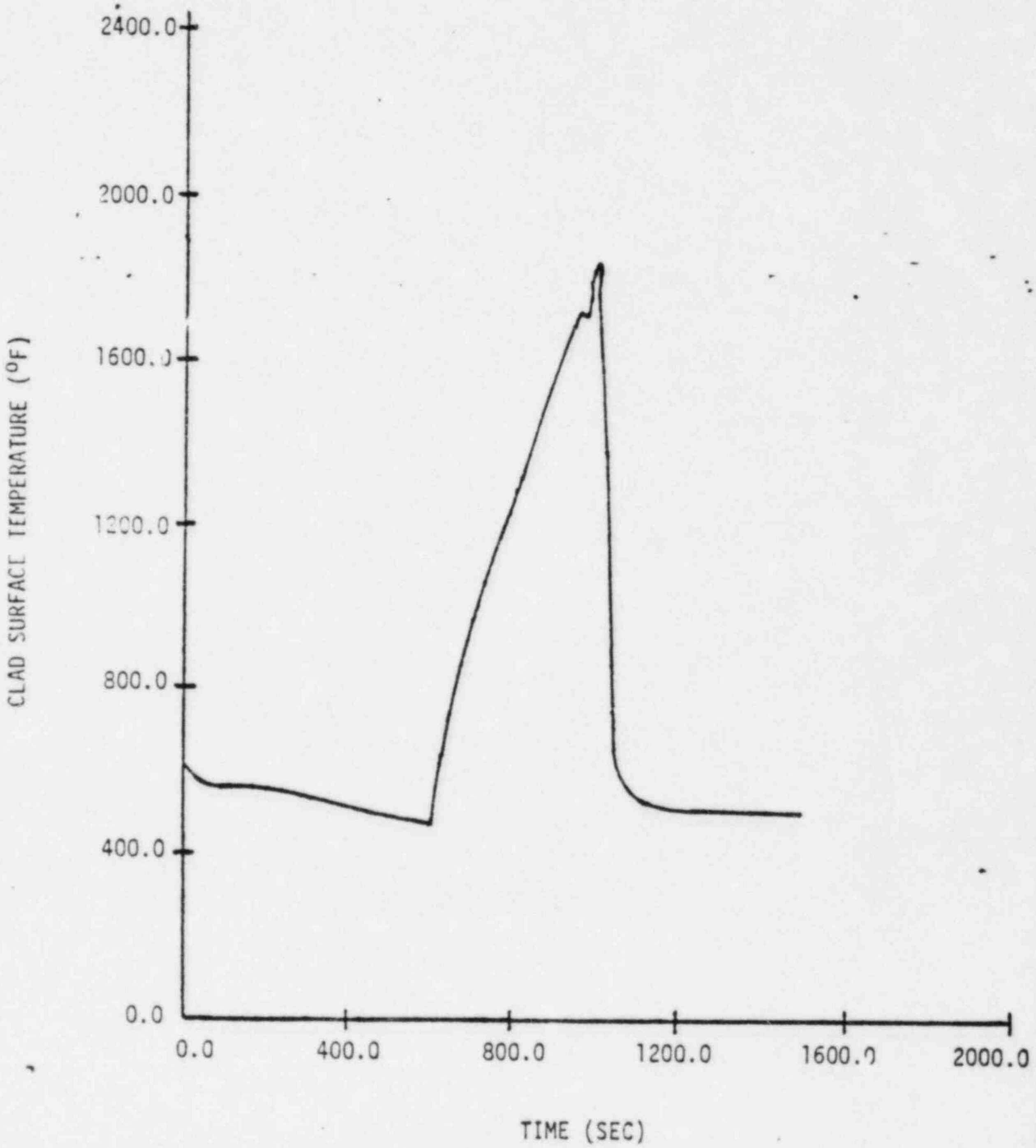


| | | |
|---|---|---|
| **Omaha Public Power District**<br>**Fort Calhoun Station**<br>**Unit No. 1** | 0.075 $FT^2$ COLD LEG BREAK AT PUMP DISCHARGE-HOT SPOT CLAD SURFACE TEMPERATURE (SMALL BREAK ANALYSIS) | Figure 14.15-31H |

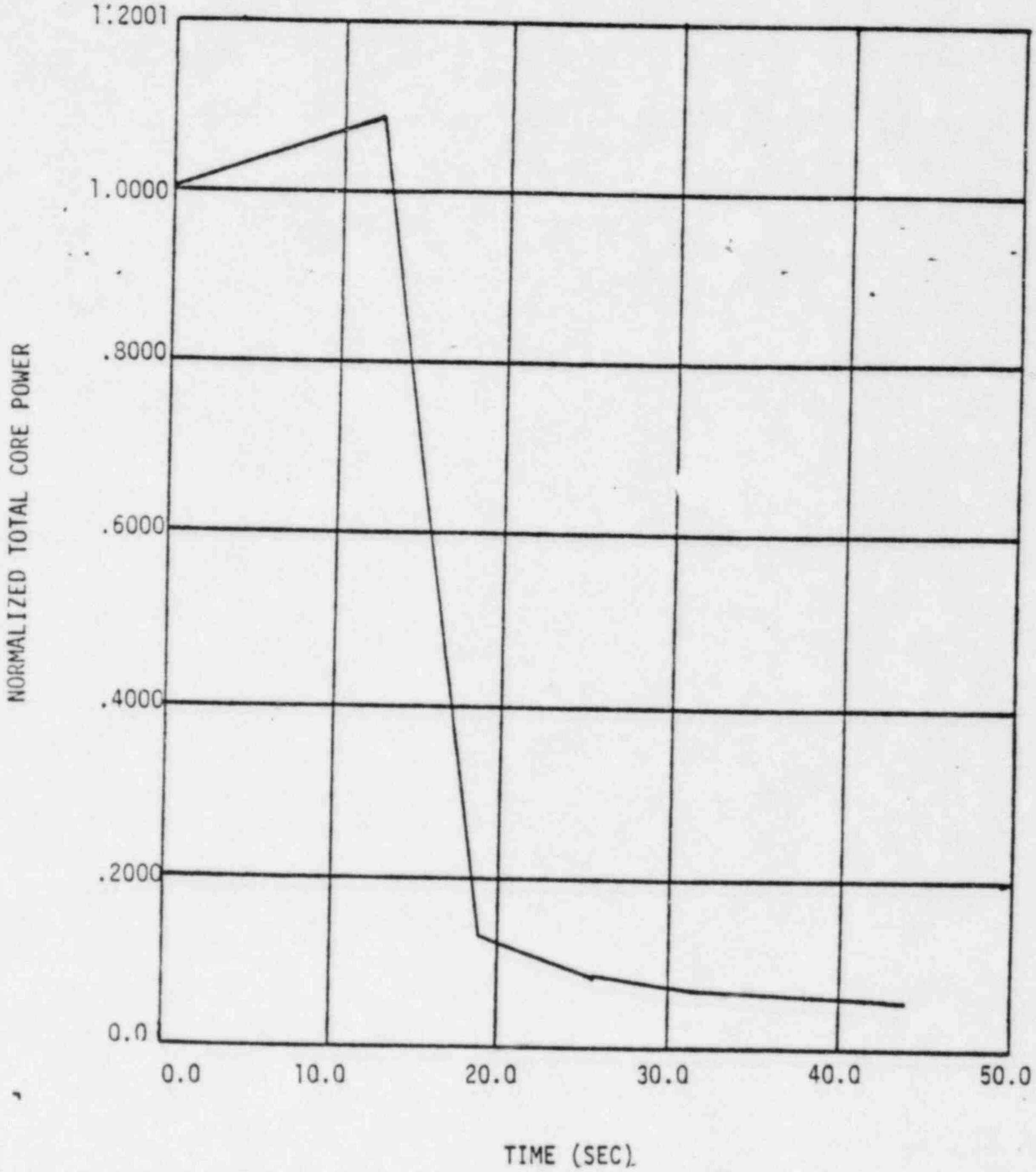


| Omaha Public Power District<br>Fort Calhoun Station<br>Unit No. 1 | 0.05 $FT^2$ COLD LEG BREAK AT PUMP DISCHARGE-NORMALIZED TOTAL CORE POWER (SMALL BREAK ANALYSIS) | Figure 14.15-32A |
|---|---|---|

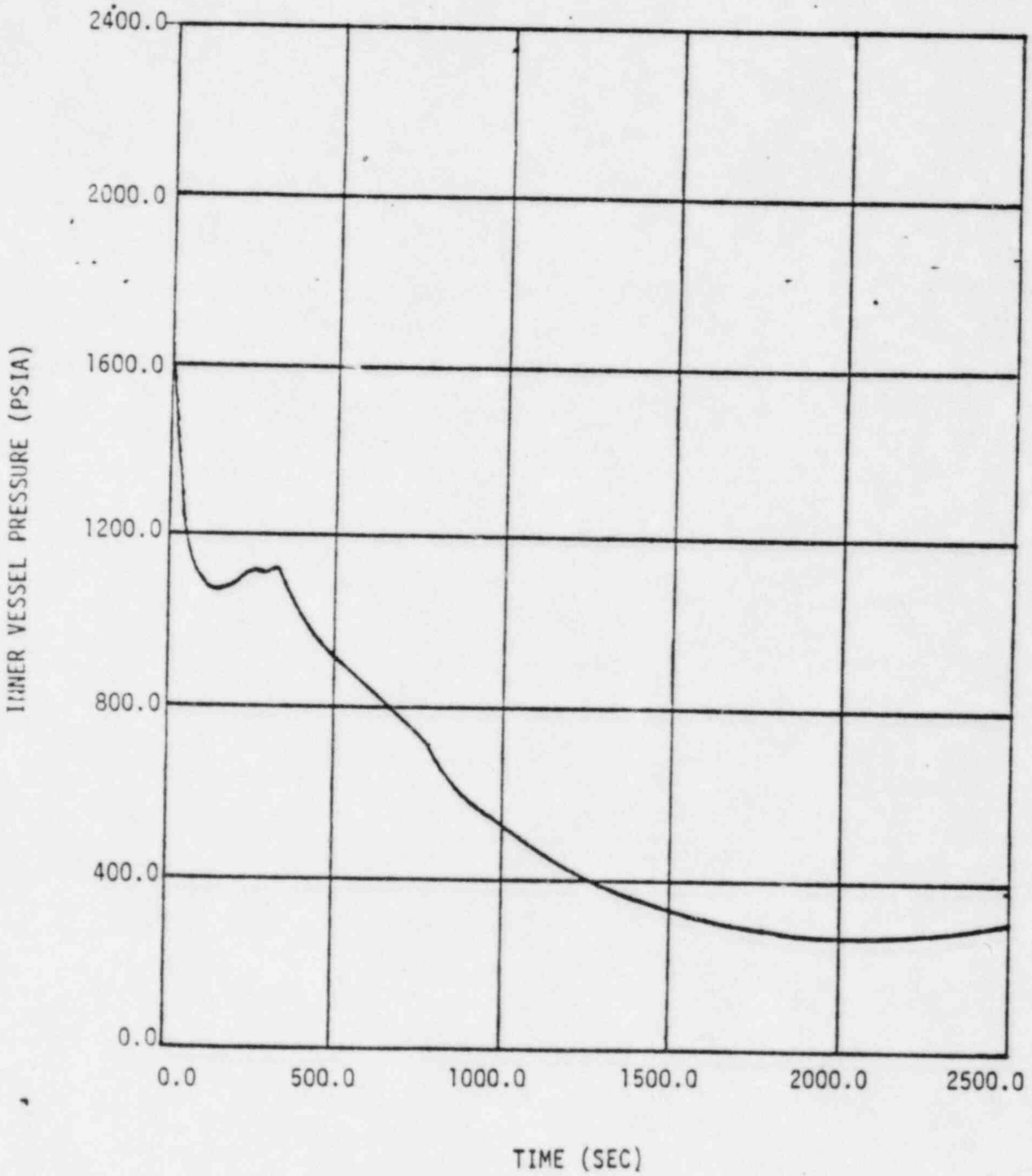


| | | |
|---|---|---|
| Omaha Public Power District<br>Fort Calhoun Station<br>Unit No. 1 | 0.05 $FT^2$ COLD LEG BREAK AT PUMP DISCHARGE-INNER VESSEL PRESSURE (SMALL BREAK ANALYSIS) | Figure 14.15-32B |

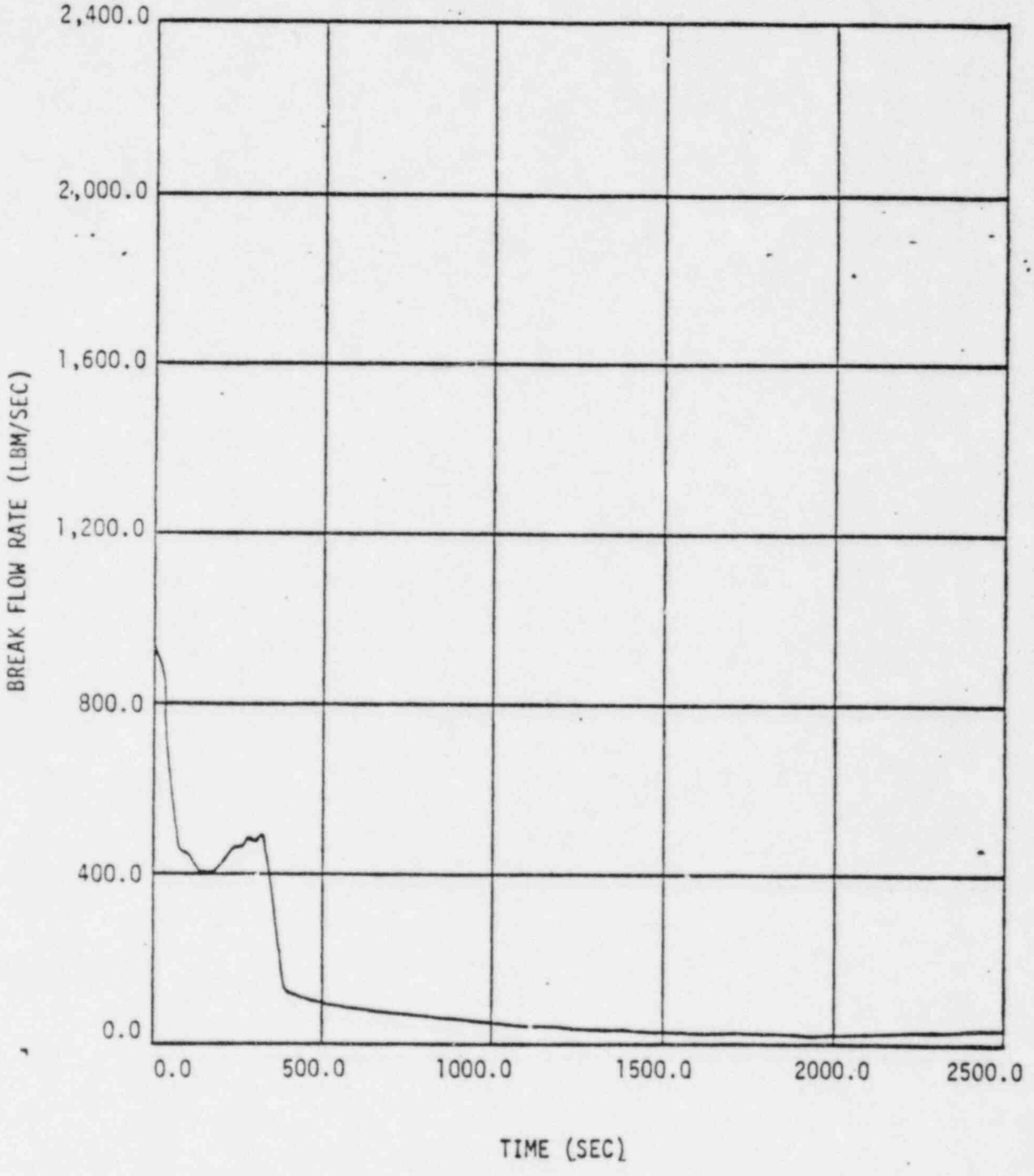


| | | |
|---|---|---|
| Omaha Public Power District<br>Fort Calhoun Station<br>Unit No. 1 | 0.05 FT$^2$ COLD LEG BREAK AT PUMP DISCHARGE - BREAK FLOW RATE (SMALL BREAK ANALYSIS) | Figure 14.15-32C |

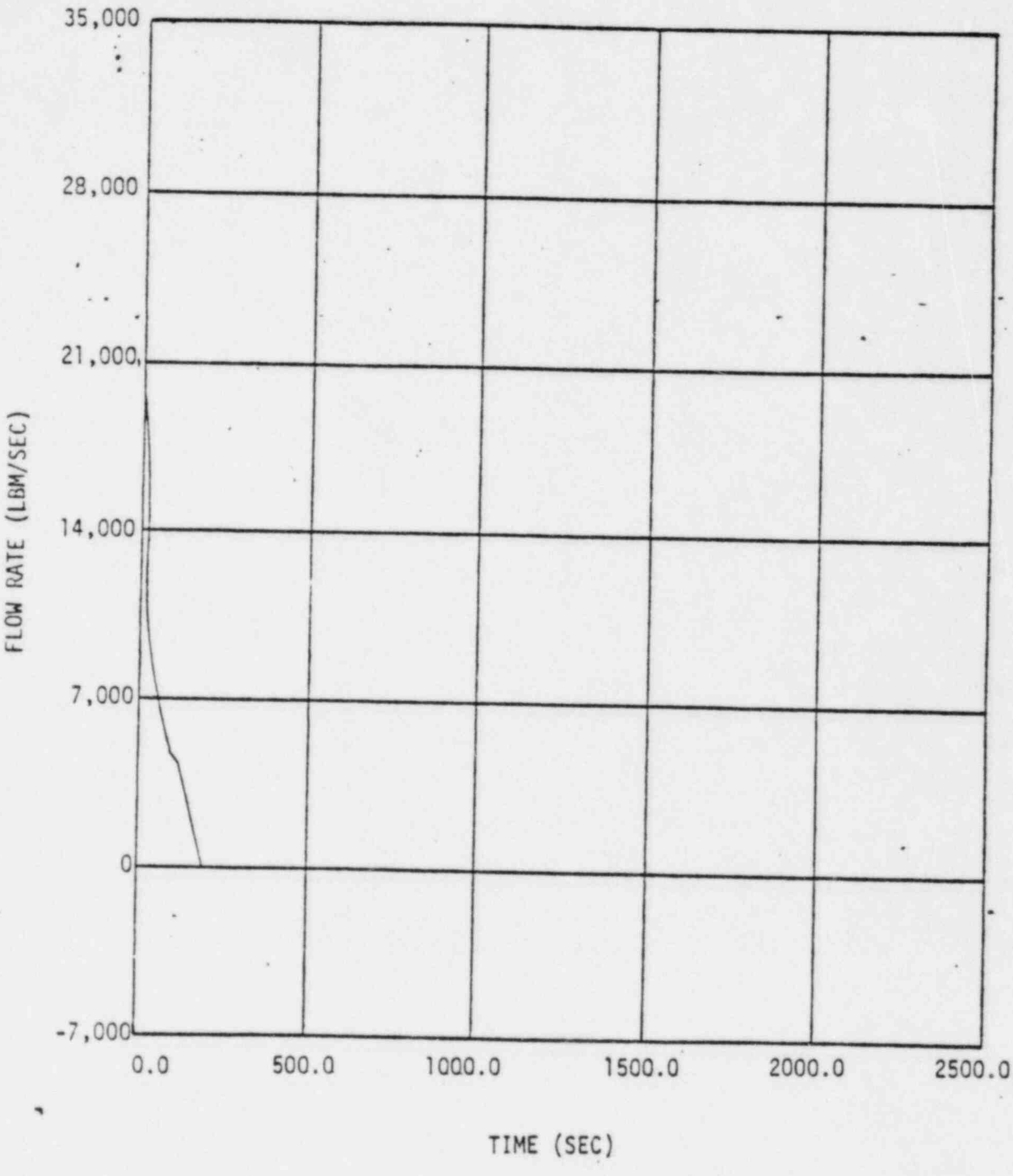


| | | |
|---|---|---|
| Omaha Public Power District<br>Fort Calhoun Station<br>Unit No. 1 | 0.05 $FT^2$ COLD LEG BREAK AT PUMP DISCHARGE - INNER VESSEL INLET FLOW RATE (SMALL BREAK ANALYSIS) | Figure 14.15-32D |

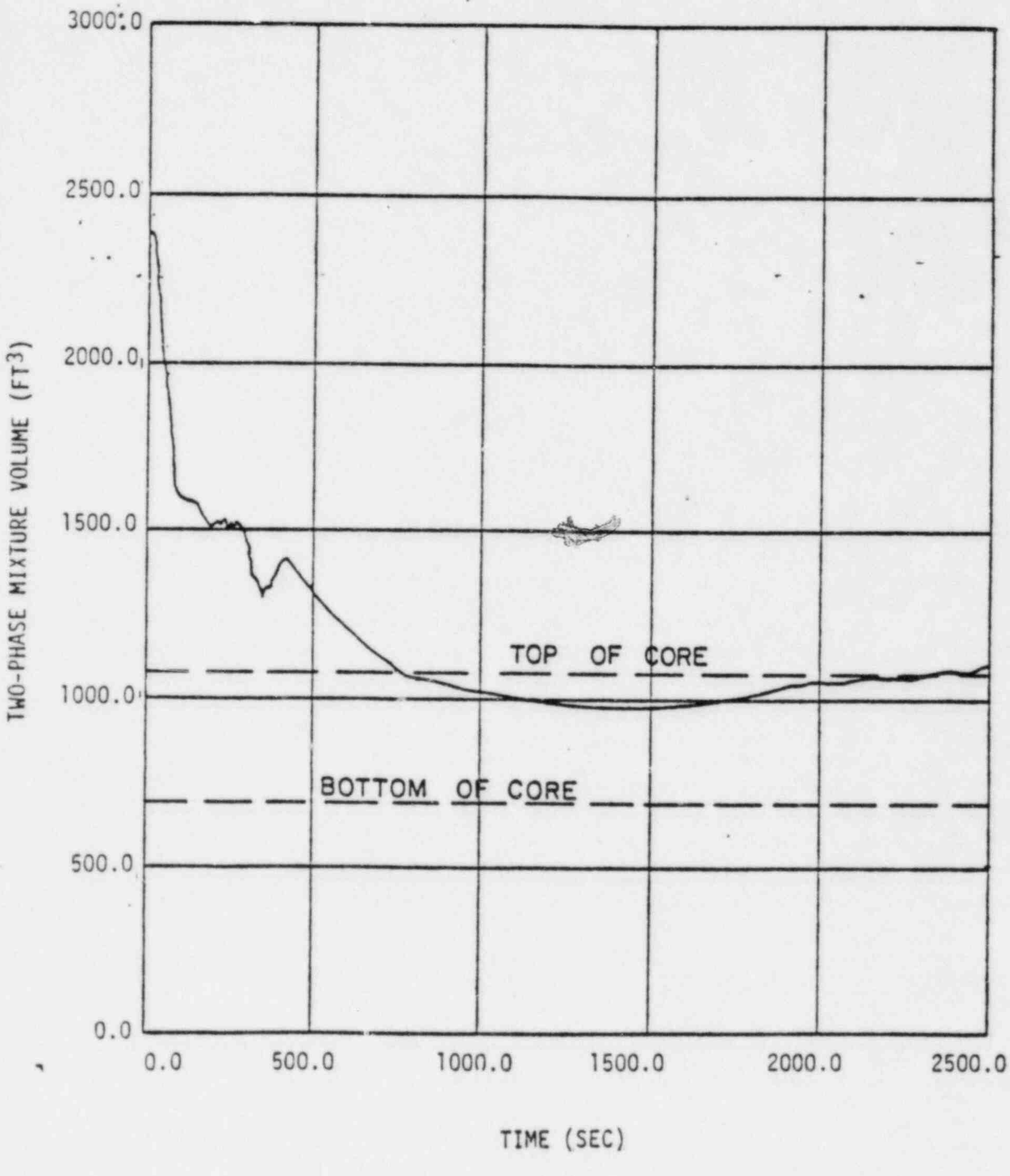


| | | |
|---|---|---|
| Omaha Public Power District<br>Fort Calhoun Station<br>Unit No. 1 | SMALL BREAK ANALYSIS<br>.05 $FT^2$ COLD LEG BREAK AT<br>PUMP DISCHARGE - INNER VESSEL<br>TWO-PHASE MIXTURE VOLUME | Figure<br>14.15-32E |

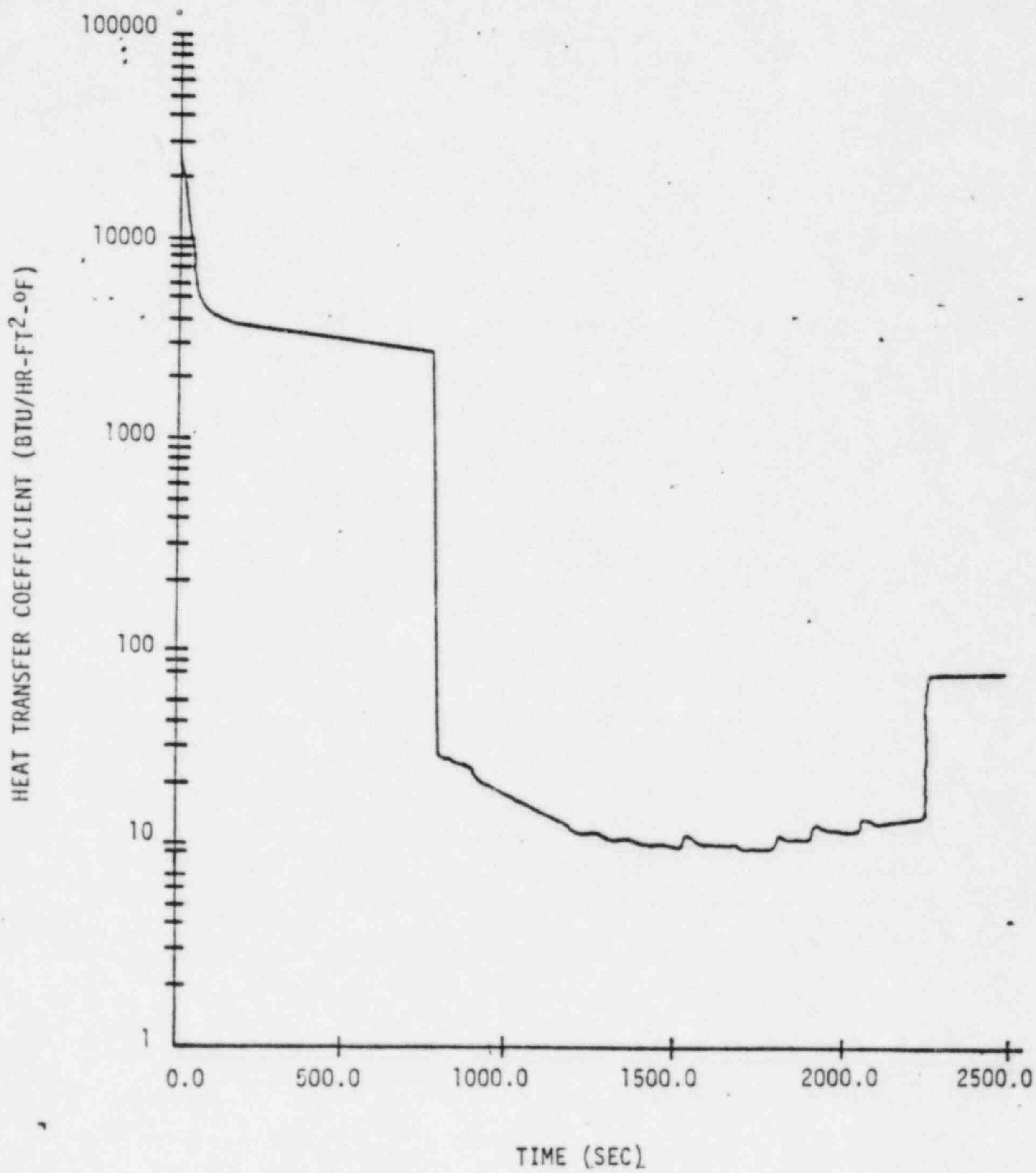


| | | |
|---|---|---|
| Omaha Public Power District<br>Fort Calhoun Station<br>Unit No. 1 | 0.05 $FT^2$ COLD LEG BREAK AT PUMP DISCHARGE-HOT SPOT HEAT TRANSFER COEFFICIENT (SMALL BREAK ANALYSIS) | Figure 14.15-32F |

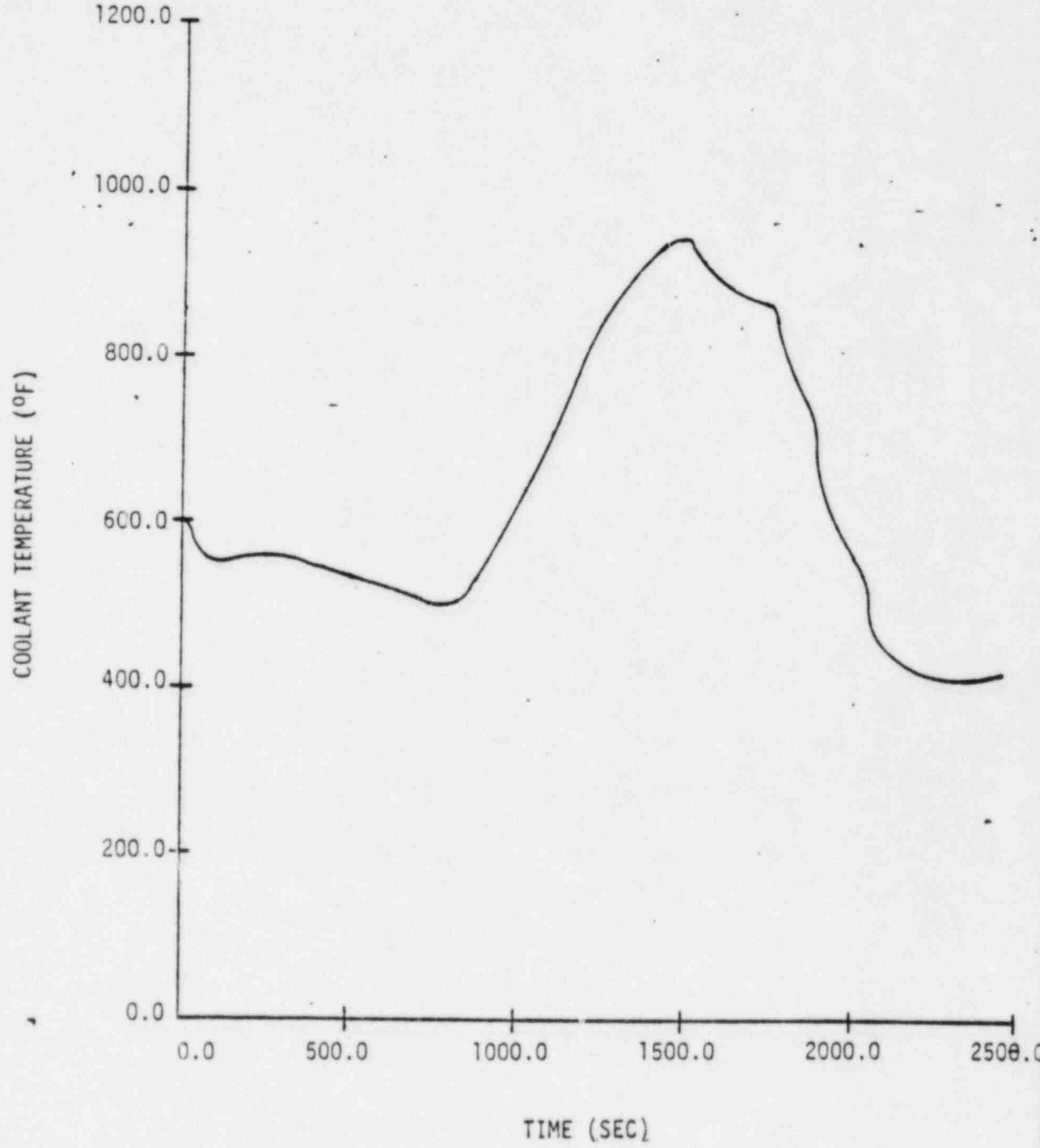


| | | |
|---|---|---|
| Omaha Public Power District<br>Fort Calhoun Station<br>Unit No. 1 | 0.05 FT² COLD LEG BREAK AT PUMP DISCHARGE - CHANNEL COOLANT TEMPERATURE AT HOT SPOT (SMALL BREAK ANALYSIS) | Figure 14.15-32G |

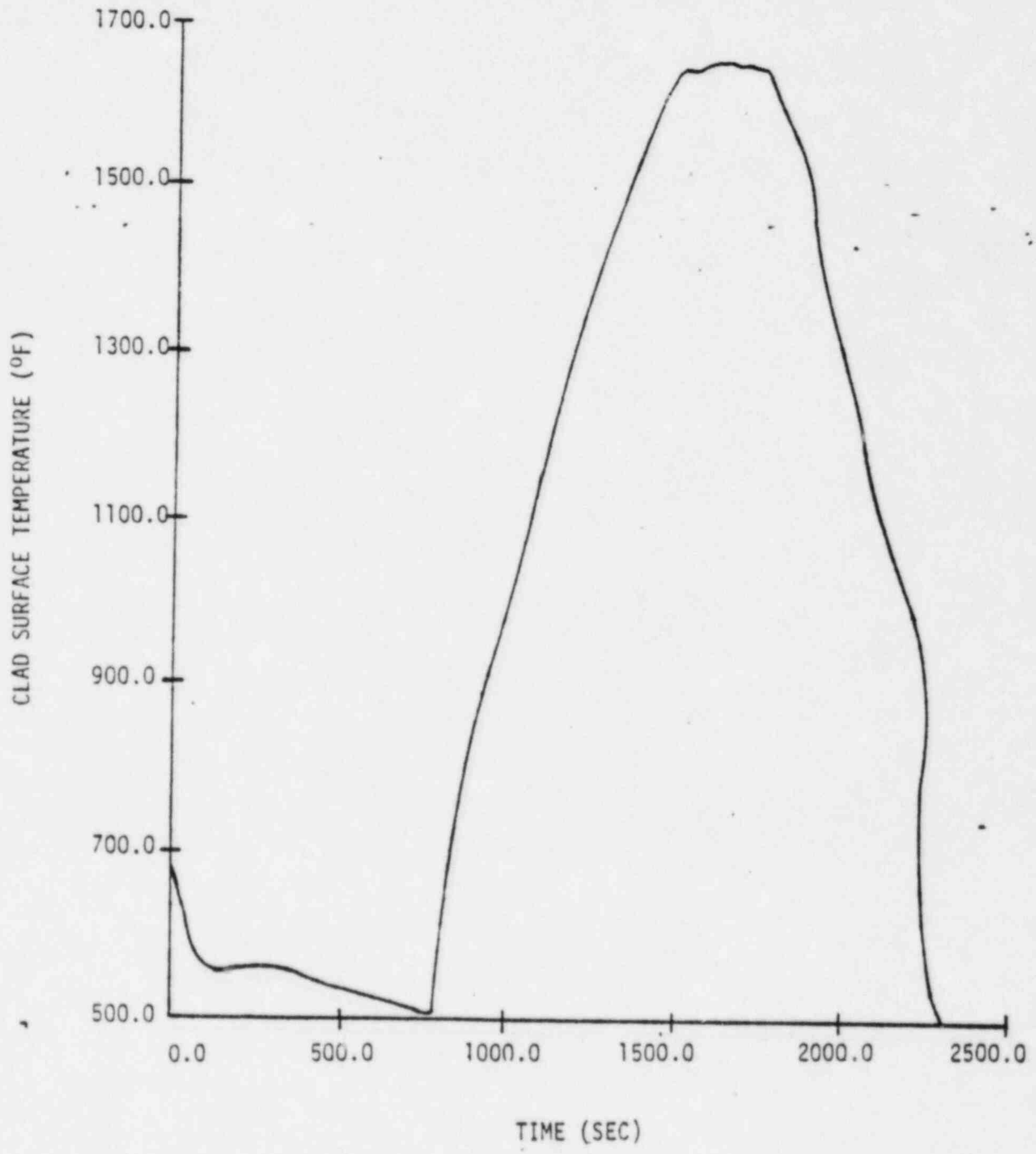


| | | |
|---|---|---|
| Omaha Public Power District<br>Fort Calhoun Station<br>Unit No. 1 | 0.05 FT$^2$ COLD LEG BREAK AT PUMP DISCHARGE - HOT SPOT CLAD SURFACE TEMPERATURE (SMALL BREAK ANALYSIS) | Figure 14.15-32H |

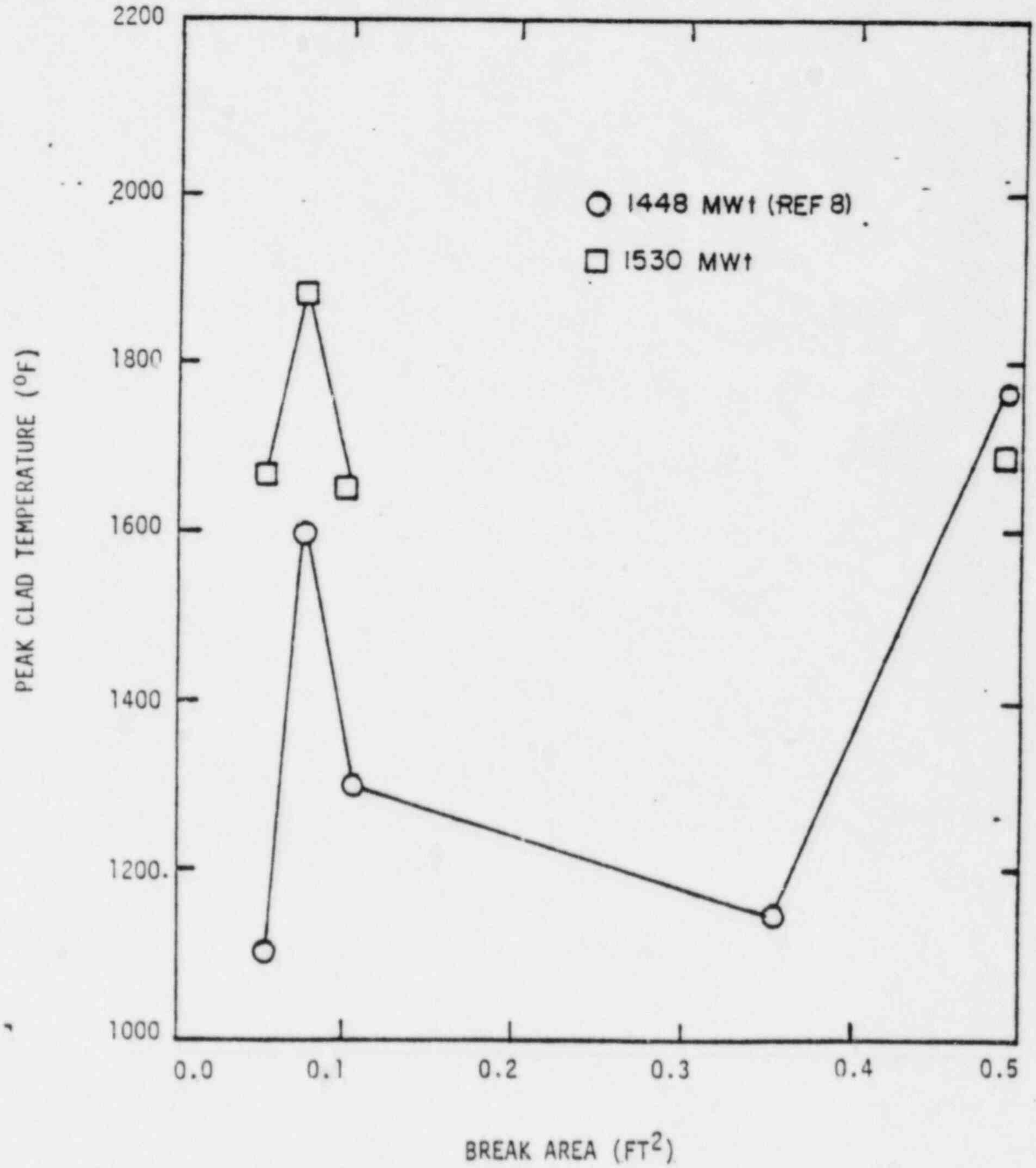


| Omaha Public Power District<br>Fort Calhoun Station<br>Unit No. 1 | PEAK CLAD TEMPERATURE<br>AS A FUNCTION OF BREAK AREA | Figure<br>14.15-33 |
|---|---|---|

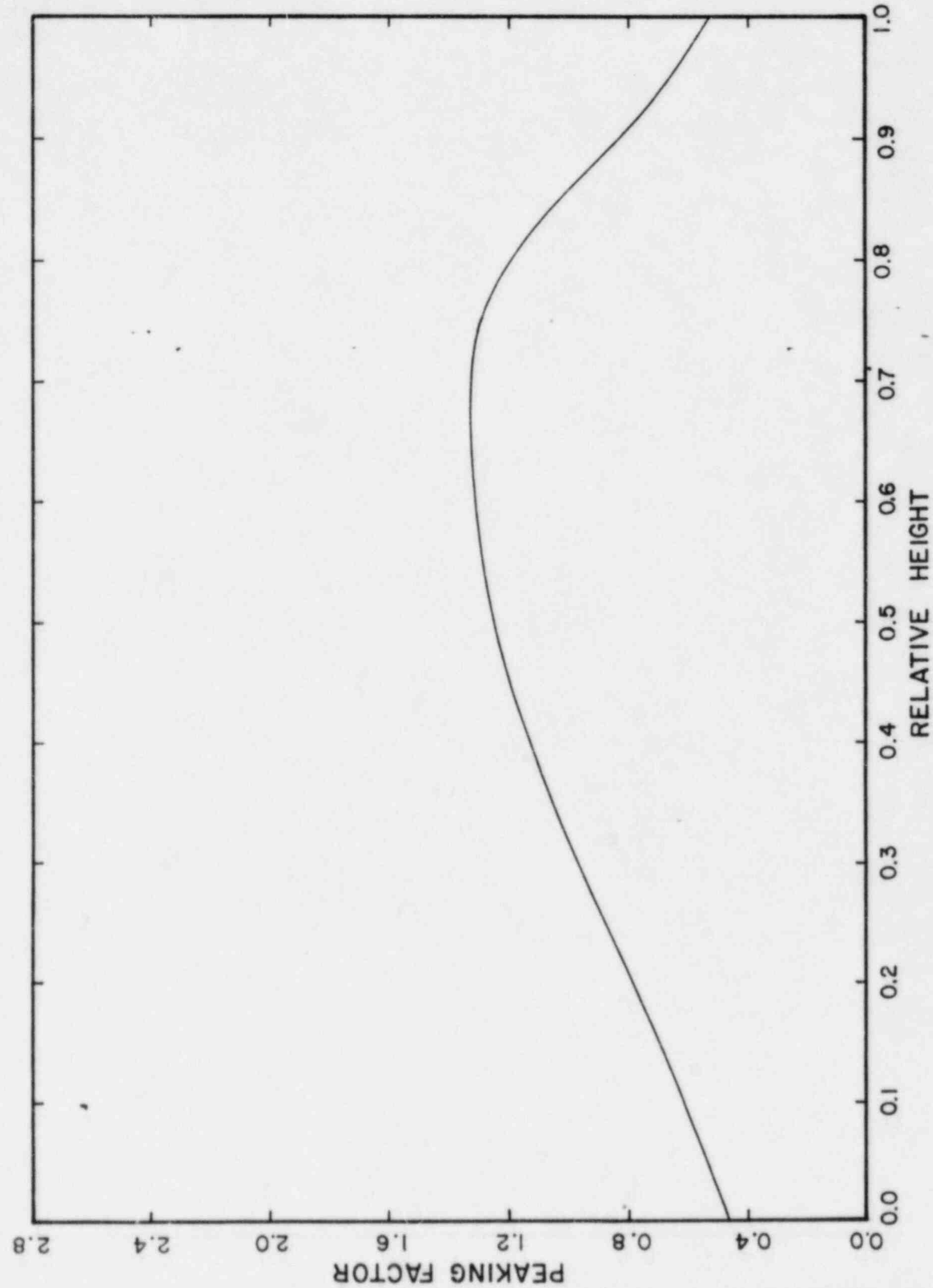


| | | |
|---|---|---|
| OMAHA PUBLIC POWER DISTRICT<br>FORT CALHOUN STATION<br>UNIT NO. 1 | Cycle 8 Axial Power Profile<br>with Peak at X/L = 0.7 | Figure<br>14.15-34 |

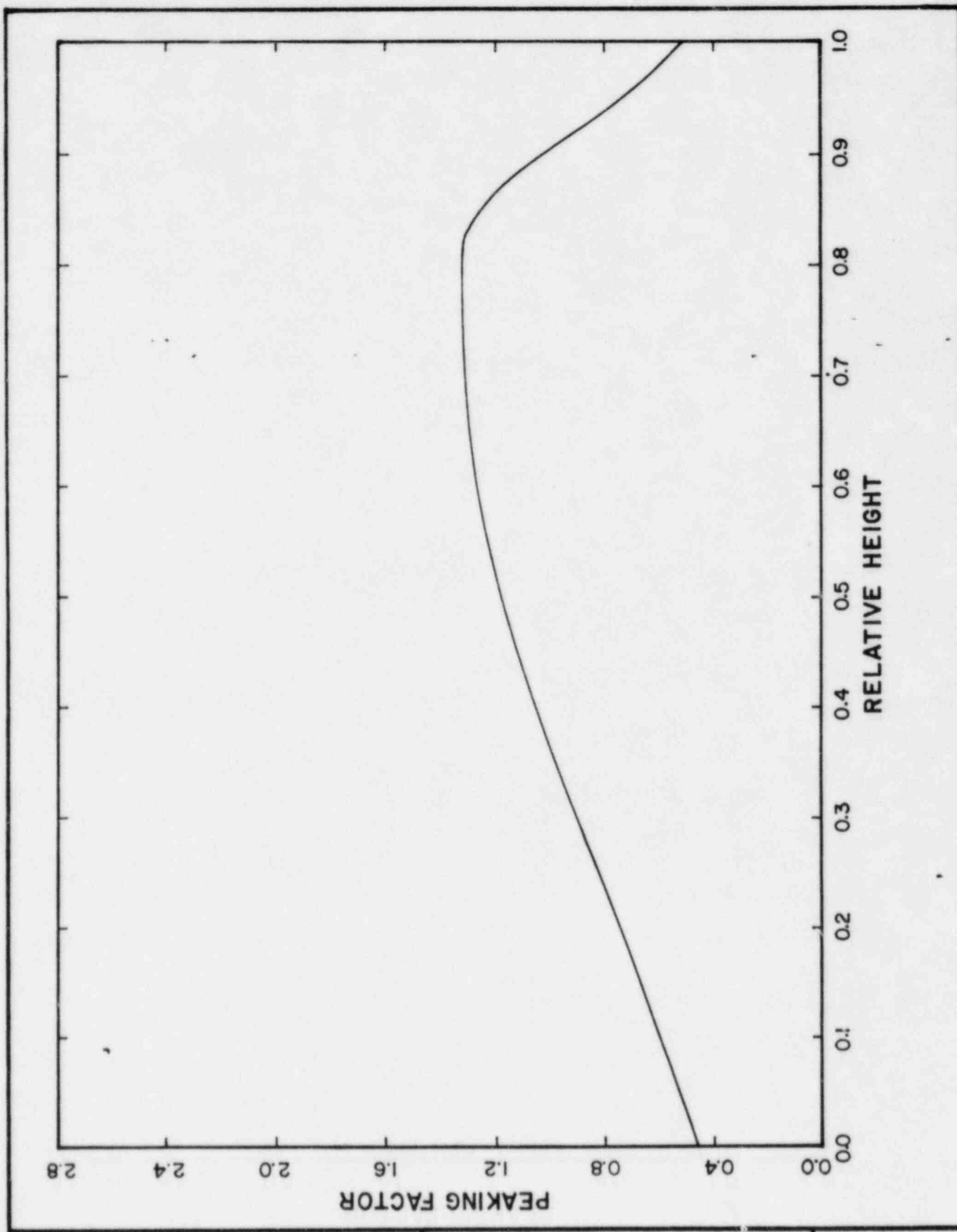


| | | |
|---|---|---|
| OMAHA PUBLIC POWER DISTRICT<br>FORT CALHOUN STATION<br>UNIT NO. 1 | Cycle 8 Axial Power Profile<br>with Peak at X/L = 0.8 | Figure<br>14.15-35 |

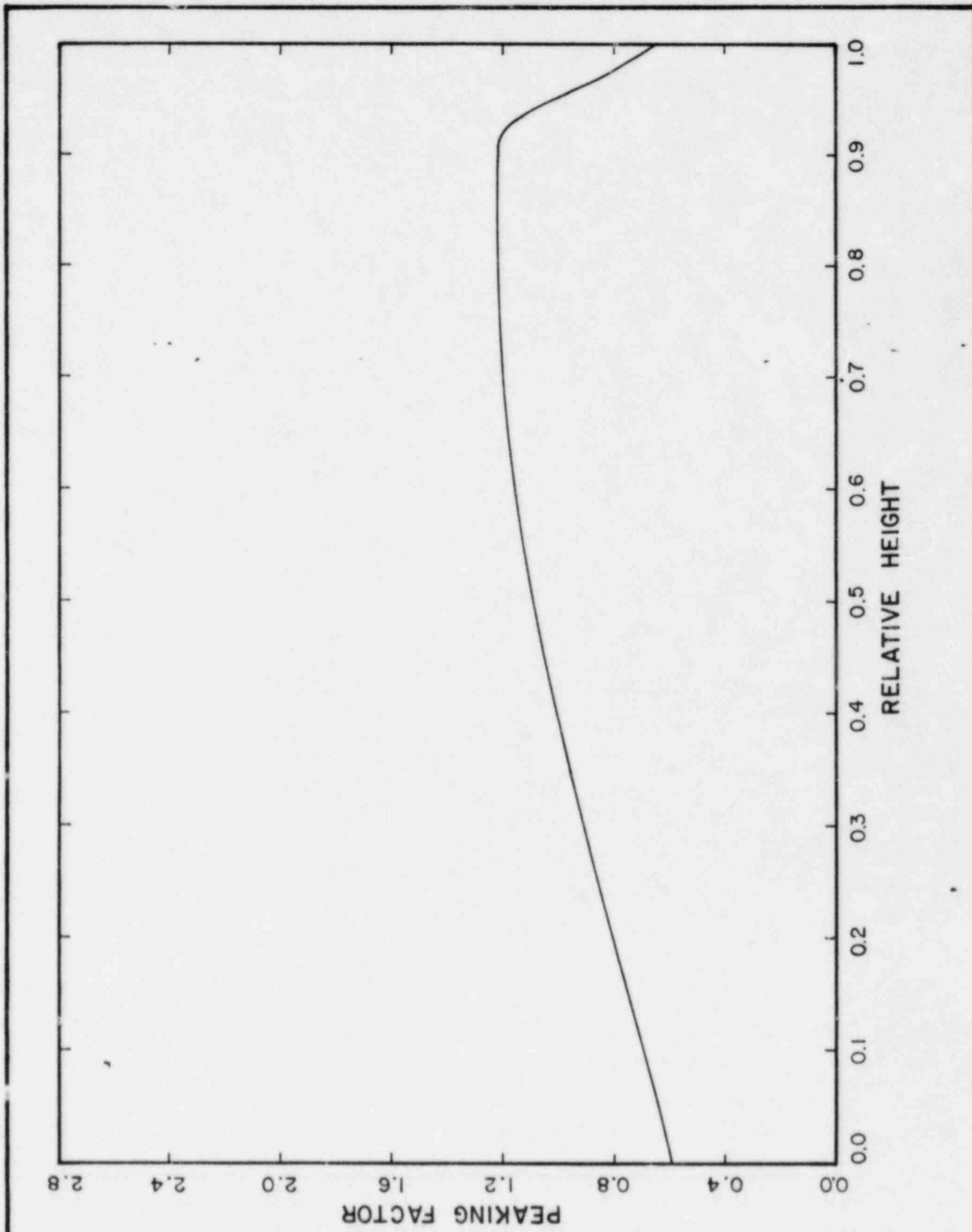


| OMAHA PUBLIC POWER DISTRICT<br>FORT CALHOUN STATION<br>UNIT NO. I | Cycle 8 Axial Power Profile<br>with Peak at X/L = 0.9 | Figure<br>14.15-36 |
|---|---|---|

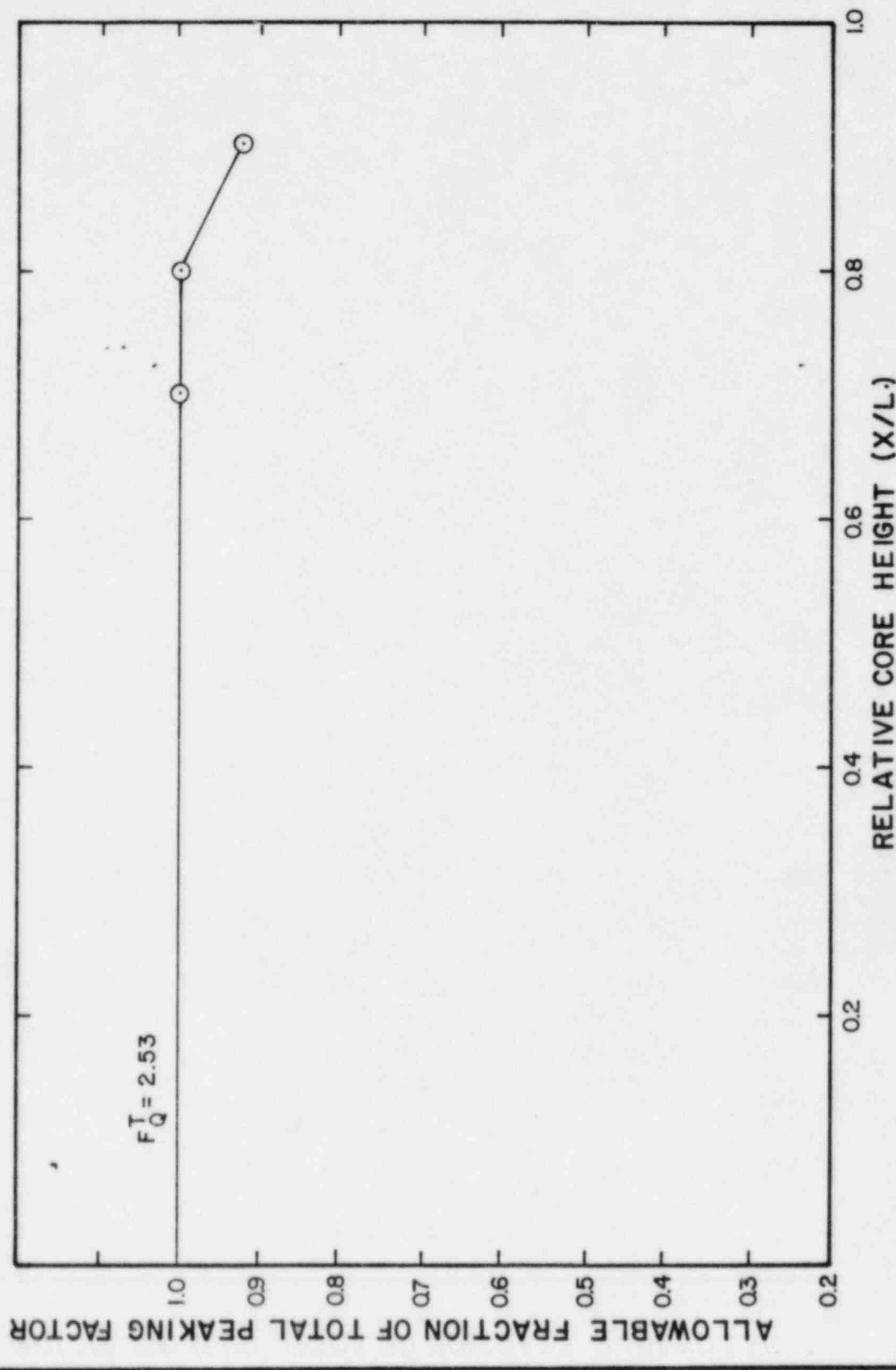


| | | |
|---|---|---|
| OMAHA PUBLIC POWER DISTRICT<br>FORT CALHOUN STATION<br>UNIT NO. 1 | Cycle 8 Limits on Total Peaking Versus Axial Power Peak Location | Figure<br>14.15-37 |

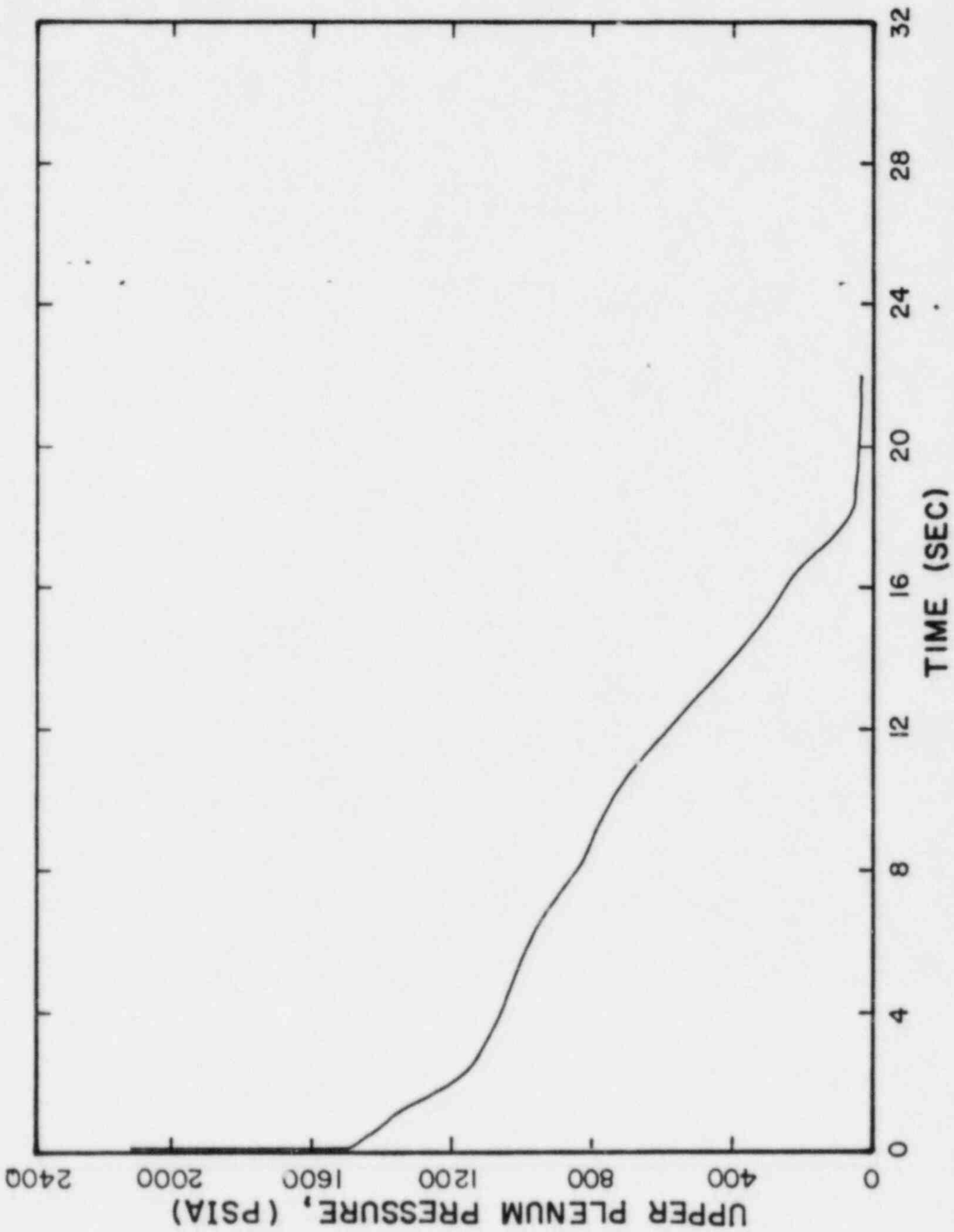


| | | |
|---|---|---|
| OMAHA PUBLIC POWER DISTRICT<br>FORT CALHOUN STATION<br>UNIT NO. 1 | Cycle 8 Blowdown System<br>Pressure, 1.0 DECLG Break | Figure<br>14.15-38 |

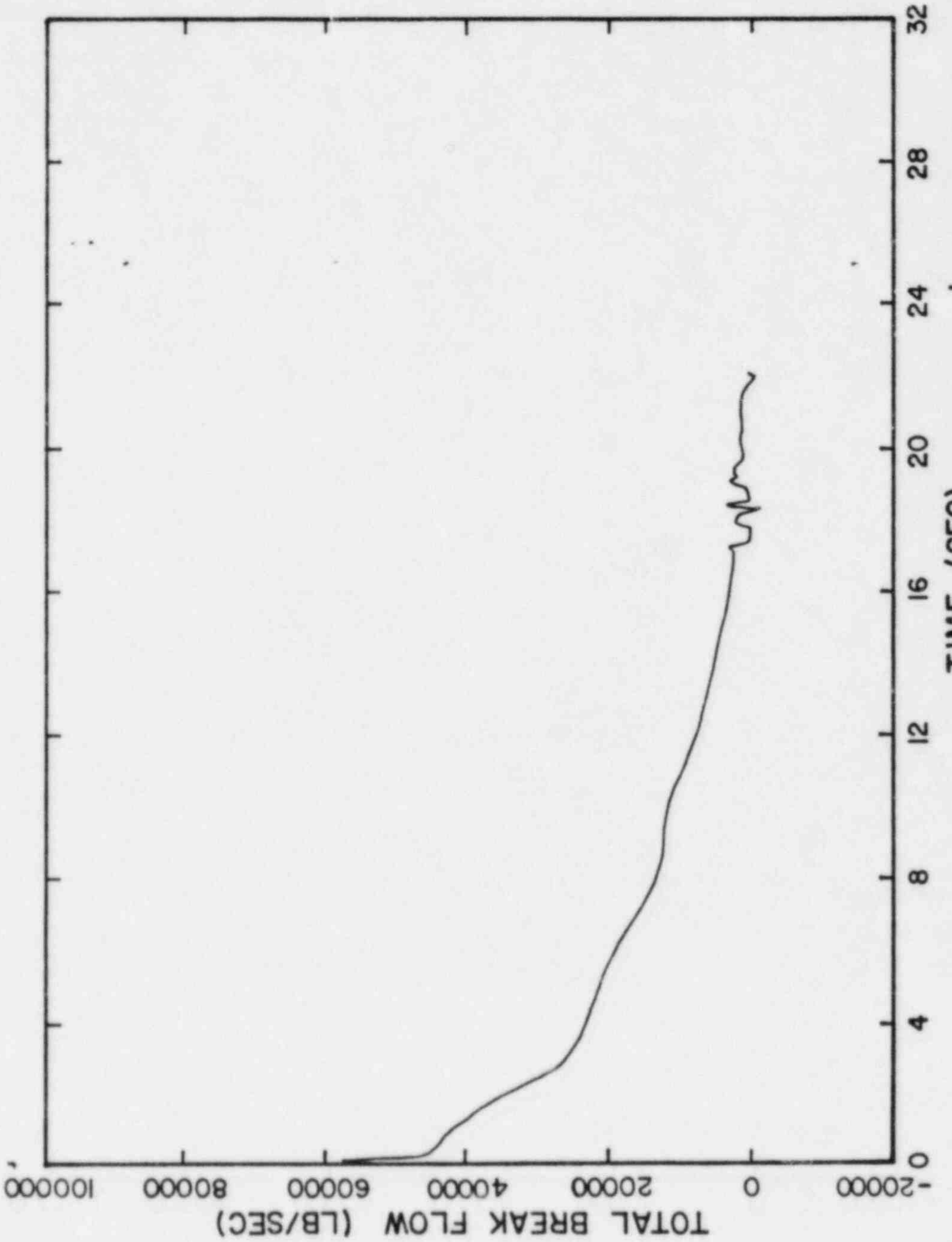


| OMAHA PUBLIC POWER DISTRICT<br>FORT CALHOUN STATION<br>UNIT NO. 1 | Cycle 8 Blowdown Total Break<br>Flow Rate, 1.0 DECLG Break | Figure<br>14.15-39 |
|---|---|---|

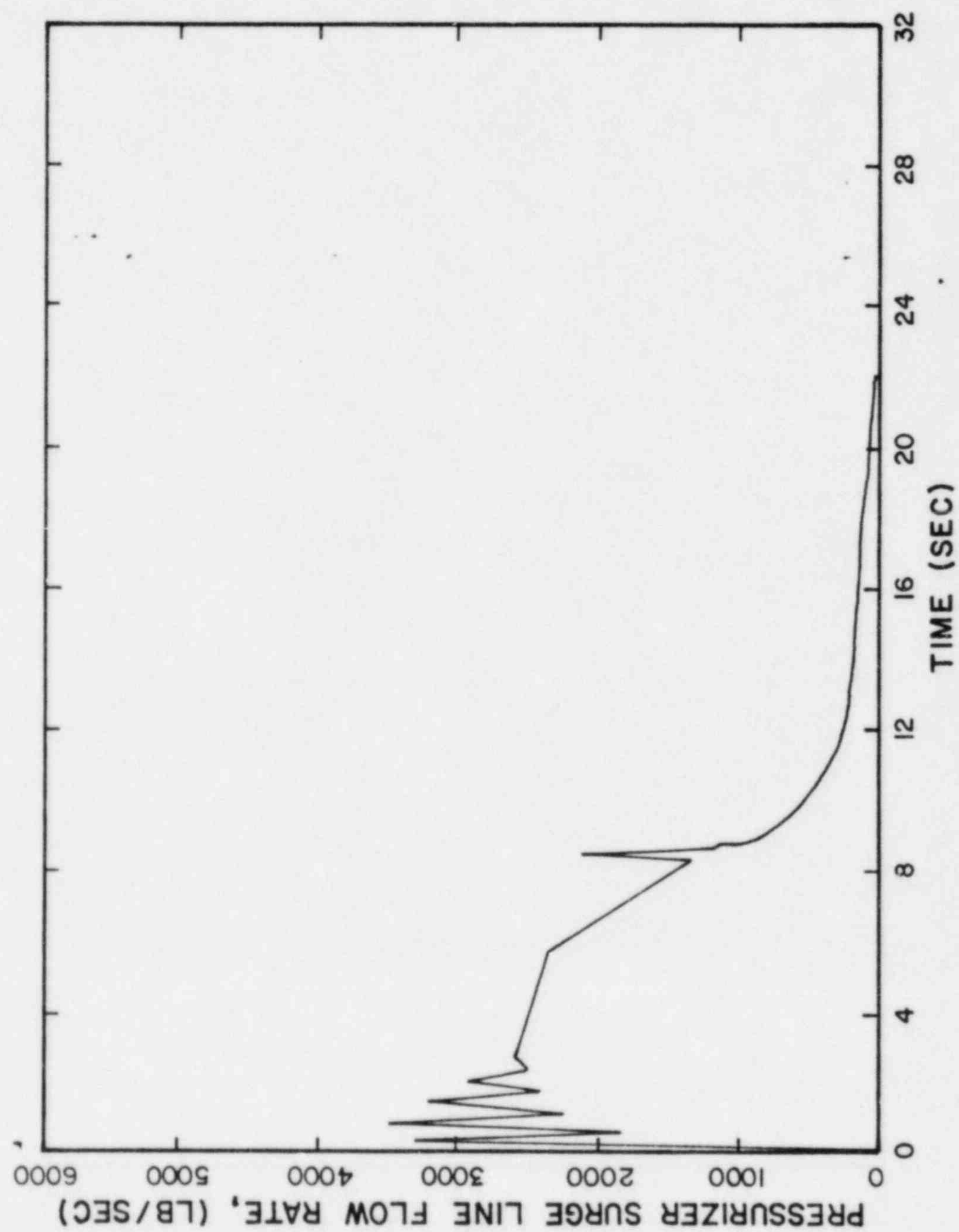


| | | |
|---|---|---|
| OMAHA PUBLIC POWER DISTRICT<br>FORT CALHOUN STATION<br>UNIT NO. I | Cycle 8 Pressurizer Surge Line Flow Rate, 1.0 DECLG Break | Figure 14.15-40 |

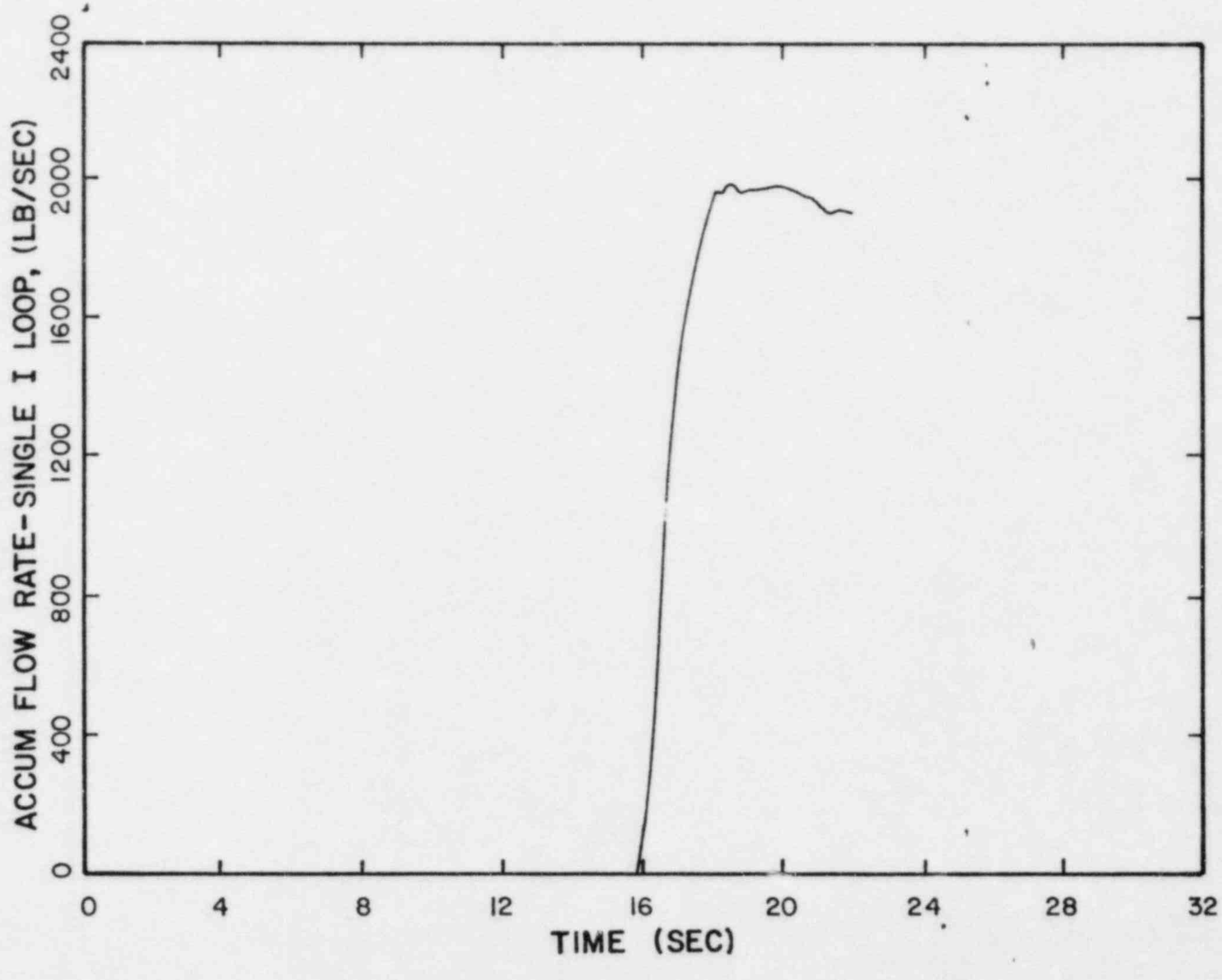


OMAHA PUBLIC POWER DISTRICT
FORT CALHOUN STATION
UNIT NO. 1

Cycle 8 Single Intact Loop
Accumulator Flow Rate,
1.0 DECLG Break

Figure
14.15-41

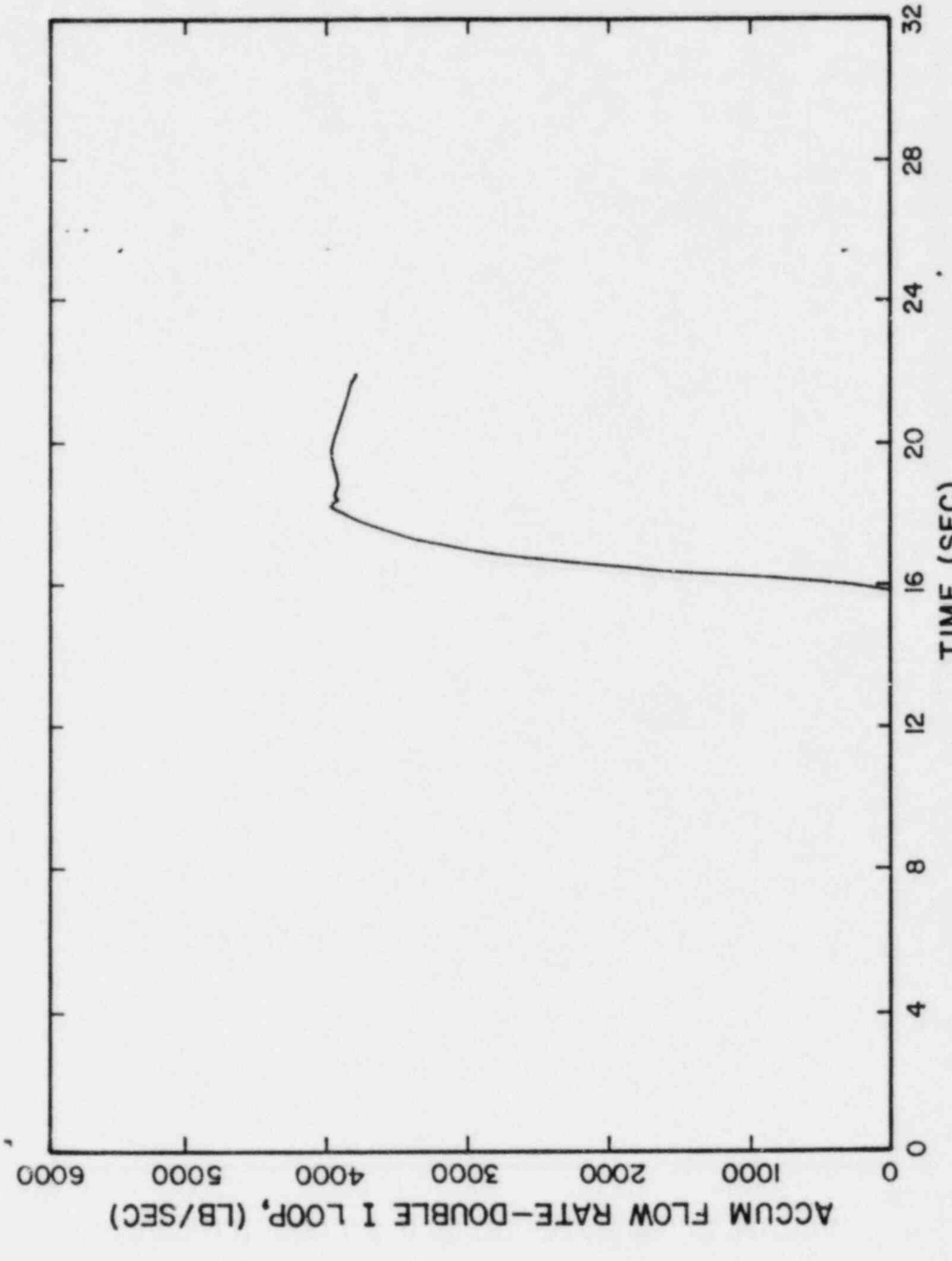


| OMAHA PUBLIC POWER DISTRICT<br>FORT CALHOUN STATION<br>UNIT NO. 1 | Cycle 8 Double Intact Loop<br>Accumulator Flow Rate,<br>1.0 DECLG Break | Figure<br>14.15-42 |
|---|---|---|

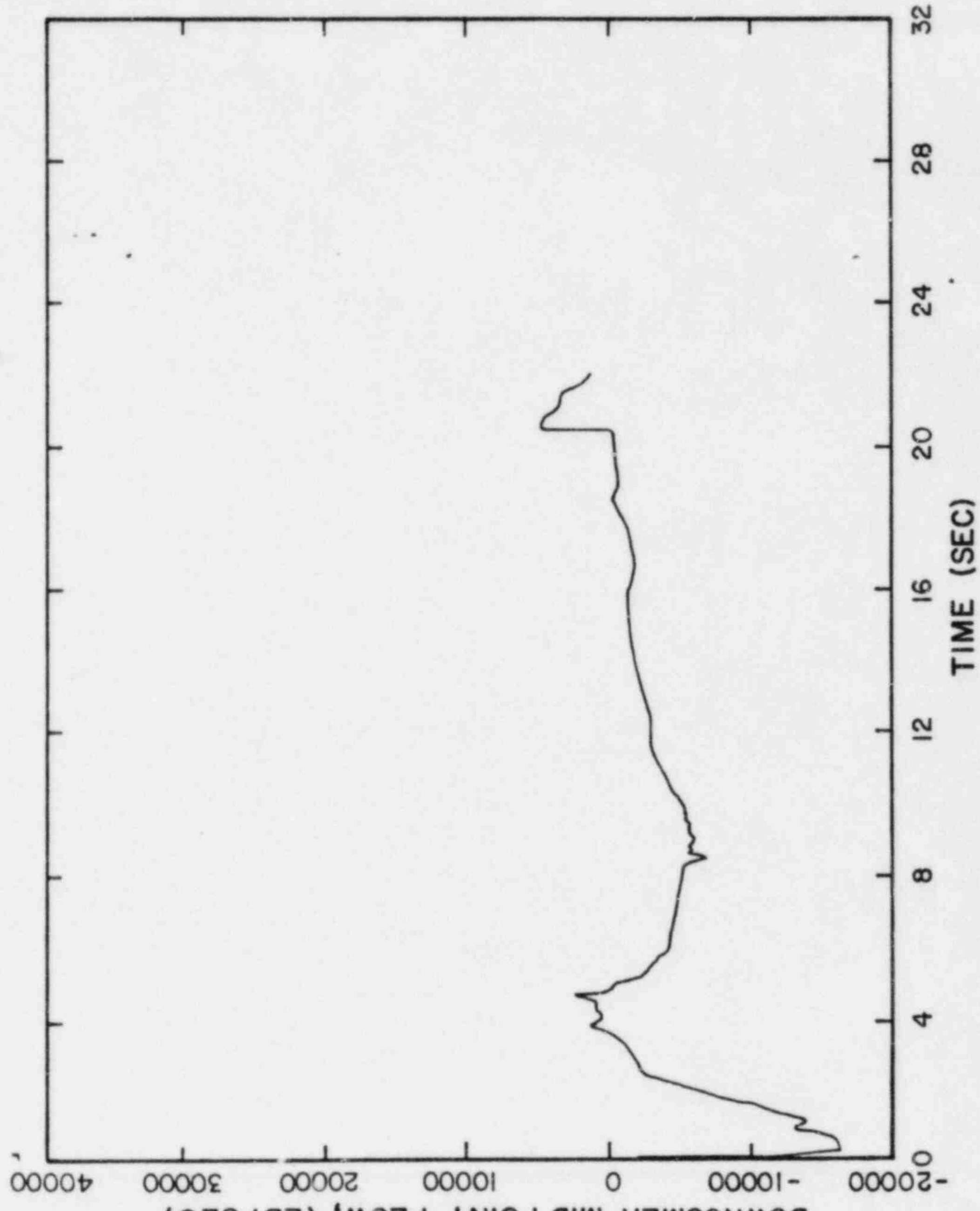


| | | |
|---|---|---|
| OMAHA PUBLIC POWER DISTRICT<br>FORT CALHOUN STATION<br>UNIT NO. 1 | Cycle 8 Downcomer Flow Rate,<br>1.0 DECLG Break | Figure<br>14.15-43 |

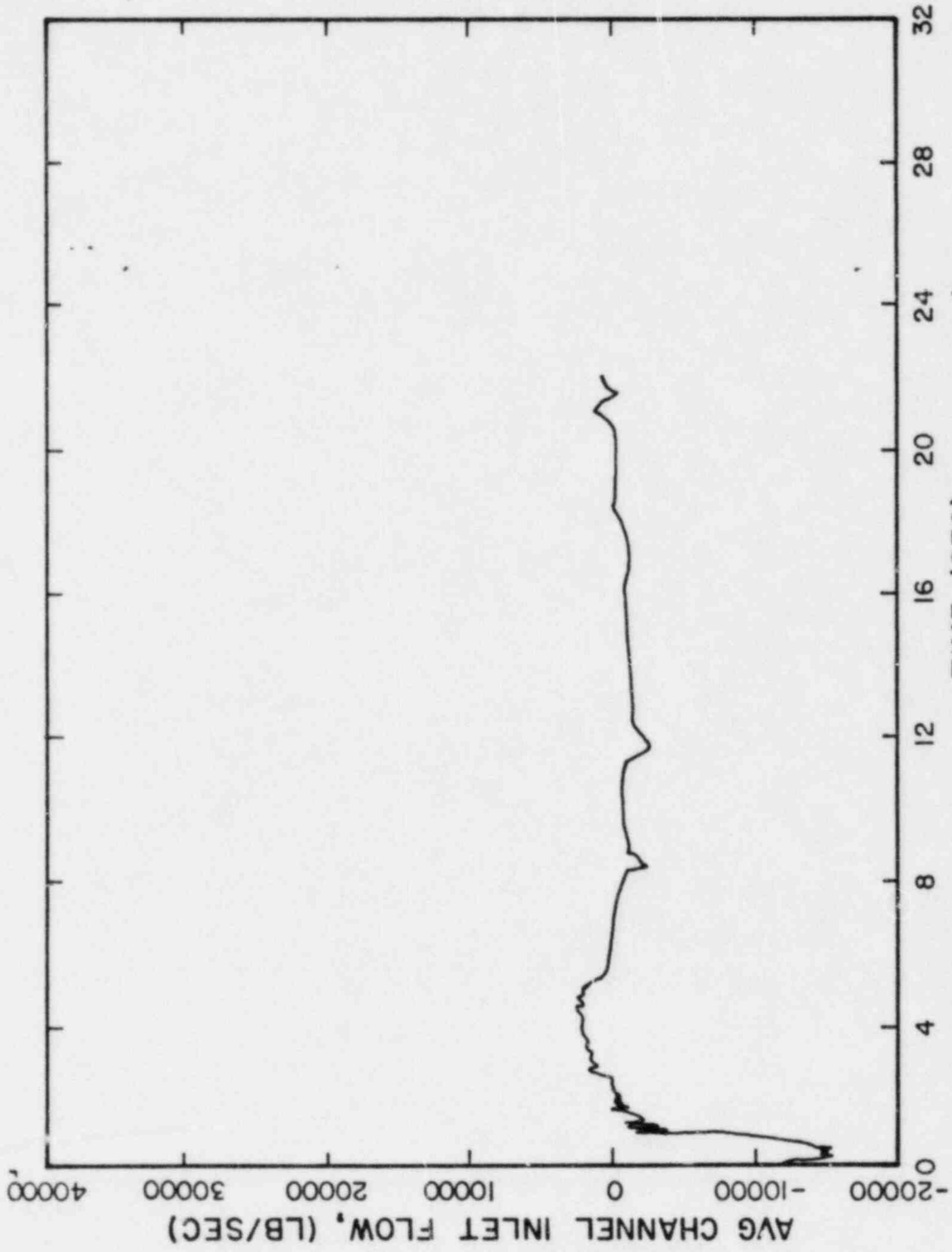


| | | |
|---|---|---|
| OMAHA PUBLIC POWER DISTRICT<br>FORT CALHOUN STATION<br>UNIT NO. 1 | Cycle 8 Average Channel Inlet Flow Rate, 1.0 DECLG Break | Figure<br>14.15-44 |

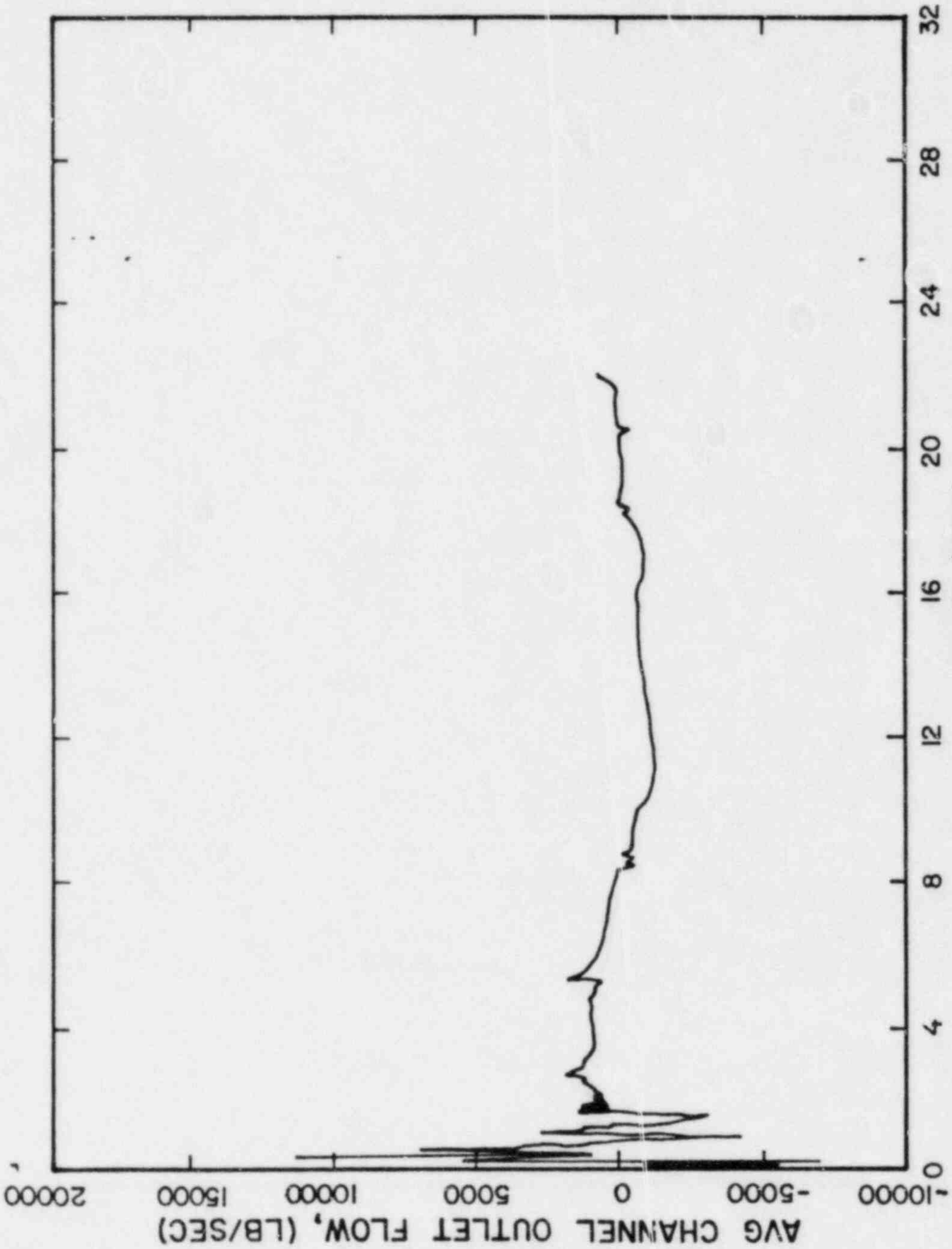


| | | |
|---|---|---|
| OMAHA PUBLIC POWER DISTRICT<br>FORT CALHOUN STATION<br>UNIT NO. 1 | Cycle 8 Average Channel Outlet Flow Rate, 1.0 DECLG Break | Figure 14.15-45 |

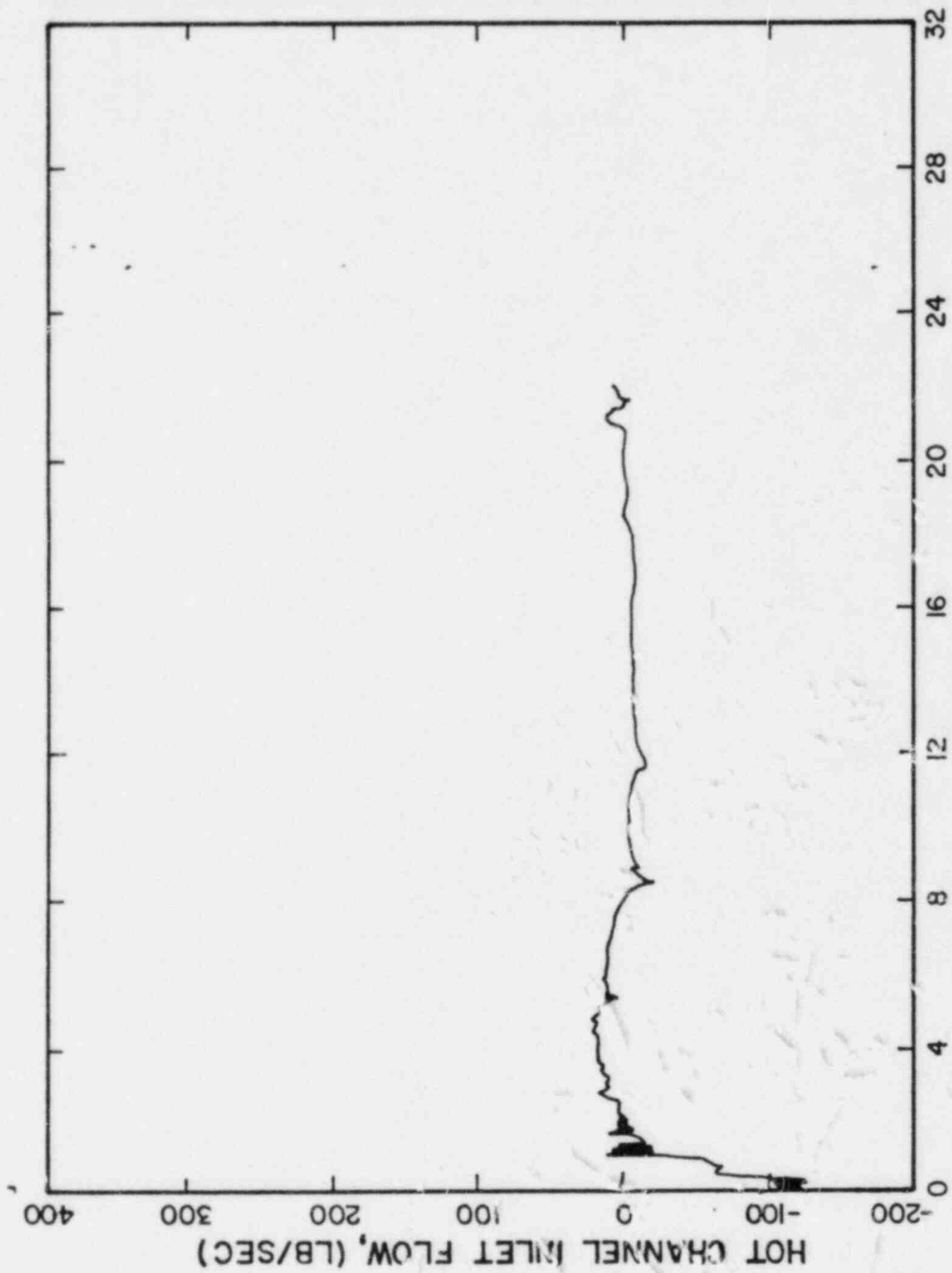


| | | |
|---|---|---|
| OMAHA PUBLIC POWER DISTRICT<br>FORT CALHOUN STATION<br>UNIT NO. I | Cycle 8 Hot Channel Inlet<br>Flow Rate, 1.0 DECLG Break | Figure<br>14.15-46 |

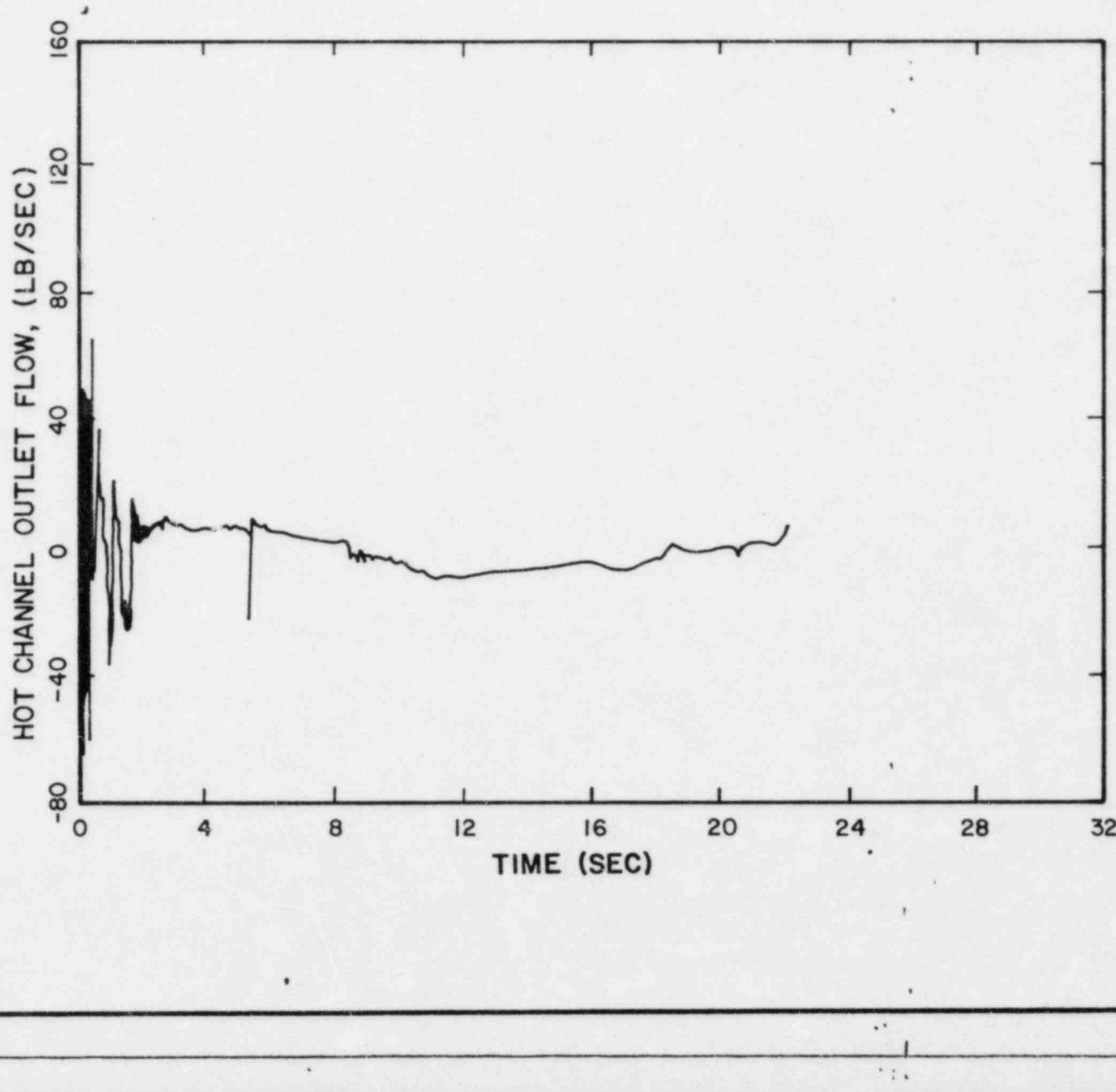


OMAHA PUBLIC POWER DISTRICT
FORT CALHOUN STATION
UNIT NO. 1

Cycle 8 Hot Channel Outlet Flow Rate, 1.0 DECLG Break

Figure 14.15-47

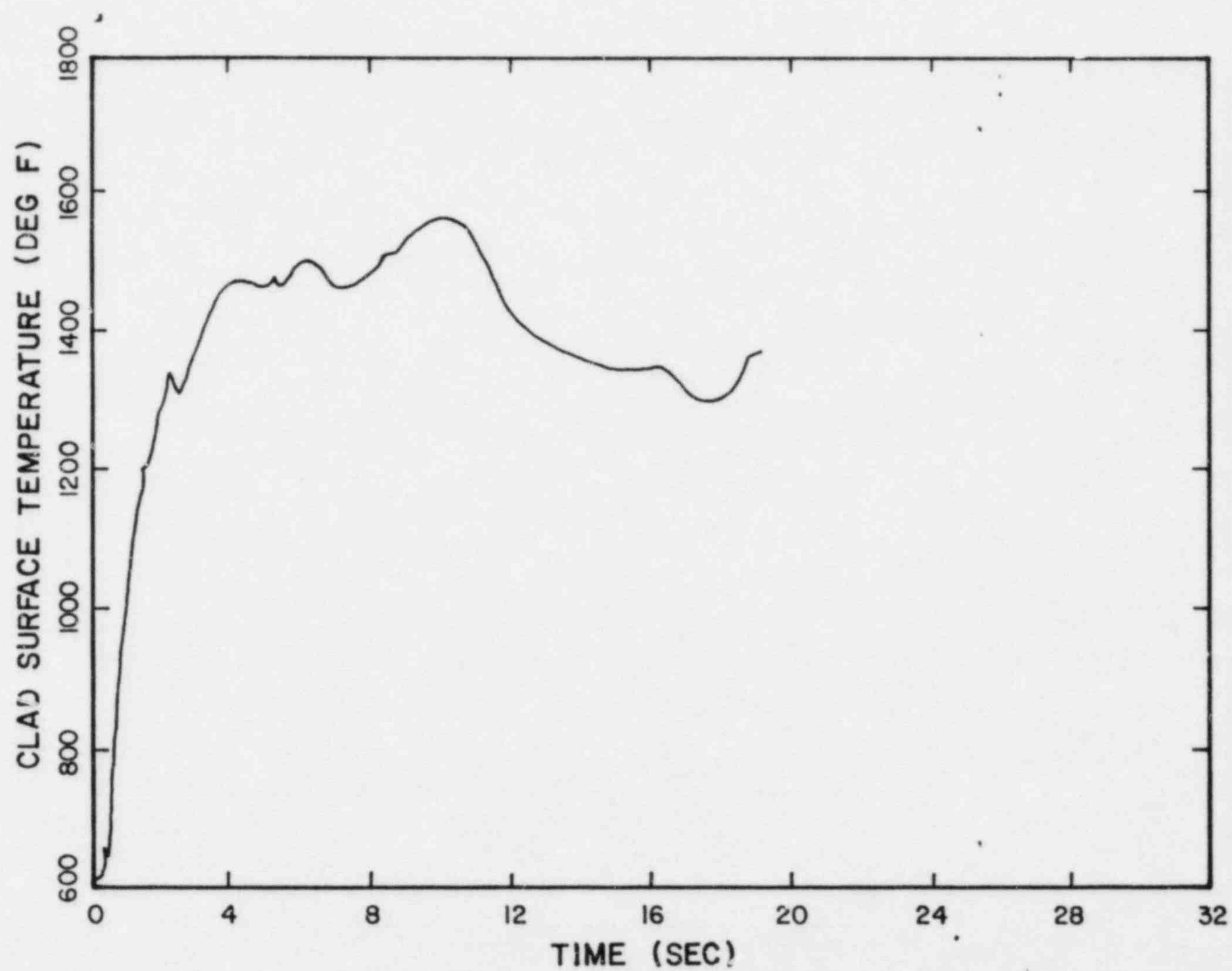


OMAHA PUBLIC POWER DISTRICT
FORT CALHOUN STATION
UNIT NO. 1

Cycle 8 PCT Node Blowdown
Cladding Surface Temperature,
1.0 DECLG Break

Figure
14.15-48

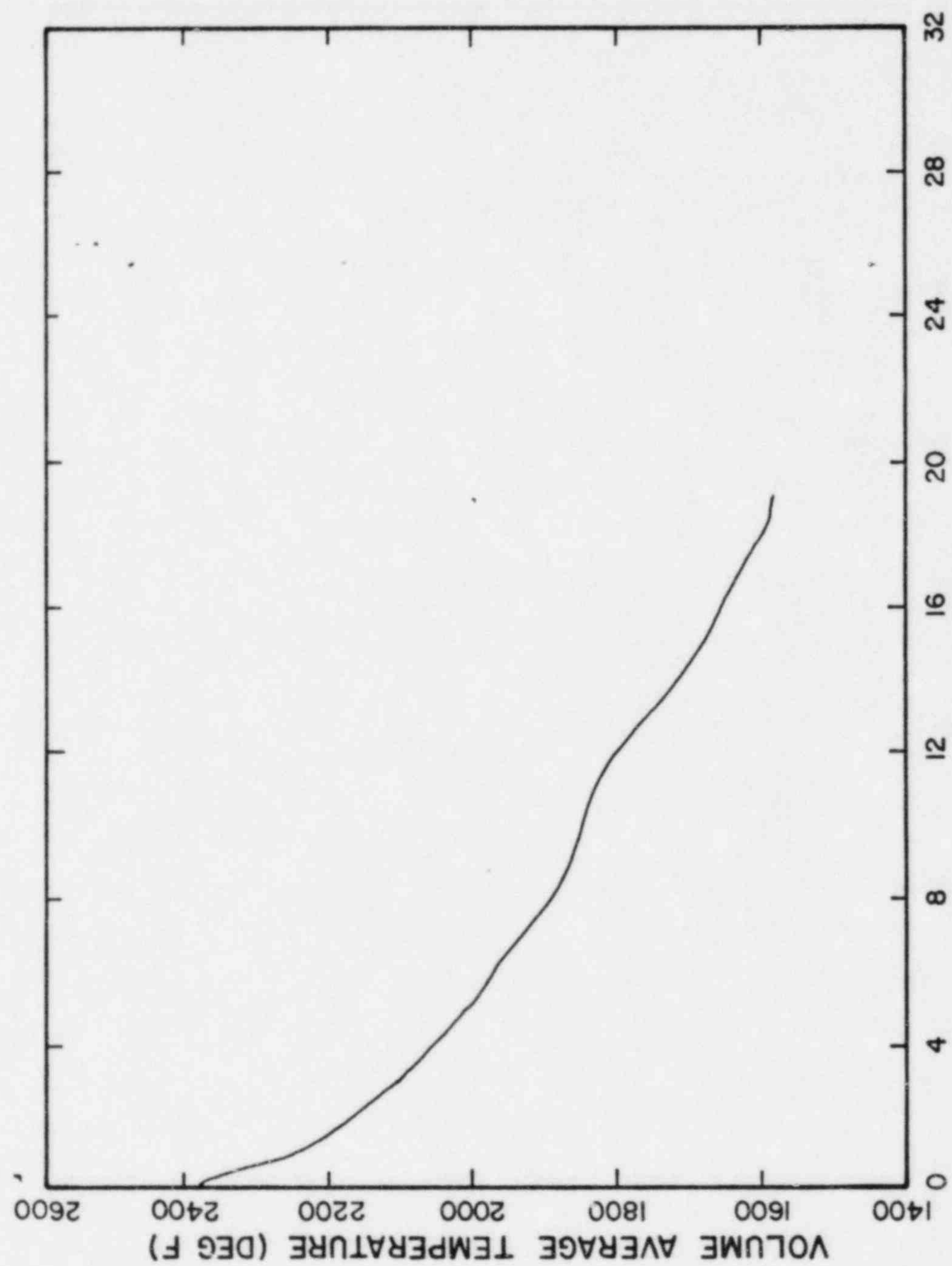


| | | |
|---|---|---|
| OMAHA PUBLIC POWER DISTRICT<br>FORT CALHOUN STATION<br>UNIT NO. 1 | Cycle 8 PCT Node Blowdown<br>Volumetric Average Fuel<br>Temperature, 1.0 DECLG Break | Figure<br>14.15-49 |

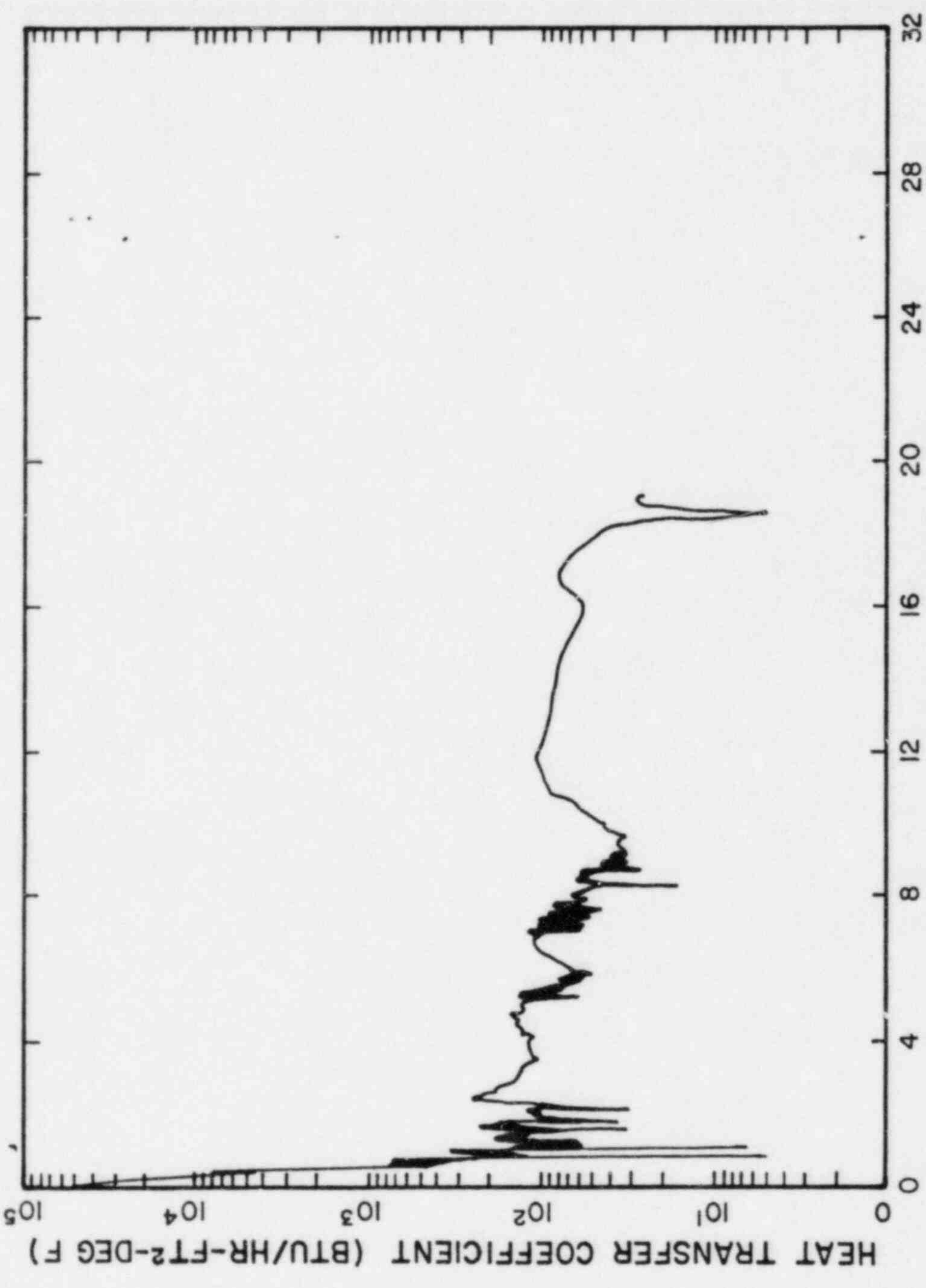


| | | |
|---|---|---|
| OMAHA PUBLIC POWER DISTRICT<br>FORT CALHOUN STATION<br>UNIT NO. 1 | Cycle 8 PCT Node Blowdown Heat Transfer Coefficient, 1.0 DECLG Break | Figure 14.15-50 |

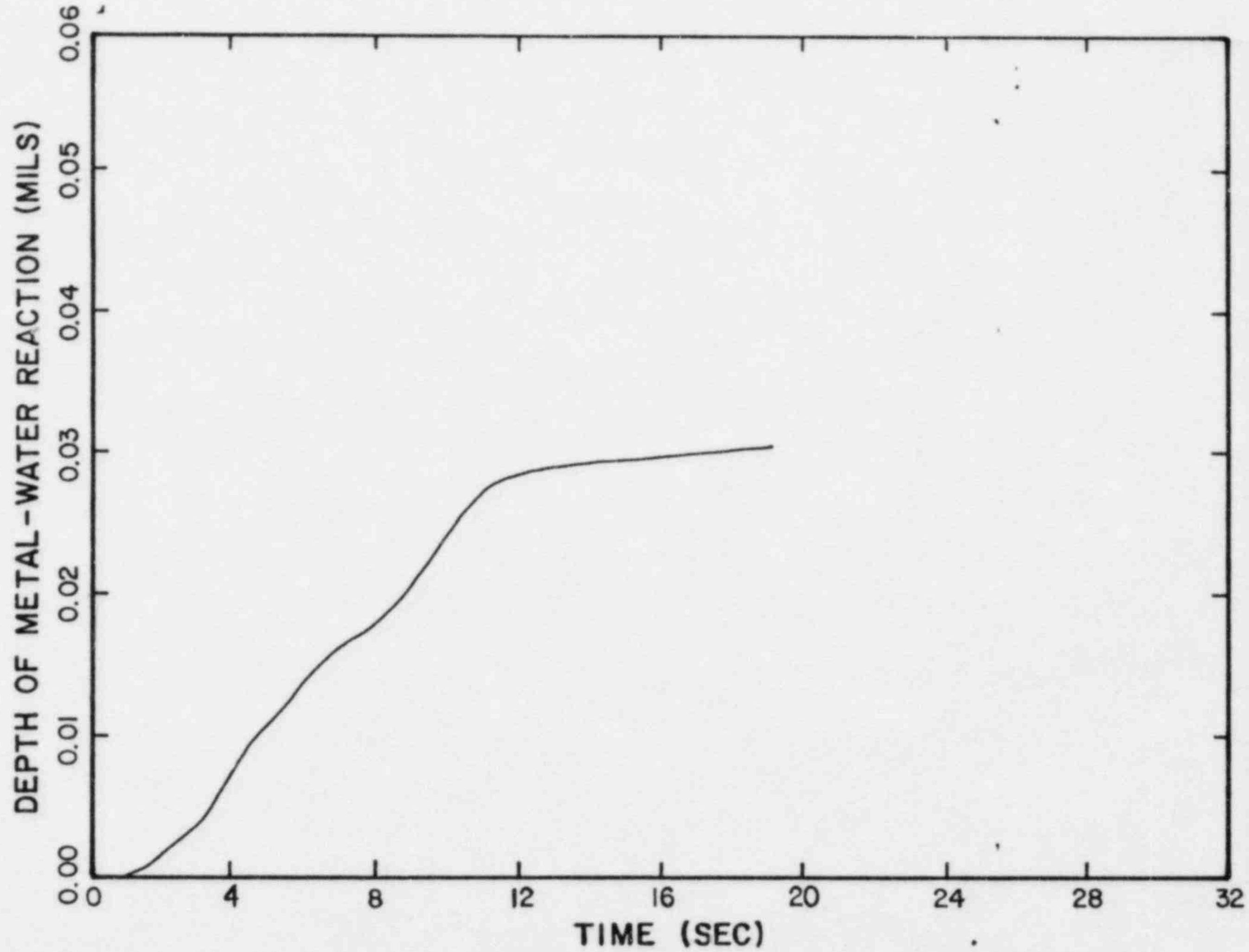


OMAHA PUBLIC POWER DISTRICT
FORT CALHOUN STATION
UNIT NO. 1

Cycle 8 PCT Node Blowdown
Depth of Zirconium-Water
Reaction, 1.0 DECLG Break

Figure
14.15-51

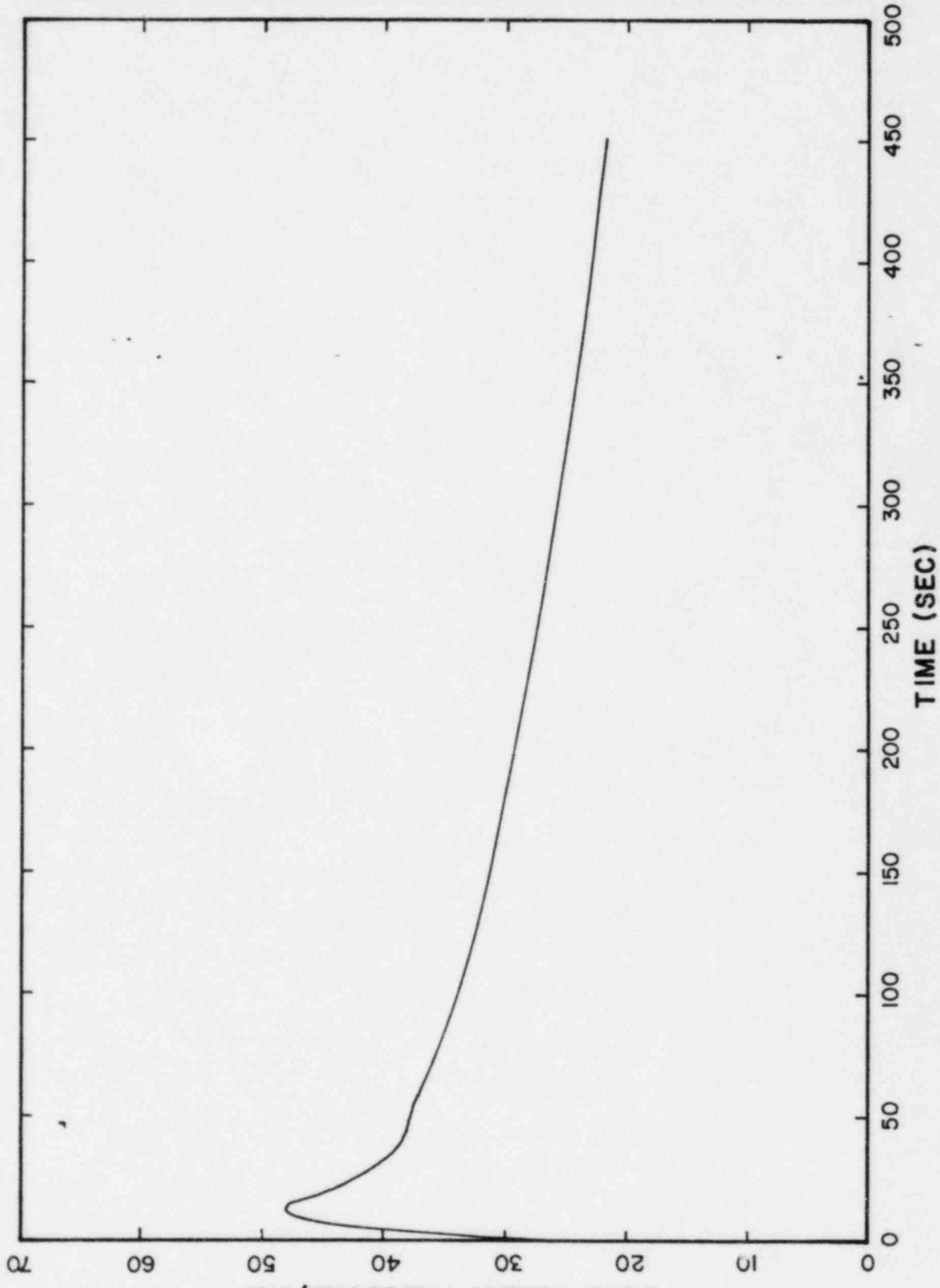


| OMAHA PUBLIC POWER DISTRICT<br>FORT CALHOUN STATION<br>UNIT NO. 1 | Cycle 8 Containment Pressure<br>Versus Time, 1.0 DECLG Break | Figure<br>14.15-52 |
|---|---|---|

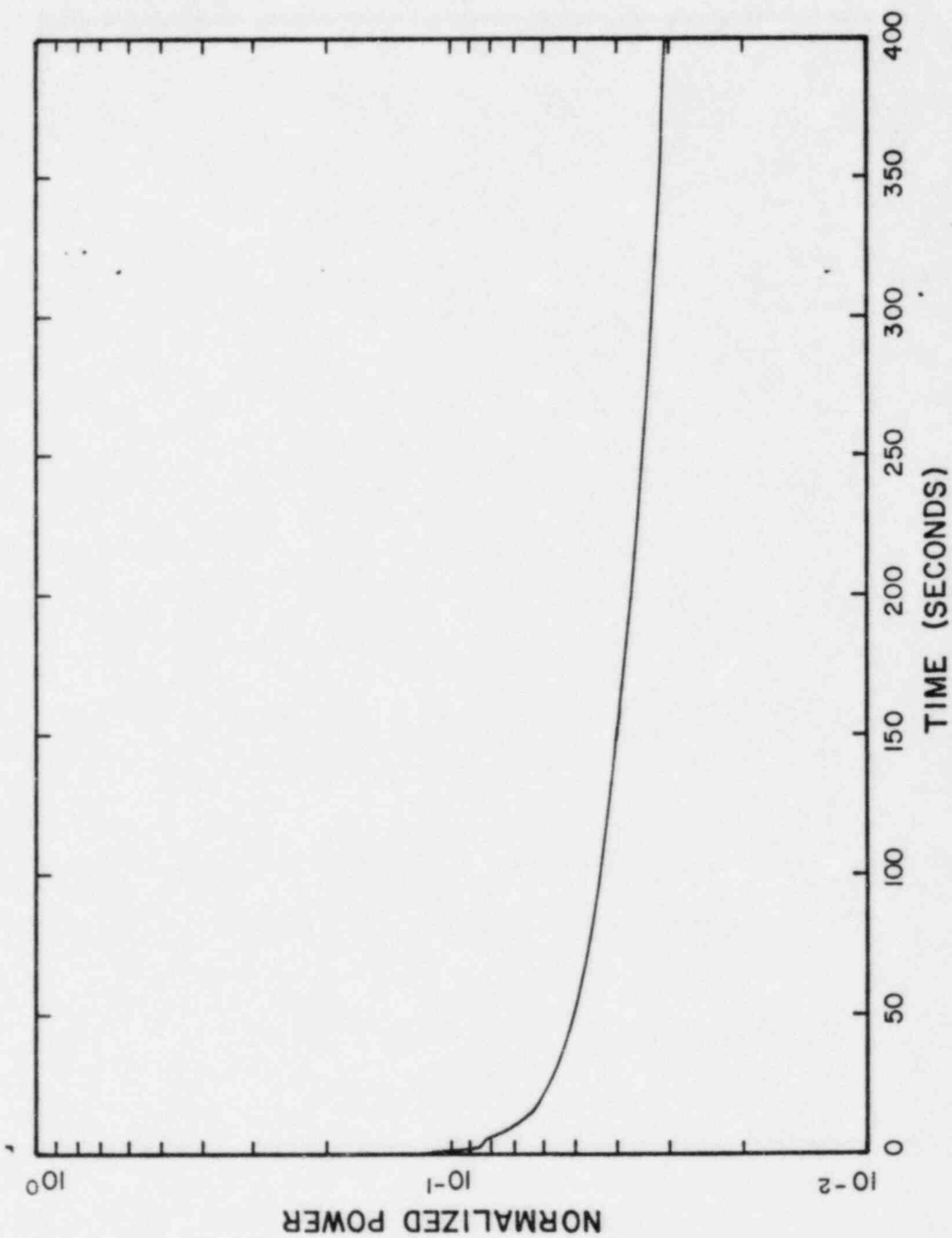


| | | |
|---|---|---|
| OMAHA PUBLIC POWER DISTRICT<br>FORT CALHOUN STATION<br>UNIT NO. 1 | Cycle 8 Normalized Core Power, 1.0 DECLG Break | Figure 14.15-53 |

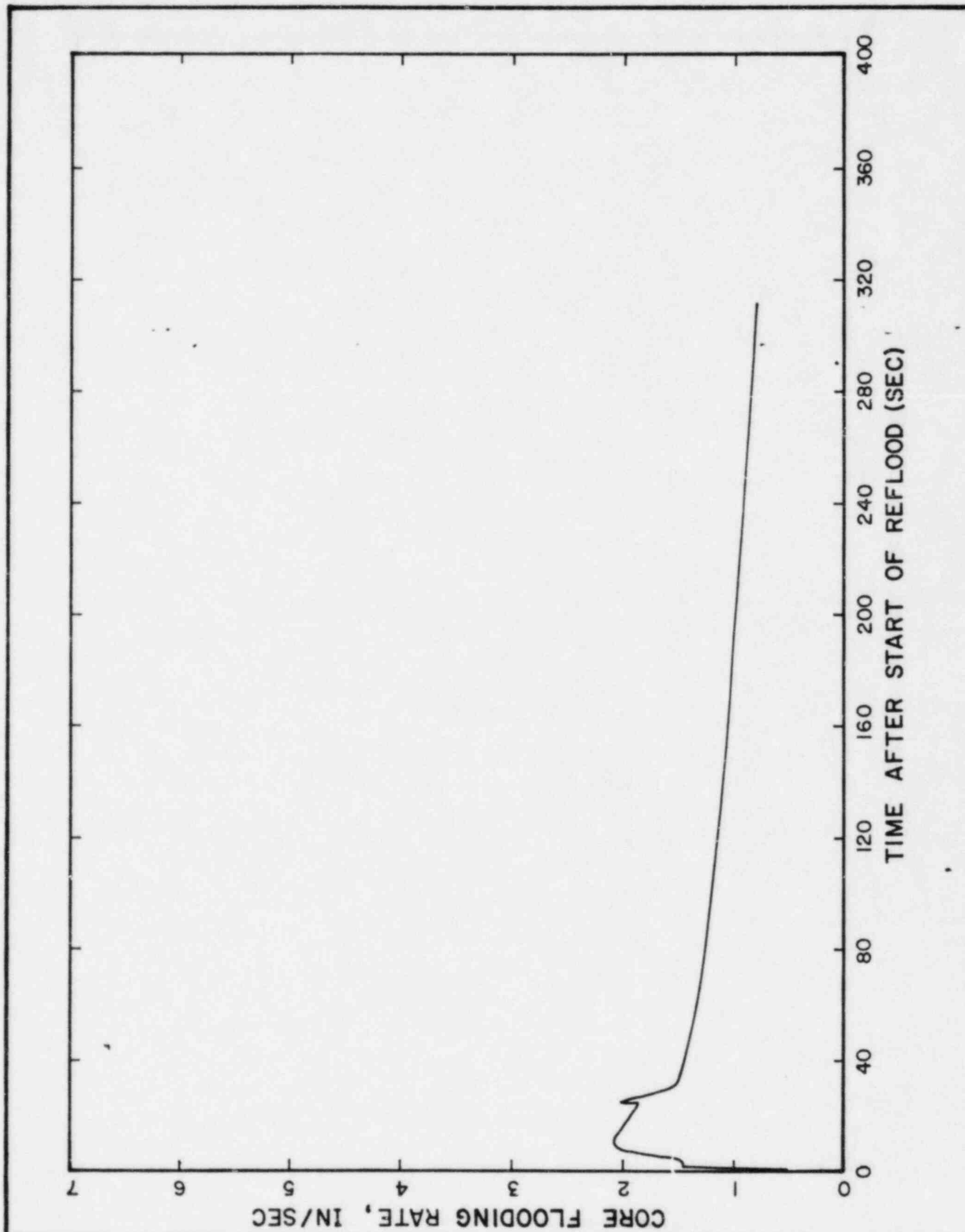


| | | |
|---|---|---|
| OMAHA PUBLIC POWER DISTRICT<br>FORT CALHOUN STATION<br>UNIT NO. 1 | Cycle 8 Core Reflooding Rate,<br>1.0 DECLG Break | Figure<br>14.15-54 |

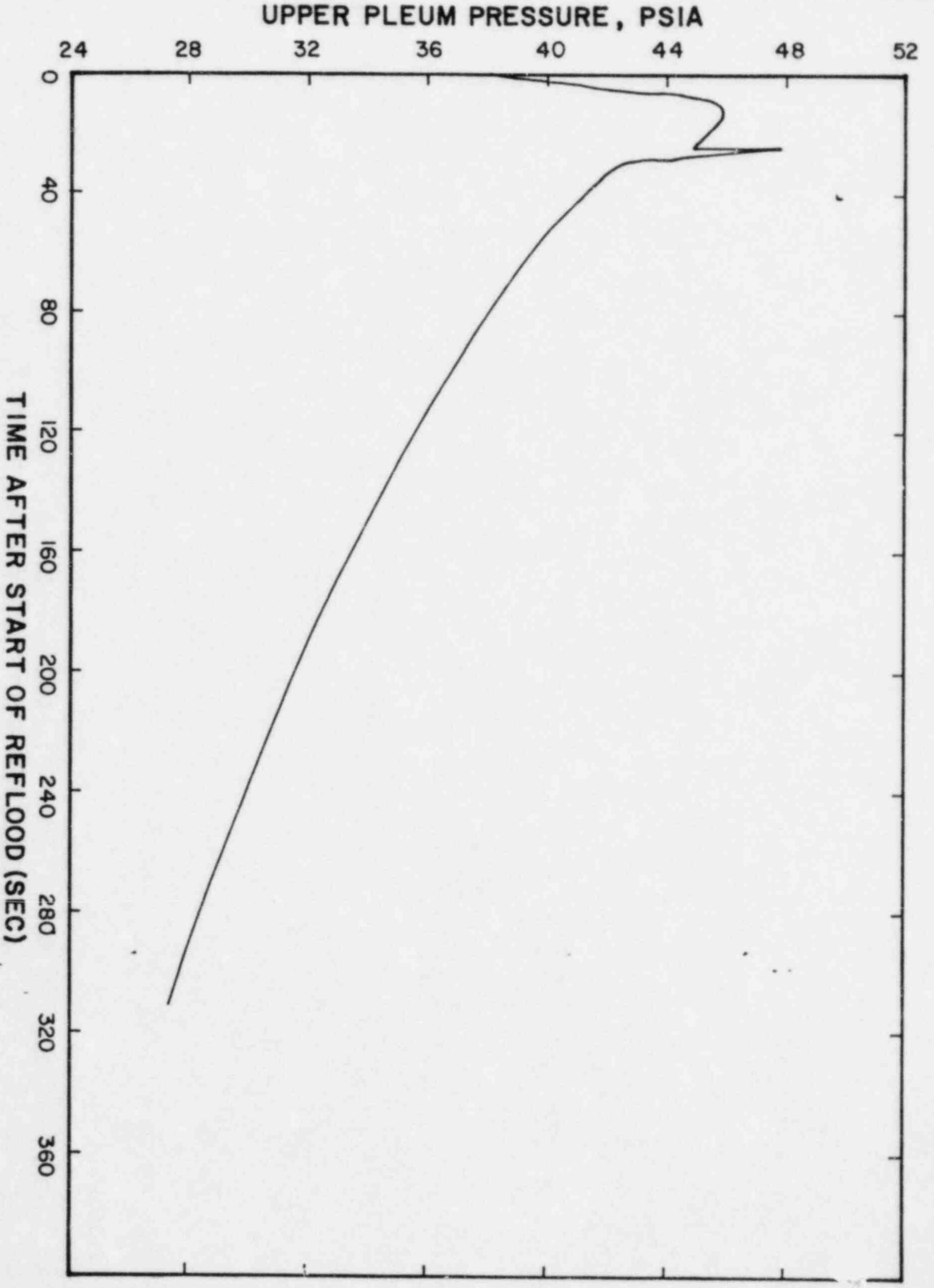


OMAHA PUBLIC POWER DISTRICT
FORT CALHOUN STATION
UNIT NO. 1

Cycle 8 Reflood System Pressure, 1.0 DECLG Break

Figure 14.15-55

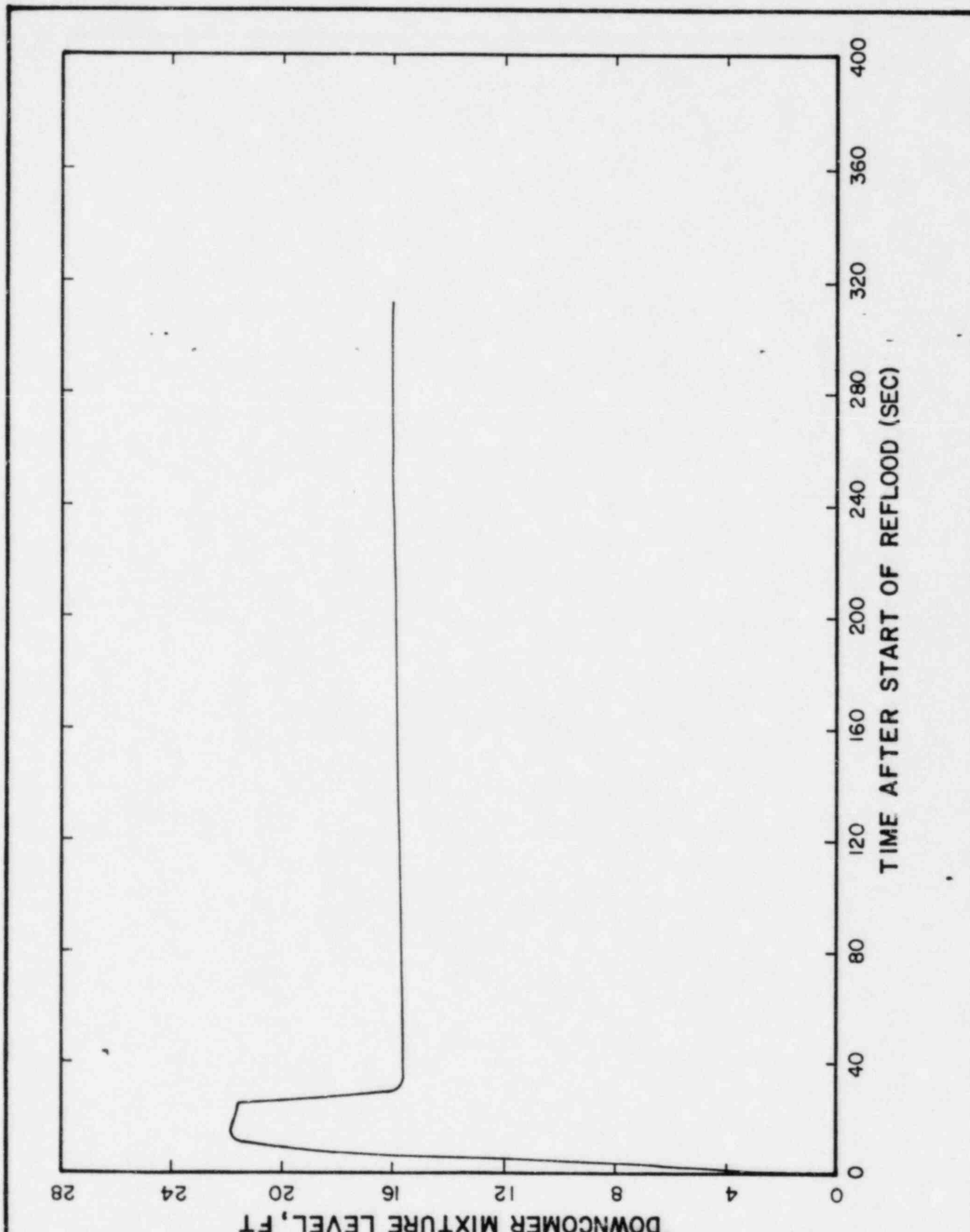


| OMAHA PUBLIC POWER DISTRICT<br>FORT CALHOUN STATION<br>UNIT NO. 1 | Cycle 8 Reflood Downcomer Mixture Level, 1.0 DECLG Break | Figure<br>14.15-56 |
|---|---|---|

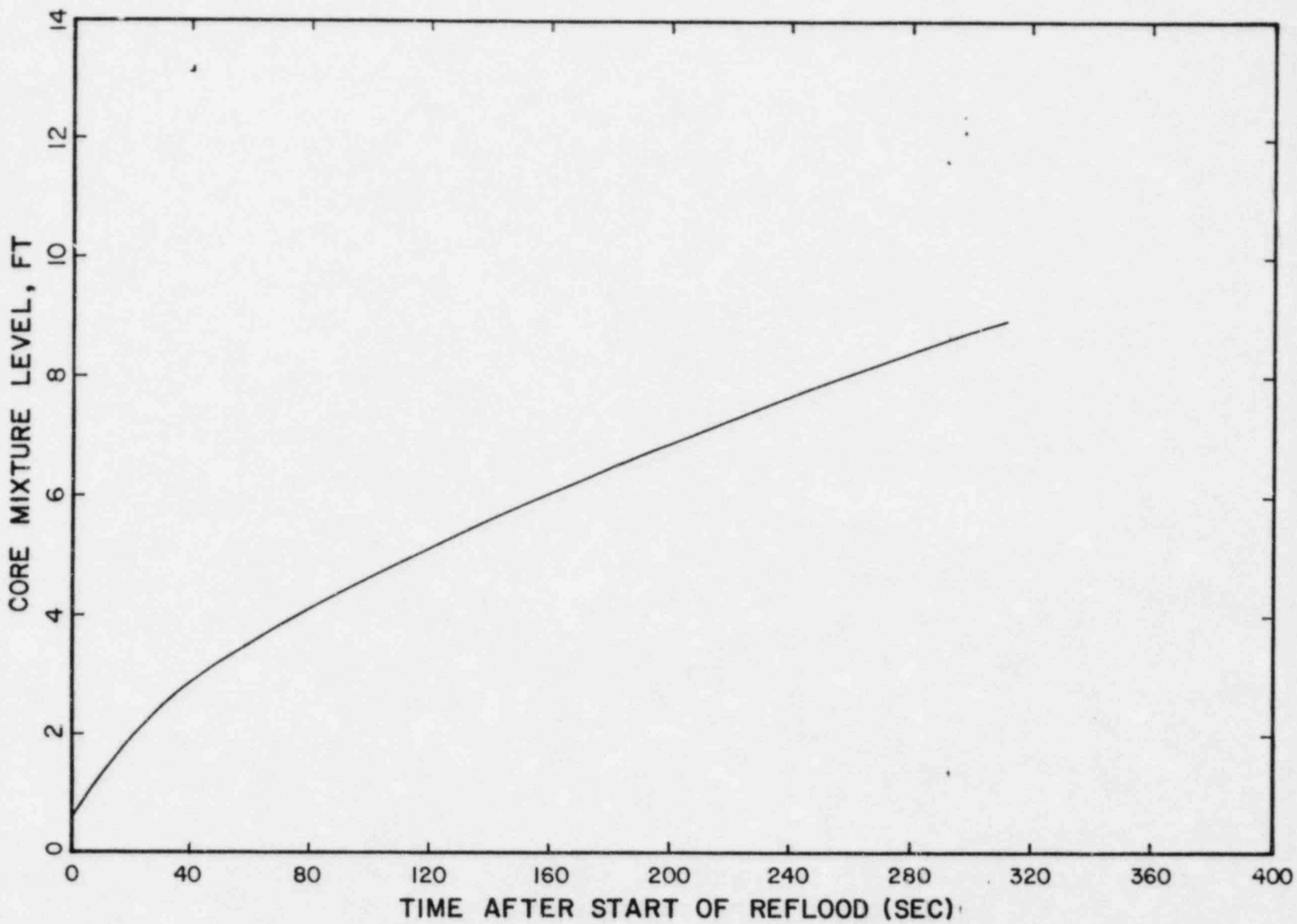


OMAHA PUBLIC POWER DISTRICT
FORT CALHOUN STATION
UNIT NO. 1

Cycle 8 Reflood Core Mixture Level, 1.0 DECLG Break

Figure 14.15-57

OMAHA PUBLIC POWER DISTRICT
FORT CALHOUN STATION
UNIT NO. 1

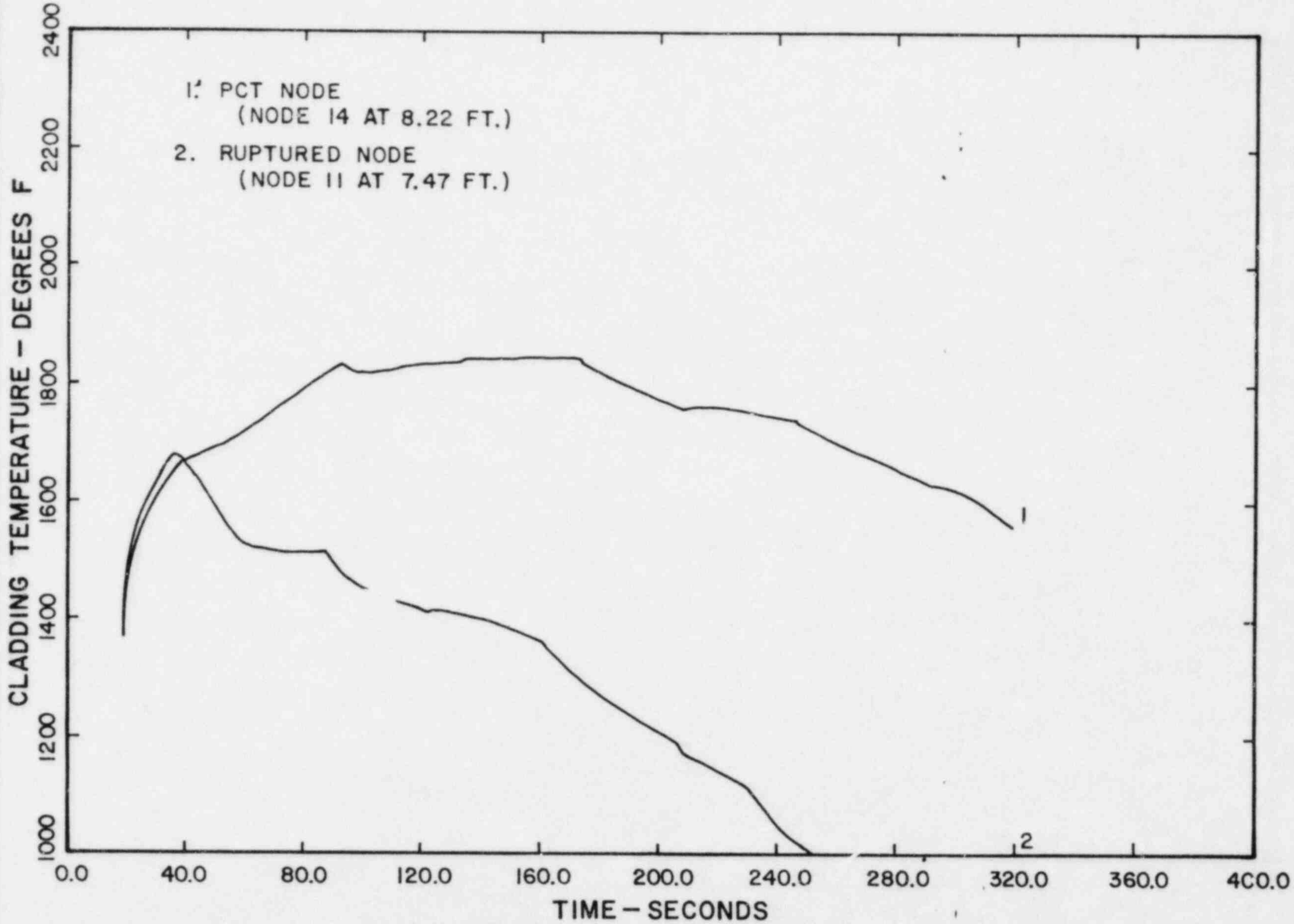


Cycle 8 Cladding Surface Temperature During Heatup, 0.7 X/L, BOL, 1.0 DECLG Break

Figure 14.15-58

OMAHA PUBLIC POWER DISTRICT
FORT CALHOUN STATION
UNIT NO. 1

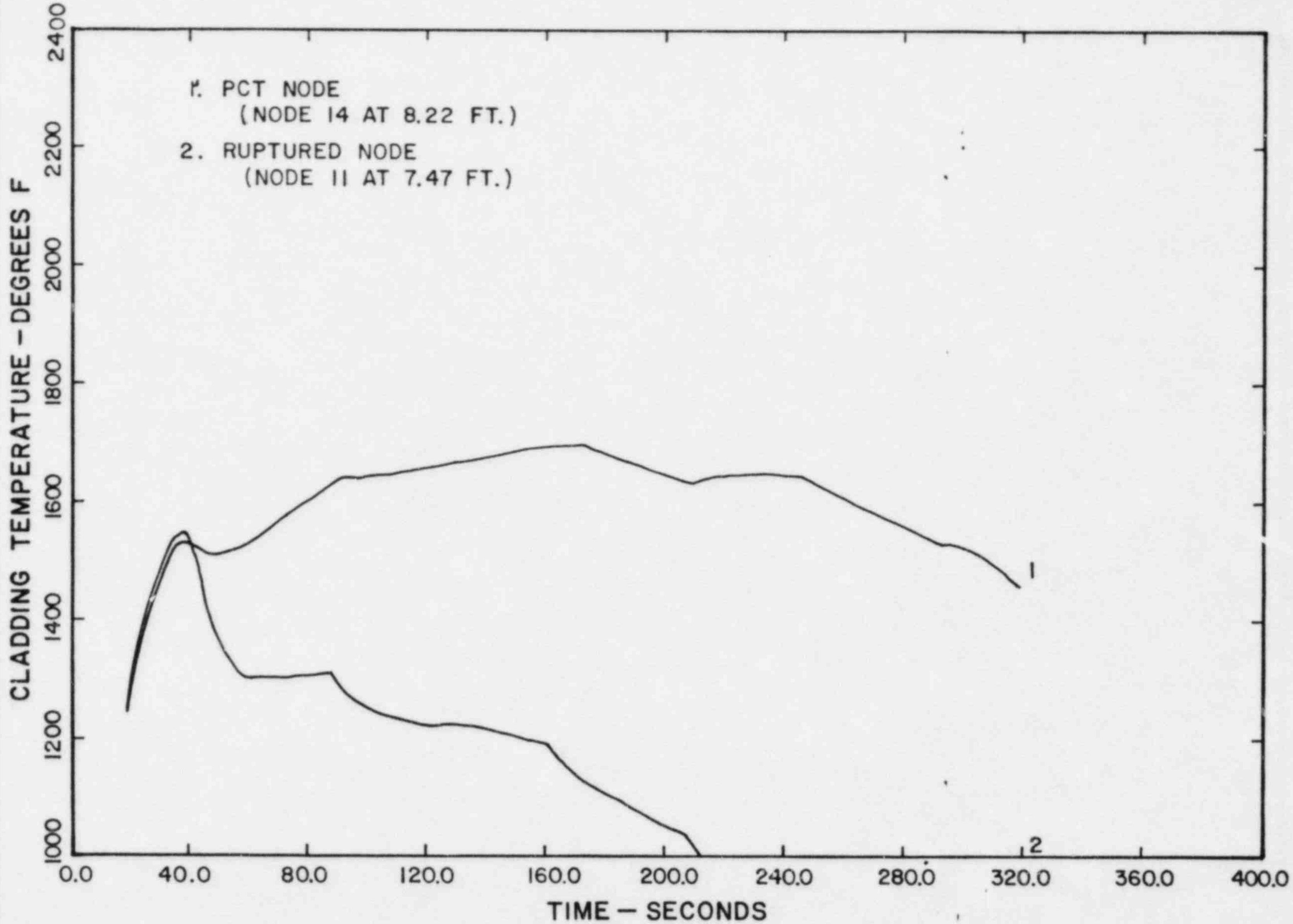


Cycle 8 Cladding Surface Temperature During Heatup, 0.7 X/L, EOL, 1.0 DECLG Break

Figure 14.15-59

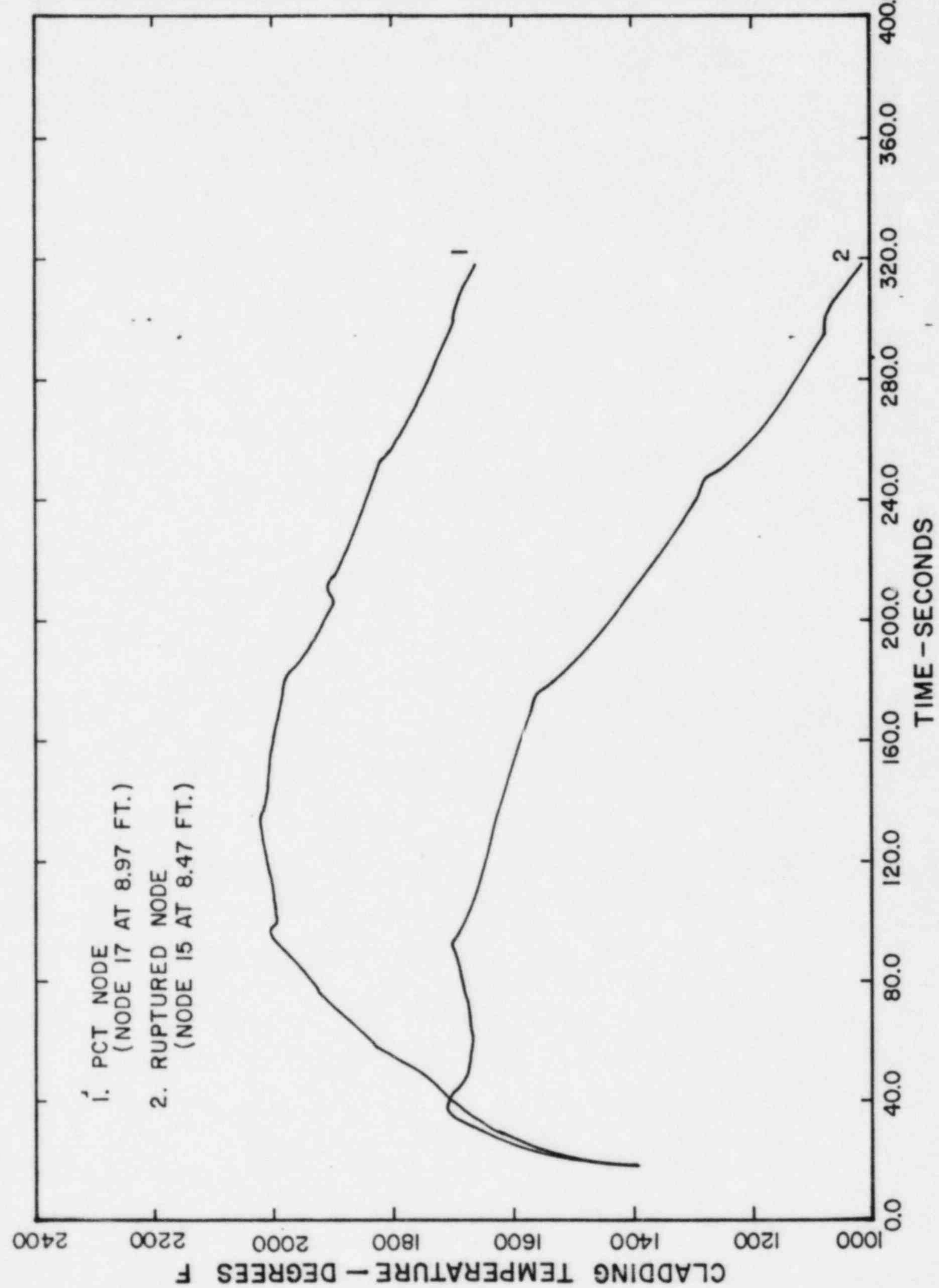


| | | |
|---|---|---|
| OMAHA PUBLIC POWER DISTRICT<br>FORT CALHOUN STATION<br>UNIT NO. 1 | Cycle 8 Cladding Surface Temperature During Heatup, 0.8 X/L, BOL, 1.0 DECLG Break | Figure 14.15-60 |

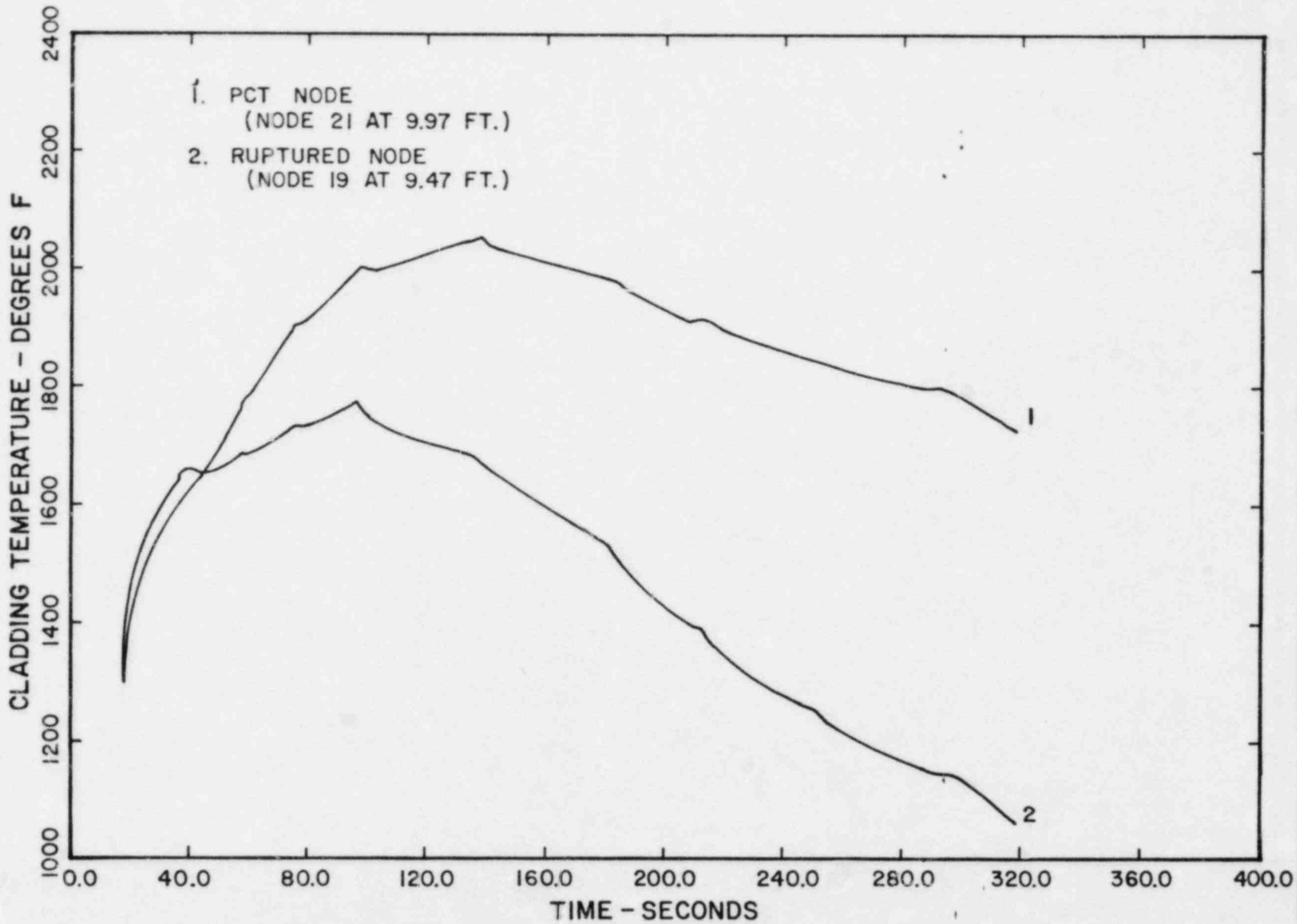


OMAHA PUBLIC POWER DISTRICT
FORT CALHOUN STATION
UNIT NO. 1

Cycle 8 Cladding Surface Temperature During Heatup, 0.9 X/L, BOL, 1.0 DECLG Break

Figure 14.15-61

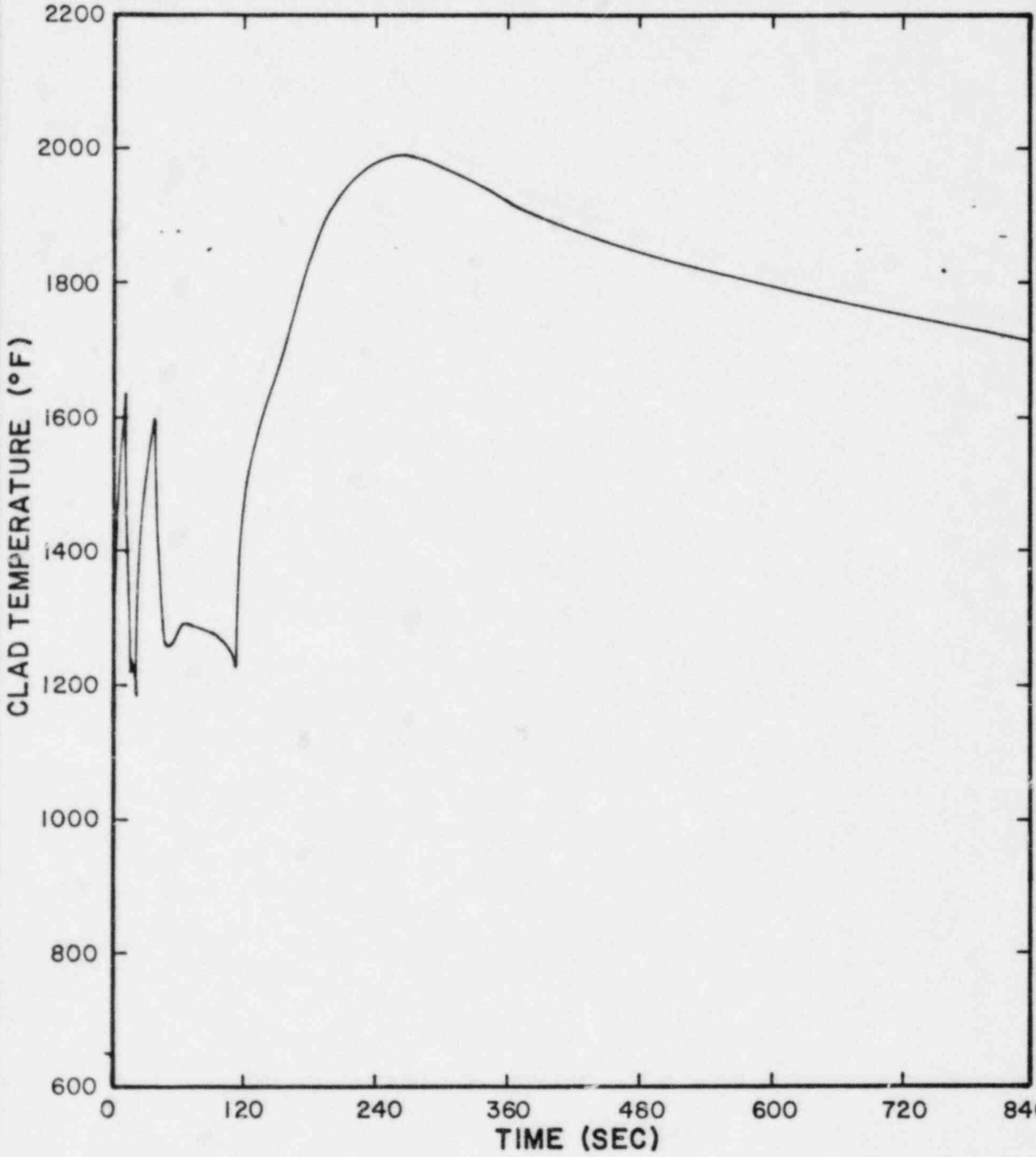


| | | |
|---|---|---|
| OMAHA PUBLIC POWER DISTRICT<br>FORT CALHOUN STATION<br>UNIT NO. 1 | Batch D, 1.0 x Double Ended Guillotine Break at Pump Discharge Leg; Clad Temperature of Neighboring Pins in the Radiation Enclosure | Figure 14.15-62 |

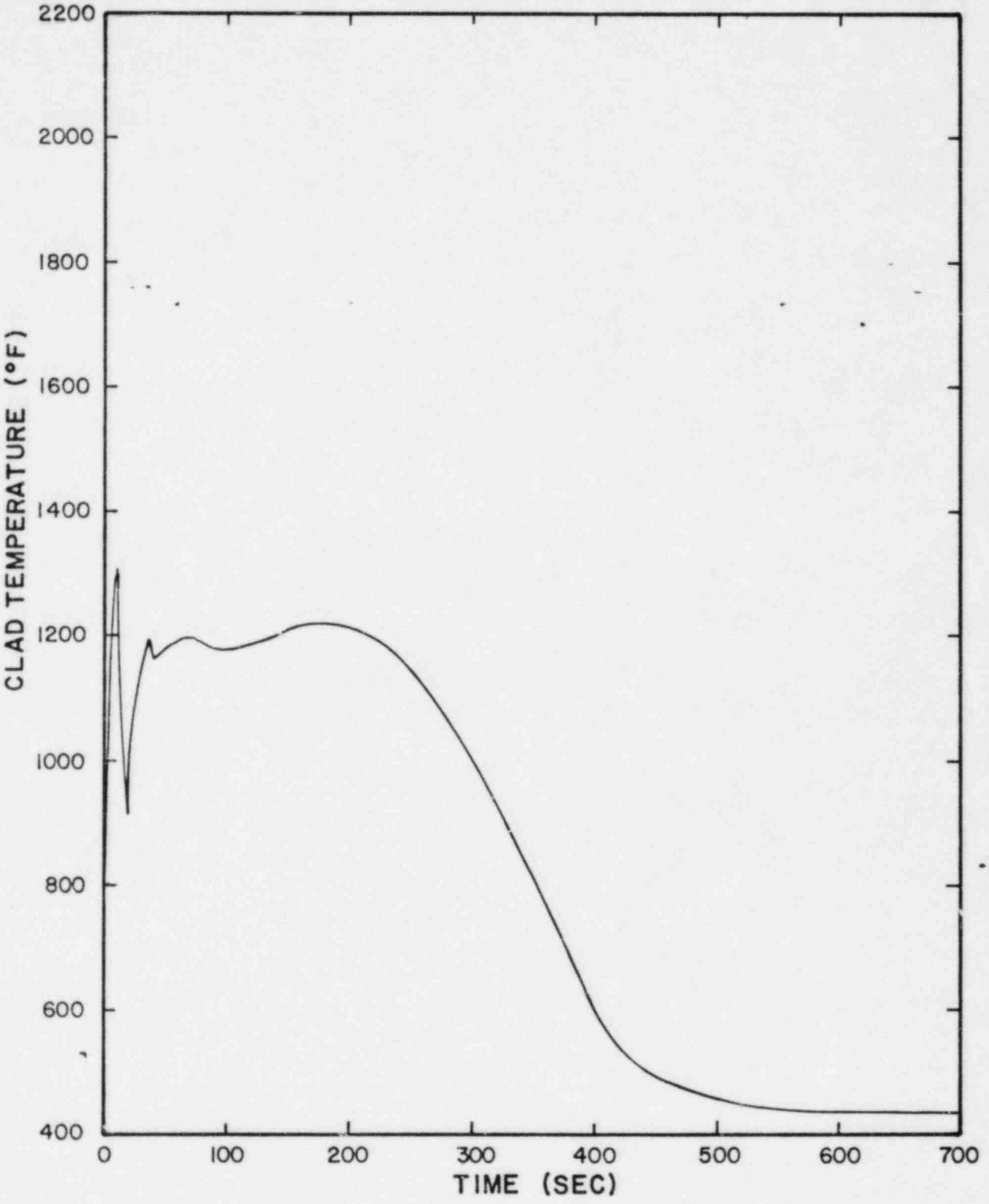


| | | |
|---|---|---|
| OMAHA PUBLIC POWER DISTRICT<br>FORT CALHOUN STATION<br>UNIT NO. 1 | Batch D, 1.0 x Double Ended Guillotine Break at Pump Discharge Leg; Peak Clad Temperature | Figure<br>14.15-63 |

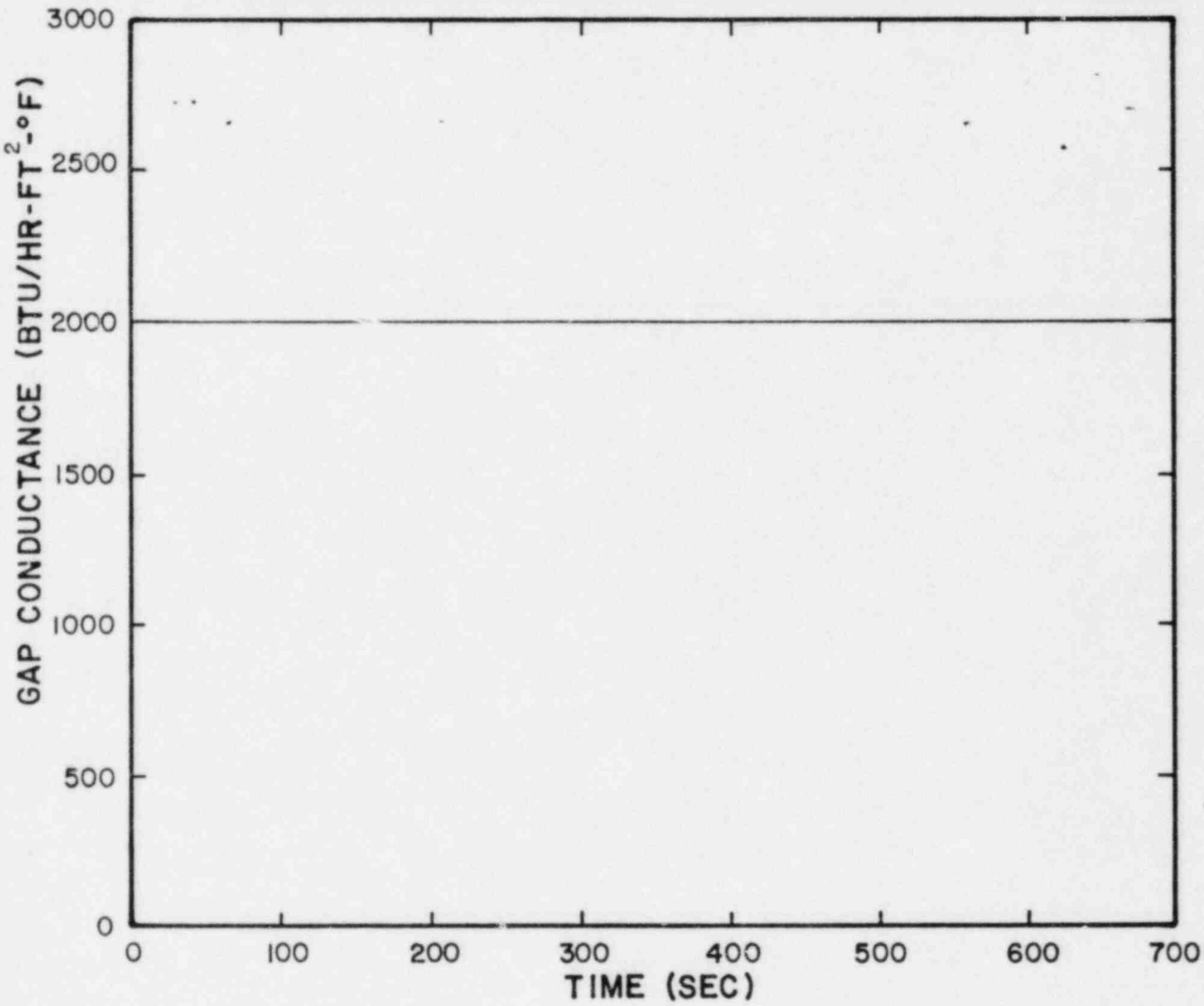


| | | |
|---|---|---|
| OMAHA PUBLIC POWER DISTRICT<br>FORT CALHOUN STATION<br>UNIT NO. 1 | Batch D, 1.0 x Double Ended Guillotine Break at Pump Discharge Leg; Hot Spot Gap Conductance | Figure 14.15-64 |

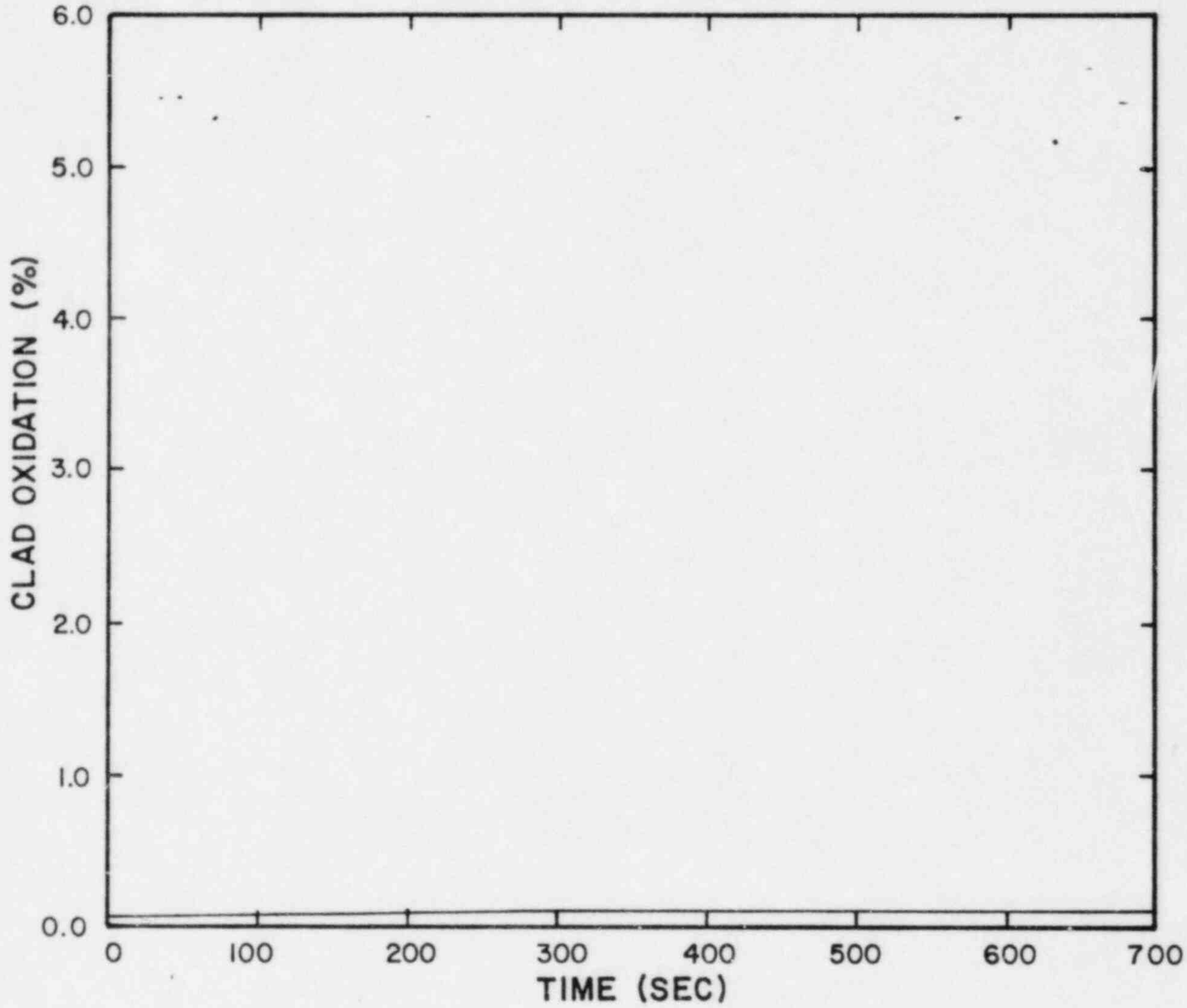


| | | |
|---|---|---|
| OMAHA PUBLIC POWER DISTRICT<br>FORT CALHOUN STATION<br>UNIT NO. I | Batch D, 1.0 x Double Ended Guillotine Break at Pump Discharge Leg; Peak Local Clad Oxidation | Figure 14.15-65 |

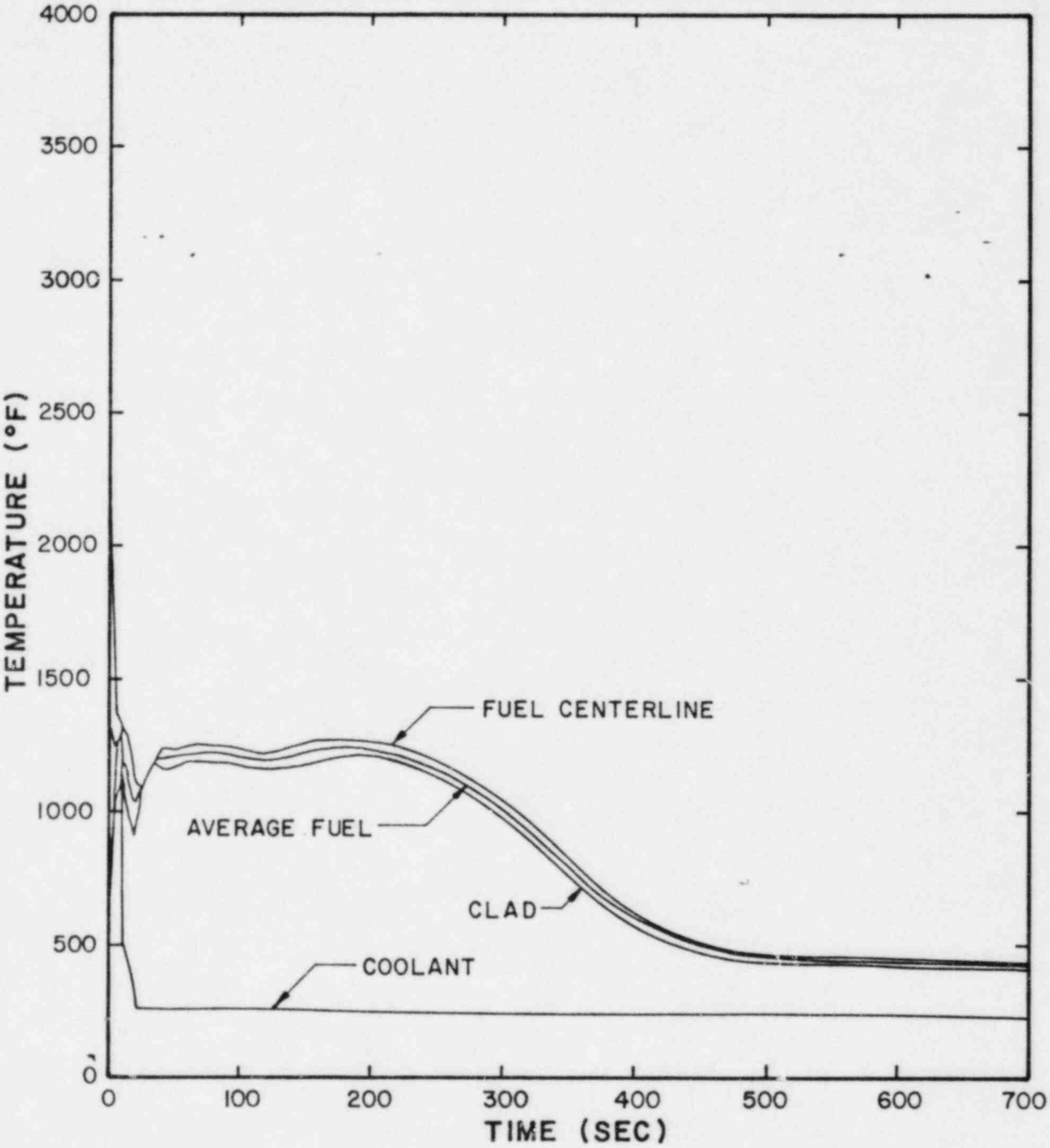


| | | |
|---|---|---|
| OMAHA PUBLIC POWER DISTRICT<br>FORT CALHOUN STATION<br>UNIT NO. 1 | Batch D, 1.0 x Double Ended Guillotine Break at Pump Discharge Leg; Clad Temp., Centerline Fuel Temp., Avg. Fuel Temp., and Coolant Temp for the Hottest Node | Figure 14.15-66 |

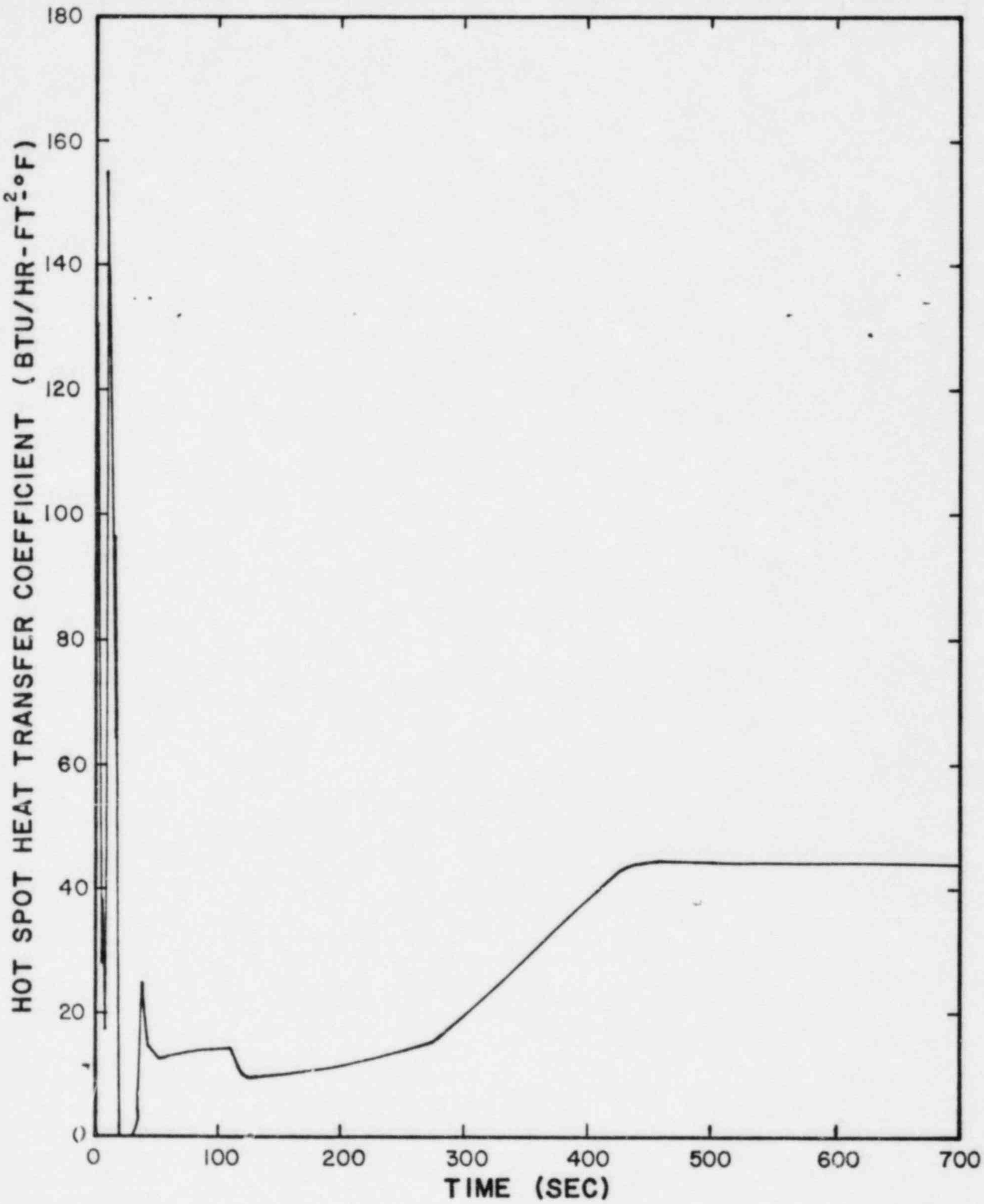


| | | |
|---|---|---|
| OMAHA PUBLIC POWER DISTRICT<br>FORT CALHOUN STATION<br>UNIT NO. 1 | Batch D, 1.0 x Double Ended Guillotine Break at Pump Discharge Leg; Hot Spot Heat Transfer Coefficient | Figure 14.15-67 |

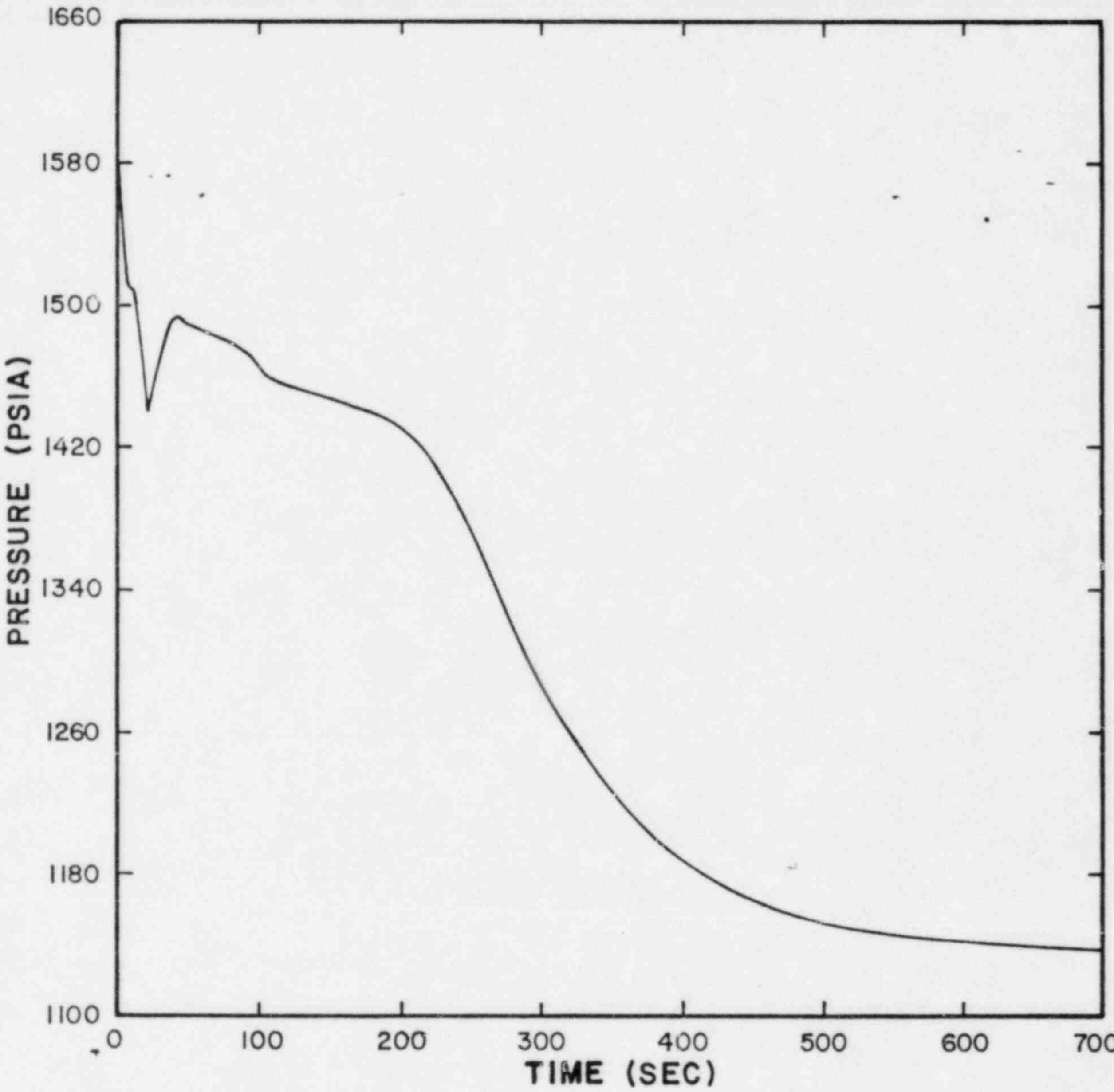


| | | |
|---|---|---|
| OMAHA PUBLIC POWER DISTRICT<br>FORT CALHOUN STATION<br>UNIT NO. 1 | Batch D, 1.0 x Double Ended Guillotine Break at Pump Discharge Leg; Hot Rod Internal Gas Pressure | Figure 14.15-68 |